VACUUM VALVES
IN
PULSE TECHNIQUE

VACUUM VALVES IN PULSE TECHNIQUE

BY

P. A. NEETESON

Philips Central Application Laboratories, Eindhoven

Second revised and enlarged edition

1959

PHILIPS' TECHNICAL LIBRARY

Publisher's note :
This book is published in English, German and French

The book contains 202 pages, 155 figures

U.D.C. 621.374

1st edition 1955
2nd enlarged edition 1959

PREFACE

The use of the electron tube in electric circuits has spread within the last few decades over a vast new field, the field of pulse technique.
Some of these applications of the tube have already become a normal part of modern life, for instance in television and automatic telephony. Further, there are important applications in special spheres, like radar, telemetering and electronic counting apparatus, not to mention the rapidly expandings sphere of electronic computers. The introduction of the electron tube into electric circuitry was chiefly the work of practical men. Gradually, the special properties and possibilities of the tube were studied and the number of uses to which it could be put increased considerably, as it became known how the tube could be treated within the network.
In pulse technique, however, the tube is generally used for quite another type of operation, there being two distinct operating states, in one of which no current or very little current is drawn and the tube is cut off. The other state is that in which a heavy anode current flows and the tube is fully conducting. The change-overs between these two states occur suddenly and are accompanied by certain related transient phenomena in the network. The tube operates as a "switch".
Although there are many known applications of the tube for this type of use, the mathematical treatment of the switching phenomena is still a closed book to many users. It is the main aim of this book to indicate the methods of determining the behaviour of a network in which electronic tubes are used as switches. The better mastery of this material may then lead to still more efficient use, and even to new applications of the tube in this type of circuit.
After a few introductory chapters, dealing with such subjects as the opening and closing of switches in networks and some principles of operational calculus, there follows a chapter in which a thorough treatment of the vacuum-tube as a switch is given. This chapter is sub-divided into a treatment of the grid circuit and of the anode circuit, both for the triode and the pentode. The last chapters deal with three very important and widely used circuits known collectively as multivibrators — these are the bistable, monostable and astable multivibrators.
The subject matter of this book does not spring from a mere desire to theorize — in the contrary, it was actually prompted by a problem that arose in practice

and that necessitated a deeper investigation by the author into the dynamic phenomena of one of these pulse circuits. By deriving a theoretical treatment of these phenomena and confirming it in practice, the operation became easier to understand and practical conclusions could be drawn, giving rise, for instance, to the development of special tubes having particularly favourable properties for use in pulse techniques.
The book will thus be useful for those who may already be engaged in pulse techniques but who are not yet conversant with the mathematical treatment of the electrical phenomena which occur in these special circuits. It will further be of help to those who are specializing in this branch of electronics and may also find application in training institutes.
Thanks are due to Mr Harley-Carter, A.M.I.E.E., London, and Mr H. P. White, London, for reading the English text.

August 1955 *The Author*

PREFACE TO THE SECOND EDITION

The fact that within a few years a second edition of this book, treating a rather specialized material, has been necessary, is of course a great satisfaction to the author. It makes him believe that the new edition will also find its way to those interested in the subjects of pulse technique in electronics, the more so as it has been possible to extend the contents of the book with an extra chapter and an extensive literature reference. The new chapter treats a special class of pulse circuitry formed by several kinds of blocking oscillators, thereby illustrating the applicability of the switching theory to this field of magnetically coupled electronic devices.

The multivibrator circuits together with the blocking oscillators cover the most important part of fundamental pulse circuits containing vacuum tubes as the active elements. Therefore it is believed that the incorporation of the new chapter makes the book a more complete whole.

June 1959 *The Author*

CONTENTS

1. INTRODUCTION

The theoretical analysis of linear electrical networks which has been developed thoroughly during the past century by many workers in this field has reached a certain degree of perfection.

The first stage in this development was the study of the behaviour of passive networks when subjected to the influence of electromotive forces or electrical currents of periodic nature and having such small amplitudes that the components included in the networks never lose their typical linear properties. In other words, the values which determine the behaviour of the components are independent of the amplitudes.

Typical components of passive linear networks are resistances, capacitances, self- and mutual inductances. These are best known in their classical form as linear components. Modern development of electrical circuitry, however, takes increasing advantage of the possibilities offered among others by new magnetic and dielectric materials having hysteresis and saturation properties to construct typical non-linear components. Examples of these are self-inductances of coils with more or less saturated magnetic cores (iron alloys, iron-dust cores, ferrites such as ferroxcube), capacitors with barium titanate dielectric, voltage-dependent resistances (VDR), resistances with negative or positive temperature-coefficient (NTC and PTC resistances resp.).

Returning to our starting point, it can be stated that the mathematical treatment of passive, linear network behaviour has been mastered very well, some examples of noteworthy tools being Fourier analysis of periodical waveforms, that enables the response of networks to these waveforms to be calculated as the response to the superposition of single sine wave functions, and also the introduction of complex functions instead of sine functions.

A further and very important step in the development of network-analysis was the study of the response of passive linear networks to non-periodic, discontinuous wave forms. This was commenced with a marvellous mathematical intuition by Heaviside, then greatly widened and mathematically established by other outstanding mathematicians and physicists, resulting in the new technique of calculating the response of networks to input-currents or -voltages known as operational

calculus. Even non-linear, passive networks of not too complex non-linear nature have been mathematically analysed.

Since the invention of the electronic vacuum tube, a new "component" has entered network-design so rapidly and completely that it hardly has a parallel in any other technical development of modern time. Thus an essentially non-linear, non-passive component, the electron tube, is introduced into electrical networks.

The electron tube is a non-passive component because direct-current power is constantly fed to it, thus making it possible to give the tube amplifying properties for signals with varying amplitude, the most widespread application being the modulation of a direct anode current by means of a varying grid voltage, resulting in a more or less proportional variation of the potential drop across an anode load-resistor.

This "more or less" must be added, because it is difficult to get a linear relationship between grid voltage variation and resulting anode current variation (linear anode current – grid voltage characteristic). Linearity is more closely approached as the excursions of the grid voltage variation to either side of a fixed operating point on the characteristic become smaller. Then the well-known equivalent circuits of the electron tube amplifier can be used to simplify the analysis of the network containing the tube. These equivalent circuits are either a voltage source μe_g in series with the internal anode resistance R_i, or a current source Se_g in parallel with R_i, μ and S being the amplification factor and the transconductance respectively, e_g the applied grid voltage variation.

Under these circumstances, the electron tube can be incorporated in the network of more conventional components as another linear (amplifying) element and mathematically treated as such.

In the use of electron tubes in pulse techniques, however, these conditions are generally far from being satisfied. The tube must, on the other hand, be considered as an essentially non-linear element. It is generally switched from one discrete state into another, viz. from the fully conducting state into cut-off condition or vice versa. In the conducting state it represents a given (internal) resistance between anode and cathode. When, in addition, grid current occurs, another (internal) resistance is present between the grid and the cathode. In the non-conducting state, these resistances have assumed very high values, practically infinite. It may thus be stated that, at sudden transitions from one state to the other, resistances are switched on or off in the circuit in which the tube is included.

It will be clear that this kind of operation of tubes in pulse techniques

is quite different from the familiar operation in conventional amplifiers, and must be considered as a switching action. Some external cause, usually a rather steep voltage step in either the positive or the negative direction applied to the control grid, should bring the tube as rapidly as possible from one discrete position to the other.

Because of the already widespread and still ever increasing use of electron tubes in pulse techniques, such as electronic counter-apparatus and computing devices, scalers and radiation counters for atomic research and X-ray application, pulse modulation systems, radar, television and the like, it seems worth while to examine the behaviour of these tubes in pulse applications. This will be the principal aim of this book. After a general treatment of the behaviour of an electronic vacuum tube when subjected to sudden voltage changes at its control grid, some special circuits, well known in practice and often used as fundamental units in pulse devices, will be dealt with. Theoretical analysis will prove to be useful in investigating the influence of several tube characteristics on the behaviour of the circuits as a whole. The circuits to be considered are the three members of the multivibrator family, viz. the bistable, the monostable and the astable multivibrator.

As already mentioned, operational calculus has offered elegant solutions of transient phenomena in electrical networks. It will prove to be useful too in solving the problems related with transients in switched electron tubes.

Relatively few basic principles of this operational calculus will be sufficient to deal with the transient problems related with electron tubes as circuit components, and to solve these problems. These basic elements will be considered in the next section.

2. BASIC THEORY OF SWITCHING

As previously mentioned, in pulse techniques the electronic tube must be regarded as a non-linear element. In the conducting state, internal anode resistance and, generally, also internal grid resistance must be taken into account, whereas in the non-conducting or cut-off state, these resistances have disappeared. If the tube is suddenly switched from one state to the other by a negative or positive-going voltage step at the control grid, these internal resistances are switched off or on respectively in the circuit containing the tube.

Operational network analysis indicates how to incorporate these discontinuities and their consequences in calculations of the circuit behaviour.

Before proceeding to a more detailed discussion of circuits with switching tubes, a short general survey of switch actions will be given.

2.1. SUDDEN SHORT-CIRCUITING OF TWO POINTS OF A NETWORK

In fig. 1.2, AB represents a passive linear network in which currents flow and voltages occur as a result of an externally applied voltage $E(t)$, which is a function of time. The voltage between points P and Q of the network will be denoted by $V(t)$. At the instant $t = t_0$, points P and Q are short-circuited, so that the voltage between these points is zero for $t \geqslant t_0$. The effect of this sudden short-circuiting on the current and voltage situation of the network can now be determined by imagining a voltage source with zero internal resistance being present between P and Q from the instant $t = t_0$ onwards, the time function of this voltage being such that the voltage $V(t)$ originally present between P and Q is just compensated from the instant t_0 onwards. This voltage source, occurring when the switch is closed, can be represented by the expression:

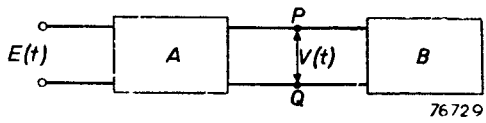

Fig. 1–2.
Passive network in which the externally applied voltage $E(t)$ produces a voltage $V(t)$ between points P and Q.

$$V_c(t) = -V(t) \,.\, U(t - t_0), \quad \ldots\ldots\ldots \quad (1.2)$$

in which $U(t-t_0)$ represents a unit step function occurring at the instant $t = t_0$. In other words, from this instant onwards the voltage $V(t)$ must be multiplied by -1 to obtain the time function $V_c(t)$.

The voltages and currents in the network now consist of two superimposed components, namely one component originating from $E(t)$ as it would be without the sudden disturbance caused by points P and Q being short-circuited, and the other component caused by $V_c(t)$, i.e. by the short-circuiting effect. Since it has been assumed that the input voltage source $E(t)$ has zero internal resistance or that its internal resistance is incorporated in the network, this voltage source may be considered as a short-circuit for calculating the effect of $V_c(t)$.

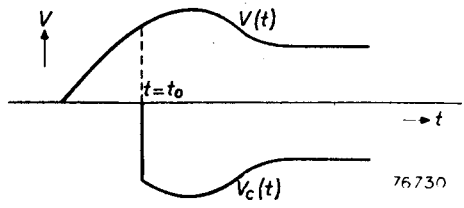

Fig. 2–2.
Example of the time function $V_c(t)$.

Fig. 2.2 illustrates an example of the time function $V_c(t)$.

2.2. SUDDEN BREAKING OF A CONNECTION IN A NETWORK

In the passive network AB shown in fig. 3.2, a current $I(t)$, which is caused by the input voltage $E(t)$, flows between points P and Q through the resistance R. This resistance will be assumed to be suddenly disconnected from point Q at the instant $t = t_0$. From the instant t_0 onwards, current can obviously no longer pass from P to Q. This is equivalent to the resistance R suddenly becoming infinitely large. The effect of this discontinuity on the network can be described as follows.

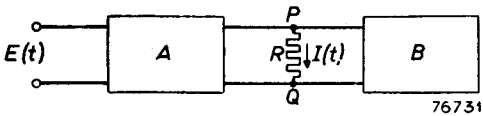

Fig. 3–2.
Passive network in which the externally applied voltage $E(t)$ produces a current $I(t)$ through the branch PQ.

From the instant $t = t_0$ onwards, voltages and currents in the network consist of two components, namely one component due to $E(t)$ and calculated as if no discontinuity had occurred, and a second component, superimposed on the other, which is caused by the sudden disconnection of R and calculated by assuming an imaginary current source with infinitely large internal resistance to be present between points P and Q, the voltage source $E(t)$ being short-circuited and the value of the current source being such that the current $I(t)$, which would be present without the disturbance, is just compensated.

This imaginary current source, occurring when the switch is opened, will be denoted by $I_0(t)$, and, in analogy with eq. (1.2), it can be described by:

$$I_0(t) = -I(t) \cdot U(t - t_0). \quad \ldots\ldots\ldots \quad (2.2)$$

This expression can be represented by the curve shown in fig. 2.2, provided $V(t)$ and $V_c(t)$ are replaced by $I(t)$ and $I_0(t)$ respectively.

3. APPLICATION OF THE THEORY TO SIMPLE SWITCHING CIRCUITS

Before proceeding to the discussion of practical switching devices containing electron tubes, some simple switching circuits will be investigated, containing a switch whose nature will be left out of consideration.

3.1. IDEAL SWITCH WITHOUT INTERNAL RESISTANCE AND PARALLEL CAPACITANCE

The circuit will be assumed to consist of a resistance R in series with a switch S connected to a constant voltage V_b (see fig. 1.3).

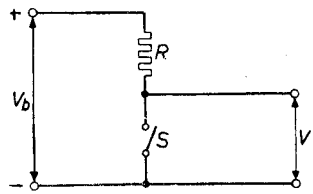

Fig. 1–3.
Ideal switch without internal resistance and parallel capacitance connected to a constant voltage V_b via the resistance R.

If the voltage source has an internal resistance, this may be imagined to be incorporated in the value of R. It is now of interest to know the form of the voltage V across the switch. It will be clear that so long as switch S is open, V will have the same value as V_b, whereas V will be zero when the switch is closed.

Opening the switch at the instants $t_1, t_3, \ldots$ and closing it at the instants $t_2, t_4 \ldots$ will therefore result in a voltage as depicted in fig. 2.3.

By way of illustration, the theory outlined in sections 2.1 and 2.2 will now be applied. First the case of the switch being closed will be considered. From this instant onwards, a voltage source V_c is to be incorporated in this circuit instead of the switch, so that V_c has the same value as, but is opposite in sign to, the voltage V that would be present if the switch had not been closed.

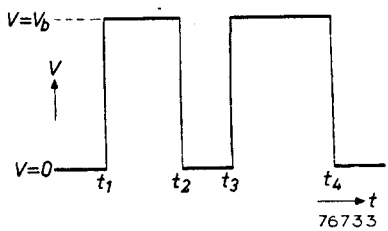

Fig. 2–3.
Voltage V produced across the switch S shown in fig. 1–3 when S is opened at the instants $t_1, t_3, \ldots$ and closed at the instants $t_2, t_4, \ldots$

Hence, $V_c = -V_b$, the situation being as represented by fig. 3.3. The actual voltage V across the switch is now equal to the superposition of

the original voltage $+V_b$ and the effect of V_c, viz. $-V_b$, resulting in zero voltage. The voltage across R was originally zero, whereas, after the switch has been closed, a current $I = V_c/R$ flows through R, producing a voltage drop $-V_c$ across R. The combined effect of these two components is $0 - V_c$ or $+V_b$.

There is obviously no point in applying this method to such simple switching circuits, but it does give an insight in the mechanism and proves the validity of the theory.

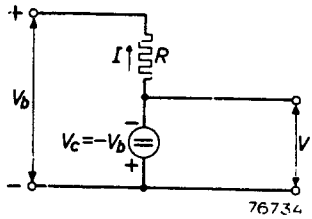

Fig. 3–3.
Circuit equivalent to that shown in fig. 1–3 when switch S is closed.

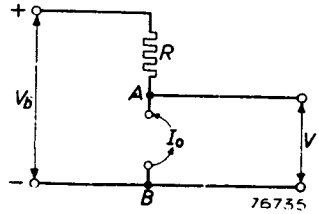

Fig. 4–3.
Circuit equivalent to that shown in fig. 1–3 when switch S is opened.

Considering the opening of the switch, it will be clear that, from the instant of opening onwards, a current source $I_0 = -V_b/R$ must be imagined to be present at the terminals of the switch (see fig. 4.3). This current gives rise to a voltage drop across R, as a result of which the potential of point A with respect to B is $-I_0R$ or $+V_b$.

The voltage between A and B was originally zero, resulting in a voltage $V = V_b$. Before the switch was opened, a current $I = -I_0$ was flowing in the downward direction through R, whereas, after the switch has been opened, this current is compensated by the current I_0, resulting in zero voltage drop across R.

3.2. SWITCH WITH INTERNAL RESISTANCE

Since ideal switches are non-existent, a better approximation of an actual switch is obtained by assuming it to have a certain internal resistance r, r being taken to be much smaller than R.

Fig. 5.3 shows the circuit with the switch open. The voltage across the switch will obviously be $V = V_b$ and will drop to a value

$$V = V_b \cdot r/(R + r)$$

when the switch is closed. Opening the switch at the instants t_1, t_3 . . . and closing it at the instants t_2, t_4 . . . will result in a voltage V as shown

in fig. 6.3. Compared with the previous case, the amplitude of the pulse-shaped voltage V has decreased by an amount $V_b \cdot r/(R + r)$. The flanks of the pulses will, however, still have an infinitely steep slope.

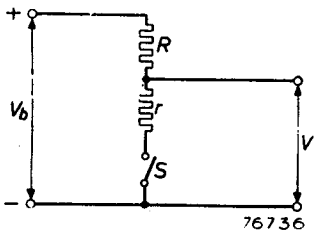

Fig. 5–3.
Switch with internal resistance r connected to a constant voltage V_b via the resistance R.

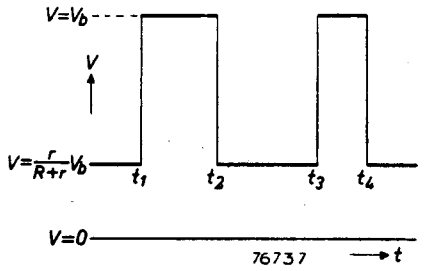

Fig. 6–3.
Voltage V produced across the switch shown in fig. 5–3 when this is opened at the instants t_1, t_3, ... and closed at the instants t_2, t_4, ...

The validity of the theory given in Sections 2.1 and 2.2 will once again be shown. Closing the switch at the instant $t = t_0$ gives for $t \geqq t_0$ a superposition of the original state and the effect of a voltage source $V_c = -V_b$ as represented in fig. 7.3. This voltage gives rise to a current

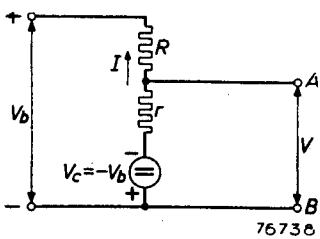

Fig. 7–3.
Circuit equivalent to that shown in fig. 5–3 when switch S is closed.

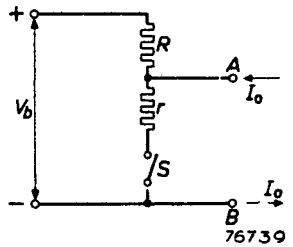

Fig. 8–3.
Circuit equivalent to that shown in fig. 5–3 when switch S is opened.

$I = V_c/(R + r) = -V_b/(R + r)$. This current produces a voltage drop of $-rI = V_b \cdot r/(R + r)$ across r. The total effect of V_c on the potential between A and B is therefore given by:

$$V_c + \frac{r}{R+r} \cdot V_b = -V_b + \frac{r}{R+r} \cdot V_b = -\frac{R}{R+r} \cdot V_b.$$

This voltage must be superimposed on the original voltage $+V_b$, which gives for the total voltage between A and B:

$$V = V_b - \frac{R}{R+r} \cdot V_b = \frac{r}{R+r} \cdot V_b.$$

The opposite case, when the switch is opened at the instant $t = t_0$, can be investigated by assuming a current source $I_0 = -V_b/(R + r)$ to be present between A and B for $t \geqq t_0$ (see fig. 8.3). This current produces a voltage drop across R, which results in a potential of

$$V_b \,.\, R/(R + r)$$

being produced between A and B. This must be added to the voltage already present between these points for $t < t_0$, namely $V_b \,.\, r/(R + r)$, which gives $V = V_b$ for $t \geqslant t_0$.

3.3. SWITCH WITH INTERNAL RESISTANCE AND PARALLEL CAPACITANCE

In practice, all switches will have not only an internal resistance, but also a stray capacitance connected in parallel. Fig. 9.3 shows the circuit with the switch open. The voltage V is equal to V_b when the switch has been open for a sufficient length of time, so that no transient effects due to a preceding switching action remain.

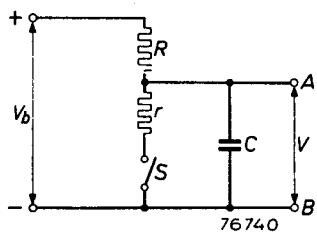

Fig. 9–3.
Switch with internal resistance r and parallel capacitance C connected to a constant voltage V_b via the resistance R.

When the switch is now closed at an instant which, for the sake of convience will be denoted by $t = 0$, the situation depicted in fig. 10.3 will arise.

With the aid of Thévenin's theorem this circuit can be replaced by the equivalent circuit shown in fig. 11.3, in which the voltage source V_b with its series resistance R is replaced by a current source $I = V_b/R$ with parallel resistance R.

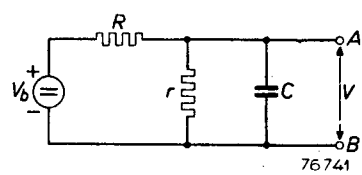

Fig. 10–3.
Circuit equivalent to that shown in fig. 9–3 when switch S is closed at $t = 0$.

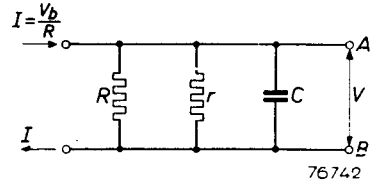

Fig. 11–3.
Equivalent circuit of fig. 10–3 according to Thévenin's theorem.

The circuit of fig. 11.3 may be replaced by the simplified circuit shown in fig. 12.3, in which $R_{eq} = R \,.\, r/(R + r)$. According to Kirchhoff's laws:

$$R_{eq} \cdot \frac{di_1}{dt} + \frac{1}{C} \cdot i_1 = \frac{1}{C} \cdot I, \quad \ldots\ldots\ldots \quad (1.3)$$

a possible solution of which is:

$$i_1 = I + Ae^{at} \quad \ldots\ldots\ldots\ldots \quad (2.3)$$

Substitution of eq. (2.3) in eq. (1.3) and introducing the initial condition $V = V_b$ for $t = 0$, gives:

$$A = \frac{V_b}{R_{eq}} - I \text{ and } a = -\frac{1}{R_{eq}C}.$$

Since

$$V = R_{eq}(I + Ae^{-t/R_{eq}C}), \quad \ldots\ldots \quad (3.3)$$

it may therefore be written:

$$V = \frac{V_b}{R + r} \cdot (r + Re^{-t/R_{eq}C}) \quad \ldots \quad (4.3)$$

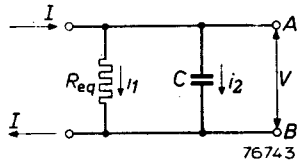

Fig. 12–3. Circuit according to that shown in fig. 11–3 in which the resistances R and r connected in parallel are replaced by the equivalent resistance R_{eq}.

After a sufficiently long time, V approximates to:

$$V_\infty = \frac{r}{R + r} \cdot V_b, \quad \ldots\ldots\ldots \quad (5.3)$$

whilst for $t = 0$ the initial value is:

$$V = V_0 = V_b \quad \ldots\ldots\ldots\ldots \quad (6.3)$$

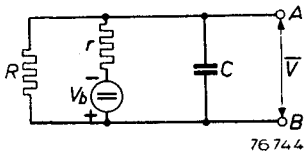

Fig. 13–3. Circuit for calculating transient effects.

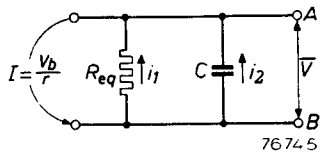

Fig. 14–3. Equivalent circuit of fig. 13–3 according to Thévenin's theorem.

For calculating the transients with the aid of the above theory, it is necessary to introduce a voltage $V_c = -V_b$ (see fig. 13.3) in series with the resistance r, and to add to the voltage V_b present before the switch was closed the voltage $\overline{V}$ across A and B due to V_c. With the aid of Thévenin's theorem, the circuit of fig. 13.3 can be replaced by the equivalent circuit shown in fig. 14.3, in which:

$$R_{eq} = \frac{rR}{r + R} \quad \ldots\ldots\ldots \quad (7.3)$$

The current i_1 is given by eq. (1.3), whilst for the general solution eq. (2.3) is applicable. Now, for $t = 0$, i.e. the instant at which the switch is closed, the voltage across the capacitance C cannot suddenly rise to a certain value; hence, $V = 0$ or $i_1 = 0$, for $t = 0$. Substitution in eq. (2.3) gives:

$$A = -I, \quad . \quad . \quad . \quad . \quad . \quad . \quad . \quad . \quad . \quad . \quad . \quad . \quad . \quad (8.3)$$

and from eqs (2.3) and (1.3):

$$a = -\frac{1}{R_{eq}C}, \quad . \quad . \quad . \quad . \quad . \quad . \quad . \quad . \quad . \quad . \quad . \quad . \quad (9.3)$$

whence:

$$i_1 = I\,(1 - e^{-t/R_{eq}C}),$$

or:

$$V = -i_1 R_{eq} = -IR_{eq}\,(1 - e^{-t/R_{eq}C}). \quad (10.3)$$

From eq. (7.3) and considering that $I = V_b/r$:

$$\overline{V} = -\frac{R}{R+r} \cdot V_b\,(1 - e^{-t/R_{eq}C}) \quad . \quad . \quad . \quad . \quad . \quad . \quad (11.3)$$

The total voltage across A and B after the switch has been closed is therefore:

$$V = V_b + \overline{V} = \frac{r}{R+r} \cdot V_b + \frac{R}{R+r} \cdot V_b e^{-t/R_{eq}C}. \quad (12.3)$$

This expression corresponds to eq. (4.3) derived in the conventional way.

Closing the switch thus results in the potential between points A and B changing from the initial value $V_0 = V_b$ to a final value

$$V_\infty = V_b \,.\, r/(R + r),$$

according to an exponential law with a time constant $T_c = R_{eq}C$.

Assuming, now, that the switch has been closed for a sufficiently long time, so that the final state in which $V = V_\infty = V_b \,.\, r/(R + r)$ is practically reached, the situation represented in fig. 15.3 will arise when the switch is opened. It is convenient to set the instant t at which the switch is opened equal to 0 in a new time scale. For $t < 0$, the voltage between points A and B was $V = V_b \,.\, r/(R + r)$ (see eq. (5.3)), a constant current $I_\infty = V_b/(R + r)$ flowing through the internal resistance r of the switch. At $t = 0$, this current suddenly drops to zero and remains zero for all times $t \geq 0$. This can be accounted for by feeding a current I_0 in the opposite direction, as represented in fig. 15.3,

this current being equal to the value of I_∞ quoted above, which gives:

$$I_0 = \frac{V_b}{R + r} \quad \ldots\ldots\ldots\ldots \quad (13.3)$$

The voltage V is now the superposition of the original voltage, which is already present between points A and B for $t < 0$, and a voltage which results from the effect of the current source I_0. This latter component can be calculated by means of the circuit given in fig. 16.3, which is identical to that shown in fig. 15.3, except for the omission of the direct voltage source $+V_b$, which plays no part in the transient effects to be determined.

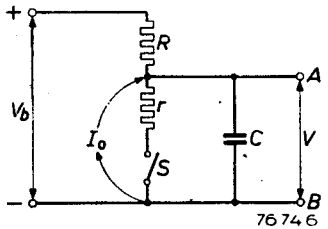

Fig. 15–3.
Circuit according to that shown in fig. 9–3 when switch S is opened after having been closed for a certain time.

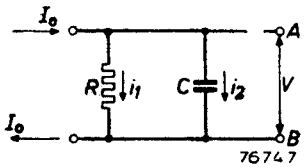

Fig. 16–3.
Circuit identical to that shown in fig. 15–3, but for the omission of the direct voltage source $+V_b$, which plays no part in the transient effects under investigation.

A comparison of figs 16.3 and 12.3 reveals that these circuits are identical, so that the solutions of V in the case of the circuit shown in fig. 16.3 will be the same as those given by eq. (3.3), provided R_{eq} and I are replaced by R and I_0 respectively. Hence:

$$\overline{V} = R\,(I_0 + Ae^{-t/RC}), \quad \ldots\ldots\ldots \quad (14.3)$$

$\overline{V}$ denoting that this is only part of the total voltage V between A and B.

The integration constant A is now defined by the initial condition $V = V_b \,.\, r/(R + r)$ for $t = 0$, i.e. $\overline{V} = 0$ for $t = 0$. Hence:

$$0 = R\,(I_0 + A) \text{ or } A = -I_0,$$

so that, from eqs (13.3) and (14.3):

$$\overline{V} = \frac{RV_b}{R + r} \,.\, (1 - e^{-t/RC}).$$

The total voltage between A and B for $t \geqq 0$ is the sum of $\overline{V}$ and V_∞, which gives:

$$V = V_b - \frac{R}{R+r} \cdot V_b e^{-t/RC} \quad . \quad . \quad . \quad . \quad . \quad (15.3)$$

Summarizing, it can thus be stated that after opening the switch the voltage V increases from its initial value $V_b \cdot r/(R+r)$ at $t = 0$ to the final value V_b according to an exponential law with a time constant $T_0 = RC$.

This time constant is thus always larger than the time constant T_c, in other words: the time constant of the transient phenomena at opening a switch exceeds that at closing a switch. The smaller the internal resistance r of the switch with respect to the external resistance R of the circuit, the more pronounced will be the difference in time constants, namely:

$$\frac{T_c}{T_0} = \frac{R_{eq}C}{RC} = \frac{r}{R+r} \quad . \quad . \quad . \quad . \quad . \quad . \quad . \quad . \quad . \quad (16.3)$$

Fig. 17.3 gives a graphical representation of the voltage V when the switch is opened at the instants t_1, t_3 . . . and closed at the instants t_2, t_4, . . .

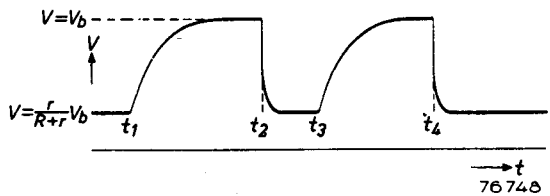

Fig. 17–3.
Voltage V as a function of time, produced in the circuit shown in fig. 15–3 when switch S is opened at the instants t_1, t_3, . . . and closed at the instants t_2, t_4 . . .

It will be clear that periodical opening and closing of the switch with time intervals T that are small compared with the largest time constant $T_0 = RC$, will result in the voltage V assuming a waveform as depicted in fig. 18.3, saw-tooth voltages thus being produced, whereas, if T is much larger than the largest time constant of the circuit, voltages with a pulsatory waveform will be generated. Both waveforms are well known and frequently applied in modern electronics, such as television, radar and computer devices.

The preceding simple treatise on switching circuits makes it possible to draw some *general conclusions.*

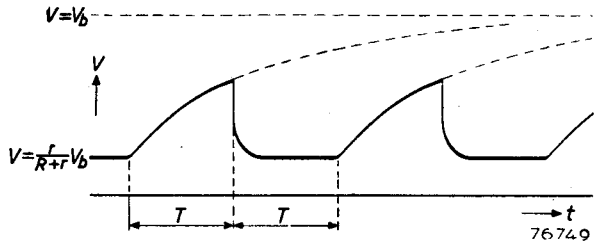

Fig. 18–3.
Saw-tooth voltage produced when switch S is opened and closed with time intervals T which are small compared with the largest time constant $T_0 = RC$.

For generating pulses it is advantageous to aim at a switch the internal resistance of which is as low as possible, in order to increase the pulse amplitude. At the same time the switch should have a very small parallel capacitance in order to obtain pulses with steep flanks. Negative-going flanks will always be steeper than positive-going flanks. For generating saw-tooth shaped signals it will as a rule be necessary to add extra parallel capacitance.

4. SIMPLE TREATMENT OF ELECTRON TUBES AS SWITCHES

By applying positive- or negative-going voltage steps to the control grid, an electronic vacuum tube can be converted from the non-conducting (cut-off) state to the conducting state and vice versa. The anode-to-cathode resistance of a cut-off tube is infinitely large and corresponds to an open switch, whereas a conducting tube represents a certain (internal) resistance between the anode and cathode and may be considered as a closed switch having internal resistance and necessarily a certain parallel capacitance. A negative-going pulse is required for opening the "switch" and a positive-going pulse for closing it.

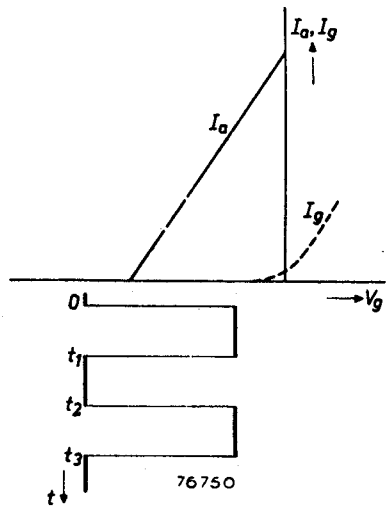

Fig. 1-4.
Idealized $I_a = f(V_g)$ characteristic of a tube to which a square wave voltage is applied.

It will be assumed that ideal, perfectly square-wave shaped voltage steps are applied to the control grid of the electron tube, the anode current being completely cut off at the lowest potential level of these steps and their amplitude being such that the point at which grid current starts to flow is not reached (see fig. 1.4).

When a suitable resistance is incorporated between the anode and the H.T. line, the resulting anode voltage variations will be as shown in figs 2.4*a* and *b*. Provided the largest time constant (product of anode load resistance and anode-to-cathode capacitance) is small compared with the switching time intervals t_1, $t_2 - t_1$, $t_3 - t_2$, etc., the anode voltage variations will be pulse-shaped as depicted in fig. 2.4*a*, whereas saw-tooth shaped voltage variations as depicted in fig. 2.4*b* will be produced when this time constant is large compared with the switching time intervals.

This section is confined to the generation of pulse-shaped signals, and reference to saw-tooth generation circuits will be omitted. Readers

who are interested in the latter subject are referred to the literature quoted in footnote [1]).

Fig. 2*c*.4 shows the oscillogram of the driving pulses applied to the control grid of the electron tube. Comparison of fig. 2*a*.4 and fig. 2*c*.4 reveals that the circuit provides a kind of pulse amplification with, however, a certain amount of distortion. It will be clear that this distortion, manifest in a decrease of the slope of the pulse flanks and in the

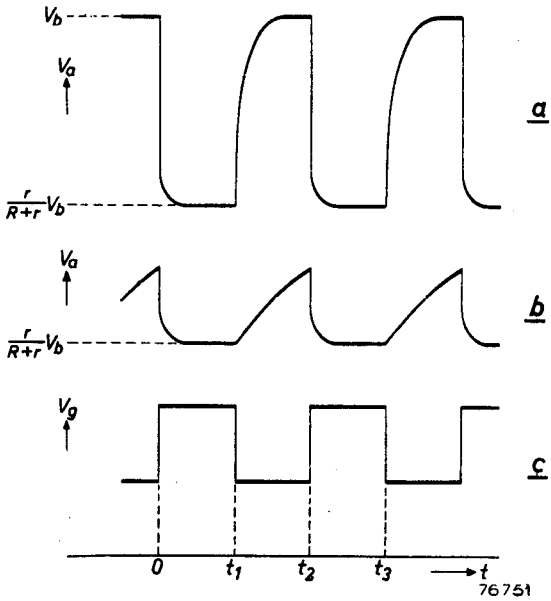

Fig. 2–4.
When the square-wave voltage represented in (*c*) is applied to the control grid of a tube with a load resistor incorporated in the anode lead, the anode voltage variations will assume the forms shown in (*a*) or (*b*).

originally sharp-edged transitions being rounded off, can be minimized by keeping the time constants of the switch as small as possible. This can be achieved by making the anode load resistance fairly small, thus improving the slope of both pulse flanks, but at the same time decreasing their amplitude. By decreasing the internal resistance of the tube, the slope of the negative-going flanks will be improved, whilst the amplitude will be increased. Finally, a reduction of the stray capacitance of the anode circuit will steepen both pulse flanks. The specific requirements

[1]) P. A. Neeteson, Flywheel Synchronization of Time-Base Generators, Electr. Appl. Bull. 12, pp 154 and 179, 1951, and P. A. Neeteson, Flywheel Synchronization of Saw-Tooth Generators, Monograph 2 of the series of books on Television Receiver Design, Philips' Techn. Library 1953.

for switching tubes are, therefore, low internal resistance and low output capacitance.

For generating pulse-shaped voltages in the anode circuit, the driving voltages applied to the control grid should be of the same nature. The obvious method of generating such voltages is to apply a regenerative process by feeding a fraction of the anode signal back to the control grid in antiphase. This is indeed the principle on which many types of relaxation oscillators, such as the multivibrator, are based (see the literature quoted in footnote [1]) page 17).

The multivibrator, which spontaneously generates pulse-shaped signals, is a *free-running* or *astable multivibrator*. This type of multivibrator has no stable state, but continuously changes from one quasi-stable position to the other. In one position, one of the two tubes which constitute the multivibrator is conducting (closed switch) and the other tube is cut off (open switch), whereas in the other position these conditions are reversed. Reversal takes place periodically with time intervals that depend on a time constant determined by the circuit elements of the coupling network between the tubes.

The *bi-stable multivibrator* or *flip-flop circuit* has two discrete, stable positions which can be changed only by applying a driving signal (trigger pulse) to the circuit.

An intermediate form is the *monostable* or *one-shot multivibrator*. This circuit has only one stable condition in which it always remains when no external signal is applied. By suitably applying a triggering signal, this type of multivibrator suddenly changes from its stable state to a quasi-stable state in which the functions of the conducting and non-conducting tubes are reversed. The circuit remains in this condition during a period of time which depends on a time constant of the coupling network between the tubes.

In several subsequent sections detailed investigation of the action of pulsed electron tubes will be given, and the three types of multivibrators just mentioned, being important and fundamental circuits in a lot of pulse devices, will also be discussed. Before proceeding, however, to the main purpose of the book, some elements will be given of the operational calculus, which is required for attainment of the results aimed for.

No strict mathematical derivations must be expected, the only purpose of the following sections being to give the reader an idea of the lines along which the final results have been attained. For those readers, acquainted with operational calculus methods, these sections will contain little new information and could be safely omitted.

5. SOME ELEMENTS OF THE OPERATIONAL CALCULUS

Basically, the operational calculus offers an elegant method of solving differential equations. When the response of a network to a unit-step function is known, it is possible to calculate its response to an input function of arbitrary form by considering this function as the sum of a sequence of small step functions. It was *Heaviside* who introduced the unit-step function as the basic discontinuity.

According to the procedure of the operational calculus, the operation d/dt, i.e. differentiation with respect to time, may be considered as an algebraic quantity, which is denoted, for example, by the operator p. A rigorous proof of the permissibility of this method can be given by means of the Laplace transform, which is beyond the scope of this section. However, in order to make the reader familiar with the operational calculus, the response of a few fundamental circuits to a unit-step function will first be derived in the classical way of solving differential equations, after which it will be shown with which operational expressions the results thus obtained correspond.

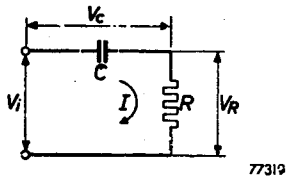

Fig. 1–5.
Simple RC network to which a step function V_i is applied.

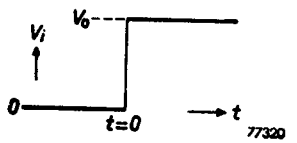

Fig. 2–5.
Step function applied to the circuit shown in fig. 1–5.

First the circuit shown in fig. 1.5 will be considered. The input voltage V_i will be taken to be a step function as depicted in fig. 2.5, i.e., the value of V_i suddenly jumps from zero to V_0 at the instant $t = 0$, and remains at V_0 for $t \geqq 0$.

By means of Kirchhoff's laws, the following relation between the current I flowing in the circuit and the input voltage V_i can easily be derived, giving:

$$\frac{1}{C} . I + R . \frac{dI}{dt} = \frac{dV_i}{dt} . \quad . \quad . \quad . \quad . \quad . \quad . \quad . \quad . \quad . \quad (1.5)$$

The solution of this differential equation is:

$$I = \frac{V_0}{R} \cdot e^{-t/RC} \quad \ldots\ldots\ldots\ldots \quad (2.5)$$

Expression (2.5) reveals that the current I flowing through the network, as a result of applying a unit-step voltage V_i (i.e. $V_0 = 1$ at the instant $t = 0$) is equal to:

$$I = \frac{1}{R} \cdot e^{-t/RC} U(t), \quad \ldots\ldots\ldots\ldots \quad (3.5)$$

in which $U(t)$ represents the unit-step function which is zero for $t < 0$ and unity for $t \geqq 0$.

According to the operational calculus, expression (1.5) may be rewritten as:

$$\left(\frac{1}{C} + Rp\right) I = pV_i \quad \ldots\ldots\ldots\ldots \quad (1a.5)$$

In other words: the relation between the two quantities I and V_i is defined by the operational expression:

$$\frac{I}{V_i} = \frac{p}{\frac{1}{C} + Rp} \quad \ldots\ldots\ldots\ldots \quad (1b.5)$$

It is also possible to express I in a symbolic, operational form, which gives:

$$I = \frac{1}{R}\left[\frac{p}{\frac{1}{RC} + p}\right] U(t) \quad \ldots\ldots\ldots\ldots \quad (4.5)$$

It can be seen from expressions (3.5) and (4.5) that the operator between square brackets, which operates on a unit-step function, can be translated into a time function, namely:

$$\left[\frac{p}{\frac{1}{RC} + p}\right] \equiv e^{-t/RC} \quad \ldots\ldots\ldots\ldots \quad (5.5)$$

The voltage V_C across the capacitance C is obviously given by:

$$V_C = \frac{\int_0^t I dt}{C},$$

or, from expressions (2.5) and (3.5):

$$V_C = (1 - e^{-t/RC})\, V_0 U(t) \quad \ldots\ldots\ldots \quad (6.5)$$

On the other hand, $I = C \cdot dV_C/dt$ and $I = (V_i - V_C)/R$, which gives:

$$\frac{1}{R} \cdot V_C + C \cdot \frac{dV_C}{dt} = \frac{1}{R} \cdot V_i,$$

whence:

$$\left(\frac{1}{RC} + p\right) V_C = \frac{1}{RC} \cdot V_i \quad \ldots\ldots\ldots \quad (7.5)$$

or:

$$V_C = \left[\frac{\frac{1}{RC}}{\frac{1}{RC} + p}\right] V_0 U(t) \quad \ldots\ldots\ldots \quad (7a.5)$$

It follows from expressions (6.5) and (7*a*.5) that the operator between square brackets can now be translated into the following time function:

$$\left[\frac{\frac{1}{RC}}{\frac{1}{RC} + p}\right] \equiv 1 - e^{-t/RC} \quad \ldots\ldots\ldots \quad (8.5)$$

In a generalized form, the relations (5.5) and (8.5) indicate that, when in any network the relation between a quantity to be investigated and an input function is given by the operational expressions $p/(a + p)$ or $a/(a + p)$, this quantity will be e^{-at} or $1 - e^{-at}$, respectively, if the input is a unit-step function occurring at the instant $t = 0$. (If this instant were $t = t_0$, the response of the network would be the same time function shifted in time over a period t_0. This may be taken into account by substituting $t - t_0$ for t in all time functions.)

In order to find the operational expression that links two electrical quantities in a network and which may have the dimension of an impedance or an admittance or may be a dimensionless transfer factor, it will be useful first to determine the a.c. impedance, admittance or transfer factor expressed in the conventional complex form with $j\omega$, which, in fact, originates from a time differentiation. Subsequently, $j\omega$ must be replaced by the operator p.

This is illustrated in the example given above. Referring again to fig. 1.5, the a.c. impedance of the network is:

$$Z(j\omega) = R + \frac{1}{j\omega C}, \quad \ldots\ldots\ldots \quad (9.5)$$

so that:

$$I = \frac{V_i}{R + \frac{1}{j\omega C}}, \quad \ldots\ldots\ldots \quad (10.5)$$

or:

$$\frac{I}{V_i} = \frac{1}{R + \frac{1}{j\omega C}}.$$

Substitution of $j\omega$ by p gives:

$$\frac{I}{V_i} = \frac{1}{R + \frac{1}{pC}},$$

or:

$$\frac{I}{V_i} = \frac{p}{\frac{1}{C} + Rp}. \quad \ldots\ldots\ldots \quad (11.5)$$

Expression (11.5) is identical to expression (1*b*.5).

If V_i is a sine function, the relation between V_C and V_i can be expressed as follows:

$$V_C = \frac{\frac{1}{j\omega C}}{R + \frac{1}{j\omega C}} \cdot V_i \quad \ldots\ldots \quad (12.5)$$

Substitution of $j\omega$ by p gives:

$$V_C = \frac{\frac{1}{pC}}{R + \frac{1}{pC}} \cdot V_i,$$

or:

$$V_C = \frac{\frac{1}{RC}}{p + \frac{1}{RC}} \cdot V_i \quad \ldots\ldots \quad (13.5)$$

which is identical to expression (7.5).

The two transformations:

$$\left[\frac{p}{a+p}\right] \equiv e^{-at} \quad \ldots\ldots \quad (14.5)$$

and

$$\left[\frac{a}{a+p}\right] \equiv 1 - e^{-at} \quad \ldots\ldots \quad (15.5)$$

are of particular importance, for it will often be possible to write a more complex operational expression as the sum of several expressions similar to expression (14.5) and (15.5), namely by splitting it up in partial fractions (Heaviside's Expansion Theorem) [2]).

This will be clarified by means of an example that will be met later, when the bi-stable multivibrator is dealt with. The value of the operational impedance between points a and b of the network shown in fig. 3.5 will now be investigated. For the sake of simplicity, the following notations will be introduced for the time constants:

$$\left.\begin{aligned} R_g C_g &= T_g \\ R_a C_a &= T_a \\ RC &= T \end{aligned}\right\}, \quad \ldots\ldots \quad (16.5)$$

and for the resistance ratios:

$$\left.\begin{aligned} \frac{R_g}{R_g + R + R_a} &= \varepsilon_g \\ \frac{R}{R_g + R + R_a} &= \varepsilon \\ \frac{R_a}{R_g + R + R_a} &= \varepsilon_a \end{aligned}\right\} \quad \ldots\ldots \quad (17.5)$$

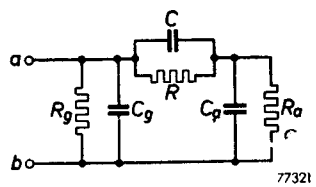

Fig. 3–5.
Network of a more complex nature to which a step function is applied.

[2]) Readers who are interested in this subject are referred to V. Bush, Operational Circuit Analysis, John Wiley and Sons Inc. New York, 1929, and T. H. Turney, Heaviside's Operational Calculus Made Easy, Chapman and Hall Ltd., London, 1946.

The final result of deriving the operational impedance [3]) is:

$$Z(p) = R_{eq} \cdot \frac{1 + Ap}{1 + Bp + Ep^2}, \quad \ldots\ldots \quad (18.5)$$

where R_{eq}, i.e. the d.c. impedance between points a and b, is given by:

$$R_{eq} = \frac{R_g (R + R_a)}{R_g + R + R_a},$$

whilst

$$A = \frac{RT_a + R_a T}{R + R_a}, \quad \ldots\ldots \quad (18a.5)$$

$$B = \varepsilon_g (T + T_a) + \varepsilon (T_g + T_a) + \varepsilon_a (T_g + T), \quad \ldots\ldots \quad (18b.5)$$

and

$$E = \varepsilon_g T T_a + \varepsilon T_g T_a + \varepsilon_a T_g T. \quad \ldots\ldots \quad (18c.5)$$

Expression (18.5) can now be split into two partial fractions by first writing the denominator as:

$$E\left(p^2 + \frac{B}{E} \cdot p + \frac{1}{E}\right) = E\,(p - p_1)\,(p - p_2), \quad \ldots\ldots \quad (19.5)$$

where p_1 and p_2 are the roots of the second order equation

$$p^2 + \frac{B}{E} \cdot p + \frac{1}{E} = 0.$$

Hence:

$$p_1 = -\frac{B}{2E} + \sqrt{\frac{B^2}{4E^2} - \frac{1}{E}}, \quad \ldots\ldots \quad (19a.5)$$

and

$$p_2 = -\frac{B}{2E} - \sqrt{\frac{B^2}{4E^2} - \frac{1}{E}} \quad \ldots\ldots \quad (19b.5)$$

Expression (18.5) thus becomes:

$$Z(p) = \frac{R_{eq}}{E} \cdot \frac{1 + Ap}{(p - p_1)\,(p - p_2)}.$$

[3]) It is stressed here that the operational impedance should not be confused with the conventional concept of impedance. (In fact, this also applies to a complex impedance in a.c. network theory.) An operational impedance is only an auxiliary quantity which proves to be most useful for investigating and solving transient phenomena. It links a voltage and a current in such a way that its dimension is that of an impedance.

This expression can be split into two partial fractions, namely:

$$Z(p) = \frac{R_{eq}}{E} \cdot \left(\frac{1 + Ap_1}{p_1 - p_2} \cdot \frac{1}{p - p_1} - \frac{1 + Ap_2}{p_1 - p_2} \cdot \frac{1}{p - p_2} \right) =$$

$$= R_{eq} \left\{ - \frac{1 + Ap_1}{Ep_1 \cdot (p_1 - p_2)} \cdot \frac{-p_1}{-p_1 + p} + \frac{1 + Ap_2}{Ep_1 (p_1 - p_2)} \cdot \frac{-p_2}{-p_2 + p} \right\} =$$

$$= R_{eq} \left(F_1 \cdot \frac{-p_1}{-p_1 + p} + F_2 \cdot \frac{-p_2}{-p_2 + p} \right) \quad \ldots\ldots\ldots\ldots \quad (20.5)$$

Applying the transformation according to expression (15.5) now gives for the response of the network shown in fig. 3.5 to a unit-step input current at the terminals a and b, a voltage across these terminals which is equal to:

$$V_{ab}[1] = R_{eq} \{ F_1 (1 - e^{p_1 t}) + F_2 (1 - e^{p_2 t}) \} \quad \ldots\ldots \quad (21.5)$$

The constants F_1 and F_2 can be combined and rearranged so that expression (21.5) becomes:

$$V_{ab}[1] = R_{eq} \{ 1 + Ke^{p_1 t} - (1 + K) e^{p_2 t} \}, \quad \ldots\ldots \quad (21a.5)$$

where:

$$K = \frac{p_2 (1 + Ap_1)}{p_1 - p_2} \quad \ldots\ldots\ldots\ldots \quad (22.5)$$

It will be clear that in the case of a current step of amplitude I, applied to terminals a and b, the resulting voltage across these terminals will be:

$$V_{ab}[I] = IR_{eq} \{ 1 + Ke^{p_1 t} - (1 + K) e^{p_2 t} \} \quad \ldots\ldots \quad (21b.5)$$

At the instant when the step occurs (for $t = 0$) this voltage is zero. This is obvious because a steep front can be considered as the commencement of a signal of very high frequency and between points a and b a chain of capacitances which smoothes this H.F. signal is present. After a very long time (theoretically an infinite time), the voltage V_{ab} becomes equal to IR_{eq}, i.e. the static condition is reached.

In the preceding comments the response of a network to a step function was considered. The determination of the response to an arbitrary time function is possible by applying the *superposition theorem*. This theorem can easily be made plausible with the aid of fig. 4.5.

In the most general case the input function $e(t)$ starts at the instant $t = 0$ with a step having an amplitude $e(0)$. It is assumed that for $t > 0$ the dependence of the input function on time can be represented

by the smooth curve $e\,(t)$. This curve is approximated by a sequence of small step functions separated in time by equal intervals $\Delta\lambda$ and

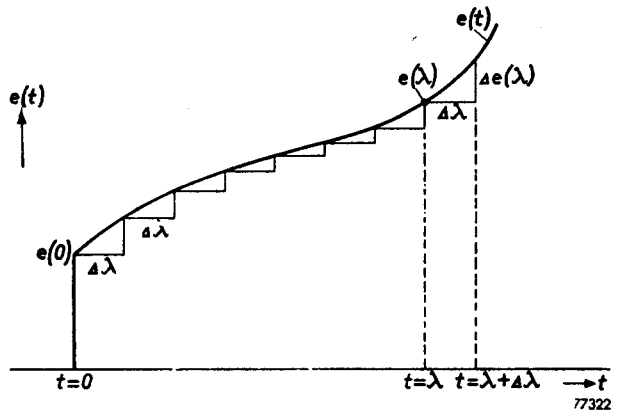

Fig. 4–5.
Approximation of an arbitrary time function by a sequence of small steps.

having an amplitude $\Delta e\,(\lambda)$. The response of the network to one of these elemental step functions is given by:

$$\Delta i\,(t) = \Delta e\,(\lambda)\,A\,(t - \lambda), \quad . \quad . \quad . \quad . \quad . \quad . \quad . \quad (23.5)$$

where $A\,(t)$ represents the response of the network to a unit step occurring at the instant $t = 0$.

The slope of the curve $e\,(t)$, i.e. $e'\,(t) = de\,(t)/dt$ at the point $t = \lambda$, is:

$$e'\,(\lambda) \approx \frac{\Delta e\,(\lambda)}{\Delta\lambda} \quad . \quad . \quad . \quad . \quad . \quad . \quad . \quad . \quad . \quad . \quad (24.5)$$

The smaller the time interval $\Delta\lambda$, the better will be the approximation. From expression (24.5):

$$\Delta e\,(\lambda) = e'\,(\lambda)\,\Delta\lambda \quad . \quad . \quad . \quad . \quad . \quad . \quad . \quad . \quad . \quad (24a.5)$$

Substituting expression (24*a*.5) in expression (23.5) gives:

$$\Delta i\,(t) = A\,(t - \lambda)\,e'\,(\lambda)\,\Delta\lambda \quad . \quad . \quad . \quad . \quad (25.5)$$

At the instant $t = \lambda$, the total response of the network to all preceding step functions will obviously be the superposition of the responses to the elemental step functions as represented by expression (25.5) and the initial step $e\,(0)$. Hence:

$$i\,(t) = e\,(0)\,A\,(t) + \sum_{\lambda=0}^{\lambda=t} A\,(t - \lambda)\,e'\,(\lambda)\,\Delta\lambda \quad . \quad . \quad . \quad . \quad . \quad (26.5)$$

The nearer $\Delta\lambda$ approximates to zero, the more exact will be the approximation of the time function $e(t)$ by the sequence of small step functions. The exact response of the network to the function $e(t)$ at the instant t is therefore given by:

$$i(t) = e(0)\, A(t) + \lim_{\Delta\lambda \to 0} \sum_{\lambda=0}^{\lambda=t} A(t-\lambda)\, e'(\lambda)\, \Delta\lambda, \quad . \quad . \quad . \qquad (27.5)$$

which, by definition, is the integral function:

$$i(t) = e(0)\, A(t) + \int_0^t A(t-\lambda)\, e'(\lambda)\, d\lambda, \quad . \quad . \quad . \quad . \quad . \qquad (28.5)$$

where $e(0)$ corresponds to $e(t)$ for $t = 0$, $A(t-\lambda)$ corresponds to $A(t)$, the variable t being replaced by $t-\lambda$, and $e'(\lambda)$ represents $de(t)/dt$ for $t = \lambda$.

When it is possible to express the input time function $e(t)$ in its related operational function $e(p)$, this rather cumbersome integrating process can be avoided. According to expression (8.5), a voltage

$$e(t) = e_0 (1 - e^{-t/T})$$

can, for example, be "transformed" into a p-function:

$$e(p) \equiv e_0 \cdot \frac{1}{1 + Tp}.$$

In an operational impedance $Z(p)$, this voltage will produce a current $I(p) = e(p)/Z(p)$. This expression must finally be transformed back into a time function $I(t) \equiv I(p)$.

In this section an attempt has been made to give a rough idea of the methods which are offered by the operational calculus to determine transient phenomena in a network. The principles outlined above have proved sufficient for calculating the problems related to pulsed electronic tubes. For a rigorous mathematical treatment and the derivation of the formulae used, reference is made to the literature quoted in the footnotes.

6. FUNDAMENTAL TREATMENT OF ELECTRON TUBES AS SWITCHING ELEMENTS

In section 4, for the sake of simplicity, no grid current was taken into consideration. In relatively few applications of the electron tube in pulse techniques this simplification will permit to obtain a good approximation of its real behaviour. In the majority of cases, where tubes are switched into the conducting state and remain for a longer or shorter period in this condition, grid current is certain to occur and play an important part in the transient phenomena caused by the switching action. This part may be a disturbing one, and therefore unwanted, or it may be useful, for instance by stabilizing the operating point of the tube (automatic grid current bias). Therefore, the effect of grid current cannot be neglected and it seems justified to start a general investigation of the behaviour of an electron tube in pulsed circuits by considering its input or control grid circuit.

6.1. THE GRID CIRCUIT

The ideal step-function, showing a discontinuity with infinitesimal slope, cannot be realized in practice, because of stray capacitances always present in switching and pulse generating circuits. In the foregoing sections, the influence of parallel stray capacitances of switches on the slope of pulse fronts has been discussed.

Generally, these pulse flanks will have a shape that can be described as an exponential function of time, or a sum of exponential time functions with different time constants. These pulse flanks traverse the grid-base of the electronic tube either starting at a high negative grid potential below the cut-off value and rising quickly up to values near to or even greater than zero, or starting at positive or zero grid potential and falling steeply to a value below cut-off potential.

In the first case the electronic tube suddenly starts conducting anode current as well as grid current (the switch is closed), in the latter case both anode- and grid current are abruptly cut off (the switch is opened). Both cases will be treated in the following sub-sections.

6.1.1. A POSITIVE-GOING STEEP CHANGE OF GRID POTENTIAL

The grid-to-cathode potential is assumed to have been at a constant value V_0 below cut-off for a sufficiently long period preceding the instant

$t = 0$ to ensure that any transients originating from possible former switching actions have completely died out. From the instant $t = 0$ onwards (so for $t \geqq 0$), the grid potential V_g changes with time according to an exponential function with a time constant $1/a$, starting at the initial value V_0 and tending to a final value V_1, that is assumed to be zero or positive ($V_1 \geqq 0$). The grid voltage change $V_g(t)$ can be represented analytically by the expression

$$V_g(t) = V_1 - (V_1 - V_0)\, e^{-at} \quad . \quad . \quad . \quad . \quad . \quad . \quad . \quad (1.6)$$

and graphically as depicted in fig. 1.6. Here, the dash-dot line represents the cut-off voltage level, indicated by E_c. As soon as the grid voltage $V_g(t)$ passes this level (at the instant $t = t_1$), anode current starts to flow in the tube and the switching action starts. The anode current increases at a rate determined by the rate of change of $V_g(t)$. With a triode, the anode voltage change also influences the anode current change, whereas it is well known that this influence is negligible with pentodes.

The reactions of the anode circuit of the tube, however, will be considered separately in later sections.

The rise in $V_g(t)$, however, will not continue until the value V_1, because of the influence of grid current, starting at a value of the grid potential near zero. Because of this grid current, the grid potential, ultimately attained, will be limited to a value not much different from zero. In this way, the anode current is restricted so that the tube can operate without being seriously damaged, as would otherwise occur. So the grid current action is a useful one here, as it stabilizes the anode current within certain limits. This will now be further investigated.

As a rule, grid current starts to flow as soon as the grid potential reaches a value of a few tenths of a volt negative with respect to cathode, and sharply rises when the grid potential passes zero and becomes positive. The general shape of the grid current – grid voltage characteristic is represented in fig. 2.6. The slope of this characteristic is a measure

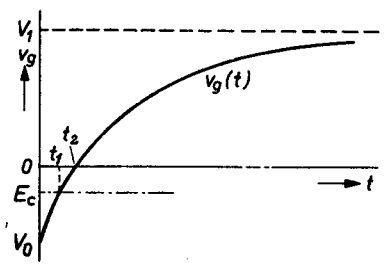

Fig. 1–6.

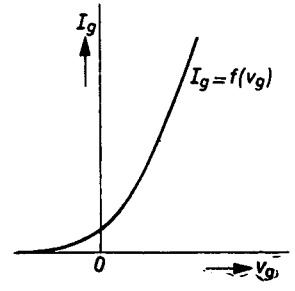

Fig. 2–6.

for the internal grid resistance. By approximating to the characteristic with simpler shaped curves, the influence of grid current on grid voltage and therefore on anode current and -voltage changes can be determined.

A first, rather rough, approximation is the assumption of an internal grid resistance zero as soon as the grid-to-cathode potential becomes zero or positive (see fig. 3.6), in other words: grid and cathode are short-circuited for values of $V_g \geqq 0$. This means that, from the instant $t = t_2$ onwards (see fig. 1.6), the function $V_g(t)$ remains at zero, as represented in fig. 4.6.

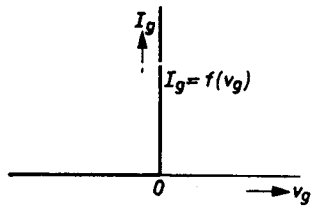

Fig. 3-6.

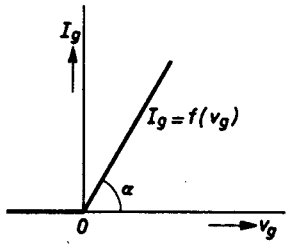

Fig. 5-6.

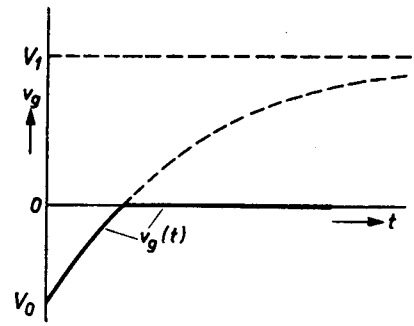

Fig. 4-6.

A better approximation is the assumption of a finite value of the internal grid resistance r_g for values of $V_g \geqq 0$, the grid current-grid voltage characteristic then being as represented in fig. 5.6, where

$$\cot \alpha = r_g, \text{ thus } V_g = r_g I_g \quad . \quad . \quad . \quad . \quad . \quad . \quad . \quad (2.6)$$

From the instant $t = t_2$ onwards (see fig. 1.6), the external grid circuit is shunted by a resistance r_g. The effect of this sudden switching of a resistance r_g in parallel with the external circuit Z_g originally present, can be calculated by assuming a voltage source $V_c(t)$ operating from the instant $t = t_2$ onwards, and superimposing its action on the grid to the initial grid voltage represented by expression (1.6). The value of $V_c(t)$ is to be taken equal to $V_g(t)$ from (1.6), but with opposite sign. This can be expressed by

$$V_c(t) = -V_g(t)\, U(t - t_2) \, , \quad . \quad . \quad . \quad . \quad . \quad . \quad . \quad (3.6)$$

where $U(t - t_2)$ represents a unit step function that is zero for $t < t_2$ and unity for $t \geqq t_2$.

Now $V_g(t)$ is defined by expression (1.6). For values of $t < t_1$, the grid voltage $V_g(t)$ is below the cut-off value (see fig. 1.6) and consequently no anode current flows. At the instant $t = t_1$, the tube starts conducting and the switching action commences. The grid voltage change from this instant onwards will be of particular interest, and therefore it is practical to introduce a new time scale τ, such that $\tau = t - t_1$, or, in other words, the instant t_1 is the zero point of the new time scale.

Then expression (1.6) is identical to the following:

$$V_g(\tau) = V_1 - (V_1 - E_c)\, e^{-a\tau}, \quad \ldots\ldots \quad (4.6)$$

where E_c is given by (see fig. 1.6):

$$E_c = V_1 - (V_1 - V_0)\, e^{-at_1} \quad \ldots\ldots\ldots \quad (5.6)$$

At the instant $t = t_2$, the grid voltage $V_g(t)$ is zero, that is in the τ scale at the instant $\tau = t_2 - t_1 = \tau_0$, which is defined by the condition:

$$V_g(\tau_0) = 0 = V_1 - (V_1 - E_c)\, e^{-a\tau_0} \quad \ldots\ldots\ldots \quad (6.6)$$

Substituting this relation into (4.6) gives

$$V_g(\tau) = V_1 - V_1\, e^{-a(\tau - \tau_0)}, \quad \ldots\ldots\ldots\ldots \quad (7.6)$$

which is valid only for $\tau \geqq \tau_0$.

Because the internal grid resistance r_g is present from the instant $\tau = \tau_0$ onwards, a second component must be added to $V_g(\tau)$, as given by (7.6). This second component can be calculated from the circuit diagram of fig. (6.6), where Z_g represents the total externally connected grid circuit impedance, whilst r_g is the internal grid-to-cathode resistance as determined by the characteristic of fig. (5.6).

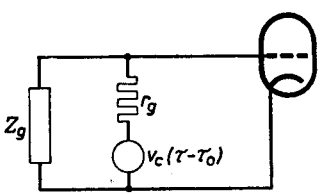

Fig. 6-6.

From (3.6) and (7.6) it follows that:

$$V_c(\tau - \tau_0) = -V_1\,(1 - e^{-a(\tau - \tau_0)}) \quad \ldots\ldots \quad (8.6)$$

In order to be able to calculate the extra grid voltage component caused by $V_c(\tau - \tau_0)$, the impedance Z_g must be further specified. The external grid circuit will be assumed to be as depicted in fig. 7.6, where V_i re-

presents a voltage source $V_i U(t)$, and V_1 a constant voltage source, both sources having zero internal impedance. V_i brings the grid at the

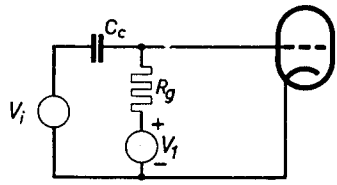

Fig. 7–6.

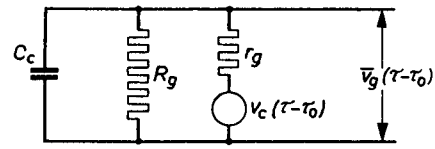

Fig. 8–6.

instant $t = 0$ to the initial value V_0, after which the change of the grid voltage is as given by expr. (1.6).

The grid-voltage component $V_g(\tau - \tau_0)$ due to $V_c(\tau - \tau_0)$ can now be calculated from the circuit diagram of fig. 8.6

As an example, the operational method, to be applied here, will be given completely.

The operational impedance Z_g of C_c and R_g in parallel is:

$$Z_g = \frac{R_g}{1 + R_g C_c p}.$$

The ratio of $\overline{V}_g$ to V_c is:

$$\frac{\overline{V}_g(\tau - \tau_0)}{V_c(\tau - \tau_0)} = \frac{Z_g}{Z_g + r_g} =$$

$$= \frac{R_g}{R_g + r_g} \frac{1}{1 + R_v C_c p}, \text{ where } R_v = \frac{r_g R_g}{R_g + r_g}. \quad . \quad . \quad . \quad . \quad (9.6)$$

$$\overline{V}_g(\tau - \tau_0) = \frac{R_g}{R_g + r_g} \frac{1}{1 + T_v p} [V_c(\tau - \tau_0)], \quad . \quad . \quad . \quad (10.6)$$

where

$$T_v = R_v C_c, \quad . \quad . \quad . \quad . \quad . \quad . \quad . \quad . \quad . \quad . \quad . \quad (11.6)$$

or, written symbolically:

$$\overline{V}_g(\tau - \tau_0) = A(p)\ [V_c(\tau - \tau_0)].$$

Now two ways of solving this problem can be followed. The first is to "translate" the p-function $A(p)$ into a time-function $A(t)$, and then to apply the superposition theorem, as expressed by (28.5).

The second way of solving the problem is to "translate" the time function $V_c(\tau - \tau_0)$ into a corresponding p-function.

Following the second method, we obtain for the corresponding p-

function of $V_c(\tau - \tau_0) = V_1(1 - e^{-a(\tau-\tau_0)})$, on introducing a new time variable $\lambda = \tau - \tau_0$, according to (15.5):

$$V_c(\lambda) = -V_1(1 - e^{-a\lambda}) \equiv -V_1 \frac{a}{a+p} \quad \ldots \quad (12.6)$$

Then expr. (10.6) becomes:

$$\overline{V}_g(\lambda) \equiv -V_1 \cdot \frac{R_g}{R_g + r_a} \cdot \frac{1}{1 + T_v p} \cdot \frac{a}{a+p}.$$

Splitting into partial fractions gives:

$$\overline{V}_g(\lambda) \equiv -V_1 \frac{R_g}{R_g + r_a} \cdot \frac{a}{1 - aT_v} \left[-T_v \frac{1}{1 + T_v p} + \frac{1}{a} \frac{1}{1 + \frac{1}{a}p} \right].$$

Converting back into a time function according to expr. (15.5) gives:

$$\overline{V}_g(\lambda) = -V_1 \frac{R_g}{R_g + r_g} \cdot \frac{a}{1 - aT_v} \left[-T_v \left(1 - e^{-\frac{\lambda}{T_v}}\right) + \frac{1}{a}(1 - e^{-a\lambda}) \right]$$

or:

$$\overline{V}_g(\tau - \tau_0) = -V_1 \frac{R_g}{R_g + r_g} \left[1 + \frac{aT_v}{1 - aT_v} e^{-\frac{\tau-\tau_0}{T_v}} - \frac{1}{1 - aT_v} e^{-a(\tau-\tau_0)} \right]. \quad (13.6)$$

Now, it will be clear from fig. 7.6 that the time constant $1/a$ with which the grid voltage changes exponentially from the value V_0 to the value V_1, must be equal to $R_g C_c$.

So:

$$a = \frac{1}{R_g C_c} \quad \ldots \quad (14.6)$$

Combined with (11.6), we see that:

$$aT_v = \frac{R_v}{R_g} = \frac{r_g}{R_g + r_g} \text{ (see 9.6)}. \quad \ldots \quad (15.6)$$

Substituting (15.6) into (13.6) gives:

$$\overline{V}_g(\tau - \tau_0) = -V_1 \left[\frac{R_g}{R_g + r_g} + \frac{r_g}{R_g + r_g} e^{-\frac{\tau-\tau_0}{T_v}} - e^{-a(\tau-\tau_0)} \right]. \quad (16.6)$$

This, finally, is the component that must be added to the grid voltage $V_g(\tau - \tau_0)$ that would have been present if no sudden change in the grid circuit occurred at the instant $\tau = \tau_0$. So the resulting grid voltage change $\overline{\overline{V}}_g(\tau - \tau_0)$ from $\tau = \tau_0$, or $t = t_2$ onwards is the sum of expressions (7.6) and (16.6):

$$\overline{\overline{V}}_g(\tau - \tau_0) = \frac{r_g}{R_g + r_g} V_1 \left(1 - e^{-\frac{\tau - \tau_0}{T_v}}\right) \quad \ldots\ldots (17.6)$$

Introducing (14.6) into (7.6) gives a value for the grid voltage change as follows:

$$V_g(\tau - \tau_0) = V_1 \left(1 - e^{-\frac{\tau - \tau_0}{R_g C_c}}\right) \quad \ldots\ldots (18.6)$$

This is the time function the grid voltage would assume when no change in the grid circuit would have appeared at the instant $\tau = \tau_0$. The effect of the sudden starting of grid current at the instant $\tau = \tau_0$ on the grid voltage is that from $\tau = \tau_0$ onwards expression (17.6) represents this voltage instead of (18.6). The grid voltage change is now an exponential function with a much smaller time constant $R_g C_c$ than it was for $\tau < \tau_0$. For this period, the time constant was $R_g C_c$. The ratio of the time constants is:

$$\frac{R_v}{R_g} \text{ or } \frac{r_g}{R_g + r_g} \text{ (see expr. 15.6).}$$

The final value that the grid voltage will attain is no longer V_1, but a much smaller amount, viz.

$$\frac{r_g}{R_g + r_g} V_1.$$

There is no discontinuity in the grid voltage value at $\tau = \tau_0$, as both the expressions (18.6) and (17.6) are zero at the instant $\tau = \tau_0$.

But there is also no discontinuity in the slope of the time function at this instant, which can be seen by differentiating both (18.6) and (17.6) with respect to time. These first derivatives are respectively:

$$\left[\frac{dV_g(\tau - \tau_0)}{d\tau}\right]_{\tau=\tau_0} = \frac{V_1}{R_g C_c}\left[e^{-\frac{\tau - \tau_0}{R_g C_c}}\right]_{\tau=\tau_0} = \frac{V_1}{R_g C_c}$$

$$\left[\frac{d\overline{\overline{V}}_g(\tau - \tau_0)}{d\tau}\right]_{\tau=\tau_0} = \frac{r_g}{R_g + r_g} \cdot V_1 \cdot \frac{1}{T_v}\left[e^{-\frac{\tau - \tau_0}{T_v}}\right]_{\tau=\tau_0} =$$

$$= \frac{r_g}{R_g + r_g} \frac{R_g + r_g}{r_g R_g C_c} V_1 = \frac{V_1}{R_g C_c}.$$

The influence of grid current, approximated by the foregoing method of calculation is graphically represented in fig. 9.6.

If the approximation as used above is considered unsatisfactory, a

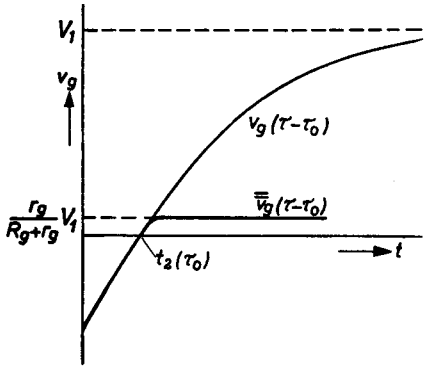

Fig. 9–6.

better one is the assumption of a grid current-grid voltage characteristic of the form given in fig. 10.6. This characteristic consists of two straight lines AB and BC with different slopes; it is a far better approximation of the $I_g - V_g$ characteristic in practice, as represented in fig. 2.6.

At the instant when $V_g(t)$ reaches a value V_{g1}, a discontinuity occurs similar to that previously discussed, which occurred at $V_g(t) = 0$ (see fig. 5.6).

The difference between the two cases will be fully discussed. For the moment it will be stated only that a resistance r_{g1}, a form of internal grid resistance, is shunted across the grid circuit as soon as $V_g(t)$ attains a value $\geqq V_{g1}$. This resistance is to be determined from the slope of the characteristic, viz. $r_{g1} = \cot \alpha_1$ (fig. 10.6). The effect of this discontinuity is that $V_g(t)$ tends exponentially with a smaller time constant $R_{v1}C_c$ instead of R_gC_c to a smaller final value V_{11} instead of V_1. The resistance R_{v1} is the resultant value of the parallel connection of R_g and r_{g1}.

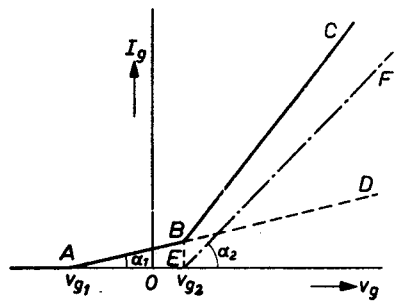

Fig. 10–6.

Again, at the instant when $V_g(t)$ reaches the value V_{g2}, another discontinuity appears, to be interpreted as shunting the grid circuit by another "internal grid resistance" $r_{g2} = \cot \alpha_2$, where α_2 is a measure of the slope of the characteristic line EF in fig. 10.6. The part BC of the $I_g - V_g$ characteristic is the superposition of the "resistance lines" AD and EF.

From the value V_{g2} onwards, the grid voltage tends exponentially with a still smaller time constant $R_{v2}C_c$ ($< R_{v1}C_c$) to a final voltage

value V_{12}, that is again smaller than V_{11} (R_{v2} is the resistance resulting from the shunting of R_{v1} by r_{g2}).

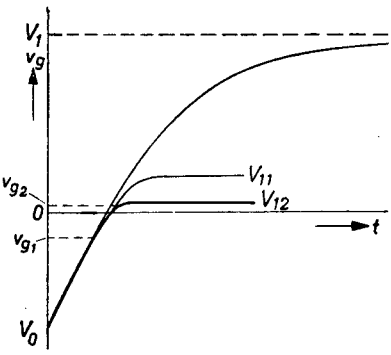

Fig. 11-6.

The change in grid voltage will then be roughly as indicated in fig. 11.6 by the strongly drawn curve.

The influence of the approximated $I_g - V_g$ characteristic of fig. 5.6 could be defined by the introduction of an auxiliary voltage source $V_c\,(t - t_2)$ as represented in the circuit of fig. 6.6. This will be discussed once more in a simple way with the sole purpose of being able to apply the same argument at a better date to derive methods of solving the problem of the discontinuities in a grid circuit as represented by the $I_g - V_g$ characteristic of fig. 10.6.

So, with the $I_g - V_g$ characteristic of fig. 5.6, grid current starts at the instant when V_g equals zero and tends to positive values. For $V_g < 0$, the circuit of fig. 7.6 is valid, and can be replaced by that of

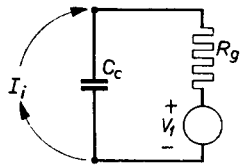

Fig. 12-6.

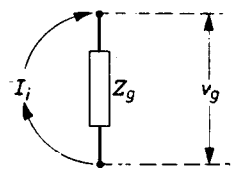

Fig. 13-6.

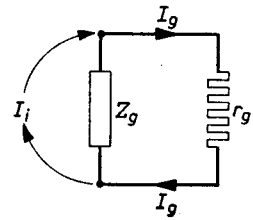

Fig. 14-6.

fig. 12.6, where $I_i = C_c p V_i$ ($p = d/dt$ = differentiation with respect to time). More general is the circuit of fig. 13.6, where Z_g may represent any impedance in the grid circuit. The grid voltage V_g is given by the relation:

$$V_g = Z_g I_i. \quad \ldots\ldots\ldots\ldots \quad (19.6)$$

As soon as $V_g \geqq 0$, a grid current I_g starts flowing in parallel with Z_g, and having a relation to the grid voltage, now indicated by $\overline{V}_g$, as follows:

$$I_g = \frac{\overline{V}_g}{r_g} \quad \ldots\ldots\ldots\ldots \quad (20.6)$$

This situation (for $\overline{V}_g \geqq 0$) can be represented by the circuit of fig. 14.6. Consequently, a current of $I_i - I_g$ now flows in Z_g, instead of

the whole of I_i, as was the case for $V_g < 0$. The voltage across Z_g will then be:

$$V_{zg} = Z_g (I_i - I_g) \quad \ldots\ldots\ldots\ldots \quad (21.6)$$

Introducing the value of I_g from (20.6) and considering that:

$$V_{zg} = \overline{V}_g; \text{ gives } \overline{V}_g = Z_g I_i - \frac{Z_g}{r_g} \overline{V}_g$$

or:

$$\overline{V}_g = \frac{r_g}{r_g + Z_g} Z_g I_i \quad \ldots\ldots\ldots\ldots \quad (22.6)$$

Substituting (19.6) gives:

$$\overline{V}_g = \frac{r_g}{r_g + Z_g} V_g \quad \ldots\ldots\ldots\ldots \quad (23.6)$$

This expression can also be written:

$$\overline{V}_g = V_g - \frac{Z_g}{r_g + Z_g} V_g \quad \ldots\ldots\ldots\ldots \quad (24.6)$$

For better understanding, the meaning of V_g and $\overline{V}_g$ is once again given here: V_g is the grid voltage as it would be without grid current starting at a value $V_g \geqq 0$, whilst $\overline{V}_g$ is the actual value of the grid voltage from the instant when grid current started.

Expression (24.6) is the superposition of V_g and a component that originates from a voltage source $V_c = -V_g$ introduced into the circuit in the way depicted in fig. 15.6. Comparing with fig. 6.6 shows that these figures are identical.

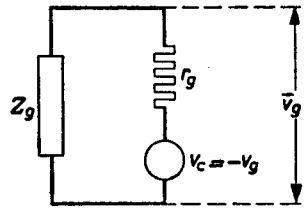

Fig. 15–6.

The same reasoning will now be applied to the case where the $I_g - V_g$ characteristic has a shape as depicted in fig. 10.6. As soon as V_g reaches a value V_{g1} (and not zero!), grid current starts according to the characteristic AD from fig. 10.6.

A current I_g depending on V_g in the following way

$$I_g = \frac{V_g - V_{g1}}{r_{g1}} \quad \ldots\ldots\ldots\ldots \quad (25.6)$$

flows parallel to Z_g.

The current through Z_g is no longer I_i, but less, viz. $I_i - I_g$, giving a voltage across Z_g:

$$V_{zg} = \overline{V}_g = Z_g (I_i - I_g) \quad \ldots\ldots\ldots\ldots \quad (26.6)$$

Substituting I_g from expr. (25.6) gives:

$$\overline{V}_g = Z_g I_i - \frac{Z_g}{r_{g1}} (\overline{V}_g - V_{g1}) , \quad . \quad . \quad . \quad . \quad . \quad . \quad (27.6)$$

or:

$$\overline{V}_g = \frac{r_{g1}}{r_{g1} + Z_g} \left[Z_g I_i + \frac{Z_g}{r_{g1}} V_{g1} \right] \quad . \quad . \quad . \quad . \quad . \quad . \quad (28.6)$$

Remembering now that for $V_g < V_{g1}$ the whole input current I_i passed through Z_g, giving a grid voltage: $V_g = Z_g I_i$, and that this would be maintained if no grid current I_g started, expression (28.6) can be written:

$$\overline{V}_g = \frac{r_{g1}}{r_{g1} + Z_g} V_g + \frac{Z_g}{r_{g1} + Z_g} V_{g1}, \quad . \quad . \quad . \quad . \quad . \quad . \quad (29.6)$$

or:

$$\overline{V}_g = V_g - \frac{Z_g}{r_{g1} + Z_g} (V_g - V_{g1}) \quad . \quad . \quad . \quad . \quad . \quad . \quad (30.6)$$

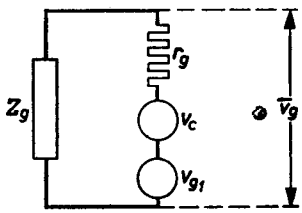

Fig. 16-6.

On comparing this result with expression (24.6), it will be seen that an important difference exists. The auxiliary voltage source to be introduced to account for the sudden starting of grid current is not equal to $-V_g$, but to $-(V_g - V_{g1})$. This is represented in fig. 16.6, where $V_c = -V_g$. If the constant voltage source V_{g1} were omitted, then fig. 16.6 could be considered as the auxiliary circuit necessary for calculating the response of the grid circuit to the sudden switching of a real resistance r_{g1} in parallel to Z_g at the instant when V_g reaches the value V_{g1}. The time function $V_c(t)$, in connection with a given function of $V_g(t)$, is represented in fig. 17.6. $V_c(t)$ shows an initial voltage step $-V_{g1}$. The combination $-(V_g - V_{g1})$, however, has an initial value zero. In fig. (18.6) this combination is represented by the function V_{c1}.

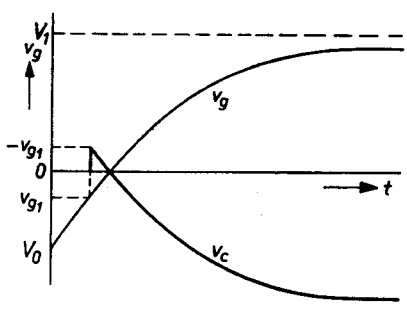

Fig. 17-6.

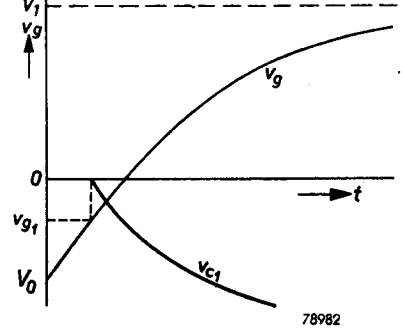

Fig. 18-6.

It is now possible to determine the response of the grid circuit to a grid-current characteristic according to fig. 10.6. It will be assumed that V_g reaches the value V_{g1} at the instant $t = t_1$ and the value V_{g2} at the instant $t = t_2$. For $0 \leqq t \leqq t_1$, equation (1.6) determines the grid voltage change. Introducing the instant $t = t_0$ when $V_g(t) = E_c$, the cut-off voltage, as the zero-point of a new time scale $\tau = t - t_0$, changes equation 1.6 into:

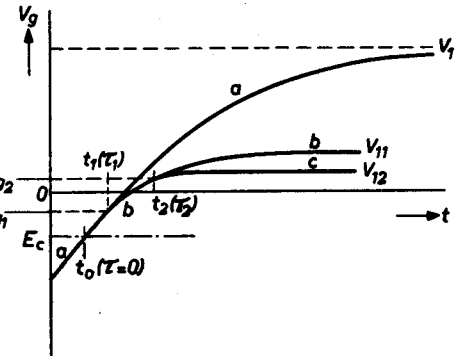

Fig. 19–6.

$$V_g(\tau) = V_1 - (V_1 - E_c) \cdot e^{-a\tau}. \quad (31.6)$$

For a survey of the time scale t and τ, fig. 19.6 has been given.

For $t = t_1$ or $\tau = \tau_1 = t_1 - t_0$:

$$V_g(\tau_1) = V_{g1} = V_1 - (V_1 - E_c)\, e^{-a\tau_1}. \quad (32.6)$$

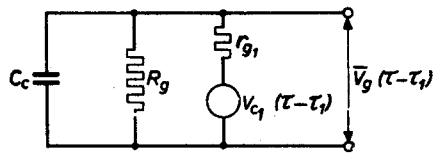

Fig. 20–6.

From $t = t_1$ onwards, the grid voltage can be supposed to contain two components, viz. $V_g(\tau)$, as given by (31.6), and the grid voltage $V_g(\tau - \tau_1)$ due to a voltage source $V_{c1}(\tau - \tau_1) = V_{g1} - V_g(\tau)$ as represented in fig. (20.6).

$$V_{c1}(\tau - \tau_1) = V_1 - (V_1 - E_c)\, e^{-a\tau_1} - V_1 + (V_1 - E_c)\, e^{-a\tau} =$$
$$= -(V_1 - E_c)\, e^{-a\tau_1} \{1 - e^{-a(\tau - \tau_1)}\}.$$

Substituting:

$$V_{g1} - V_1 = -(V_1 - E_c)\, e^{-a\tau_1}. \quad (32.6)$$

from (32.6) gives

$$V_{c1}(\tau - \tau_1) = -(V_1 - V_{g1}) \{1 - e^{-a(\tau - \tau_1)}\} \quad (33.6)$$

Indicating the total grid voltage between the instants t_1 and t_2 by $V_g^*(\tau - \tau_1)$, this voltage is given by:

$$V_g^*(\tau - \tau_1) = V_g(\tau) + \overline{V}_g(\tau - \tau_1).$$

$V_g(\tau - \tau_1)$ can be calculated by the same operational methods as given in the previous case. Only the final result will be given here:

$$V_g^*(\tau - \tau_1) = V_1 - (V_1 - V_{g1}) \left[\frac{R_g}{R_g + r_{g1}} + \frac{r_{g1}}{R_g + r_{g1}}\, e^{-\frac{\tau - \tau_1}{R_{g_1} C_c}} \right], \quad (34.6)$$

where:

$$R_{v1} = \frac{r_{g1} R_g}{R_g + r_{g1}} \quad \ldots\ldots\ldots\ldots \quad (35.6)$$

If $V_{g1} = 0$, expression (34.6) is identical to expression (17.6), as should be expected.

For large values of τ, expr. (34.6) tends to the final value:

$$V_{11} = \frac{r_{g1}}{R_g + r_{g4}} V_1 + \frac{R_g}{R_g + r_{g4}} V_{g1} \quad \ldots\ldots \quad (36.6)$$

(compare fig. 11.6).

At the instant $t = t_2$ or $\tau = \tau_2 = \tau_2 - t_0$, the grid voltage $V_g^* (\tau - \tau_1)$ reaches the value V_{g2} and another discontinuity appears, because of the suddenly increasing slope of the I_g - V_g characteristic (see fig. 10.6).

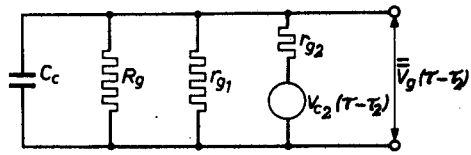

Fig. 21-6.

An extra voltage source $V_{c2} (\tau - \tau_2) = -V_g^* (\tau - \tau_1) + V_{g2}$ (see fig. 21.6) causes a component $\overline{\overline{V}}_g (\tau - \tau_2)$ across the grid circuit, that must be added to the voltage originally present, $V_g^* (\tau - \tau_1)$, continued for $\tau > \tau_2$, as if no change had taken place. The final result of operational calculations is that the total grid voltage V_g^{**} for $t > t_2$ or $\tau > \tau_2$ is

$$V_g^{**} (\tau - \tau_2) = \left(\frac{r_{g1}}{R_g + r_{g1}} V_1 + \frac{R_g}{R_g + r_{g1}} V_{g1} \right) \frac{r_{g2}}{R_{v1} + r_{g2}} +$$

$$+ V_{g2} \frac{R_{v1}}{R_{v1} + rg_2} - \left(\frac{r_{g1}}{R_g + r_{g1}} V_1 + \frac{R_g}{R_g + r_{g1}} V_{g1} - \right.$$

$$\left. - V_{g2} \right) \frac{r_{g2}}{R_{v1} + r_{g2}} e^{-\frac{\tau - \tau_2}{R_{v2} C_c}}, \quad \ldots\ldots\ldots\ldots\ldots\ldots \quad (37.6)$$

where:

$$R_{v2} = \frac{R_{v1} r_{g2}}{R_{v1} + r_{g2}} \quad \ldots\ldots\ldots\ldots \quad (38.6)$$

r_{g1} and r_{g2} are given by

$r_{g1} = \cot \alpha_1$; $r_{g2} = \cot \alpha_2$ (see fig. 10.6)

R_{v1} is given by expr. (35.6).

For $\tau \to \infty$, expr. 37.6 tends to a final value

$$V_{12} = \left(\frac{r_{g1}}{R_g + r_{g1}} V_1 + \frac{R_g}{R_g + r_{g1}} V_{g1}\right) \frac{r_{g2}}{R_{v1} + r_{g2}} + V_{g2} \frac{R_{v1}}{R_{v1} + r_{g2}} \qquad (39.6)$$

(compare fig. 11.6).

If $\alpha_2 = 0$, or $r_{g2} = \infty$, in other words: if no second discontinuity would appear at $V_g = V_{g2}$ (see fig. 10.6), then expression (37.6) changes into expr. (34.6) as should be expected. This will be shown.

Expression (34.6) can be written:

$$V_g^* (\tau - \tau_1) = \frac{r_{g1}}{R_g + r_{g1}} V_1 +$$

$$+ \frac{R_g}{R_g + r_{g1}} V_{g1} - (V_1 - V_{g1}) \frac{r_{g1}}{R_g + r_{g1}} e^{-\frac{\tau - \tau_0}{R_{v1} C_c}} \quad . \quad . \quad . \quad . \quad . \quad (40.6)$$

For $\tau = \tau_2$, this will be:

$$V_{g2} = \frac{r_{g1}}{R_g + r_{g1}} V_1 + \frac{R_g}{R_g + r_{g1}} V_{g1} - (V_1 - V_{g1}) \frac{r_{g1}}{R_g + r_{g1}} e^{-\frac{\tau_2 - \tau_1}{R_{v1} C_c}} \quad . \quad . \quad (41.6)$$

Now, for $r_{g2} = \infty$, $R_{v2} = R_{v1}$, and (37.6) becomes:

$$V_g^{**} = \left(\frac{r_{g1}}{R_g + r_{g1}} V_1 + \frac{R_g}{R_g + r_{g1}} V_{g1}\right)\left(1 - e^{-\frac{\tau - \tau_2}{R_{v1} C_c}}\right) + V_{g2} e^{-\frac{\tau - \tau_2}{R_{v1} C_c}} \quad . \quad . \quad (42.6)$$

Substituting (41.6) gives:

$$V_g^{**} = \frac{r_{g1}}{R_g + r_{g1}} V_1 + \frac{R_g}{R_g + r_{g1}} V_{g1} - (V_1 - V_{g1}) \frac{r_{g1}}{R_g + r_{g1}} e^{\frac{\tau - \tau_1}{R_{v1} C_c}} \quad . \quad . \quad (43.6)$$

This is identical to (34.6).

For a clear survey, a review of the formulae will be given.

During the time interval $0 \leqq t \leqq t_1$, the grid voltage is:

$$V_g (t) = V_1 - (V_1 - V_0) e^{-\frac{t}{R_g C_c}} \quad . \quad . \quad . \quad . \quad . \quad . \quad . \quad . \quad (1.6)$$

This function is represented by curve $a - a$ in fig. 19.6.

During the time interval $t_1 \leqq t \leqq t_2$, the grid voltage is:

$$V_g^* (t) = V_1 - \left(V_1 - V_{g1}\right)\left(\frac{R_g}{R_g + r_{g1}} + \frac{r_{g1}}{R_g + r_{g1}} e^{-\frac{t - t_1}{R_{v1} C_c}}\right) \quad . \quad . \quad (34.6)$$

This function is represented by curve $b - b$ in fig. 19.6.

Its validity may be checked by calculating the value at the instant $t = t_1$. Substituting $t = t_1$ in (34.6) gives $V_g^*(t_1) = V_{g1}$, as should be expected.

For times $t \geqq t_2$, the grid voltage is:

$$V_g^{**}(t) = \left(\frac{r_{g1}}{R_g + r_{g1}} V_1 + \frac{R_g}{R_g + r_{g1}} V_{g1}\right) \frac{r_{g2}}{R_{v1} + r_{g2}} + V_{g2} \frac{R_{v1}}{R_{v1} + r_{g2}} -$$

$$- \left(\frac{r_{g1}}{R_g + r_{g1}} V_1 + \frac{R_g}{R_g + r_{g1}} V_{g1} - V_{g2}\right) \frac{r_{g2}}{R_{v1} + r_{g2}} e^{-\frac{t - t_2}{R_{v1} C_c}} \quad . \quad . \quad . \quad (37.6)$$

This function is represented by curve $c - c$ in fig. 19.6.

A phenomenon often observed in positive-going steep voltage waveforms applied to the grid of an electron tube is the overshoot, which appears as a short "pip" at the top of the positive-going wavefront (see fig. 22.6). The occurrence of overshoot depends upon the shape of the grid current – grid voltage characteristic and on the initially applied voltage waveform at the grid.

The first relationship will be clear if the case of a characteristic according to fig. (3.6) is considered. Then the grid-to-cathode internal resistance becomes zero as soon as the grid voltage reaches zero, and

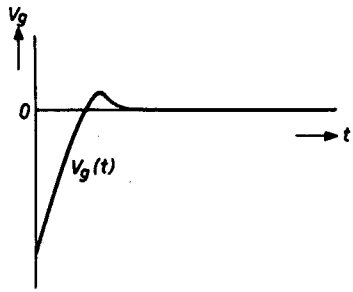

Fig. 22–6.

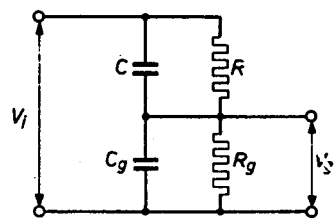

Fig. 23–6.

no further increase in grid-to-cathode voltage is possible (compare fig. 4.6). Thus no overshoot will be possible. If the I_g - V_g characteristic has the shape of fig. 5.6, however, then overshoot may occur, particularly as the angle α becomes smaller, i.e. the internal grid resistance r_g higher.

Furthermore, the occurrence of overshoot will depend on the waveform of the grid voltage as it would be when no discontinuity in the form of grid current appears. In the earlier case of input grid voltage, as represented by fig. (19.6) curve $a - a$ and by expression (1.6), no overshoot is originally present, and neither waveforms influenced

by grid current show overshoot. (Compare fully drawn curve of fig. 9.6 and expr. (17.6), curves $b - b$ and $c - c$ of fig. 19.6 and expressions (34.6) and (37.6)).

It will be of interest to deal with a case of input voltage waveform that shows overshoot, and to investigate again the influence of grid current. Consider the circuit of fig. (23.6), where R_g represents a grid leak resistance, C_g a grid stray capacitance, and an input voltage V_i is applied to the grid via a resistance R and a capacitance C in parallel.

If V_i has the shape of a voltage step of amplitude $+V$, occurring at the instant $t = 0$, what will be the grid voltage change from the instant $t = 0$ onwards?

Mathematically, V_i is defined as follows:

$$\left.\begin{aligned} V_i &= 0 \quad \text{for } t < 0 \\ V_i &= V \quad \text{for } t \leqslant 0 \end{aligned}\right\} \text{ or } V_i = VU(t), \quad \ldots\ldots \quad (44.6)$$

where $U(t)$ represents the unit voltage step. To start with, no discontinuities are assumed to occur. It can be seen immediately that the voltage step is attenuated by the capacitive voltage divider, formed by C and C_g, so that a fraction $\frac{C}{C + C_g}$ of the total step V appears across the output leads. In other words: at the instant $t = 0$ the voltage $V_g(t)$ is

$$V_g(0) = \frac{C}{C + C_g} V \quad \ldots\ldots\ldots \quad (45.6)$$

But immediately after the application of the voltage step, a distribution of the electric charge on the capacitances starts in such a way that finally a steady voltage of value $\frac{R_g}{R + R_g} V$ will be present at the output leads. In other words: for infinite time, $V_g(t)$ will be:

$$V_g(\infty) = \frac{R_g}{R + R_g} V \quad \ldots\ldots\ldots \quad (46.6)$$

Now, if:

$$\frac{C}{C + C_g} > \frac{R_g}{R + R_g}, \quad \ldots\ldots\ldots\ldots \quad (47.6)$$

or, virtually, the same condition, if:

$$CR < C_g R_g, \quad \ldots\ldots\ldots\ldots \quad (48.6)$$

then the voltage $V_g(t)$ will show overshoot, as depicted in fig. (24.6). If:

$$\frac{C}{C + C_g} = \frac{R_g}{R + R_g} \quad \ldots\ldots\ldots \quad (49.6)$$

or:

$$CR = C_g R_g \,, \quad \ldots\ldots\ldots \quad (50.6)$$

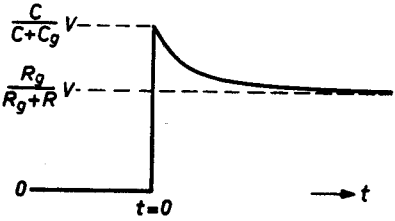

Fig. 24–6.

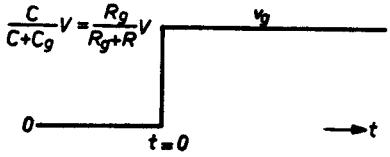

Fig. 25–6.

then the grid voltage $V_g(t)$ is an attenuated copy of the input voltage waveform, that is to say:

$$V_g(t) = \frac{C}{C + C_g} VU(t). \quad \ldots\ldots\ldots \quad (51.6)$$

or:

$$V_g(t) = \frac{R_g}{R + R_g} VU(t) \quad \ldots\ldots\ldots \quad (52.6)$$

(see fig. 25.6).
If:

$$\frac{C}{C + C_g} < \frac{R_g}{R + R_g} \,, \quad \ldots\ldots\ldots \quad (53.6)$$

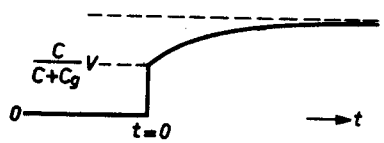

Fig. 26–6.

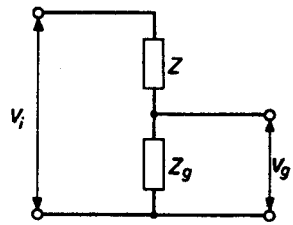

Fig. 27–6.

or

$$CR < C_g R_g \quad \ldots\ldots\ldots \quad (54.6)$$

then the initial value of $V_g(t)$ is smaller than the final value, and the term "undershoot" could be applied. This case is depicted in fig. (26.6). These results will be derived by operational calculus. The circuit of fig. (23.6) is represented by that of fig. (27.6), where:

$$\frac{1}{Z} = \frac{1}{R} + pC \quad \ldots\ldots\ldots\ldots \quad (55.6)$$

$$\frac{1}{Z_g} = \frac{1}{R_g} + pC_g \quad \ldots\ldots\ldots\ldots \quad (56.6)$$

It can be seen that:

$$V_g(t) = \frac{Z_g}{Z + Z_g} V_i$$

or:

$$V_g(t) = \frac{1/Z}{1/Z_g + 1/Z} V_i \quad \ldots\ldots\ldots \quad (56.6)$$

or:

$$V_g(t) = \frac{1/R + pC}{1/R + 1/R_g + p(C + C_g)} V_i \quad \ldots\ldots \quad (58.6)$$

or:

$$V_g(t) = \frac{R_g}{R + R_g} \frac{1 + RCp}{1 + R_v(C + C_g)p} V_i \quad \ldots\ldots \quad (59.6)$$

where:

$$R_v = \frac{RR_g}{R + R_g} \quad \ldots\ldots\ldots\ldots \quad (60.6)$$

Substituting

$$T = RC \quad \ldots\ldots\ldots\ldots \quad (61.6)$$

and

$$T_v = R_v(C + C_g) \quad \ldots\ldots\ldots\ldots \quad (62.6)$$

gives

$$V_g(t) = \frac{R_g}{R + R_g} \frac{1 + Tp}{1 + T_v p} V_i \quad \ldots\ldots\ldots \quad (63.6)$$

or:

$$V_g(t) = \frac{R_g}{R + R_g} \left[1 + \frac{(T - T_v)p}{1 + T_v p}\right] V_i \quad \ldots\ldots\ldots \quad (64.6)$$

With expression (44.6) this gives:

$$V_g(t) = \frac{R_g}{R + R_g} V \left[U(t) + \frac{T - T_v}{T_v} e^{-\frac{t}{T_v}} \right] \quad \ldots\ldots \quad (65.6)$$

(see expr. (14.5))

From (61.6) and (62.6) it can be derived that:

$$\frac{T - T_v}{T_v} = \frac{RC - R_g C_g}{R_g (C + C_g)} \quad \ldots\ldots\ldots \quad (66.6)$$

so:

$$V_g(t) = \frac{R_g}{R + R_g} V \left[U(t) + \frac{RC - R_g C_g}{R_g (C + C_g)} e^{-\frac{t}{T_v}} \right] \quad \ldots \quad (67.6)$$

From this expression it follows immediately that the final value of $V_g(t)$ will be:

$$V_g(\infty) = \frac{R_g}{R + R_g} V \text{ (compare with (46.6)).}$$

Furthermore, for $RC = R_g C_g$ there will be no overshoot, as $V_g(t)$ in that case is:

$$V_g(t) = \frac{R_g}{R + R_g} V \,.\, U(t).$$

This is the attenuated input voltage step, as already mentioned before. If $RC > R_g C_g$, the initial value of $V_g(t)$ will be larger than the final value, and then overshoot occurs.

If $RC < R_g C_g$, $V_g(0)$ will be smaller than $V_g(\infty)$:

$$V_g(0) = \frac{R_g}{R + R_g} V \left[1 + \frac{RC - R_g C_g}{R_g (C + C_g)} \right],$$

or:

$$V_g(0) = \frac{C}{C + C_g} V.$$

Compare these results with figs (24, 25 and 26.6).

From expression (64.6) it follows that for $T = T_v$, or, what is the same condition, $RC = R_g C_g$, the output voltage $V_g(t)$ of the network

of fig. (23.6) is a true, though attenuated copy of the input voltage, no matter what is the shape of the latter:

$$V_g(t) = \frac{R_g}{R + R_g} V_i, \quad \ldots\ldots\ldots \quad (68.6)$$

if:

$$CR = C_g R_g.$$

The time constant determining the exponential function with which the voltage $V_g(t)$ changes from the initial step to its final value (see figs. 24.6 and 26.6), is given by:

$$T_v = R_v (C + C_g), \quad \ldots\ldots\ldots \quad (62.6)$$

and with (60.6):

$$T_v = \frac{RR_g}{R + R_g} (C + C_g) \quad \ldots\ldots\ldots \quad (69.6)$$

This is the product of the resultant resistance of R and R_g in parallel and the resultant capacitance of C and C_g in parallel.

Now, the influence of grid current will be investigated, working with a characteristic as represented by fig. 5.6. So, as soon as the grid voltage V_g is $\geqq 0$, a resistance r_g must be incorporated in parallel to the grid circuit. In the circuit of fig. 23.6 a negative constant bias voltage V_0 in series with R_g is assumed to be present, of a value sufficiently large to keep the grid voltage below the cut-off value E_c for all times < 0 (see fig. 28.6). At the instant $t = 0$, the input voltage V_i suddenly jumps from the value V_1 to the value V_2, which can be interpreted by assuming a voltage step

$$V \,.\, U(t) = (V_2 - V_1)\, U(t) \quad (70.6)$$

to occur.

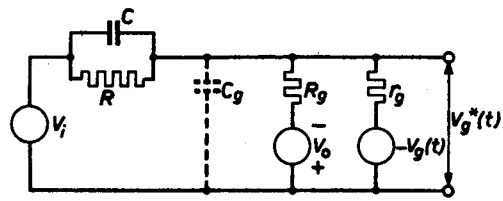

Fig. 28–6.

This voltage step is assumed to have such a value as to apply a reduced voltage step

$$\frac{C}{C + C_g} V$$

to the grid of the tube, of sufficient amplitude to make the grid voltage immediately > 0.

Thus, at the same instant $t = 0$ when the voltage step occurs, the

internal grid resistance r_g is switched in parallel with R_g and the resultant grid voltage $V_g^*(t)$ can be calculated as the sum of two components, viz. the grid voltage $V_g(t)$ as it would be when no grid current appeared, and the response $V_g(t)$ of the grid circuit to a voltage source $-V_g(t)$ in series with r_g (see fig. 28.6).

The initial condition of the grid circuit is then:

$$V_i = V_1 \text{ for } t < 0. \quad \ldots\ldots\ldots\ldots \quad (71.6)$$

and thus:

$$V_g = V_{g0} = \frac{R_g}{R + R_g} V_1 - \frac{R}{R + R_g} V_0 \quad \ldots\ldots \quad (72.6)$$

V_{g0} is negative to a value below cut-off.

At $t = 0$, a step

$$V_i = V \,.\, U(t) = (V_2 - V_1) \,.\, U(t)$$

occurs and for

$$t \geqq 0, \quad V_i = V_2.$$

$V_g(t)$ is the sum of the steady state component, given by (72.6) and the transient component, given by (67.6)

$$V_g(t) = V_{g0} + \frac{R_g}{R + R_g} V \left[1 + \frac{RC - R_g C_g}{R_g (C + C_g)} e^{-\frac{t}{T_v}}\right] \quad \ldots \quad (73.6)$$

The effect of the voltage source $-V_g(t)$ in the circuit of fig. (28.6) at the grid is:

$$V_g(t) = \frac{R_v}{R_v + r_g} \frac{1}{1 + T_{v1} p} \left[-V_g(t)\right] \quad \ldots\ldots \quad (74.6)$$

The result of calculating this by operational methods and adding it to $V_g(t)$ is:

$$V_g^*(t) = V_g(t) + V_g(t) =$$
$$= \frac{r_g}{R_v + r_g} \left[V_{g0} + \frac{R_g}{R + R_g}\right] V \left(1 + \frac{RC - R_g C_g}{R_g (C + C_g)} e^{-\frac{t}{T_{v1}}}\right), \quad \ldots \quad (75.6)$$

where:

$$T_{v1} = \frac{r_g}{R_v + r_g} T_v \quad \ldots\ldots\ldots\ldots \quad (76.6)$$

Comparing $V_g^*(t)$ with $V_g(t)$, the same remarks can be made as when expressions (17.6) and (18.6) were compared to one another, viz. the effect of the sudden starting of grid current is that the grid voltage tends to a smaller final value with a smaller time constant when grid current appears, than would be the case without this discontinuity occurring.

As can be seen from expr. (75.6), the conditions whether or not overshoot will occur are the same as for expr. (73.6).

6.1.2. A NEGATIVE-GOING STEEP CHANGE OF GRID POTENTIAL

In the foregoing section the initial state of the grid was with a grid-potential below cut-off value. Then a steep positive-going voltage transferred the grid into the conducting state. Now, the other case will be considered, the grid being conducting and then a negative-going voltage being applied. The change of grid voltage will be investigated.

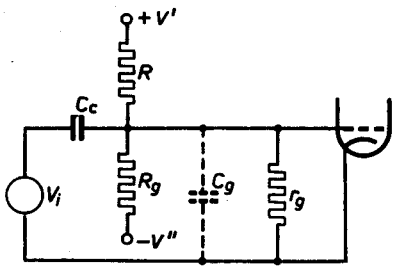

Fig. 29–6.

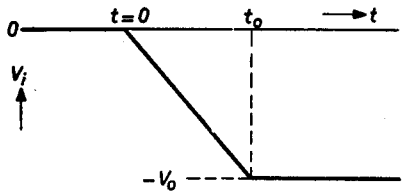

Fig. 30–6.

Referring to fig. 29.6, it can be seen that the D.C. grid potential can be controlled by suitable choice of the positive and negative D.C. voltage sources V' and V'' resp. and by the ratio of the resistances R and R_g. The resistance r_g represents the internal grid resistance, defined by a grid current – grid voltage characteristic according to fig. 5.6.

The D.C. potential at the grid will be:

$$V_{g0} = \frac{r_g R_g V' - r_g R V''}{r_g R_g + r_g R + R R_g} \quad \ldots\ldots\ldots \quad (77.6)$$

This D.C. voltage V_{g0} must be zero or positive.

It is assumed that at the instant $t = 0$ an input voltage V_i of the shape indicated in fig. 30.6 is applied. At this instant transient phenomena will commence and be superimposed upon the steady state that was present for $t < 0$.

For the calculation of these transients, the circuit of fig. 31.6 must be considered. This can be transformed into that of fig. 32.6, where

$$R_v = \frac{RR_g}{R + R_g} \quad \ldots\ldots\ldots\ldots \quad (78.6)$$

The current source I_i is given by the expression:

$$I_i = C_c \frac{dV_i}{dt} \quad \ldots\ldots\ldots\ldots \quad (79.6)$$

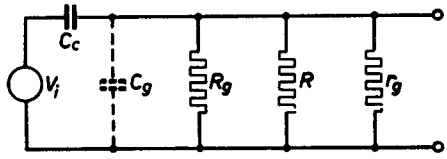

Fig. 31–6.

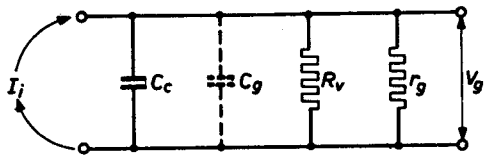

Fig. 32–6.

V_i changes linearly from the instant $t = 0$ until $t = t_0$, with a slope

$$\frac{dV_i}{dt} = -\frac{V_0}{t_0}, \text{ so:}$$

$$I_i = -C_c \frac{V_0}{t_0} \quad \ldots\ldots\ldots\ldots \quad (80.6)$$

This value is valid for $0 \leqq t \leqq t_0$. For $t > t_0$, however, $V_i = V_0$. This is a constant value, so:

$$I_i = 0 \text{ for } t > t_0.$$

In other words: I_i is the superposition of two step-functions:

$$I_i = C_c \frac{V_0}{t_0}\left[-U(t) + U(t - t_0)\right], \quad \ldots\ldots \quad (81.6)$$

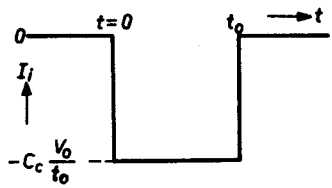

Fig. 33–6.

or I_i is a negative pulse function with an amplitude

$$-C_c \frac{V_0}{t_0}$$

and a pulse width t_0 seconds.

This is represented in fig. 33.6. When the operational impedance of the network of fig. 32.6 is known, the response of this circuit to this input function I_i is easy to calculate.

The operational impedance is:

$$Z(p) = \frac{R_{v1}}{1 + T_{v1}p}, \quad \ldots\ldots\ldots \quad (82.6)$$

where:

$$R_{v1} = \frac{R_v r_g}{R_v + r_g} \quad \ldots\ldots\ldots \quad (83.6)$$

$$T_{v1} = R_{v1} C_i \quad \ldots\ldots\ldots \quad (84.6)$$

$$C_i = C_c + C_g \quad \ldots\ldots\ldots \quad (85.6)$$

C_g is the input capacitance of the grid circuit, including grid-to-cathode and wiring capacitances.

The response of this impedance to a current step function $I_i U(t)$ is

$$V_g(t) = I_i R_{v1} (1 - e^{-t/Tv_1}) \quad \ldots\ldots\ldots \quad (86.6)$$

The total grid voltage, including the steady state, will be for $0 \leqq t \leqq t_0$:

$$V_g(t) = V_{g0} - C_c \frac{V_0}{t_0} R_{v1} (1 - e^{-t/Tv_1}) \quad \ldots\ldots \quad (87.6)$$

For further calculation of the transient phenomena it is necessary to discriminate between two possibilities.

First, it is possible that the grid voltage, represented by expression (87.6), will not pass below zero within the time t_0, the rise time of the input-voltage change (see fig. 30.6).

Then there will be no new discontinuity due to the grid current suddenly ceasing. The circuit remains unchanged and the expression (87.6) is valid until the instant t_0, when the positive step in I_i causes another transient response, given by

$$V_g(t - t_0) = +C_c \frac{V_0}{t_0} R_{v1} (1 - e^{-(t-t_0)/Tv_1}) \quad \ldots\ldots \quad (88.6)$$

For $t \geqq t_0$, the total grid voltage is the sum of expressions (87.6) and (88.6):

$$V_g(t) = V_{g0} - C_c \frac{V_0}{t_0} R_{v1} \left[e^{t_0/Tv_1} - 1 \right] e^{-t/Tv_1} \quad \ldots \quad (89.6)$$

The shape of this function is as represented in fig. 34.6.

This first case will, however, not occur frequently in practice, as the D.C. grid voltage V_{g0} will generally be only slightly positive, and

the value of V_0 will be large enough to drive the grid voltage negative within a time that is shorter than t_0 seconds.

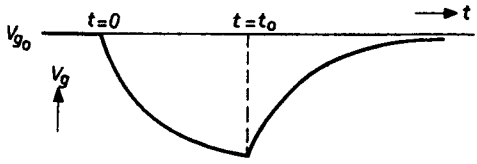

Fig. 34–6.

This is the second possibility we will have to investigate. However, before doing so, the dividing limit between these two cases will be considered.

This limit is reached when at the instant $t = t_0$ the grid voltage (expression 87.6, fig. 34.6) becomes zero. This is expressed by the following relation:

$$0 = V_{g0} - C_c \frac{V_0}{t_0} R_{v1} (1 - e^{-t_0/Tv_1}) \quad . \quad . \quad . \quad . \quad . \quad (90.6)$$

According to (84.6) and (85.6):

$$T_{v1} = R_{v1} (C_c + C_g).$$

In practice C_c will generally be much larger than C_g. Therefore:

$$T_{v1} \approx R_{v1} C_c,$$

and expression (90.6) can be written:

$$V_{g0} = V_0 \frac{T_{v1}}{t_0} (1 - e^{-t_0/T_{v1}}) \quad . \quad . \quad . \quad . \quad . \quad . \quad . \quad (91.6)$$

or:

$$\frac{V_{g0}}{V_0} = \frac{T_{v1}}{t_0} (1 - e^{-t_0/Tv_1}) \quad . \quad . \quad . \quad . \quad . \quad . \quad . \quad . \quad (92.6)$$

Substituting:

$$V_0 = \beta V_{g0} \quad . \quad . \quad . \quad . \quad . \quad . \quad . \quad . \quad . \quad . \quad . \quad (93.6)$$

and

$$t_0 = \alpha T_{v1} \quad . \quad . \quad . \quad . \quad . \quad . \quad . \quad . \quad . \quad . \quad . \quad (94.6)$$

changes expr. (92.6) into:

$$\beta = \frac{\alpha}{1 - e^{-\alpha}} \quad . \quad . \quad . \quad . \quad . \quad . \quad . \quad . \quad . \quad . \quad . \quad (95.6)$$

$$\lim_{\alpha \to 0} \beta = 1.$$

In the graph of fig. 35.6, the relation (95.6) is shown, and it is clear that, with fixed values of V_{g0} and T_{v1}, the less steep its negative-going flank, the higher will be the input voltage amplitude V_0 to drive the grid completely out of its conducting state.

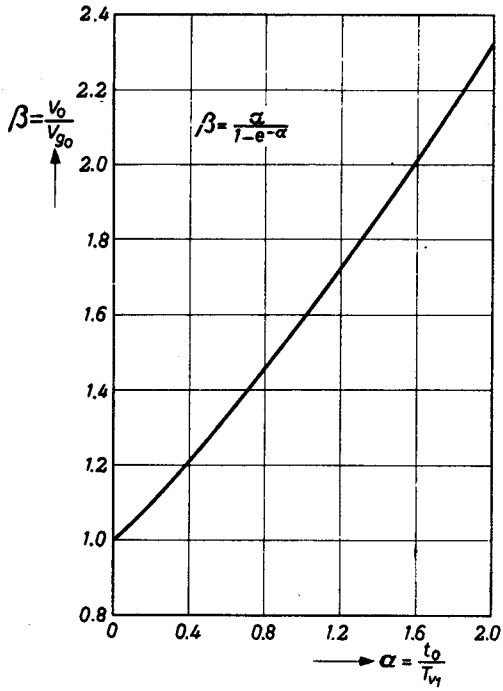

Fig. 35–6.

The second case, where the grid voltage reaches zero at an instant $t_1 < t_0$ will now be considered. At this instant, t_1, the grid current disappears and r_g in fig. (31.6) suddenly becomes infinite. This causes new transients in the circuit that can be calculated by methods indicated in section 2. The process to be applied is as follows: The current i_g flowing in r_g before the instant t_1 must be determined, the expression for i_g applying also for $t > t_1$ if no discontinuity appears.

The effect of suddenly increasing r_g to an infinite value, or to interrupt i_g, can be accounted for by assuming from the instant $t = t_1$ onwards that a current source I_0 is present at the terminals of the former r_g, I_0 being of opposite polarity but equal in value to i_g. Then the grid voltage for $t \geqq t_1$ will be the sum of the grid voltage $V_g(t)$ that was calculated for the original situation with r_g present, and of a component $\overline{V}_g(t)$ that is caused by the response of the circuit to the current I_0.

The first component is represented by expression (87.6), and is valid in the circuit of fig. 36.6.

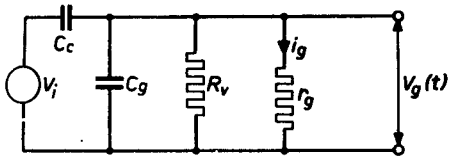

Fig. 36–6.

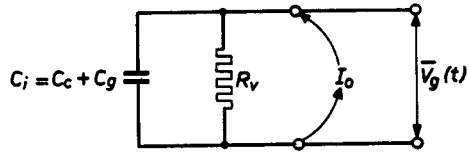

Fig. 37–6.

The second component can be calculated from the circuit of fig. 37.6, where $| I_0 | = | i_g |$, and i_g is given by:

$$i_g(t) = \frac{V_{g0} - C_c \frac{V_0}{t_0} R_{v1} (1 - e^{-t/Tv_1})}{r_g} \quad \ldots\ldots \quad (96.6)$$

(see expr. 87.6 and fig. 36.6).

At the instant $t = t_1$, the grid voltage is zero; consequently $i_g(t_1)$ is also zero. For calculating the new transients starting at the instant t_1, it is convenient to introduce a new time scale τ, with its zero point at $t = t_1$ so

$$\tau = t - t_1 \quad \ldots\ldots \quad (97.6)$$

In this new time scale the expression 87.6 reads as follows:

$$V_g(\tau) = -C_c \frac{V_0}{t_0} R_{v1} e^{-t_1/Tv_1} (1 - e^{-\tau/Tv_1}) \quad \ldots\ldots \quad (98.6)$$

The value t_1 is defined by the condition that $v_g(t)$ (see expr. 87.6) is zero for $t = t_1$; so:

$$V_{g0} = C_c \frac{V_0}{t_0} R_{v1} (1 - e^{-t_1/Tv_1}) \quad \ldots\ldots \quad (99.6)$$

Substituting this expr. in (98.6) yields for $\tau \geqq 0$:

$$V_{g1}(\tau) = -(R_{v1} | I_i | - V_{g0}) (1 - e^{-\tau/Tv_1}), \quad \ldots\ldots \quad (100.6)$$

where:

$$| I_i | = C_c \frac{V_o}{t_0} \quad \ldots\ldots \quad (101.6)$$

Expression (100.6) gives the first component of the total grid voltage for $t \geqq t_1$. The second component $\overline{V}_g(t)$ or $\overline{V}_g(\tau)$ can be calculated from fig. (37.6). The result is:

$$V_g(\tau) = \frac{R_v}{r_g}(V_{g0} - R_{v1} \mid I_i \mid)\left[1 + \frac{r_g}{R_v} e^{-\tau/Tv_1} - \frac{R_v + r_g}{R_v} e^{-\tau/Tv}\right], \quad (102.6)$$

where:

$$R_v = \frac{RR_g}{R + R_g}, \quad \ldots\ldots\ldots\ldots \quad (78.6)$$

and:

$$T_v = R_v C_i.$$

The resulting grid voltage $V_{g_{II}}(\tau)$ for $t \geqq t_1$ is the sum of $V_g(\tau)$ and $V_g(\tau)$ (expressions 100.6 and 102.6):

$$V_{g_{II}}(\tau) = V_g(\tau) + \overline{V}_g(\tau)$$

$$V_{g_{II}}(\tau) = -(R_{v1} \mid I_i \mid - V_{g0}) \frac{R_v + r_g}{r_g}(1 - e^{-\tau/Tv}) \quad \ldots \quad (103.6)$$

Now, at the instant $t = t_0$, another discontinuity occurs, viz. the input current I_i jumps back from a value $-C_c \frac{V_0}{t_0}$ to zero.

This causes a transient response:

$$\overline{\overline{V}}_g(\tau) = R_v \mid I_i \mid (1 - e^{-(\tau - t_0 + t_1)/Tv}) \quad \ldots \quad (104.6)$$

This new component must be superimposed on the grid voltage, originating from former transients, viz. $V_{g_{II}}(\tau)$ (expr. 103.6).

The resulting grid voltage is:

$$V_{g_{III}}(\tau) = -\frac{R_v + r_g}{r_g}(R_{v1} \mid I_i \mid - V_{g1})(1 - e^{-\tau/Tv}) +$$

$$+ R_v \mid I_i \mid (1 - e^{-(\tau - t_0 + t_1)/Tv}). \quad \ldots\ldots\ldots\ldots \quad (105.6)$$

At a certain instant $t = t_2$ (or $\tau = \tau_0$) this voltage reaches a value zero, and at that instant grid current starts again, in other words: resistance r_g is once again shunted across the grid circuit. Thus, from this instant $t = t_2$ onwards, a new component must be taken into account. This can be calculated by imagining a voltage source $V_c(\tau)$ being present in series with r_g, as represented in fig. 38.6.

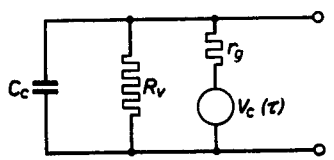

Fig. 38-6.

This voltage $V_c(\tau)$ is equal to the grid voltage $V_{III}(\tau)$ from expression (105.6), but with opposite sign.

The response of the network to $V_c(\tau)$ results in a grid voltage component:

$$-V_{g0}\left[\frac{R_v}{r_a}-\frac{r_g+R}{r_g}e^{-(\tau-\tau_0)/Tv}+e^{-(\tau-\tau_0)/Tv_1}\right].$$

This must be added to the voltage $V_{g_{III}}(\tau)$ (expr. 105.6), giving for the grid voltage at $t \geqq t_2$ the following expression:

$$V_{g_{IV}}(\tau) = V_{g0}(1-e^{-(\tau-\tau_0)/Tv_1}). \quad . \quad . \quad . \quad . \quad (106.6)$$

As is expected, the final value of the grid voltage is V_{g0} again.

In fig. 39.6 a survey is given of the various phases through which the grid voltage passes.

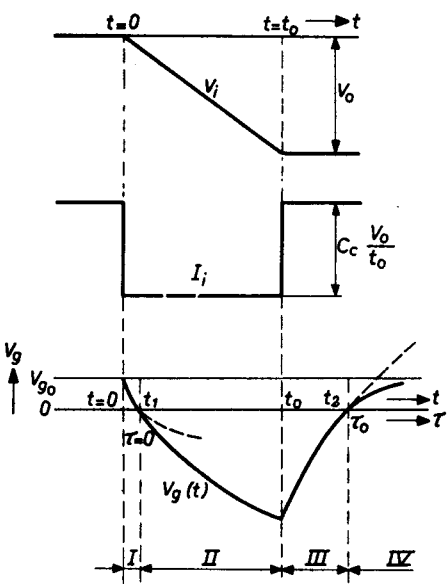

Fig. 39–6.

The first phase I commences at the instant $t = 0$, where the input voltage starts falling with a linear slope to the final, constant value $-V_0$. The second phase II commences at the instant $t = t_1$, when grid current disappears. The third phase III commences at $t = t_0$, when the input voltage V_i no longer changes.

The last phase IV is for times $t > t_2$. At $t = t_2$. the grid current starts again.

The changes from phase I into II and from phase III into IV occur continuously. This can be shown by calculating the first derivative with respect to time of the grid voltage changes at the instants $t = t_1$ and $t = t_2$. It will be found that:

$$\frac{d}{dt}\left[V_{g_I}(\tau)\right]_{t=t_1} = \frac{d}{dt}\left[V_{g_{II}}(\tau)\right]_{t=t_1}$$

and

$$\frac{d}{dt}\left[V_{g_{III}}(\tau)\right]_{t=t_2} = \frac{d}{dt}\left[V_{g_{IV}}(\tau)\right]_{t=t_2}$$

To give a quick survey, the expressions of the grid voltage changes in the various phases will be summarized again:

During phase I: $0 \leqq t \leqq t_1$:

$$V_{g_I}(t) = V_{g0} - |I_i| R_{v1} (1 - e^{-t/Tv_1}) \quad . \quad . \quad . \quad . \quad (87.6)$$

Final value: $V_{g_I}(\infty) = V_{g0} - |I_i| R_{v1}$.

During phase II: $t_1 \leqq t \leqq t_0$ or $0 \leqq \tau \leqq t_0 - t_1$:

$$V_{g_{II}}(\tau) = -(R_{v1} |I_i| - V_{g0}) \frac{R_v + r_g}{r_g} (1 - e^{-\tau/Tv}) \quad . \quad (103.6)$$

$$V_{g_{II}}(\infty) = -(R_{v1} |I_i| - V_{g0}) \frac{R_v + r_g}{r_g} = \frac{R_v + r_g}{r_g} V_0 - R_v |I_i| .$$

During phase III: $t_0 \leqq t \leqq t_2$ or $t_0 - t_1 \leqq \tau \leqq \tau_0$:

$$V_{g_{III}}(\tau) = -(R_{v1} |I_i| - V_{g0}) \frac{R_v + r_g}{r_g} (1 - e^{-\tau/Tv}) +$$

$$+ R_v |I_i| (1 - e^{-(\tau - t_0 + t_1)/Tv}) \quad . \quad . \quad . \quad . \quad . \quad . \quad . \quad . \quad . \quad . \quad . \quad . \quad (105.6)$$

$$V_{g_{III}}(\infty) = \frac{R_g V' - R V''}{R + R_g} .$$

During phase IV: $t \geqq t_2$ or $\tau \geqq \tau_0$:

$$V_{g_{IV}}(\tau) = V_{g0} (1 - e^{-(\tau - \tau_0)/Tv_1}) \quad . \quad . \quad . \quad . \quad (106.6)$$

$$V_{g_{IV}}(\infty) = V_{g0}.$$

It is interesting to consider the value of t_1 with respect to t_0, for it will be clear from the foregoing and especially from fig. 39.6 that the ultimate negative amplitude of the grid voltage will be larger as the grid current is cut off earlier, in other words: as t_1 becomes smaller with respect to t_0. In order to suppress the anode current of the tube with a given input voltage of amplitude V_0 and time of rise t_0, the peak negative grid voltage will have to be sufficiently high to pass the value of grid voltage for anode current cut-off.

The influence of the values of V_0 and t_0 on t_1 for given values of the circuit and tube constants and voltage sources R, R_g, C_c, C_g, r_g, V' and V'' can be investigated by closer examination of expression (99.6):

$$V_{g0} = V_0 \frac{T_{v1}}{t_0} (1 - e^{-t_1/Tv_1}) ,$$

or:
$$1 - e^{-t_1/Tv_1} = \frac{\alpha}{\beta} \quad \ldots\ldots\ldots\ldots \quad (107.6)$$

(see expressions (93.6) and (94.6).

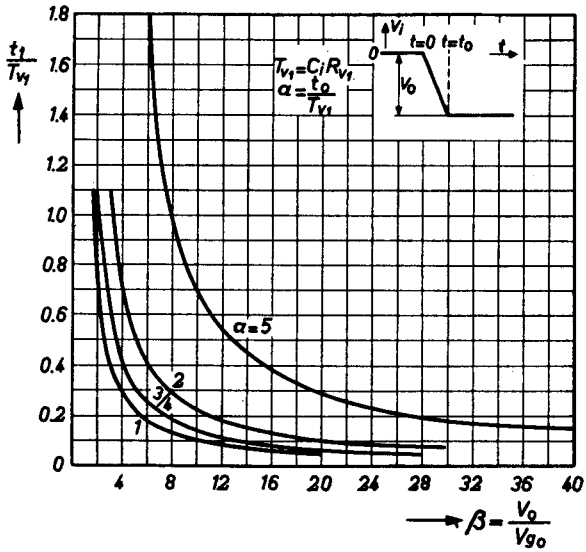

Fig. 40–6.

The value $\frac{t_1}{T_{v1}}$ as a function of β (or V_0) with α (or t_0) as a parameter is represented graphically in fig. 40.6, whilst in fig. 41.6 the value $\frac{t_1}{t_0}$ is represented as a function of α (or t_0) with β (or V_0) as parameter. If $\beta = \alpha$, then t_1 would be infinitely large, but in practice t_1 cannot be larger than t_0, so the ordinate in the graph of fig. 41.6 cannot become greater than 1.

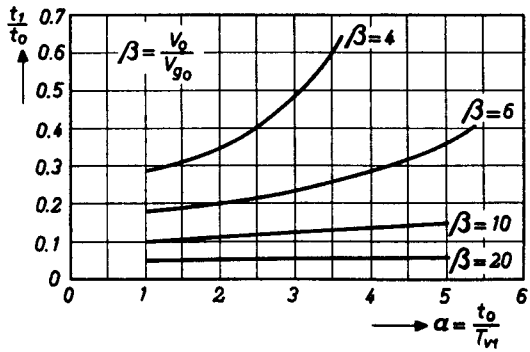

Fig. 41–6.

6.1.3. DIODE CIRCUITS

The results of the study of the behaviour of grid circuits when subjected to the influence of sudden steep positive- or negative-going voltage changes, as derived in the preceding sections, will also be useful for the investigation of the response of diode circuits. For vacuum-tube diodes the same current-voltage characteristic approximations as given in figs 5.6 and 10.6 can be applied. The resistance of a vacuum diode in the reversed current direction, often called the "back resistance", can be taken to be infinite. However, another large category of diodes, viz. crystal diodes, selenium rectifiers and the like, have a back resistance of finite value. In that case, the diode current-voltage characteristic can, to a close approximation, be represented by the graph of fig. 42.6. Indeed, in practice the current is zero for zero voltage, which is different from the case of vacuum tubes. The back resistance R_b of diodes, having a characteristic like that of fig. 42.6, will be:

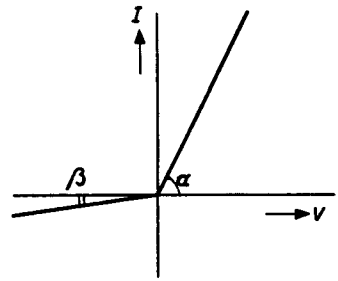

Fig. 42–6.

$$R_b = \cot \beta \, , \quad \ldots \ldots \ldots \ldots \quad (108.6)$$

whilst the forward resistance will be:

$$R_f = \cot \alpha \, . \quad \ldots \ldots \ldots \ldots \quad (109.6)$$

The behaviour of such diodes in a network when subjected to a change in input voltage which passes the value zero can be described in the following way. For negative values of diode voltage the diode is represented by its back resistance as depicted in fig. 43.6, where the block A

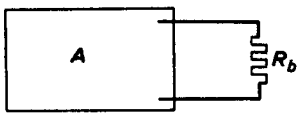

Fig. 43–6.

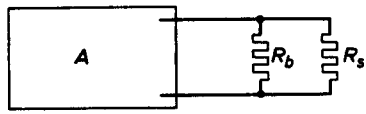

Fig. 44–6.

represents an arbitrary network in which the diode is incorporated.

For positive diode voltages the diode is represented by its forward resistance R_f. When the voltage across the diode changes from negative to positive, then it can be assumed that, at the instant its value is zero, a resistance R_s is suddenly shunted across R_b of such a value that:

$$R_f = \frac{R_b \cdot R_s}{R_b + R_s}, \quad \ldots\ldots\ldots \quad (110.6)$$

or:

$$R_s = \frac{R_b \cdot R_f}{R_b - R_f} \quad \ldots\ldots\ldots \quad (111.6)$$

(see fig. 44.6).

The sudden shunting of R_b by R_s causes transients which can be calculated in the way outlined in previous sections.

In the same way, the change of the diode voltage from positive to negative values will be accompanied by transient phenomena which can be described by the sudden omission of R_s from the circuit at the instant the diode voltage passes zero, and calculated by the same methods. It should be borne in mind, however, that disturbing effects may occur, when switching certain kinds of semi-conductor diodes, caused by inherent inertia phenomena such as hole-storage in Germanium diodes.

6.2. THE ANODE CIRCUIT

If the grid voltage change of a tube has been determined by any method given in the foregoing sections, then the next problem will be to investigate the anode circuit of the tube and, if possible, to derive expressions which represent the anode current and voltage as functions of time.

When using idealized characteristics, this can be performed for triodes as well as for pentodes.

6.2.1. TRIODES

The idealized characteristics of a triode, giving the relation between the anode current I_a and the anode voltage V_a with the grid voltage V_g as parameter, are represented in fig. 45.6. The main difference between practical characteristics and these idealized ones is given by the lower dotted curved parts of the otherwise straight lines.

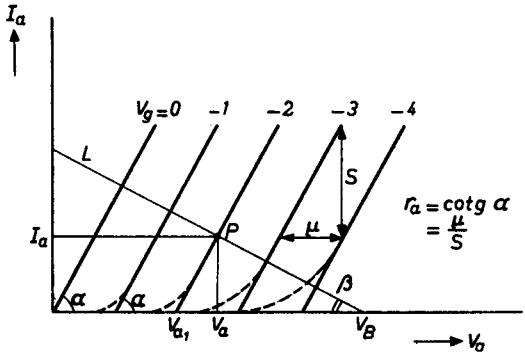

Fig. 45–6.

When an anode supply voltage V_B is available and fed to the anode via a load resistance R_a, then the operating point of the tube

defined by the value of V_g will be situated on the loadline L that intersects the horizontal axis at $V_a = V_B$ and has a slope $\cot \beta = R_a$.

The situation of a point P is characterized by the following relations:

$$I_a = \frac{V_a - V_{a1}}{r_a},$$

where:

$$V_{a1} = -\mu V_g \quad \ldots\ldots\ldots\ldots \quad (112.6)$$

and $r_a = \cot \alpha =$ internal anode resistance, thus:

$$I_a = \frac{V_a + \mu V_g}{r_a} = \frac{V_a}{r_a} + S V_g, \quad \ldots\ldots\ldots \quad (113.6)$$

where $S =$ transconductance of the tube.

It can be seen from the characteristics that the cut-off grid voltage E_c is dependent on the value of V_B, viz.

$$V_B = -\mu E_c \quad \ldots\ldots\ldots\ldots \quad (114.6)$$

(compare expr. 112.6).

If the anode load is a pure resistance, then dynamic operating conditions will all be situated on the load line L. In practice, however, some stray capacitance will always be present, and at steep changes of grid voltage the operating point can change to such values that, temporarily, it will no longer be situated on the load line. It can be assumed that a static condition exists with P as the operating point of the tube (see fig. 46.6), and also that the grid voltage falls below the cut-off value in a time that is small compared with the time constant in the anode circuit (anode load resistance times anode stray capacitance). The anode current will suddenly become zero, but the anode voltage cannot change to its final value V_B at the same rate, and the operating point will trace the dotted line I in the direction of the arrows. In the reverse case, when V_g suddenly changes to zero, the operating point P will trace the dotted line II in the direction of the arrows.

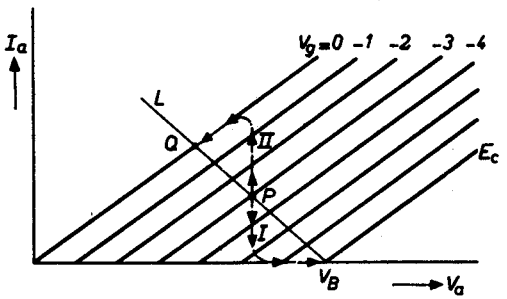

Fig. 46–6.

If, in general, an anode load impedance Z_a is present, then the values of I_a and V_a in the dynamic conditions arising from changes in grid voltage V_g will be determined by expression (113.6) and the following relation:

$$V_B - V_a = Z_a I_a \quad \ldots\ldots\ldots \quad (115.6)$$

Eliminating V_a gives an expression for I_a:

$$I_a = \frac{\mu}{r_a + Z_a}(V_g - E_c), \quad \ldots\ldots\ldots \quad (116.6)$$

in which relation (114.6) has also been substituted.

Once I_a is known, V_a can be determined from expr. (115.6).

If a pure resistance represents the anode load, then $Z_a = R_a$, and the anode current will be:

$$I_a = \frac{\mu}{r_a + R_a}(V_g - E_c), \quad \ldots\ldots\ldots \quad (117.6)$$

and the anode voltage:

$$V_a = -\frac{\mu}{r_a + R_a}(r_a E_c + R_a V_g) \quad \ldots\ldots\ldots \quad (118.6)$$

If a parallel capacitance is to be considered across R_a, then:

$$Z_a = R_a \frac{1}{1 + T_a p}, \quad \ldots\ldots\ldots \quad (119.6)$$

where $T_a = R_a C_a$, when C_a is the total output capacitance of the tube (including wiring capacitance). Now Z_a is an operational impedance, where p denotes the usual symbol for derivation with respect to time. Substituting Z_a from expr. (119.6) into expr. (116.6) gives:

$$I_a = \frac{\mu(1 + T_a p)}{r_a + R_a + r_a T_a p}(V_g - E_c),$$

or:

$$I_a = \frac{\mu}{r_a + R_a} \frac{1 + T_a p}{1 + \lambda_a T_a p}(V_g - E_c), \quad \ldots \quad (120.6)$$

where:

$$\lambda_a = \frac{r_a}{r_a + R_a} \quad \ldots\ldots\ldots\ldots \quad (121.6)$$

When V_g is a known function of time, equation (120.6) can be solved with operational calculus methods, as previously discussed. It must be remembered, however, that for values of V_g smaller than E_c, the tube is in the cut-off state and no anode current at all flows. So changes of V_g at values $V_g < E_c$ have no influence in the anode circuit. Consequently, only values of $V_g > E_c$ or values of $V_g - E_c > 0$ will cause variations in anode current according to expr. 120.6.

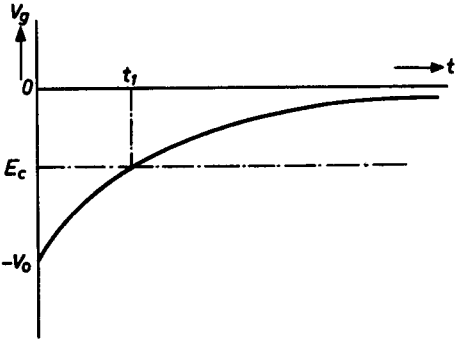

Fig. 47–6.

For example, if V_g is given by the time function:

$$V_g = -V_0 e^{-t/T} \quad . \quad . \quad . \quad . \quad . \quad . \quad . \quad . \quad . \quad (122.6)$$

(see fig. 47.6).

Then a period of time from $t = 0$ until $t = t_1$ elapses before V_g reaches a value E_c, and this instant t_1 is given by:

$$E_c = -V_0 e^{-t_1/T}$$

So:

$$V_g - E_c = -V_0 (e^{-t/T} - e^{-t_1/T}) ,$$

or:

$$V_g - E_c = -V_0 e^{-t_1/T} (e^{-(t-t_1)/T} - 1) ,$$

or:

$$V_g - E_c = E_c (e^{-\tau/T} - 1) , \quad . \quad . \quad . \quad . \quad . \quad . \quad . \quad . \quad (122a.6)$$

where $\tau = t - t_1$, a new time-scale having its zero point at the instant when $V_g - E_c$ becomes positive.

The change of the anode current with time will be determined by the expressions (120.6) and (122*a*.6):

$$I_a = \frac{-\mu E_c}{r_a + R_a} \frac{1 + T_a p}{1 + \lambda_a T_a p} (1 - e^{-\tau/T}) \quad . \quad . \quad . \quad . \quad (123.6)$$

This can be solved by the methods treated in section 5, viz. either by applying the superposition theorem (expr. 28.5) or by "translating"

the time function $1 - e^{-\tau/T}$ into the corresponding p-function $\frac{1}{1+Tp}$ according to expr. (15.5).

The latter method is the quickest and will be followed here.

Then expr. (123.6) can be written:

$$I_a = \frac{V_B}{r_a + R_a} \frac{1 + T_a p}{(1 + \lambda_a T_a p)(1 + Tp)}, \quad \ldots \quad (124.6)$$

where $-\mu E_c$ is substituted by V_B, according to (114.6).

The p-function can be split up in two partial fractions, giving:

$$I_a = \frac{V_B}{r_a + R_a} \frac{1}{T - \lambda_a T_a} \left[(1 - \lambda_a) T_a \frac{1}{1 + \lambda_a T_a p} + (T - T_a) \frac{1}{1 + Tp} \right]. \quad (125.6)$$

Transforming these p-functions back again into time functions yields:

$$I_a = \frac{V_B}{r_a + R_a} \left[1 - \frac{(1 - \lambda_a) T_a}{T - \lambda_a T_a} e^{-\tau/\lambda_a T_a} - \frac{T - T_a}{T - \lambda_a T_a} e^{-\tau/T} \right]. \quad (126.6)$$

The final value of I_a (for $t =$ infinite), will be:

$$I_a(\infty) = \frac{V_B}{r_a + R_a},$$

corresponding to the operating point Q in fig. 46.6. If the time constant T of the grid voltage change is the same as the anode circuit time constant T_a, then expr. (126.6) simplifies to:

$$I_a = \frac{V_B}{r_a + R_a} \left[1 - e^{-\tau/\lambda_a T_a} \right] \quad \ldots \ldots \quad (127.6)$$

The corresponding anode voltage change would be, according to (115.6) and (119.6):

$$V_a = V_B - \frac{R_a}{1 + T_a p} (I_a) \quad \ldots \ldots \quad (128.6)$$

I_a expressed as a p-function, can be found from (125.6), remembering that T was equated to T_a:

$$I_a = \frac{V_B}{r_a + R_a} \cdot \frac{1}{1 + \lambda_a T_a p} \quad \ldots \ldots \quad (129.6)$$

From (128.6) and (129.6):

$$V_a = V_B \left[1 - (1 - \lambda_a) \frac{1}{1 + T_a p} \cdot \frac{1}{1 + \lambda_a T_a p}\right]. \quad . \quad . \quad . \quad (130.6)$$

This can again be solved by splitting the p-function into partial fractions:

$$V_a = V_B \left[1 + \lambda_a \frac{1}{1 + \lambda_a T_a p} - \frac{1}{1 + T_a p}\right]. \quad . \quad . \quad . \quad . \quad . \quad (131.6)$$

Translating back into a time function:

$$V_a = V_B \left[\lambda_a - \lambda_a e^{-\tau/\lambda_a T_a} + e^{-\tau/T_a}\right] . \quad . \quad . \quad . \quad . \quad . \quad . \quad . \quad (132.6)$$

The foregoing treatment showed the derivation of the anode current and voltage changes caused by a positive-going grid voltage change, starting below cut-off (see fig. 47.6) and expression 122.6). The electron tube can be represented as a switch that is closed. The reverse case will now be considered, viz. the influence of a negative-going grid voltage (the switch is opened). It will be assumed that the grid voltage is zero for $t \leqq 0$, and that no transients of a former change remain. The change of the grid voltage V_g can be represented by fig. 48.6 and by the following expression:

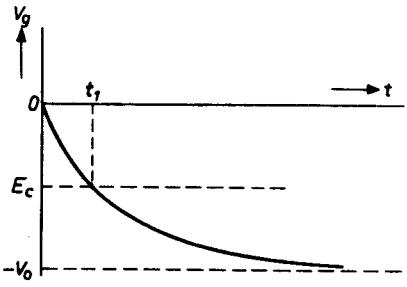

Fig. 48–6.

$$V_g = -V_0 (1 - e^{-t/T}) \quad . \quad . \quad . \quad . \quad . \quad . \quad . \quad . \quad (133.6)$$

This case of switching-off a tube is more complicated than the reverse. Depending on the values of V_0 and the time constant T from expression (133.6), several particular cases must be distinguished. In order to make this clear, it is best to start with two extreme cases.

Let it first be assumed that the time constant T_a in the anode circuit is very much larger than that of the grid voltage change T.

If then V_0 has a value that exceeds $|E_c|$, the tube is already cut off ($I_a = 0$) before the anode voltage has had any opportunity to change its value appreciably. To a good approximation, the response of the anode circuit will be the same as to a step-shaped input current which is of equal magnitude but opposite in sign to the constant current I_{a0} that was flowing in the anode circuit before the change in grid voltage

commenced (for times $t \leqq 0$). So, for times $t \leqq 0$, the voltage drop across the anode circuit is $R_a \,.\, I_{a0}$, I_{a0} being the constant anode current at $V_g = 0$ and $t \leqq 0$.

When the tube is suddenly cut off, this voltage drop tends to approach zero according to an exponential function with a time constant $T_a = R_a C_a$. (R_a = anode load resistor, C_a = total anode capacitance across R_a). In other words: the anode voltage will be for $t \geqq 0$:

$$V_a(t) = V_B - R_a I_{a0}\, e^{-t/T_a} \quad \ldots\ldots \quad (134.6)$$

The path of the operating point in the I_a - V_a characteristics will be as indicated by the dotted line in fig. 49.6, where L represents the static load line corresponding to the anode load resistor R_a.

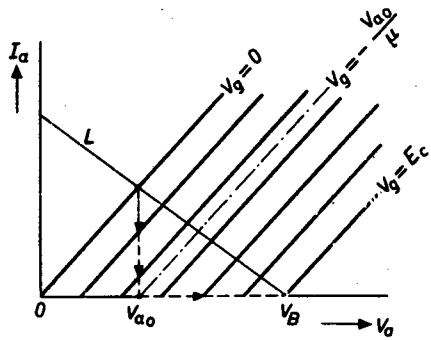

Fig. 49-6.

Another extreme case is that where $T \gg T_a$. If there were no parallel capacitance at all across R_a, the working point would be shifted from the intersection of L and the I_a - V_a characteristic at $V_g = 0$ in fig. 49.6 along the loadline down to V_B. Between these cases are many other intermediate possibilities. The static condition for times $t < 0$ is characterized by:

$$I_{a0} = \frac{V_{a0}}{r_a} \quad \ldots\ldots \quad (135.6)$$

If ΔV_g denotes in general the change in V_g taking place for $t \geqq 0$, then an anode current change ΔI_a will be caused, given by the relation

$$\Delta I_a = \frac{\Delta V_a + \mu \Delta V_g}{r_a} \quad \ldots\ldots \quad (136.6)$$

The change in voltage across the anode circuit impedance Z_a is given by $Z_a \Delta I_a$, and this must be equal to the change in anode voltage but opposite in sign:

$$\Delta V_a = -Z_a \Delta I_a \quad \ldots\ldots \quad (137.6)$$

Substituting (136.6) gives:

$$\Delta V_a = -\frac{Z_a}{Z_a + r_a} \mu \Delta V_g \quad \ldots\ldots \quad (138.6)$$

Z_a is the parallel combination of the resistance R_a and the capacitance C_a, so:

$$Z_a = \frac{R_a}{1 + R_a C_a p} \quad \ldots\ldots\ldots \quad (139.6)$$

Substituting in (138.6) gives:

$$\Delta V_a = -\mu \frac{R_a}{R_a + r_a} \frac{1}{1 + T_v p} \Delta V_g \quad \ldots\ldots \quad (140.6)$$

where:

$$T_v = \frac{r_a}{R_a + r_a} R_a C_a \quad \ldots\ldots\ldots \quad (141.6)$$

If ΔV_g is supposed to be as represented by expression (133.6), then the operational form in which ΔV_a can be expressed is as follows:

$$\Delta V_a = \frac{\mu V_0 R_a}{R_a + r_a} \frac{1}{1 + T_v p} \frac{1}{1 + Tp} \quad \ldots\ldots\ldots \quad (142.6)$$

Transformed into a time function, this expression will be:

$$\Delta V_a = \mu V_a \frac{R_a}{R_a + r_a} \left[1 - e^{-t/T} - A\,(e^{-t/T_v} - e^{-t/T})\right], \ldots \quad (143.6)$$

where:

$$A = \frac{T_v}{T_v - T} \quad \ldots\ldots\ldots \quad (144.6)$$

Now, the total anode voltage will be the sum of the initial steady state value V_{a0} and the transient value ΔV_a:

$$V_a(t) = V_{a0} + \Delta V_a \quad \ldots\ldots\ldots \quad (145.6)$$

The anode current decreases from the initial steady state value I_{a0} to zero. The instant $t = t_1$ at which it reaches zero is fixed by the condition:

$$V_a(t_1) + \mu V_g(t_1) = 0. \quad \ldots\ldots\ldots \quad (146.6)$$

Substituting expressions (145.6), (143.6) and (133.6) gives an equation for determining t_1:

$$V_{a0} + \mu V_0 \frac{R_a}{R_a + r_a} \left[1 - e^{-t_1/T} - A\,(e^{-t_1/T_v} - e^{-t_1/T})\right] -$$

$$- \mu V_0 (1 - e^{-t_1/T}) = 0. \quad \ldots\ldots\ldots \quad (147.6)$$

or:

$$V_{a0} - \mu V_0 \left[\frac{r_a}{R_a + r_a} (1 - e^{-t_1/T}) - \frac{R_a}{R_a + r_a} A \, (e^{-t_1/T_v} - e^{-t_1/T}) \right] = 0.$$

A general solution for t_1 will be difficult to derive, each practical case being considered individually and then solved for example by graphical methods.

A few special cases can be found directly, for example that already mentioned, where $T \ll T_v$. Then it can be derived that:

$$- A \, (e^{-t/T_v} - e^{-t/T}) \approx e^{-t/T} - 1,$$

and consequently $\Delta V_a = 0$ at $t = t_1$. The grid voltage changes so rapidly that the anode voltage cannot follow because of its much larger time constant. Then condition (147.6) simplifies to:

$$V_{a0} - \mu V_0 \, (1 - e^{-t_1/T}) = 0,$$

or:

$$t_1 = - T \ln \left(1 - \frac{V_{a0}}{\mu V_0} \right) \quad . \quad . \quad . \quad . \quad . \quad . \quad . \quad (148.6)$$

There is only a real solution for t_1 if:

$$\frac{V_{a0}}{\mu V_0} \leqq 1.$$

Now the value $\frac{V_{a0}}{\mu}$ represents the cut-off grid voltage of the tube at an anode voltage V_{a0}. The characteristic corresponding with this cut-off grid voltage is represented by the dash-dot line in fig. 49.6. It is clear that V_0 must be larger than this cut-off value. However, when V_0 does not exceed the absolute value of E_c, the cut-off voltage at an anode voltage equal to the supply voltage V_B, then the tube will, after an initial cut-off, sooner or later again become conducting as the anode voltage rises and tends to a final value V_B when no anode current flows. As soon as V_a reaches a value $-\mu V_g(t)$, then anode current starts to flow again. This lowers the rate of increase of V_a and it may be expected that gradually the anode voltage will tend to its final value μV_0, with the operating point of the tube at the intersection of the static loadline and the grid voltage characteristic of value $-V_0$.

This method of switching a tube will, however, not be frequently used in practice. Generally, the tube will have to be cut off rapidly and definitely, so that V_0 will have to be larger than E_c.

Another extreme case occurs when $T_v \ll T$, so that the quantity A (see expr. (144.6) is very small and expr. (147.6) simplifies to:

$$V_{a0} - \mu V_0 \frac{r_a}{R_a + r_a}(1 - e^{-t_1/T}) = 0,$$

or:

$$t_1 = -T \ln\left(1 - \frac{R_a + r_a}{r_a} \frac{V_{a0}}{\mu V_0}\right) \quad \ldots\ldots \quad (149.6)$$

To have a real value of t_1, in other words to reach a real cut-off condition, the relation

$$\frac{R_a + r_a}{r_a} \frac{V_{a0}}{\mu V_0} \leqq 1$$

must be fulfilled, or:

$$V_0 \geqq \frac{R_a + r_a}{r_a} \frac{V_{a0}}{\mu},$$

or:

$$V_0 \geqq \frac{V_B}{\mu} (= |E_c|).$$

6.2.2. PENTODES

The idealized anode current – anode voltage characteristics at a given screen grid voltage for a pentode are represented in fig. 50.6. The main deviations from this idealized form are rounded edges at the left.

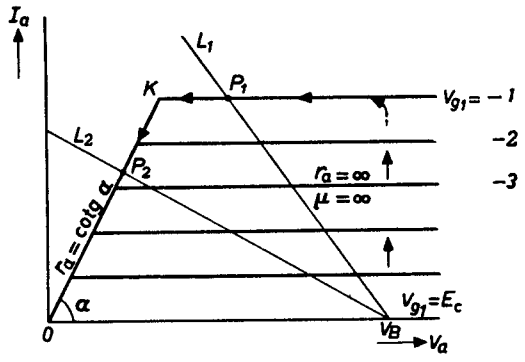

Fig. 50–6.

At low values of the anode voltage V_a, all characteristics converge approximately into one steep line through the origin of the system of coordinates. The reverse of the slope of this "bottoming" line is denoted by r_a:

$$r_a = \cot \alpha \text{ (see fig. 50.6)} \quad \ldots\ldots \quad (150.6)$$

The discontinuity of the characteristics at the "knee" complicates the response of the pentode to sudden changes in voltage at the control grid. If, for instance, the tube has been cut-off for a long period, then its anode voltage will be equal to the supply voltage V_B. If then the control-grid voltage V_{g1} is suddenly raised to a value above the cut-off voltage E_c, say —1 volt, the anode current suddenly assumes a value corresponding to the characteristic for $V_g = -1$ volt.

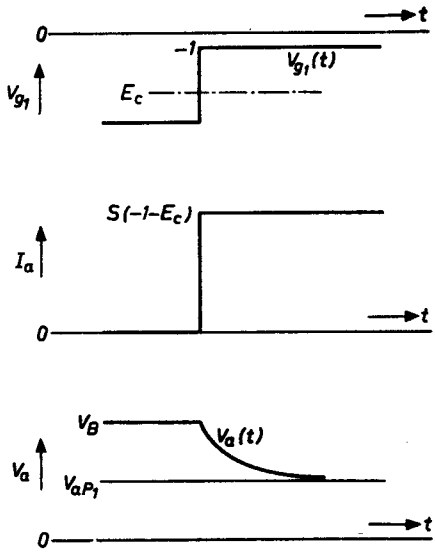

Fig. 51-6.

If the time constant of the anode circuit is large, the change in anode voltage will be very slow, compared with this sudden increase in current. The operating point of the tube will travel along the curve indicated by arrows in fig. 50.6, and finally reach a steady state at point P_1 if the anode load resistance R_a is small enough to correspond with the static loadline L_1.

If the change of V_{g1} was step-shaped, then the change of I_a will be of similar shape. The anode voltage V_a will be an exponential curve starting at a value V_B and tending to a final value corresponding with the operating point P_1 with a time constant R_aC_a. These waveforms are represented in fig. 51.6.

However, when the anode load resistance R_a happens to be large enough to correspond with loadline L_2 of fig. 50.6, then the final operating point will be P_2. Before this point is reached, the "kneepoint" K is passed, and at that instant a discontinuity occurs.

Until this instant, the anode current is constant and independent of the anode voltage. From this instant onwards, however, the anode current decreases proportionately to the anode voltage, the relation being $I_a = V_a \operatorname{tn} \alpha$, or, according to (150.6):

$$I_a = \frac{V_a}{r_a} \quad \ldots\ldots\ldots\ldots \quad (151.6)$$

This can be taken into account by the sudden switching of a resistance r_a between the anode and cathode of the pentode.

Referring to fig. 52.6, the first of two possible cases is loadline L_1, giving a final operating point P_1 when the pentode receives a positive voltage step at its control grid that jumps from a value below cut-off to the value V_{g0} corresponding to an anode current I_{a0}.

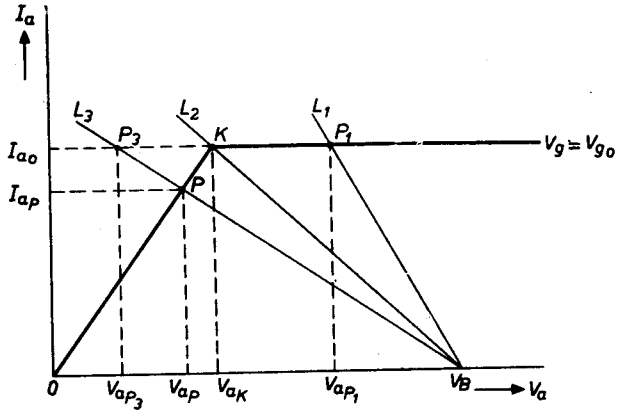

Fig.. 52-6.

Figure 51.6 gives the shape of the anode voltage, which is in mathematical form as follows:

$$V_a(t) = V_B - I_{a0}R_a(1 - e^{-t/T_a}), \quad \ldots\ldots \quad (152.6)$$

if the voltage step at the grid occurs at the instant $t = 0$.

$T_a = R_aC_a$ = time constant of anode impedance.

The second possibility is loadline L_3, whilst loadline L_2 represents the border case. For this case, expr. (157.6) would still be valid. With the case of L_3 a discontinuity occurs at the instant $t = t_1$ when V_a reaches the value

$$V_a(t_1) = V_{ak} = I_{a0}r_a \quad \ldots\ldots\ldots \quad (153.6)$$

The final value of equation (152.6) which is valid only for $t \leqq t_1$, would be $V_a(\infty) = V_{ap3}$, corresponding to a virtual operating point P_3. However, the limiting operating point will be P, corresponding to $V_a(\infty) = V_{ap}$. The current will then be:

$$I_{ap} = V_{ap}/r_a. \quad \ldots\ldots\ldots\ldots \quad (154.6)$$

Moreover:

$$\frac{V_B - V_{ap}}{R_a} = I_{ap}. \quad \ldots\ldots\ldots\ldots \quad (155.6)$$

Combining (154.6) and (155.6) gives:

$$V_{ap} = V_B \frac{r_a}{R_a + r_a}. \quad \ldots\ldots\ldots \quad (156.6)$$

From expressions (152.6) and (153.6) it follows:

$$I_{a0} r_a = V_B - I_{a0} R_a (1 - e^{-t_1/T_a}),$$

or:

$$t_1 = T_a \ln \frac{I_{a0} R_a}{I_{a0} (R_a + r_a) - V_B}. \quad \ldots\ldots\ldots \quad (157.6)$$

From fig. 52.6 it can be seen that $V_B = I_{a0} (R_{a2} + r_a)$, where R_{a2} corresponds to loadline L_2. Then, $t_1 = \infty$.

For loadline L_1 it can be seen that $I_{a0} R_{a1} = V_B - V_{ap1}$ and $I_{a0} r_a = V_{ak}$; thus:

$$t_1 = T_a \ln \frac{V_B - V_{ap1}}{V_{ak} - V_{ap1}}.$$

As $V_{ak} < V_{ap1}$, there is no real value of t_1 in that case.

For loadline L_3, however, it can be written:

$$t_1 = T_a \ln \frac{V_B - V_{ap3}}{V_{ak} - V_{ap3}},$$

and now:

$$V_{ak} > V_{ap3},$$

so t_1 has a real finite value.

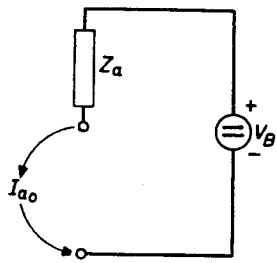

Fig. 53–6.

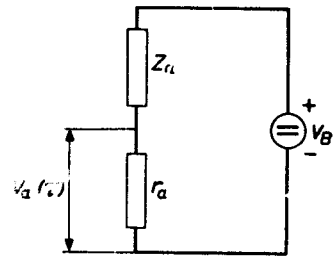

Fig. 54–6.

For times $t \leqq t_1$, the value of the anode voltage is given by expression (152.6), and the anode circuit can be represented by the diagram of fig. 53.6. The current source I_a is a step-function.

$$I_a = I_{a0} = s\,(V_{g0} - E_c) \quad \ldots\ldots\ldots \quad (158.6)$$

From the instant $t = t_1$ onwards, a resistance r_a is to be shunted across the current source I_a, and the circuit can be represented by the diagram of fig. 54.6. The instant $t = t_1$ will be considered as the origin of a new time scale $\tau = 0$ $(\tau = t - t_1)$.

The anode voltage $V_a\,(\tau)$ in this new time-scale has an intial value

$$V_a\,(0) = V_{ak} = I_{a0}\,r_a \text{ (see 153.6)} \quad \ldots\ldots\ldots \quad (159.6)$$

The final value will be:

$$V_a\,(\infty) = \frac{r_a}{Z_a + r_a}\,V_B \quad \ldots\ldots\ldots \quad (160.6)$$

The anode voltage changes from its initial value to its final value with a time constant:

$$T = \frac{r_a R_a}{R_a + r_a}\,C_a\,, \quad \ldots\ldots\ldots\ldots \quad (161.6)$$

and will be represented by the time-function:

$$V_a\,(\tau) = V_a\,(\infty) + (V_{ak} - V_a\,(\infty))\,e^{-\tau/T} \quad \ldots\ldots \quad (162.6)$$

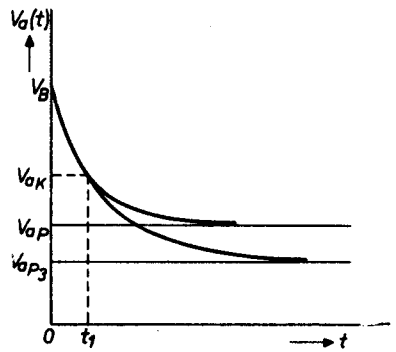

Fig. 55–6.

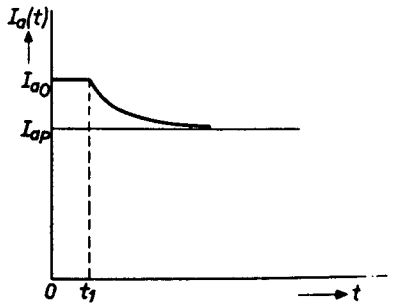

Fig. 56–6.

The values of $V_a\,(\infty)$ and V_{ak} substituted in (162.6) gives:

$$V_a\,(\tau) = \frac{r_a}{R_a + r_a}\left[V_B - \{V_B - I_{a0}\,(R_a + r_a)\}\,e^{-\tau/T}\right] \quad (163.6)$$

This is valid for $t \geqq t_1$ $(\tau \geqq 0)$, whilst for $0 < t \leqq t_1$ expr. (152.6) holds:

$$V_a(t) = V_B - I_{a0}R_a(1 - e^{-t/T_a}) \quad . \quad . \quad . \quad . \quad . \quad (152.6)$$

The anode voltage is continuous at $t = t_1$, not only in its value, but also, as can easily be checked, in its first derivative with respect to time.

The shape of $V_a(t)$ is sketched in fig. 55.6, whilst the anode current I_a as a function of time is represented in fig. 56.6.

So far, the influence of a positive-going voltage step at the control grid of a pentode on the anode circuit has been treated.

The response to a negative-going control grid voltage step will next be considered. It is again assumed that the anode load impedance is the parallel combination of a resistance R_a and a capacitance C_a, giving a time constant $T_a = C_aR_a$. Furthermore no effects of any foregoing transients are supposed to be present at the moment $t = 0$ when the voltage step at the control grid occurs. This grid voltage is V_{g0} for times $t \leqq 0$.

At $t = 0$ it jumps to a value below cut-off causing the anode current to become suddenly zero.

The capacitance C_a now starts discharging from the initial voltage value I_aR_a to its final value of zero according to an exponential time function with a time constant $T_a = R_aC_a$.

Thus the change in anode voltage will be:

$$V_a(t) = V_B - I_aR_a\,e^{-t/T_a} \quad . \quad . \quad . \quad . \quad . \quad . \quad . \quad . \quad (164.6)$$

This equation is valid no matter, whether the initial current I_a corresponds to the operation point P (loadline L_3) or P_1 (loadline L_1) in fig. 52.6.

7. THE MULTIVIBRATOR FAMILY

7.1. INTRODUCTION

The multivibrator principle is commonly used for generating or shaping pulses, pulse frequency-dividing and similar functions. As mentioned at the end of section 4, three types of multivibrators can be distinguished. First the *bistable multivibrator*, frequently called the Eccles Jordan flip-flop circuit. This offers a suitable and much used means of dividing the number of pulses per unit time by the factor two. By combining several binary dividers in cascade, division of the input pulse repetition frequency by any power of two may be accomplished. Feedback may be suitably applied between cascaded flip-flops for division. Thus the counting of pulses may be accomplished in numerical systems other than the binary one. This will often be the decimal system, which is familiar to every one who has studied arithmatic.

It will not be surprising, therefore, that the bi-stable multivibrator is a very important basic element in modern computing devices. The number of tubes used in such applications is innumerable, and special types mostly in the form of a double triode have been developed by several manufacturers.

In fact, it has been the development of a double triode for computer purposes that caused the need for more exact knowledge of the behaviour of tubes in flip-flop circuits, and this initiated the author's investigations of the transient phenomena in a bi-stable multivibrator. The theoretical results enabled us to trace the influence of tube characteristics on the behaviour of the flip-flop circuit, thus giving the tube manufacturer valuable information as to how to design tubes which will accomplish their specific tasks.

The bi-stable multivibrator will be treated extensively. Once this circuit had been analysed, it was a simpler matter to analyse the *monostable multivibrator*, a second member of the multivibrator family, in the same way. Among other applications, this type of switching device is used for pulse shaping and delaying.

The third type, the *astable* or free-running multivibrator, is a self-oscillating pulse (or sawtooth) generator needing no external triggering signal for operation, in contrast to the two types already mentioned. It is often fed, however, with external pulses, in order to synchronize its frequency with a given frequency. The application of the astable

multivibrator in television receivers is described by the author in his book "Flywheel Synchronisation of Sawtooth Generators", monograph 2 of the series Television Receiver Design, Book VIIIB of Philips' Technical Library.

In this book, only the frequency of the multivibrator signal and its synchronization is dealt with. In the present book the waveform of the astable multivibrator signals will also be considered, and the influence of the internal anode resistance of the tube on both frequenccy and waveform will be included.

7.2. THE BI-STABLE MULTIVIBRATOR

The bi-stable multivibrator — or Eccles-Jordan flip-flop circuit — incorporates two vacuum tubes which basically perform a switching operation. This involves several sudden changes in the voltages and currents in the network. An analysis of these transients is essential to obtain an insight into the operation of bi-stable multivibrators in general and of the influence of the tube characteristics in particular.

In the operation of the bi-stable multivibrator, two conditions can be distinguished, namely the static condition at which one tube is conducting, the other tube being cut off and all effects of previous trigger pulses having died out, and the dynamic condition which commences as soon as a trigger pulse is applied and ultimately leads to another static condition at which the tube that was originally conducting is cut off, whilst the tube that was originally cut off becomes conducting.

It will be clear that an investigation of the dynamic condition is of particular interest, the switching speed and the triggering sensitivity of the multivibrator being determined thereby. By applying a step-by-step method and subdividing the dynamic condition into the following three phases, its analysis is simplified.

(*a*) The first phase commences at the instant $t = 0$ at which the trigger pulse is applied. Tube *I* is assumed to be conducting prior to this instant, tube *II* then being cut off. Conditions are assumed to be such that tube *I* is immediately cut off, tube *II* remaining in the cut-off condition during this phase. The first phase is therefore characterized by the fact that the circuit may be considered as a passive network.

(*b*) The second phase commences at the instant $t = t_{II}$, at which tube *II*, which was originally cut off, becomes conducting. This phase continues until the instant t_s, at which grid current starts to flow in the conducting tube *II*.

(*c*) The third phase, commencing at the instant t_s, continues until the transients have died out.

7.2.1. FUNDAMENTAL CIRCUIT

Fig. 1.7 shows the fundamental circuit of the bi-stable multivibrator. It is assumed that both the positive H.T. supply $+V'$ and the negative

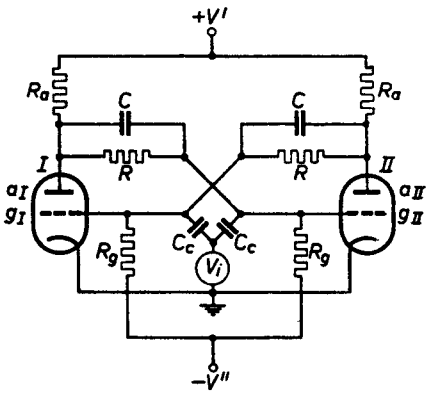

Fig. 1–7.
Fundamental circuit of the bi-stable multivibrator.

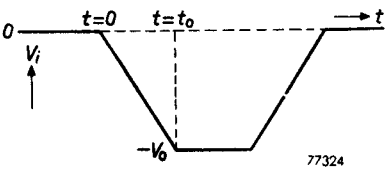

Fig. 2–7.
Input voltage V_i consisting of a negative-going trapezoidal pulse applied to the multivibrator circuit shown in fig. 1–7.

H.T. supply $-V''$ have a negligibly low internal resistance. This also applies to the input voltage source V_i. This input voltage is assumed to be a negative-going trapezoidal pulse as represented in fig. 2.7.

The multivibrator should be triggered, i.e. it should be switched over from condition 1 in which tube *I* is conducting and tube *II* is cut off, to condition 2 in which *I* is cut off and *II* is conducting, by the negative-going flank of this pulse occurring between $t = 0$ and $t = t_0$. With the exception of the anode-to-grid capacitance C_{ag} of the tubes, the stray capacitances, including interelectrode capacitances, can easily be taken into account.

Fig. 3.7 represents the circuit for condition 1, including the stray capacitances, which are indicated by broken lines. Since the left-hand tube *I* is taken to be conducting in condition 1, the internal anode resistance r_a between the anode a_1 and cathode (earth potential) and the internal grid resistance r_g between the grid g_1 and cathode have been incorporated, this grid being assumed to draw current.

If the anode-to-grid capacitances C_{agI} and C_{agII} were absent, it would be possible to split up the circuit into two parts which could be con-

sidered separately with regard to their response to an input pulse V_i. The interaction between both halves of the circuit due to these anode-to-grid capacitances, however, renders the problem more complicated,

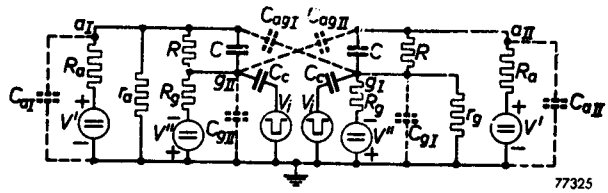

Fig. 3–7.
Equivalent circuit of the bi-stable multivibrator shown in fig. 1–7 in condition 1 (tube *I* conducting, tube *II* cut off). It should be recognized that the left-hand and right-hand halves of this equivalent circuit do not correspond to those of the circuit shown in fig. 1–7.

the more so as the influence of these capacitances is not always the same at all phases of the trigger process. When one or both tubes are conducting, a kind of Miller effect will be experienced. This may be considered as introducing additional input capacitance at the grid of the tubes by an amount $(1 + G)\, C_{ag}$, where G is an "amplification factor" determined by the ratio of the slope of the anode voltage signal to that of the grid voltage signal [4]).

For a non-conducting tube, the effect of C_{ag} will nearly be equivalent to the presence of a capacitive voltage divider between anode and grid, and will influence signals with a steep slope. For tube *I* this can be taken into account by the factor:

$$b_{\mathrm{I}} = \frac{C_{ag\mathrm{I}}}{C_{ag\mathrm{I}} + C_c + C_{g\mathrm{I}} + \dfrac{CC_{a\mathrm{II}}}{C + C_{a\mathrm{II}}}}, \quad \ldots\ldots\ldots \quad (1.7)$$

and for tube *II* by the factor:

$$b_{\mathrm{II}} = \frac{C_{ag\mathrm{II}}}{C_{ag\mathrm{II}} + C_c + C_{g\mathrm{II}} + \dfrac{CC_{a\mathrm{I}}}{C + C_{a\mathrm{I}}}} \quad \ldots\ldots\ldots \quad (2.7)$$

These factors represent the fraction of the anode voltage variation that is transmitted to the grid of the same tube due to the anode-to-grid capacitance of this tube.

For the time being, the influence of the anode-to-grid capacitances

[4]) M.I.T. Radiation Lab. Series, Vol. 19, Waveforms, p. 174.

will be disregarded. In some cases of special interest, which are dealt with in a subsequent section, a correction will be introduced to take this influence into account.

7.2.2. STATIC CONDITION

To determine the static condition, in which all transients due to previous triggering of the multivibrator may be considered to have died out, the capacitances may be omitted from the circuit. Its two halves can then be represented by the diagrams shown in fig. 4.7, fig. 4.7*a*

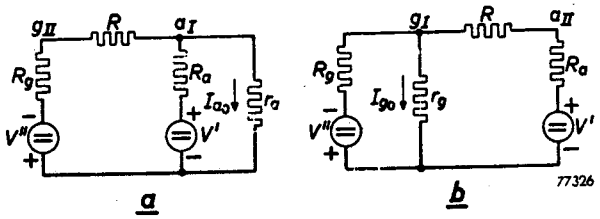

Fig. 4–7.
The two halves of the equivalent circuit shown in fig. 3–7 in the static condition; fig. 4–7*a* corresponds to the left-hand part and fig. 4–7*b* to the right-hand part of this equivalent circuit.

corresponding to the left-hand part and fig. 4.7*b* to the right-hand part of fig. 3.7.

In both circuits a constant current

$$I = \frac{V' + V''}{R_g + R + R_a} \quad \ldots\ldots\ldots\ldots \quad (3.7)$$

will always be present as a result of the two H.T. supply sources $+V'$ and $-V''$.

If no grid current I_{g0} flows in the circuit of fig. 4.7*b*, the voltage drop produced across the resistance R_g by the current I is:

$$V_{Rg1} = R_g \,.\, I = \frac{R_g}{R_g + R + R_a} \,.\, (V' + V''),$$

or, from eq. (17.5):

$$V_{Rg1} = \varepsilon_g \,(V' + V'') \,. \quad \ldots\ldots\ldots \quad (4.7)$$

Together with the voltage source $-V''$, this gives a total grid voltage:

$$V_{g1} = \varepsilon_g V' - (1 - \varepsilon_g)\, V'' \,. \quad \ldots\ldots\ldots \quad (5.7)$$

If this value is sufficiently negative, the grid current will be zero.

In practice, the conducting tube is, however, usually driven beyond the point at which grid current starts to flow. Expression (5.7) will therefore be assumed to be positive. It depends on the type of tube, and more particularly on its grid current versus grid voltage characteristic, i.e. on the value of r_g, what value the potential between grid and cathode will assume (compare section 6.1). It will usually be of the order of a few volts or even less. No great error will therefore be introduced by assuming the grid-to-cathode voltage to be zero. In so doing, it becomes possible to determine the grid current I_{g0} which flows through the resistance R_g shunted across the resistances R and R_g connected in series. The voltage drop produced by this current is:

$$-I_{g0} \cdot \frac{R_g (R + R_a)}{R_g + R + R_a} = -I_{g0} (1 - \varepsilon_g) R_g.$$

The positive voltage V_{g1} given by eq. (5.7) must be compensated by this voltage drop; hence:

$$I_{g0} (1 - \varepsilon_g) R_g = \varepsilon_g V' - (1 - \varepsilon_g) V'',$$

or:

$$I_{g0} = \frac{\varepsilon_g V' - (1 - \varepsilon_g) V''}{(1 - \varepsilon_g) R_g} \quad \ldots\ldots\ldots\ldots \quad (6.7)$$

In this case, the static grid voltage of tube I is:

$$V_{g10} = 0, \quad \ldots\ldots\ldots\ldots \quad (7.7)$$

whilst the anode voltage of tube II is:

$$V_{a110} = \frac{R}{R + R_a} \cdot V' \quad \ldots\ldots\ldots \quad (8.7)$$

In the circuit shown in fig. 4.7*a*, the same current I (eq. (3.7)) is always present, whilst the internal resistance r_a is, moreover, traversed by the anode current I_{a0}. In addition to the voltage drop caused by the current I given by eq. (3.7), a voltage drop $-\varepsilon_g R_a I_{a0}$ will be produced by I_{a0} across R_g, so that the total grid voltage will be:

$$V_{g110} = \varepsilon_g V' - (1 - \varepsilon_g) V'' - \varepsilon_g R_g I_{g0} \quad \ldots\ldots \quad (9.7)$$

Because of the currents I and I_{a0}, the total anode voltage of tube I is:

$$V_{a10} = (1 - \varepsilon_a) V' - \varepsilon_a V'' - \varepsilon_a (R_g + R) I_{a0}, \quad \ldots \quad (10.7)$$

ε_a being given by eq. (17.5).

I_{a0} can be evaluated from the tube characteristics by determining

the point of intersection of the $I_a = f(V_a)$ characteristic at $V_g = 0$ and the load line for the specified values of R_a and V'. I_{a0} can also be expressed in terms of r_a, since, according to fig. 4.7*a*, $V_{a10} = r_a \cdot I_{a0}$. From eq. (10.7):

$$I_{a0} = \frac{(1 - \varepsilon_a)\, V' - \varepsilon_a V''}{\varepsilon_a (R_g + R) + r_a} \quad \ldots\ldots\ldots \quad (11.7)$$

The anode and grid voltages of both tubes in the static condition have now been derived and are given by eqs (7.7), (8.7), (9.7) and (10.7). They are the initial conditions for the transient phenomena which occur after an input trigger pulse has been applied to both grids. These transients must be superimposed on the static voltages. There is no need to consider the H.T. voltages when calculating the transients, the influence of these voltages being included in the static conditions. The H.T. voltages are therefore omitted in the circuits which are used for determining the dynamic conditions of the bi-stable multivibrator.

7.2.3. DYNAMIC CONDITION

From the instant $t = 0$ onwards, V_i is no longer zero, but varies according to the function represented in fig. 2.7, which may be formulated as follows:

$$\left.\begin{aligned} V_i &= 0 \text{ for } t < 0 \\ V_i &= -\alpha t \text{ for } 0 \leqq t \leqq t_0 \\ V_i &= -V_0 \text{ for } t > t_0 \end{aligned}\right\}, \quad \ldots \quad (12.7)$$

where $\alpha = V_0/t_0$.

For the time being, the influence of the positive-going rear flank of V_i will not be considered. The amplitude V_0 of the pulse is assumed to be large enough to ensure that the voltage V_i traverses the entire grid base of the conducting tube I within a fraction of the time of rise t_0. This will usually be the case in practice, because the cut-off voltage of the conducting tube will be fairly small as a result of its low anode voltage. The anode current I_{a0} will therefore be assumed to drop to zero at the instant $t = 0$; in other words: the internal resistance r_a is assumed to become suddenly infinitely large at this instant.

According to the principles treated in Section 2, this discontinuity in the circuit can be accounted for by introducing a current source I_{a0} between the anode a_1 and cathode (earth), its polarity being such that the current I_{a0} previously flowing beween a_1 and cathode through

the internal resistance r_a is compensated. Hence, the left-hand part of the circuit shown in fig. 3.7 will be as depicted in fig. 5.7.

It will be clear that the same reasoning is applicable to the grid current I_{g0} which flows in the right-hand part of the circuit shown in fig. 3.7,

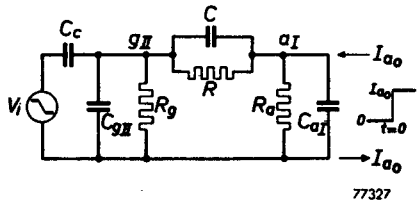

Fig. 5–7.
Left-hand part of the equivalent circuit shown in fig. 3–7 in the first phase of the dynamic condition. The current source I_{a0} introduced between the anode a_I and earth compensates the current I_{a0} previously flowing through the internal resistance r_a.

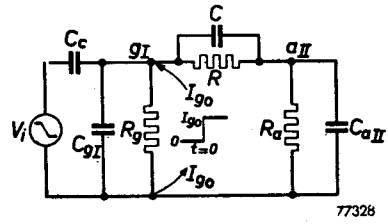

Fig. 6–7.
Right-hand part of the equivalent circuit shown in fig. 3–7 in the first phase of the dynamic condition. The current source I_{g0} introduced between the grid g_I and earth compensates the current I_{g0} previously flowing through the internal grid resistance r_g.

the approximation being even better because a much smaller decrease of the grid potential is sufficient to completely suppress the grid current (see Section 6.1.2). In the right-hand part of this circuit, a current step function I_{g0} should therefore be introduced as depicted in fig. 6.7.

The circuits of figs 5.7 and 6.7 can be further simplified by transforming the voltage source V_i with the capacitance C_c connected in series into a current source I_i with the capacitance C_c connected in parallel according to Thévenin's theorem, so that:

$$I_i = C_c \cdot \frac{dV_i}{dt} \quad \ldots\ldots\ldots\ldots \quad (13.7)$$

In that case:

$$\left.\begin{aligned} &I_i = 0 \text{ for } t < 0 \\ &I_i = -\alpha C_c \text{ for } 0 \leqq t \leqq t_0 \\ &I_i = 0 \text{ for } t > t_0 \end{aligned}\right\} \quad \ldots\ldots \quad (14.7)$$

I_i is a rectangular, negative-going pulse with a duration of t_0 seconds and an amplitude αC_c, or the superposition of a negative-going current step $-\alpha C_c$ at the instant $t = 0$, which will be denoted by $-\alpha C_c U(t)$, and a positive-going current step $+\alpha C_c$ at the instant $t = t_0$, which will be denoted by $+\alpha C_c U(t - t_0)$.

The coupling capacitance C_c is now connected in parallel with the input capacitances C_{gI} and C_{gII}. The sums $C_c + C_{gI}$ and $C_c + C_{gII}$ will be denoted by C_{iI} and C_{iII} respectively. Both circuits of figs 5.7 and 6.7 have now been reduced to the simplified circuit shown in fig. 7.7, which is identical to that shown in fig. 3.5.

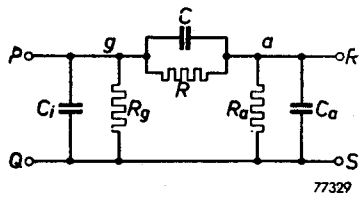

Fig. 7–7.
Simplification of the circuits shown in figs. 5–7 and 6–7 according to Thévenin's theorem.

In the right-hand part of the multivibrator shown in fig. 3.7 (represented by the equivalent circuit shown in fig. 5.7), current steps $+ I_{g0}U(t)$, $-\alpha C_c U(t)$ and $-\alpha C_c U(t - t_0)$ must be introduced at terminals P and Q. The response of a network to these current steps has been calculated in Section 5 and is given by eq. (21*b*.5), i.e. the voltage across P-Q or the grid voltage V_{gI} of tube I.

In order to calculate the anode voltage V_{aII} of tube II, the operational transimpedance from P-Q to R-S must be determined by an operational function similar to that given by eq. (18.5).

In the left-hand part of the multivibrator (see fig. 5.7), current steps $-\alpha C_c U(t)$ and $+\alpha C_c U(t - t_0)$ must be introduced at terminals P and Q, and a current step $I_{a0}U(t)$ at terminals R and S.

In order to calculate the grid voltage V_{gII} of tube II and the anode voltage V_{aI} of tube I, the operational impedances between P-Q and R-S and the operational transimpedance from R-S to P-Q must be determined. These various kinds of impedances all have a form similar to that of eq. (18.5), their denominators being the same, the only difference being the constants R_{eq} and A in the numerator.

7.2.3.1. First phase of the dynamic condition

The slope and the amplitude of the trigger pulse V_i are assumed to be so high that immediately after this pulse has been applied to the grids of the multivibrator tubes, both tubes are non-conducting, which will as a rule be the case in practice. Both grid voltages then tend to a final value, which is determined only by the H.T. supply voltages, i.e. by the current I supplied by these voltage sources; see eq. (3.7) [5]).

[5]) It should be recognized that from this instant onwards the circuit can be considered as a passive network, both tubes being non-conducting, contrary to the switch-over condition of a free-running or astable multivibrator (Abraham and Bloch type), where a regenerative action with both tubes conducting starts as soon as the non-conducting tube reaches its cut-off point.

According to eq. (5.7), this final value, which was assumed to be positive, is $\varepsilon_g V' - (1 - \varepsilon_g)\, V''$.

Sooner or later the grid voltage of one of the tubes will rise beyond the cut-off value, so that anode current will start to flow in this tube. The successful operation of the M.V. depends on which of the two tubes starts conducting. If it is the grid voltage of tube *I* that first reaches the cut-off value, the switching action of the multivibrator will be wrong, for in that case the initial static condition with tube *I* conducting and tube *II* non-conducting will ultimately be re-established, which is not the purpose in view. Conditions must therefore be chosen so that the cut-off value of tube *II* is always reached before that of tube *I*.

The first phase of the dynamic condition of the multivibrator will in any case be defined as that which covers the time interval between the instant $t = 0$, when the trigger pulse starts, and the instant at which the grid voltage of one of the tubes reaches the cut-off value.

The derivation of the time functions which represent the anode and grid voltages during this phase will not be given in full detail, since it is intended to give only a general idea of the lines along which the problem can be solved. The final results are dealt with at the end of this Section. For the time being, the anode and grid voltages will be represented by the following general formulae:

$$\left.\begin{aligned} V_{g\mathrm{I}} &= V_{g\mathrm{I}}(t) \\ V_{a\mathrm{I}} &= V_{a\mathrm{I}}(t) \\ V_{g\mathrm{II}} &= V_{g\mathrm{II}}(t) \\ V_{a\mathrm{II}} &= V_{a\mathrm{II}}(t) \end{aligned}\right\} \quad \ldots\ldots\ldots\ldots \quad (15.7)$$

It will now be indicated how to ascertain which tube starts to draw current first. In a conducting triode, the relation between the anode current I_a and the anode voltage V_a and the grid voltage V_g is given by:

$$I_a = \frac{V_a + \mu V_g}{r_a}, \quad \ldots\ldots\ldots\ldots \quad (16.7)$$

where r_a is the internal resistance and μ is the amplification factor of the tube. The cut-off value E_{co} of the grid voltage is now defined by the condition $I_a = 0$ for $V_g = E_{co}$; hence:

$$0 = V_a + \mu E_{co},$$

or:

$$E_{co} = -\frac{V_a}{\mu}. \quad \ldots\ldots\ldots\ldots \quad (17.7)$$

By means of this relation, the instants t_{I} and t_{II} at which tubes *I* and *II*

respectively reach their cut-off point can be determined. For this purpose, eqs (17.7) and (15.7) are combined in the following relations:

$$\text{for tube } I\text{: } V_{g\mathrm{I}}(t_{\mathrm{I}}) = -\frac{1}{\mu} \cdot V_{a\mathrm{I}}(t_{\mathrm{I}}), \quad \ldots \quad (18.7)$$

$$\text{and for tube } II\text{: } V_{g\mathrm{II}}(t_{\mathrm{II}}) = -\frac{1}{\mu} \cdot V_{a\mathrm{II}}(t_{\mathrm{II}}) \quad \ldots \quad (19.7)$$

These conditions depend on various quantities, namely network elements (resistances and capacitances), supply voltages (V' and V''), the time of rise of the trigger pulse (t_0), the amplitude of this pulse (V_0) and the tube characteristics I_{a0} (which depends on the internal resistance r_a) and μ. It is rather cumbersome to investigate the influence of these parameters on the values of t_{I} and t_{II}. The correct situation is that at which $t_{\mathrm{II}} < t_{\mathrm{I}}$, as the cut-off point of tube *II* will then be reached first. A change in one of the above-mentioned quantities may result in t_{I} and t_{II} assuming different values. If the changes are such that t_{II} decreases and t_{I} increases, it will be all the better, but in the reverse case there is a risk of t_{II} becoming larger than t_{I}. This will result in the multivibrator no longer operating correctly.

The expressions for the anode and grid voltages of both tubes are therefore given below. They will be of particular importance in enabling the practical conclusions to be drawn in a later section regarding the way in which tube characteristics influence the trigger sensitivity of the bi-stable multivibrator.

The time functions which represent the voltages at the anodes and grids of the tubes are defined as follows. For $0 \leqq t \leqq t_0$, the complete expressions can be calculated, but the time interval t_0 is so small that the exponential functions which constitute these expressions can be represented with great accuracy by linear functions. The expressions for $t > t_0$ are also valid for $t = t_0$, so that the voltages for $t = t_0$ can be determined from these functions. For $0 \leqq t \leqq t_0$, the voltages vary linearly with time between the initial static conditions and the calculated values for $t = t_0$. The complete expressions will therefore be given only for $t \geqq t_0$.

For tube *I* (initially conducting):

$$V_{g\mathrm{I}} = \varepsilon_g V' - (1 - \varepsilon_g)\, V'' + \\ + \left\{(1 - \varepsilon_g)\, R_g C_c \cdot \frac{V_0}{t_0} \cdot (e^{-p_1 t_0} - 1) + \varepsilon_g V' - (1 - \varepsilon_g)\, V''\right\} K e^{p_1 t} - \\ - \left\{(1 - \varepsilon_g)\, R_g C_c \cdot \frac{V_0}{t_0} \cdot (e^{-p_2 t_0} - 1) + \varepsilon_g V' - (1 - \varepsilon_g)\, V''\right\} (1 + K) e^{p_2 t}, \quad (20.7)$$

and

$$V_{a\text{I}} = (1-\varepsilon_a)\,V' - \varepsilon_a V'' + \\ + \left\{\varepsilon_a R_g C_c \cdot \frac{V_0}{t_0} \cdot (e^{-p_1 t_0} - 1)\,P + (1-\varepsilon_a)\,R_a I_{a0} L\right\} e^{p_1 t} - \\ - \left\{\varepsilon_a R_g C_c \cdot \frac{V_0}{t_0} \cdot (e^{-p_2 t_0} - 1)\,(1+P) + (1-\varepsilon_a)\,R_a I_{a0}\,(1+L)\right\} e^{p_2 t} \quad (21.7)$$

For tube *II* (initially non-conducting):

$$V_{g\text{II}} = \varepsilon_g V' - (1-\varepsilon_g)\,V'' + \\ + \left\{(1-\varepsilon_g)\,R_g C_c \cdot \frac{V_0}{t_0} \cdot (e^{-p_1 t_0} - 1)\,K + \varepsilon_g R_a I_{a0} P\right\} e^{p_1 t} - \\ - \left\{(1-\varepsilon_g)\,R_g C_c \cdot \frac{V_0}{t_0} \cdot (e^{-p_2 t_0} - 1)\,(1+K) + \varepsilon_g R_a I_{a0}\,(1+P)\right\} e^{p_2 t} \quad (22.7)$$

and

$$V_{a\text{II}} = (1-\varepsilon_a)\,V' - \varepsilon_a V'' + \\ + \varepsilon_a \left\{R_g C_c \cdot \frac{V_0}{t_0} \cdot (e^{-p_1 t_0} - 1) + \frac{\varepsilon_g}{1-\varepsilon_g} \cdot V' - V''\right\} P e^{p_1 t} - \\ - \varepsilon_a \left\{R_g C_c \cdot \frac{V_0}{t_0} \cdot (e^{-p_2 t_0} - 1) + \frac{\varepsilon_g}{1-\varepsilon_g} \cdot V' - V''\right\} (1+P)\, e^{p_2 t} \quad . \quad (23.7)$$

For the values of ε_g and ε_a reference is made to eq. (17.5); for V', V'', R_g, C_c and R_a, see fig. 1.7, and for V_0 and t_0, see fig. 2.7. The transients are determined by two time constants, namely $1/p_1$ and $1/p_2$ (see eqs (18*b*.5), (18*c*.5), (19*a*.5) and (19*b*.5)), whilst:

$$K = \frac{p_2\,(1 + A p_1)}{p_1 - p_2} \text{ (see eqs. (22.5) and (18}a\text{.5))}, \quad . \quad (24.7)$$

$$P = \frac{p_2\,(1 + T p_1)}{p_1 - p_2} \text{ (for } T \text{ see eq. (16.5))} \quad . \quad . \quad . \quad . \quad . \quad (25.7)$$

and

$$L = \frac{p_2\,(1 + D p_1)}{p_1 - p_2}, \quad . \quad . \quad . \quad . \quad . \quad . \quad . \quad . \quad . \quad (26.7)$$

where:

$$D = \frac{R}{R + R_g} \cdot T_g + \frac{R_g}{R + R_h} \cdot T \quad \text{(for } T \text{ and } T_g\text{, see eq. (16.5))} \quad (27.7)$$

7.2.3.2. Second and third phase of the dynamic condition

Disregarding the case in which the grid voltage of tube *I* reaches the cut-off value first, it will be assumed that conditions are chosen so that the required flip-flop operation is obtained. At a certain instant $t = t_{II}$, determined by eq. (19.7), tube *II* reaches a condition at which anode current starts to flow. This instant is the commencement of the second phase of the dynamic condition. For the new transients which now start, this instant $t = t_{II}$ will be taken as the zero point of a new time scale.

V_{gII} now traverses the grid base of tube *II* according to an exponential time function (see fig. 8.7). It is assumed that the part of this exponential function that is situated within the grid base is such a small fraction of the total curve that it may be considered as a linear function of time, i.e.:

$$V_{gII} = at + E_{co} \quad . \quad . \quad . \quad (28.7)$$

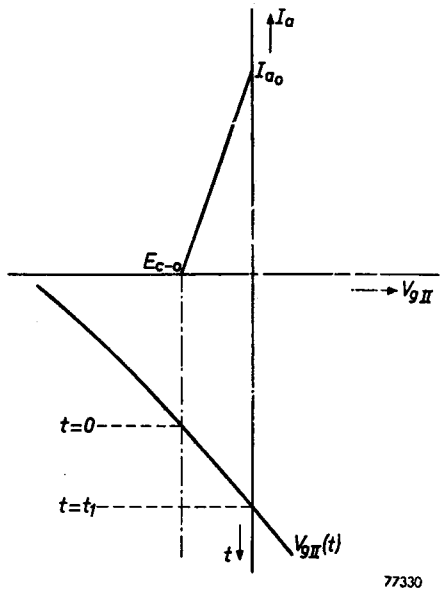

Fig. 8-7.
Grid-voltage variation V_{gII} and corresponding anode current variation I_{a0} as functions of time during the second phase of the dynamic conditions at which tube *II* becomes conducting. E_{co} represents the cut-off voltage of tube *II*.

For $t = t_1$, the grid voltage becomes zero; hence:

$$at_1 = -E_{co}, \quad . \quad . \quad . \quad . \quad . \quad . \quad . \quad . \quad . \quad . \quad (29.7)$$

or, from eq. (17.7):

$$at_1 = \frac{V_{a0}}{\mu}, \quad . \quad . \quad . \quad . \quad . \quad . \quad . \quad . \quad . \quad . \quad (30.7)$$

where E_{co} denotes the cut-off voltage corresponding to the anode voltage V_{a0} of tube *II* which is present at the instant $t = 0$ (i.e. t_{II} in the time scale of the first dynamic phase).

For values of V_{gII}, situated within the grid base, the anode current of tube *II* is defined by:

$$I_a = \frac{V_{aII} + \mu V_{gII}}{r_a} \quad . \quad . \quad . \quad . \quad . \quad . \quad . \quad . \quad . \quad (31.7)$$

V_{aII} should now be defined as a function of time. It is therefore necessary to derive another relation between I_a and V_{aII}. Now the voltage drop across the anode impedance Z_{ai}, i.e. the impedance between terminals R and S in fig. 7.7, is given bv:

$$V' - V_{aII} = Z_{ai} I_a, \quad . \quad . \quad . \quad . \quad . \quad . \quad . \quad . \quad . \quad (32.7)$$

when the constant current I (eq. (3.7)) through the voltage divider R_a, R, R_g is neglected. This current, however, results in the anode voltage at $I_a = 0$ differing from the H.T. supply voltage V', its value being an amount $(V' + V'')\, R_a/(R_g + R + R_a)$ lower than V'. Eq. (32.7) should therefore be replaced by:

$$V' - \frac{R_a}{R_g + R + R_a} \cdot (V' + V'') - V_{aII} = Z_{ai} I_a,$$

or:

$$(1 - \varepsilon_a)\, V' - \varepsilon_a V'' - V_{aII} = Z_{ai} I_a \quad . \quad . \quad . \quad . \quad . \quad . \quad (33.7)$$

This includes the assumption that the transients occurring in the anode voltage of tube *II* due to the first phase of the dynamic condition, i.e. the exponential terms of eq. (23.7), have practically disappeared for $t = t_{II}$. Eq. (33.7) can be written:

$$V_{a0} - V_{aII} = Z_{ai} I_a, \quad . \quad . \quad . \quad . \quad . \quad . \quad . \quad . \quad . \quad (34.7)$$

where:

$$V_{a0} = (1 - \varepsilon_a)\, V' - \varepsilon_a V''.$$

From eqs. (34.7) and (31.7):

$$V_{a0} - V_{aII} = \frac{V_{a0} + \mu V_{gII}}{1 + \frac{r_a}{Z_{ai}}} \quad . \quad . \quad . \quad . \quad . \quad . \quad (35.7)$$

Substitution of $V_{g\,II}$ by the value given by eq. (28.7) gives:

$$V_{a0} - V_{a\,II} = \frac{V_{a0} + \mu E_{co} + \mu at}{1 + \frac{r_a}{Z_{ai}}},$$

or, since, according to eqs (29.7) and (30.7), $V_{a0} + \mu E_{co} = 0$:

$$V_{a0} - V_{a\,II} = \frac{\mu at}{1 + \frac{r_a}{Z_{ai}}} \quad \ldots\ldots\ldots \quad (36.7)$$

Z_{ai} is an operational impedance of the form:

$$Z_{ai} = R_{ai} \cdot \frac{1 + Dp}{1 + Bp + Ep^2}, \quad \ldots\ldots\ldots \quad (37.7)$$

where:

$$R_{ai} = \frac{R_a (R + R_g)}{R_g + R + R_a}, \quad \ldots\ldots\ldots \quad (38.7)$$

and D, B and E are given by eqs (27.7), (18b.5) and (18c.5) respectively.

Combination of eqs (36.7) and (37.7) gives:

$$V_{a0} - V_{a\,II} = \frac{R_{ai}}{R_{ai} + r_a} \cdot \frac{1 + Dp}{1 + Fp + Gp^2} [\mu at], \quad \ldots \quad (39.7)$$

where:

$$F = \frac{R_{ai}}{R_{ai} + r_a} \cdot D + \frac{r_a}{R_{ai} + r_a} \cdot B, \quad \ldots\ldots \quad (39a.7)$$

and:

$$G = \frac{r_a}{R_{ai} + r_a} \cdot E. \quad \ldots\ldots\ldots \quad (39b.7)$$

Eq. (39.7) can be calculated by the operational methods indicated in Section 5, the final result being:

$$V_{a\,II} = V_{a0} - \frac{R_{ai}}{R_{ai} + r_a} \cdot V_{a0} \cdot \left\{ -\frac{Q}{p_3 t_1} \cdot (1 - e^{p_3 t}) + \frac{1 + Q}{p_4 t_1} \cdot (1 - e^{p_4 t}) + \frac{t}{t_1} \right\} \quad \ldots\ldots\ldots \quad (40.7)$$

Here eq. (30.7) has been introduced; r_a is the internal anode resistance of the tube determined by the slope of the $I_a = f(V_a)$ characteristics, whilst:

$$Q = \frac{p_4 (1 + D p_3)}{p_3 - p_4}, \quad \ldots\ldots\ldots \quad (40a.7)$$

$$p_3 = -\frac{F}{2G} \cdot \left(1 - \sqrt{1 - \frac{4G}{F^2}}\right) \quad \ldots\ldots\ldots \quad (40b.7)$$

and:

$$p_4 = -\frac{F}{2G} \cdot \left(1 + \sqrt{1 - \frac{4G}{F^2}}\right) \quad \ldots\ldots\ldots \quad (40c.7)$$

The value of t_1 can be determined from eq. (22.7) by the condition that $V_{g\,II} = 0$ for $t = t_{II} + t_1 = t_s$.

Eq. (40.7) is valid for $0 < t < t_1$. At the instant $t = t_1$ in the time scale of eq. (40.7), $V_{g\,II}$ becomes zero, and it is assumed that at this instant (commencement of the third phase) grid current starts to flow in tube *II* to such an extent that $V_{g\,II}$ is kept rigorously constant at the value zero. This implies another transient phenomenon, namely sudden short-circuiting of the grid and cathode of the tube. It can be accounted for by adding a new component:

$$V_{g\,II} = -\mu a\,(t - t_1) \quad \ldots\ldots\ldots \quad (41.7)$$

to the grid voltage. This gives rise to another term in the anode voltage of a form similar to eq. (40.7), but shifted in time by t_1 seconds. The superposition of these two components gives the following final expression for $V_{a\,II}$ at $t \geqq t_1$:

$$V_{a\,II} = \frac{r_a}{R_{ai} + r_a} \cdot V_{a0} - \frac{R_{ai}}{R_{ai} + r_a} \cdot$$

$$\cdot V_{a0} \left\{ \frac{Q}{p_3 t_1} \cdot (1 - e^{-p_3 t_1})\, e^{p_3 t} - \frac{1 + Q}{p_4 t_1} \cdot (1 - e^{-p_4 t_1})\, e^{p_4 t} \right\} \quad \ldots\ldots \quad (42.7)$$

The transient voltages at the grid and anode of tube *II* have now been derived for the complete triggering action. The grid voltage $V_{g\,II}$ is given by eq. (22.7), valid for $t_0 \leqq t \leqq t_s$, whilst $V_{g\,II} = 0$ for $t > t_s$. The anode voltage $V_{a\,II}$ is given by eq. (23.7) for $t_0 \leqq t \leqq t_{II}$, by eq. (32.7) for $t_{II} \leqq t \leqq t_s$, and by eq. (42.7) for $t > t_s$.

Tube *I* was assumed to be non-conducting during the first and second phases of the triggering action and will therefore produce no new transients as a result of anode or grid current surges.

During the second phase, the grid voltage of tube *I* can be calculated directly from the anode voltage of tube *II*, whilst the anode voltage of tube *I* depends entirely on the grid voltage of tube *II*.

Fig. 7.7 reveals that V_{g1} is determined by a voltage divider circuit between a_{II} and $_{g1}$. The operational impedance of C_i and R_g connected in parallel is:

$$Z_g = \frac{R_g}{1 + R_g C_i p} = \frac{R_g}{1 + T_g p} \quad \ldots\ldots\ldots \quad (43.7)$$

Similarly, the operational impedance of C and R connected in parallel is:

$$Z = \frac{R}{1 + RCp} = \frac{R}{1 + Tp} \quad \ldots\ldots\ldots \quad (44.7)$$

It will be clear that:

$$V_{g1} = \frac{Z_g}{Z_g + Z}[V_{aII}] \quad \ldots\ldots\ldots\ldots \quad (45.7)$$

Hence, from eqs (43.7) and (44.7):

$$V_{g1} = \beta_g V_{aII} + \beta_g \beta \cdot \frac{T - T_g}{D} \cdot \frac{p}{\frac{1}{D} + p}[V_{aII}], \quad \ldots\ldots \quad (46.7)$$

where:

$$\beta = \frac{R}{R_g + R'} \quad \ldots\ldots\ldots\ldots \quad (46a.7)$$

$$\beta_g = \frac{R_g}{R_g + R'} \quad \ldots\ldots\ldots\ldots \quad (46b.7)$$

and:

$$D = \beta T_g + \beta_g T \text{ (see eq. (27.7))} \quad \ldots\ldots \quad (46c.7)$$

Eq. (46.7) demonstrates the well-known fact that voltage division by means of two RC parallel circuits connected in series gives an undistorted copy of the input voltage, decreased according to the resistance ratios, provided the time constants of the two RC-combinations are equal. In that case $T - T_g = 0$ (compare Section 6.1).

When $T > T_g$, the voltage at g_1 will initially exceed its final value (overshoot), whereas, when $T < T_g$, this voltage will gradually increase until the final value is reached without ever being exceeded.

It should be noted that in eq. (46.7) the value of V_{aII} which should be substituted must not contain the constant term V_{a0}, the latter being incorporated in the static conditions of V_{g1}. From eq. (46.7) it can be calculated that, for $0 \leqq t \leqq t_1$ (second phase of the dynamic condition):

$$V_{g1} = \beta_g \cdot \frac{R_{ai}}{R_{ai} + r_a} \cdot V_{a0} \cdot \left[Q \left\{ \frac{1}{p_3 t_1} + \frac{\beta (T - T_g)}{t_1 (1 + D p_3)} \right\} (1 - e^{p_3 t}) - \right.$$

$$- (1 + Q) \left\{ \frac{1}{p_4 t_1} + \frac{\beta (T - T_g)}{t_1 (1 + D p_4)} \right\} (1 - e^{p_4 t}) -$$

$$\left. - \beta \cdot \frac{T - T_g}{t_1} \cdot \left\{ \frac{Q}{1 + D p_3} - \frac{1 + Q}{1 + D p_4} + 1 \right\} (1 - e^{-t/D}) - \frac{t}{t_1} \right], \quad . \quad . \quad (47.7)$$

whilst for $t \geqq t_1$ (third phase of the dynamic condition):

$$V_{g1} = -\beta_g \cdot \frac{R_{ai}}{R_{ai} + r_a} \cdot V_{a0} \cdot \left[Q \left\{ \frac{1}{p_3 t_1} + \frac{\beta (T - T_g)}{t_1 (1 + D p_3)} \right\} (1 - e^{-p_3 t_1}) e^{p_3 t} - \right.$$

$$- (1 + Q) \left\{ \frac{1}{p_4 t_1} + \frac{\beta (T - T_g)}{t_1 (1 + D p_4)} \right\} (1 - e^{-p_4 t_1}) e^{p_4 t} -$$

$$\left. - \beta \cdot \frac{T - T_g}{t_1} \cdot \left\{ \frac{Q}{1 + D p_3} - \frac{1 + Q}{1 + D p_4} + 1 \right\} (1 - e^{t_1/D}) e^{-t/D} + 1 \right]. \quad (48.7)$$

To obtain the complete value of V_{g1} in the second and the third phase, these expressions must be added to eq. (20.7). In doing so, it should be remembered that the zero point of the time scale of eqs (47.7) and (48.7) corresponds to $t = t_{11}$ in the time scale of eq. (20.7).

The last voltage occurring in the second and third phases that should be determined is V_{a1}. It has already been shown that V_{a1} depends only on V_{g11}, which is entirely determined by eq. (22.7) until the instant $t = t_s$, when it drops to zero. For $t > t_s$, V_{g11} remains zero. This discontinuity can be accounted for by assuming a voltage of opposite sign but equal to V_{g11} being present between g_{11} and cathode from the instant $t = t_s$ onwards. Part of this voltage will be passed on to a_1 via the voltage divider formed by R-C, R_a-C_a (see fig. 7.7), which gives:

$$V_{a1} = \frac{Z_a}{Z_a + Z} \cdot [V_{g11}], \quad . \quad . \quad . \quad . \quad . \quad . \quad . \quad . \quad . \quad (49.7)$$

where:

$$Z_a = \frac{R_a}{1 + T_a p}, \quad . \quad . \quad . \quad . \quad . \quad . \quad . \quad . \quad . \quad (49a.7)$$

and (see eq. (44.7)):

$$Z = \frac{R}{1 + Tp}. \quad . \quad . \quad . \quad . \quad . \quad . \quad . \quad . \quad . \quad (49b.7)$$

From eqs. (49.7), (49*a*.7) and (49*b*.7):

$$V_{a1} = \gamma_a V_{g11} + \gamma_a \gamma \cdot \frac{T - T_a}{a} \cdot \frac{p}{\frac{1}{A} + p} [V_{g11}], \quad . \quad . \quad . \quad . \quad (50.7)$$

where:

$$\left.\begin{aligned} \gamma_a &= \frac{R_a}{R + R_a} \\ \gamma &= \frac{R}{R + R_a} \end{aligned}\right\}, \quad . \quad . \quad . \quad . \quad . \quad . \quad . \quad . \quad . \quad (50a.7)$$

and:

whilst $T = RC$, $T_a = R_a C_a$, and, according to eq. (18*a*.5):

$$A = \gamma T_a + \gamma_a T.$$

By writing eq. (22.7):

$$V_{g11} = V + V_1 e^{p_1 t} + V_2 e^{p_2 t}, \quad . \quad . \quad . \quad . \quad . \quad . \quad . \quad (51.7)$$

where V, V_1 and V_2 are constants, it follows from eq. (50.7) that:

$$\begin{aligned} V_{a1} = &- \gamma_a V - \gamma_a V_1 e^{p_1 t_s} \left\{1 + \gamma (T - T_a) \cdot \frac{p_1}{1 + p_1 A}\right\} e^{p_1 t} - \\ &- \gamma_a V_2 e^{p_2 t_s} \left\{1 + \gamma (T - T_a) \cdot \frac{p_2}{1 + p_2 A}\right\} e^{p_2 t} + \\ &+ \gamma_a \gamma (T - T_a) \left\{\frac{p_1}{1 + p_1 A} \cdot V_1 e^{p_1 t_s} + \frac{p_2}{1 + p_2 A} \cdot V_2 e^{p_2 t_s}\right\} \cdot e^{-t/A} \quad . \quad . \quad (52.7) \end{aligned}$$

The zero point of the time scale of eq. (52.7) corresponds to $t = t_s$ in the time scale of eq. (21.7). The total voltage V_{a1} is the sum of eqs (21.7) and (52.7).

Since the circuit has been assumed to be symmetrical, it will be clear that after a sufficiently long time, when the trigger transients have died out, the final values of the grid and anode voltages of tube *I* must be equal to the initial values of the corresponding voltages of tube *II* and vice versa. Denoting the final values by the index ∞, it should follow from the expressions derived above that:

$$V_{g1\infty} = V_{g11 0}, \qquad V_{a1\infty} = V_{a11 0},$$
$$V_{g11\infty} = V_{g10} \quad \text{and} \quad V_{a11\infty} = V_{a10}.$$

It will be shown below that this is indeed the case.

According to eqs (20.7) and (48.7), for $t = \infty$:

$$V_{g\mathrm{I}\infty} = \varepsilon_g V' - (1 - \varepsilon_g)\, V'' - \beta_g \cdot \frac{R_{ai}}{R_{ai} + r_a} \cdot V_{a0} \quad . \qquad (53.7)$$

Now V_{a0} is the constant term from eq. (23.7), viz.

$$V_{a0} = (1 - \varepsilon_a)\, V' - \varepsilon_a V'',$$

whilst, according to eq. (38.7), $R_{ai} = \varepsilon_a (R + R_g)$, which gives:

$$V_{g\mathrm{I}\infty} = \varepsilon_g V' - (1 - \varepsilon_g)\, V'' - \frac{\beta_g \varepsilon_a (R + R_g)}{\varepsilon_a (R + R_g) + r_a} \cdot V_{a0} =$$

$$= \varepsilon_g V' - (1 - \varepsilon_g)\, V'' -$$

$$- \frac{\varepsilon_g R_a}{\varepsilon_a (R + R_g) + r_a} \cdot \left\{(1 - \varepsilon_a)\, V' - \varepsilon_a V''\right\} . \quad . \quad . \quad . \quad . \quad . \quad . \quad . \quad . \quad (54.7)$$

From eqs (54.7) and (11.7):

$$V_{g\mathrm{I}\infty} = \varepsilon_g V' - (1 - \varepsilon_g)\, V'' - \varepsilon_g R_a I_{a0}, \quad . \quad . \quad . \quad . \quad . \quad . \quad (55.7)$$

which is identical to the value of $V_{g\mathrm{II}0}$ given by eq. (9.7).

From eqs (21.7) and (52.7) it can be seen that:

$$V_{a\mathrm{I}\infty} = (1 - \varepsilon_a)\, V' - \varepsilon_a V'' - \gamma_a V =$$

$$= (1 - \varepsilon_a)\, V' - \varepsilon_a V'' - \frac{R_a}{R + R_a} \left\{\varepsilon_g V' - (1 - \varepsilon_g)\, V''\right\} =$$

$$= \frac{R_g + R}{R_g + R + R_a} \cdot V' - \frac{R_a}{R_g + R + R_a} \cdot V'' - \frac{R_a R_g}{(R + R_a)(R_g + R + R_a)} \cdot V' +$$

$$+ \frac{R_a}{R + R_a} \cdot \frac{R + R_a}{R_g + R + R_a} \cdot V'' =$$

$$= \frac{(R_g + R)(R + R_a) - R_a R_g}{(R + R_a)(R_g + R + R_a)} \cdot V' = \frac{R}{R + R_a} \cdot V', \quad . \quad . \quad . \quad . \quad . \quad (56.7)$$

which is identical to the value of $V_{a\mathrm{II}0}$ given by eq. (8.7).

$V_{g\mathrm{II}\infty}$ is obviously equal to $V_{g\mathrm{I}0}$, both quantities being zero.

According to eq. (40.7):

$$V_{a\mathrm{II}\infty} = \frac{r_a}{R_{ai} + r_a} \cdot V_{a0} = \frac{r_a}{R_{ai} + r_a} \cdot \left\{(1 - \varepsilon_a)\, V' - \varepsilon_a V''\right\} \qquad (57.7)$$

According to eqs (10.7) and (11.7):

$$V_{a10} = \left\{(1-\varepsilon_a)\,V' - \varepsilon_a V''\right\}\left\{1 - \frac{\varepsilon_a (R_g + R)}{\varepsilon_a (R_g + R) + r_a}\right\} =$$

$$= \frac{r_a}{\varepsilon_a (R_g + R) + r_a} \cdot \left\{(1-\varepsilon_a)\,V' - \varepsilon_a V''\right\}, \quad \ldots\ldots \quad (58.7)$$

which is identical to the value of $V_{aII\infty}$ given by eq. (57.7).

It should be recognized that the derivation of the expressions which give the flip-flop operation in a mathematical form is not restricted to symmetrical circuits. In practice, one of the anode circuits is often loaded by a subsequent bi-stable multivibrator circuit, so that in any case the capacitive loads of both anode circuits are no longer equal. An example of this asymmetrical loading will be dealt with in a subsequent section.

7.2.4. VARIATIONS OF THE FUNDAMENTAL CIRCUIT

7.2.4.1. Bi-stable multivibrator with automatic grid bias

Instead of incorporating the separate negative grid bias supply $-V''$ in the multivibrator circuit as shown in fig. 1.7, automatic negative grid bias may be applied by inserting a by-passed cathode resistor in the circuit (see fig. 9.7).

If the time constant of the cathode circuit is sufficiently large, the voltage drop thus produced may be considered as a constant voltage source, at least during the triggering action. This voltage drop depends, however, on the value of the anode current in the static condition. This condition can be described by the following values of the grid and anode voltages with respect to earth:

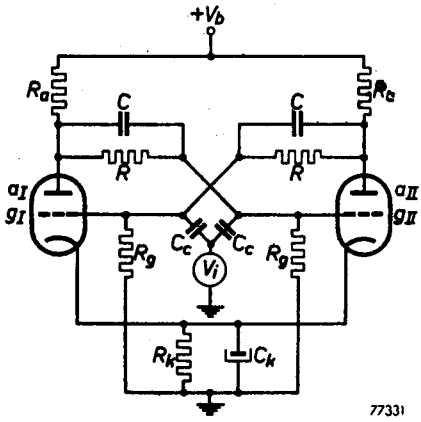

Fig. 9–7.
Bi-stable multivibrator circuit in which automatic grid bias is obtained by means of the by-passed cathode resistor R_k.

$$\left.\begin{aligned} V_{gI10} &= \varepsilon_g V_b - \varepsilon_g R_a I_{a0} \\ V_{a10} &= (1-\varepsilon_a)\,(V_b - I_{a0} R_a) \\ V_{g10} &= \varepsilon_g V_b - I_{g0}\,(1-\varepsilon_g)\,R_g \\ V_{aI10} &= V_b - \frac{\varepsilon_a}{1-\varepsilon_g} \cdot (V_b - R_k I_{a0}) \end{aligned}\right\} \quad \ldots\ldots \quad (59.7)$$

The grid current I_{g0} can be determined by assuming V_{g10} to be equal to the static cathode voltage $V_k = R_k (I_{a0} + I_{g0})$, which gives:

$$I_{a0} = \frac{\varepsilon_g V_b - R_k I_{a0}}{R_k + (1 - \varepsilon_g) R_g} \quad \ldots\ldots\ldots \quad (60.7)$$

The triggering process can be calculated in a way analogous to that previously described by taking these static initial conditions as a starting point.

7.2.4.2. Trigger pulses applied to the anodes

It will be clear that the formulae applicable to the case of the trigger pulses being applied to the anodes can be derived by behaving the procedure outlined above. The input current pulse I_i is then fed to terminals R and S of the circuit shown in fig. 7.7, whilst the coupling capacitance C_c should be added to the anode capacitances C_{aI} and C_{aII} instead of to the grid capacitances C_{gI} and C_{gII}.

7.2.4.3. Trigger pulses applied to a tap of the grid leak resistors

In the circuit shown in fig. 10.7, the trigger pulses are applied to a tap of the grid leak resistors.

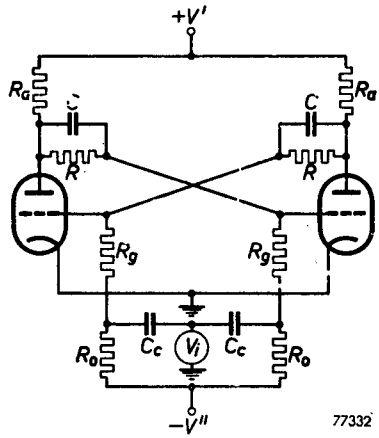

Fig. 10–7.
Bi-stable multivibrator circuit in which the trigger pulses are applied to a tap of the grid leak resistors R_g-R_0.

The transients occurring in this circuit can be calculated by means of the equivalent circuit shown in fig. 11.7, which for the sake of convenience should be compared with the circuit shown in fig. 7.7.

Taking into account the input and output capacitances of the tubes, C_g and C_a respectively (indicated by the broken lines in fig. 11.7), the denominator of the operational impedances which have to be dealt with will contain a polynomial of the third order in p. A third-order equation must therefore be solved to determine the time constants of the e-powers which form the final solution of the voltage time functions. Since there is no straightforward method for solving third-order equations, as is the case with second-order equations, each case will have to be solved after numerical values have been substituted.

An approximate solution is possible when C_g and C_a are so small that they may be neglected. The third-order denominator of the operational impedance is then reduced to the second order.

In practice, the input trigger pulses are often applied to a common tap of the grid leak resistors, so that the resistances R_0 of the circuit shown in fig. 10.7 coincide. In that case, the two halves of the multivibrator circuit are, however, no longer independent of each other and some interaction will necessarily occur. When R_0 is small compared with R_g, the previous methods of calculation may, however, be applied to a first approximation.

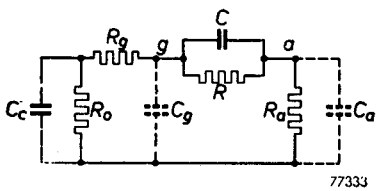

Fig. 11–7.
Equivalent circuit of the bi-stable multivibrator shown in fig. 10–7 (cf. fig. 7–7).

7.2.4.4. Trigger pulses applied to a tap of the anode resistors

The case of the trigger pulses being applied to a tap of the anode resistors is obviously analogous to that discussed in Section 7.2.4.3.

Determination of the voltage time functions can be dealt with in a similar manner using the same approximations.

7.2.5. INFLUENCE OF THE TUBE CHARACTERISTICS ON THE SENSITIVITY OF A BI-STABLE MULTIVIBRATOR

In previous sections an analysis was given of the bi-stable multivibrator or Eccles-Jordan flip-flop circuit. In the present section the method of investigating the influence of the tube characteristics on the sensitivity of the multivibrator by means of the formulae derived in the earlier sections is discussed.

7.2.5.1. Introduction

In Section 7.2.3, the trigger action of a bi-stable multivibrator or

Eccles-Jordan flip-flop circuit is investigated and explicit expressions are given for the anode and grid voltages as functions of time during the first and the second phase of the trigger action [6]). These explicit time functions offer the possibility of determining the length of time required by each tube to reach its cut-off point. The calculated time functions for the initially conducting tube *I* are denoted by $V_{gI}(t)$ and $V_{aI}(t)$, and those for the initially cut-off tube *II* by $V_{gII}(t)$ and $V_{aII}(t)$. The lengths of time t_I and t_{II} after which tubes *I* and *II* reach their respective cut-off points are then defined by the following relations:

$$V_{gI}(t_I) = -\frac{1}{\mu} \cdot V_{aI}(t_I), \quad \ldots\ldots\ldots \quad (61.7)$$

and

$$V_{gII}(t_{II}) = -\frac{1}{\mu} \cdot V_{aII}(t_{II}), \quad \ldots\ldots\ldots \quad (62.7)$$

according to expressions (18.7) and (19.7) given in section 7.2.3.1.

In these relations, the influence of the anode-to-grid capacitances of the tubes has not been incorporated. This influence can be taken roughly into account by adding to the grid voltages a component supplied by a capacitive voltage divider between the anodes and the grids. Only the transient components and not the steady-state parts of the anode voltages will be passed to the grids. Denoting these transient components by V_{aItr} and V_{aIItr} respectively, eqs (61.7) and (62.7) are then changed into:

$$V_{gI}(t_I) + b_I V_{aItr}(t_I) = -\frac{1}{\mu} \cdot V_{aI}(t_I), \quad \ldots\ldots\ldots \quad (63.7)$$

and

$$V_{gII}(t_{II}) + b_{II} V_{aIItr}(t_{II}) = -\frac{1}{\mu} \cdot V_{aII}(t_{II}) \quad \ldots\ldots\ldots \quad (64.7)$$

The voltage divider factors b_I and b_{II} are given by eqs (1.7) and (2.7) of section 7.2.1.

---

[6]) The first phase is understood to commence at the instant $t = 0$ at which the trigger pulse is applied. Tube *I* is assumed to be conducting prior to this instant, tube *II* then being cut off. Conditions are assumed to be such that tube *I* is immediately cut off, tube *II* remaining in the cut-off condition during this phase. The first phase is therefore characterized by the fact that the circuit may be considered as a passive network.

The second phase commences at the instant $t = t_{II}$, at which tube *II*, which was originally cut off, becomes conducting. This phase continues until the instant t_s, at which grid current starts to flow in the conducting tube *II* and the third phase starts. The latter continues until the transients have died out.

Once the circuit is given, it is now possible to investigate the influence of the amplitude V_0 of the negative-going flank of the input trigger pulse, provided the time of rise t_0 is kept constant. Fig. 12.7 shows the complete circuit and fig. 13.7 the shape of the trigger voltage.

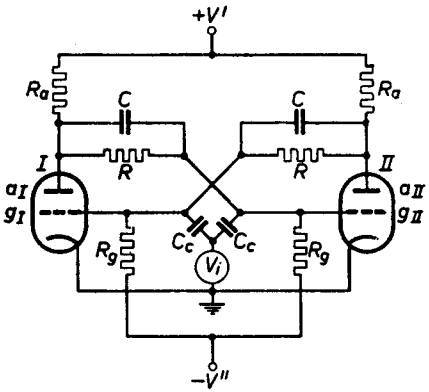

Fig. 12–7.
Fundamental circuit of the bi-stable multivibrator.

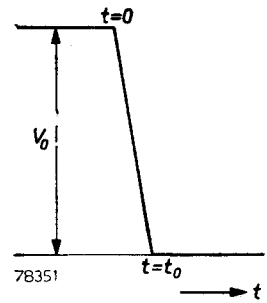

Fig. 13–7.
Negative-going trigger voltage of amplitude V_0 applied at the instant $t = o$.

When all circuit components, the supply voltages and tube characteristics, as well as the time of rise t_0 of the trigger pulse V_i, are known, it is possible to substitute a certain value of the amplitude of V_i, namely V_0, in the relations (61.7) and (62.7) or (63.7) and (64.7). By solving these relations for t_I and t_{II}, numerical values are obtained for these time periods.

When $t_I > t_{II}$, the circuit will operate in the correct way. Successive calculations for decreasing values of V_0 will eventually give a value at which t_I is equal to or even smaller than t_{II}. In the latter case, the multivibrator will no longer operate satisfactorily; the value of V_0 at which $t_I = t_{II}$ must therefore be considered as the minimum pulse amplitude at which the multivibrator will be triggered in the correct manner. This special value of V_0 will be called the critical trigger pulse amplitude V_{cr} and may be considered as a measure of the sensitivity of the multivibrator.

7.2.5.2. Influence of several tube characteristics on the sensitivity of the multivibrator

The time functions which represent the grid and anode voltages of the multivibrator from the instant $t = 0$ onwards, at which the trigger pulse is applied (see fig. 13.7), until the instant at which one

of the tubes reaches its cut-off point, are given by eqs (20.7), (21.7), (22.7) and (23.7) of Section 7.2.3.1. Strictly speaking, these equations are valid only from the instant $t = t_0$ onwards, but since these voltages depend almost linearly on the time between $t = 0$ and $t = t_0$, and the value for $t = t_0$ is given by the above-mentioned expressions, the voltages for $0 \leqq t \leqq t_0$ can be approximately represented by a linear function which starts at a value equal to the initial static condition and has a final value equal to that calculated for $t = t_0$.

It should be realized that the expressions mentioned are applicable to a symmetrical bi-stable multivibrator circuit. Since, however, it is desired to investigate, among other things, the influence of an asymmetrical capacitive load applied to one of the anode circuits, these expressions are given below for the more general case in which the two halves of the circuit are not identical.

In that case, the grid voltage of the originally conducting tube I will be:

$$V_{g\mathrm{I}}(t) = \varepsilon_g V' - (1 - \varepsilon_g)\, V'' +$$
$$+ \left\{(1 - \varepsilon_g)\, R_g C_c \cdot \frac{V_0}{t_0} \cdot (e^{-p_1 t_0} - 1) + \varepsilon_g V' - (1 - \varepsilon_g)\, V''\right\} K e^{p_1 t} -$$
$$- \left\{(1 - \varepsilon_g)\, R_g C_c \cdot \frac{V_0}{t_0} \cdot (e^{-p_2 t_0} - 1) + \varepsilon_g V' - (1 - \varepsilon_g) V''\right\} (1+K) e^{p_2 t}, \quad (65.7)$$

and the anode voltage of tube I:

$$V_{a\mathrm{I}}(t) = (1 - \varepsilon_a)\, V' - \varepsilon_a V'' +$$
$$+ \left\{\varepsilon_a R_g C_c \cdot \frac{V_0}{t_0} \cdot (e^{-p_1 t_0} - 1)\, P_1 + (1 - \varepsilon_a)\, R_a I_{a0} L\right\} e^{p_1 t} -$$
$$- \left\{\varepsilon_a R_g C_c \cdot \frac{V_0}{t_0} \cdot (e^{-p_2 t_0} - 1)\,(1 + P_1) + (1 - \varepsilon_a)\, R_a I_{a0}\,(1 + L)\right\} e^{p_2 t} \quad (66.7)$$

The grid voltage of the initially cut-off tube II will be:

$$V_{g\mathrm{II}}(t) = \varepsilon_g V' - (1 - \varepsilon_g)\, V'' +$$
$$+ \left\{(1 - \varepsilon_g)\, R_g C_c \cdot \frac{V_0}{t_0} \cdot (e^{-p_1 t_0} - 1)\, K_1 + \varepsilon_g R_a I_{a0} P_1\right\} e^{p_1 t} -$$
$$- \left\{(1 - \varepsilon_g)\, R_g C_c \cdot \frac{V_0}{t_0} \cdot (e^{-p_2 t_0} - 1)\,(1 + K_1) + \varepsilon_g R_a I_{a0}\,(1 + P_1)\right\} e^{p_2 t}, \quad (67.7)$$

and the anode voltage of tube II:

$$V_{an}(t) = (1 - \varepsilon_a)\, V' - \varepsilon_a V'' +$$
$$+ \varepsilon_a \left\{ R_g C_c \cdot \frac{V_0}{t_0} \cdot (e^{-p_1 t_0} - 1) + \frac{\varepsilon_g}{1 - \varepsilon_g} \cdot V' - V'' \right\} P e^{p_1 t} -$$
$$- \varepsilon_a \left\{ R_g C_c \cdot \frac{V_0}{t_0} \cdot (e^{-p_2 t_0} - 1) + \frac{\varepsilon_g}{1 - \varepsilon_g} \cdot V' - V'' \right\} (1 + P)\, e^{p_2 t}. \qquad (68.7)$$

In these formulae:

and

$$\left.\begin{aligned} \varepsilon_g &= \frac{R}{R_g + R + R_a} \\ \varepsilon_a &= \frac{R_a}{R_g + R + R_a} \end{aligned}\right\}, \qquad \ldots\ldots\ldots \quad (69.7)$$

whilst p_1, p_2, p_5 and p_6 are reciprocal time constants.

If both halves of the circuit were identical, p_1 and p_2 would be equal to p_5 and p_6 respectively, and, similarly, K_1 and P_1 would be equal to K and P respectively.

The way in which the various reciprocal time constants p and the quantities K, P and L depend on the circuit constants is indicated in Sections 5 and 7 (see eqs (19*a*.5), (19*b*.5), (18*a*.5), (18*b*.5), (18*c*.5), (22.5), (24.7), (25.7), (26.7) and (27.7)).

I_{a0}, which denotes the anode current of the conducting tube in the static condition, is given by eq. (11.7) of Section 7.2.2, namely:

$$I_{a0} = \frac{(1 - \varepsilon_a)\, V' - \varepsilon_a V''}{\varepsilon_a (R_g + R) + r_a}, \qquad \ldots\ldots\ldots \quad (70.7)$$

which also gives the relation between I_{a0} and the internal resistance r_a of the tube.

Eqs (63.7) and (64.7) now make it possible to investigate the influence of the tube characteristics μ, I_{a0} (or r_a, according to eq. (70.7)) and C_{ag} (contained in the term b) on the trigger sensitivity of a given circuit. For this purpose two of the three characteristics mentioned are assumed to have a certain value, after which the variation of the critical trigger amplitude of the input voltage, V_{cr}, is calculated as a function of the third characteristic.

7.2.5.2.1. *Numerical example*

An example of the calculation of the influence of tube characteristics and a capacitive load in the anode circuit will be given. The circuit

to be investigated is assumed to have the following characteristic data (compare fig. 12.7):

$V' = 150$ V; $V'' = 100$ V; $R_a = 20$ kΩ; $R = 200$ kΩ; $R_g = 200$ kΩ; $C = 100$ pF; $C_c = 40$ pF; $t_0 = 0{,}2$ μ sec.

The input capacitance at the control grid is assumed to be $C_g = 10$ pF.

This gives:

$$C_i = C_c + C_g = 50 \text{ pF (see fig. 7.7).}$$

The anode load capacitances will be denoted C_{aI} and C_{aII} resp. (see fig. 3.7). The loading of the multivibrator is assumed to be symmetrical, i.e. $C_{aI} = C_{aII}$. In that case, the reciprocal time constants p_1 and p_2 are identical to p_5 and p_6 respectively, whilst $K_1 = K$ and $P_1 = P$ (see expressions 65, 66, 67 and 68.7).

Equations (63.7) and (64.7) can then be brought into the following form:

$$(AV_0 + B)\, x_I^{\alpha} + (DV_0 + E)\, x_I + F = 0. \quad . \quad . \quad . \quad (71.7)$$

$$(AV_0 + G)\, x_{II}^{\alpha} + (DV_0 + H)\, x_{II} + K = 0, \quad . \quad . \quad (72.7)$$

where:

$$x_I = e^{p_1 t_I}. \quad . \quad . \quad . \quad . \quad . \quad . \quad . \quad . \quad . \quad . \quad . \quad . \quad (73.7)$$

$$x_{II} = e^{p_1 t_{II}}. \quad . \quad . \quad . \quad . \quad . \quad . \quad . \quad . \quad . \quad . \quad . \quad . \quad (74.7)$$

$$\alpha = \frac{p_2}{p_1}, \quad . \quad . \quad . \quad . \quad . \quad . \quad . \quad . \quad . \quad . \quad . \quad . \quad (75.7)$$

A, B, D, E, F, G, H and K are constants containing the tube characteristics μ, r_a and C_{ag}, the anode-to-grid capacitance. The anode load-capacitances C_{aI} and C_{aII} influence p_1 and p_2 as well as the constants. Now the aim is to investigate the influence of the parameters μ, r_a, C_{ag} and $C_{aI} = C_{aII} = C_a$ on the minimum trigger-voltage amplitude V_0, already denoted by V_{cr}.

The procedure to be applied is as follows:

Substitute given values of the parameters and calculate the constants A, B ...., K. If, now, $x_I = x_{II}$, then $V_0 = V_{cr}$. Then equations (71.7) and (72.7) can be written:

$$(AV_{cr} + B)\, x^{\alpha} + (DV_{cr} + E)\, x + F = 0. \quad . \quad . \quad . \quad . \quad . \quad (76.7)$$

$$(AV_{cr} + G)\, x^{\alpha} + (DV_{cr} + H)\, x + K = 0. \quad . \quad . \quad . \quad . \quad . \quad (77.7)$$

Subtract these equations, and the result will be:

$$(B - G)\, x^{\alpha} + (E - H)\, x + F - K = 0 \quad . \quad . \quad . \quad . \quad . \quad . \quad (78.7)$$

If x could be determined from this equation, then V_{cr} may be calculated from either (76.7) or (77.7) by substituting x.

However, in general, equation (78.7) will not be easily solved by conventional methods, as α is generally a rather high power and some-

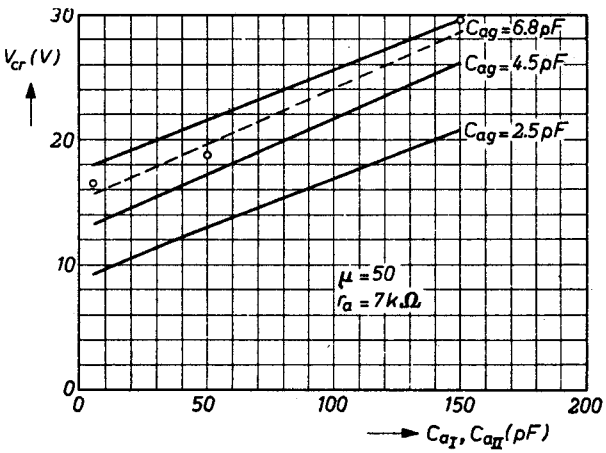

Fig. 14–7.

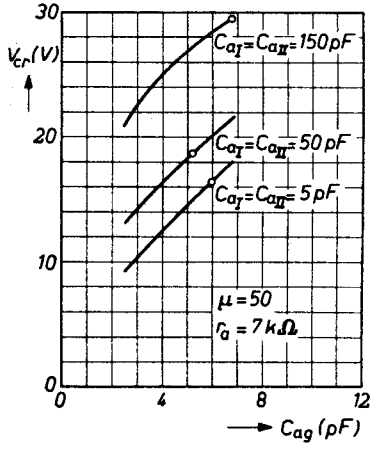

Fig. 15–7.

times not a whole number. Therefore, a graphical method is to be followed.

Put:

$$x^{\alpha} = y_1 \quad . \quad . \quad . \quad . \quad . \quad . \quad . \quad . \quad . \quad . \quad . \quad . \quad (79.7)$$

and

$$\frac{(H - E)\, x + K - F}{B - G} = y_2 \quad . \quad . \quad . \quad . \quad . \quad . \quad . \quad (80.7)$$

Plot both y functions on a graph. The point of intersection is the solution of x satisfying (78.7). Then, from (76.7) or (77.7) the critical trigger-voltage amplitude can be determined and turns out to be:

$$V_{cr} = \frac{(GE - HB)\, x + GF - KB}{\{A\,(H - E) + D\,(B - G)\}\, x + A\,(K - F)} \quad . \quad . \quad (81.7)$$

The results of calculations are represented in the following tables and depicted in figs 14.7, 15.7, 16.7 and 17.7.

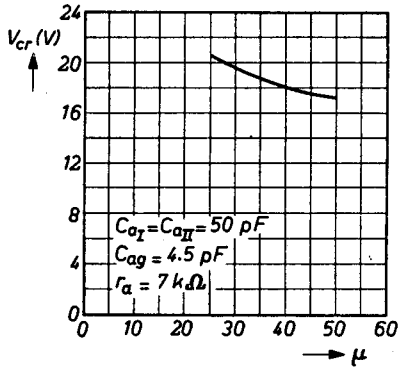

Fig. 16–7.

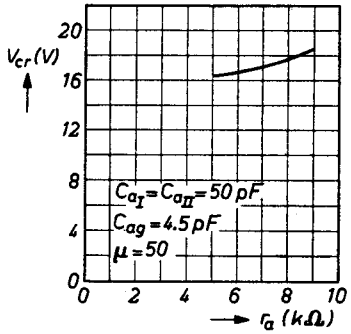

Fig. 17–7.

$C_{aI}=C_{aII}$	5	50	150	(pF)
C_{ag}				
2·5	9·2	13·0	20·8 → V_{cr} (V)	
4·5	13·4	17·2	26·0 → V_{cr} (V)	
6·8	18·0	21·6	29·5 → V_{cr} (V)	
(pF)				

This table combines the influence of the capacitive anode load C_a and the anode-to-grid capacitance C_{ag}.

The amplification factor is assumed to be 50, whilst the internal anode resistance r_a is 7 kΩ.

The influence of the amplification factor μ is given in the following table, where it is assumed that:

$$C_{aI} = C_{aII} = C_a = 50 \text{ pF}, \; C_{ag} = 4{\cdot}5 \text{ pF and } r_a = 7 \text{ k}\Omega.$$

μ	V_{cr} (V)
25	20·6
35	18·8
50	17·2

The influence of the internal anode resistance r_a is to be seen from the next table, where $C_a = 50$ pF, $C_{ag} = 4.5$ pF, and $\mu = 50$.

r_a ($k\Omega$)	V_{cr} (V)
5·4	16·3
7·0	17·2
9·0	18·6

The tables are represented graphically in figs 14.7, 15.7, 16.7 and 17.7, in which the values of all parameters are denoted.

It can be concluded from these figures, that the trigger sensitivity increases linearly with the capacitive load in the anode circuit with a mean slope

$$\frac{dV_{cr}}{dC_a} = 0{\cdot}082 \frac{V}{\text{pF}} \quad . \quad . \quad . \quad . \quad . \quad . \quad . \quad . \quad . \quad (82.7)$$

The critical trigger voltage increases approximately linearly with the anode-to-grid capacitance with a mean slope

$$\frac{dV_{cr}}{dC_{ag}} = 2 \text{ V/pF} \quad . \quad . \quad . \quad . \quad . \quad . \quad . \quad . \quad . \quad . \quad (83.7)$$

The trigger sensitivity decreases with increasing anode internal resistance and increases with increasing amplification factor. It must be borne in mind that these conclusions are not of a general character, but apply for the specific case treated.

These results of calculations can be compared with experimental investigations.

The trigger sensitivity of a double triode type E 92 CC has been measured under similar conditions as were assumed to exist in the foregoing calculations. The amplification factor of this tube is $\mu = 50$, whilst its internal anode resistance is 7 kΩ. The capacitances of the tube itself are $C_{ag} = 2{\cdot}5$ pF and $C_a = 0{\cdot}3$ pF. The wiring capacitances in the anode circuit have been assumed to amount to 5 pF, based on experimental experience. Then the trigger sensitivity is measured to be 16·5 V when no extra capacitive load is applied to the anodes, whereas it is 18·7 V with 50 pF applied between the anode and cathode of both tubes, and 29·6 V with 150 pF anode load applied. These measurements are represented by the small circles in figs 14.7 and 15.7. A mean curve drawn through these measuring points is represented by the dotted curve in fig. 14.7.

The conclusion to be drawn from these measurements is that an effective anode-to-grid capacitance of a value of about 6 pF must be present. A wiring capacitance between anode and grid of 3·5 pF would be sufficient to give this value, which is not at all abnormal.

In general, it can be said that the experimental figures are in quite good agreement with those derived from theoretical considerations.

One further check on the theory is possible.

Assuming C_{ag} to be 6 pF, the trigger sensitivity with asymmetrical capacitive anode load has been calculated. If one anode is loaded with 50 pF and the other tube has no externally applied capacitive load, then $C_{aI} = 50$ pF and $C_{aII} = 5$ pF. With these values of capacitance, the trigger sensitivity of this asymmetrically loaded bi-stable multivibrator is calculated to be 23 V, whereas it is measured to be 21 V. This also gives reasonable agreement.

7.2.5.3. The complete trigger cycle

As previously shown, the first phase of the trigger action determines the sensitivity of the circuit and also the switching time, since this depends on the instant $t = t_{II}$ at which the cut-off point of the second tube is reached and at which the definite change of state occurs in the tubes.

The time functions for the anode and grid voltages, as derived in section 7.2.3 for the complete trigger cycle, have been calculated for a numerical example nearly the same as treated in the preceding sections, and are graphically represented in figs 18.7, 19.7, 20.7 and 21.7.

The curves marked *a* are applicable to a symmetrical multivibrator, of which $C_{aI} = C_{aII} = 5$ pF, whilst the curves marked *b* and *c* apply to an asymmetrical multivibrator with $C_{aI} = 110$ pF and $C_{aII} = 5$ pF. The calculated curves are represented by the fully drawn lines. In order to comform with practice, the curves displayed by an oscilloscope and redrawn to the same scale, have also been plotted in these figures (broken lines). It should be realized that the time scale on the screen of the oscilloscope was only about one tenth of that used for the graphs, so that some inaccuracy was introduced in redrawing the steep fronts.

The multivibrator was triggered by applying negative-going pulses having an amplitude of 35 V, a width of 4 μsec and a period of 40 μsec. The time of rise of the negative-going front was 0·2 μsec.

7.2.5.3.1. *Discussion of the waveforms*

From fig. 18.7, which represents the waveform of V_{gII}, it can be clearly seen that V_{gII} reaches the cut-off value (approximately —4 V)

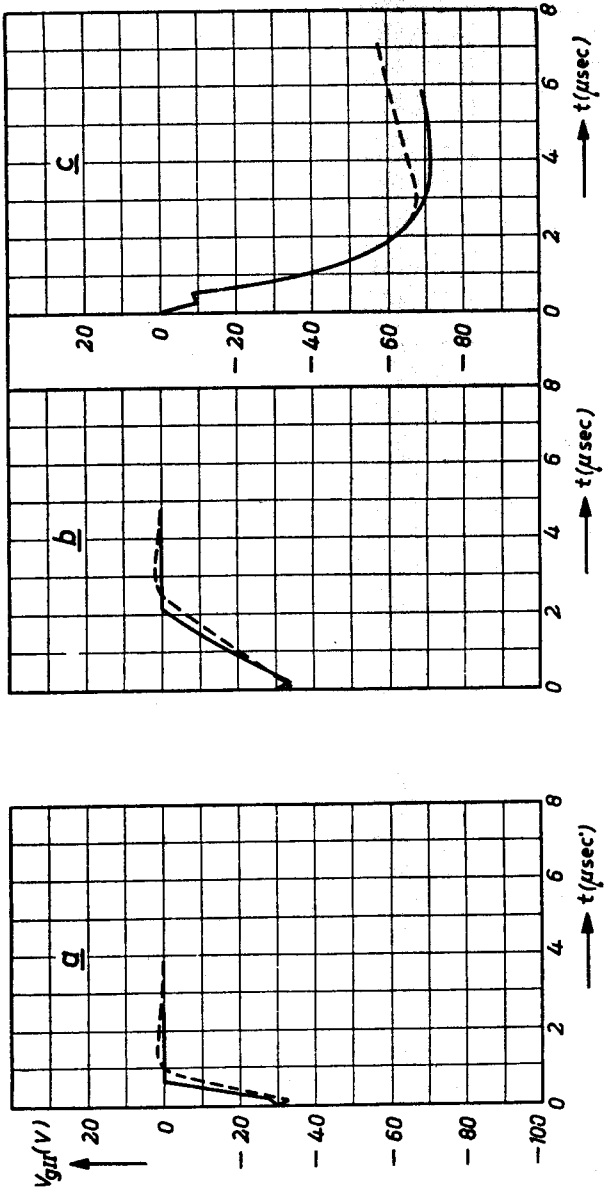

Fig. 18–7.
Calculated values (fully drawn lines) and measured values (broken lines) of V_{gII} as function of time, trigger pulses with an amplitude of 35 V, a width of 4 μsec, a period of 40 μsec and a negative-going front with a rise time of 0·2 μsec being applied. Curve *a* applies to a symmetrical multivibrator ($C_a = C_{aI} = C_{aII} = 5$ pF), tube *II* becoming conducting (and tube *I* being cut off). Curves *b* and *c* apply to an asymmetrically loaded multivibrator ($C_{aI} = 110$ pF, $C_{aII} = 5$ pF), tube *II* becoming conducting in curve *b* and being cut off by the next pulse in curve *c*.

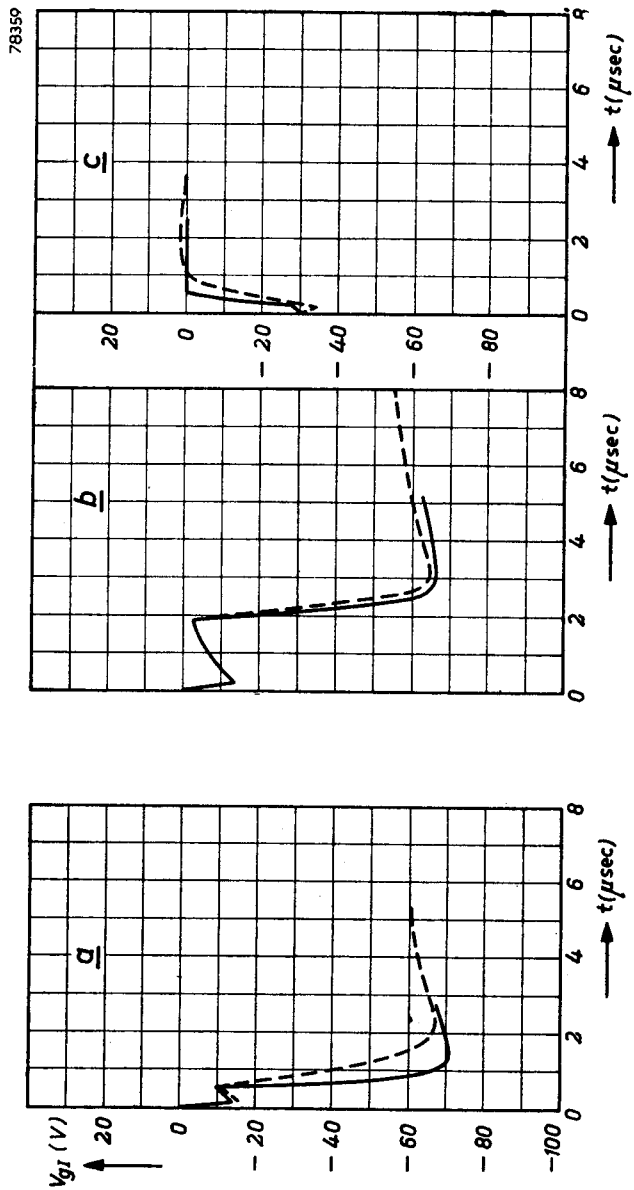

Fig. 19–7.
Oscillograms similar to those shown in fig. 18–7, representing V_{g1} as a function of time.

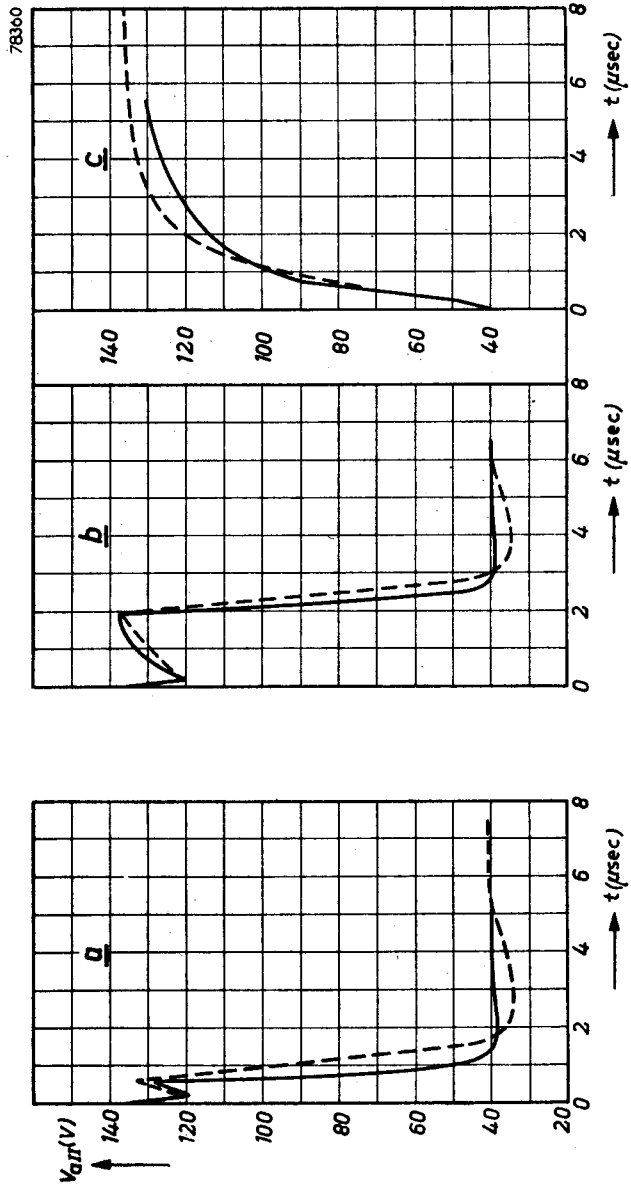

Fig. 20–7.
Oscillograms similar to those shown in fig. 18–7, representing V_{aH} as a function of time.

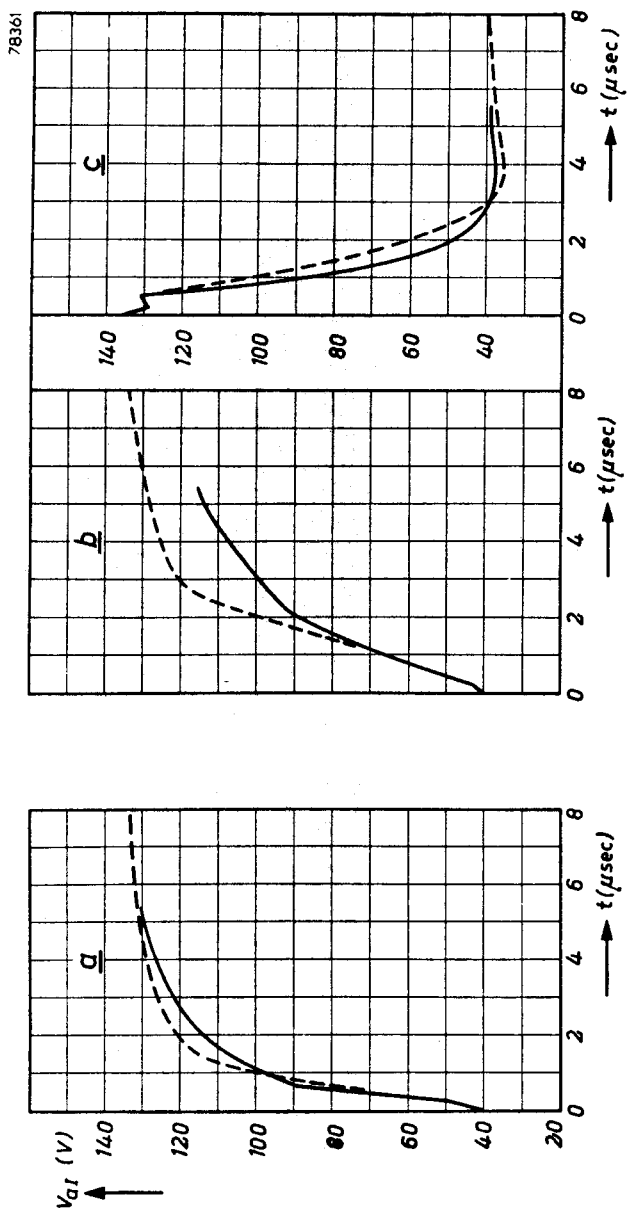

Fig. 21–7.
Oscillograms similar to those shown in fig. 18–7, representing V_{a1} as a function of time.

in a much smaller time ($t = t_{II}$) in case *a* than in case *b* (capacitive load, $C_{aI} = 110$ pF); in other words: the capacitive load considerably increases the switching time.

At the instant $t = t_{II}$, the second phase of the trigger cycle commences. Curves *a* and *b* of fig. 20.7 reveal that the anode voltage V_{aII} greatly decreases at this instant; in other words: the multivibrator is definitely triggered.

Fig. 18.7 shows that V_{gII} crosses the grid base of tube *II* and becomes

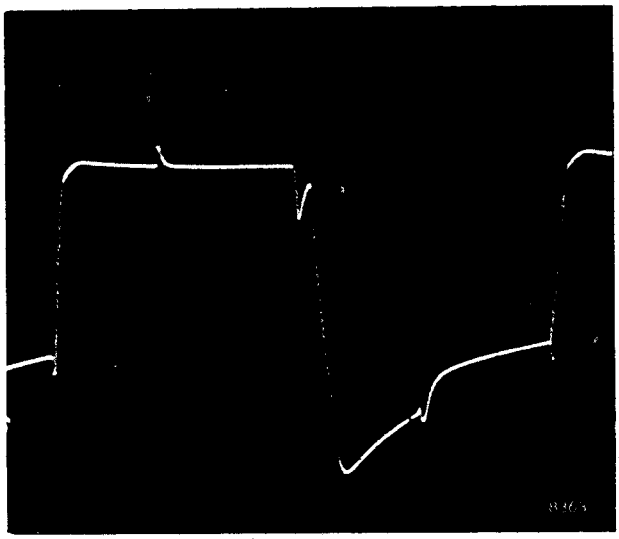

Fig. 22–7.
Oscillogram of the grid voltage of one of the triodes of a symmetrical multivibrator ($C_a = C_{aI} = C_{aII} =$ 5 pF); square-wave trigger pulses with a period of 15 μsec being applied.

zero shortly after the instant $t = t_{II}$; due to the occurrence of grid current, V_{gII} is then kept constant at this value. In practice, there is some overshoot, which should be attributed to the fact that the grid resistance is not zero, as was assumed in the calculations, but has a definite value. The influence of the discontinuity will therefore be smaller than calculated.

The fully drawn curves plotted in fig. 21.7 show the calculated effects of this discontinuity (at approximately 0·7 μsec for curve *a*, and at approximately 2 μsec for curve *b*) on the anode voltage V_{aI}. This effect could not be clearly discerned on the oscillograms [7]).

[7]) The oscillograms shown in figs 22–7 to 27–7, which apply to other trigger circuits, do show these discontinuities.

The oscillograms shown in figs. 22.7 and 23.7 refer to a symmetrical, unloaded multivibrator having the same characteristics as the circuit previously mentioned. Triggering was, however, achieved by means of square-wave pulses with a period of 15 μsec. Fig. 22.7 shows the grid voltage variation of one of the tubes; that of the other tube is obviously identical. Fig. 23.7 displays the anode voltage variation of both tubes. The discontinuity which can be clearly seen in the ascending part of the oscillogram is due to the start of grid current flow.

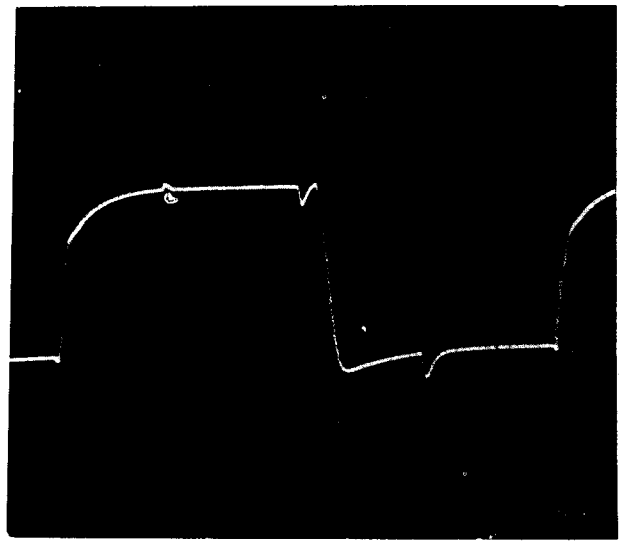

Fig. 23-7.
Oscillograms of the anode voltage of one of the triodes of a symmetrical multivibrator ($C_a = C_{aI} = C_{aII} =$ 5 pF); square-wave trigger pulses with a period of 15 μsec being applied.

Figs. 24.7, 25.7, 26.7 and 27.7 show the oscillograms of the grid and anode voltages of an asymmetrical multivibrator, triggered by negative-going pulses having a width of 40 μsec, a period of 60 μsec and an amplitude of 35 V. The component values are once again identical to those of the previous circuits; C_{aI} and C_{aII} were 110 pF and 5 pF respectively.

The variation of V_{gII} is displayed by the oscillogram shown in fig. 24.7; the negative-going front should be compared with curve *c* of fig. 18.7, and the positive-going front with curve *b* of this figure.

Fig. 25.7 shows the variation of V_{gI}; this should be compared with curves *b* and *c* of fig. 19.7.

Fig. 26.7 gives the oscillogram of V_{aII} and should be compared with curves *b* and *c* of fig. 20.7.

Finally, the oscillogram of fig. 27.7 shows the variation of V_{aI}, and should be compared with curves *b* and *c* of fig. 21.7.

In the curves representing the calculated time functions, the influence of the positive rear flanks of the trigger pulses have been disregarded. In practice, care should be taken that these positive, differentiated pulses do not disturb the normal triggering of the multivibrator. These pulses should not, for example, drive the non-conducting tube (i.e. the initially conducting tube *I*) back into its grid base. Curves *a* and *b* of fig. 19.7

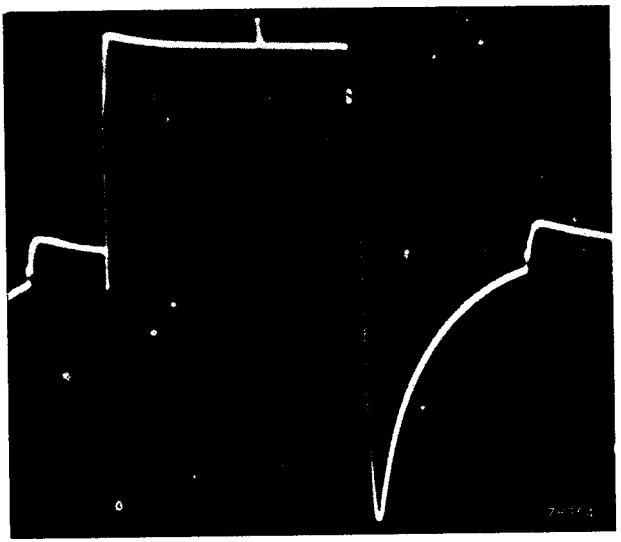

Fig. 24–7.
Oscillogram showing the grid voltage variation V_{gII} of tube *II* of an asymmetrically loaded multivibrator ($C_{gI} = 110$ pF, $C_{aII} = 6$ pF), negative-going trigger pulses with a width of 40 μsec, a period of 60 μsec and an amplitude of 35 V being applied.

reveal the considerable overshoot of V_{gI} in the negative direction, its final value being —30 V. It would therefore be advantageous to choose the width of the trigger pulse in such a way that the positive-going rear flank coincides with this overshoot region. This will not be possible, however, when a flip-flop unit is triggered by a preceding flip-flop unit, because the pulses produced thereby are always roughly square in shape and the positive-going flank will always occur just between two negative-going flanks.

There is a compensating effect of the negative anode pulse of the conducting tube on the positive pulse at the grid of the non-conducting tube. This is clearly shown by the oscillogram of fig. 22.7, where the

grid voltage gradually increases. About half way in this region the effect of the positive differentiated pulse can be seen. Initially, the voltage tends to rise, but the slightly delayed negative pulse at the anode of the conducting tube is passed to the grid of the non-conducting tube via the speed-up capacitor C, and even overcompensates the positive input pulse, so that a negative pulse results.

The final static conditions for the curves *a* and *b* of figs 18.7, 19.7, 20.7 and 21.7 are: $V_{gI} = -30$ V, $V_{aI} = 136$ V, $V_{gII} = 0$ V and

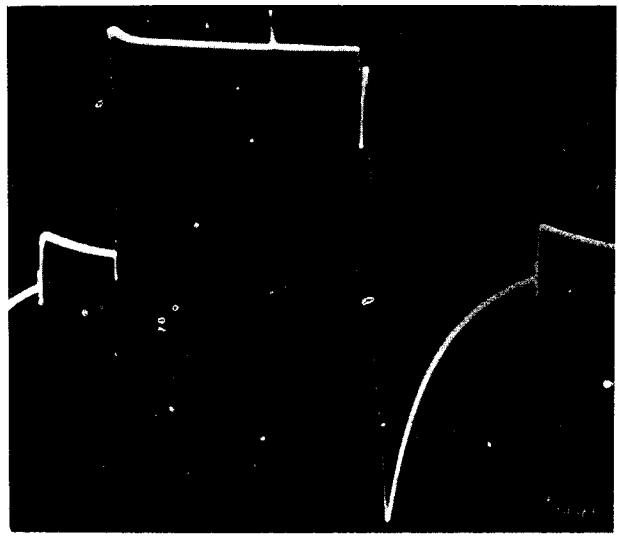

Fig. 25–7.
Oscillogram similar to that shown in fig. 24–7, displaying the grid voltage variation V_{gI} of tube *I*.

$V_{aII} = 40$ V. The functions are now reversed, tube *I* being cut off and tube *II* being conducting. The next negative-going flank of V will trigger the multivibrator once again. In the case of a symmetrical circuit ($C_{aI} = C_{aII} = 5$ pF), the waveforms during this new trigger action can easily be calculated from the theoretical results by changing the indices I and II in all formulae,the waveform of V_{gII} thus being identical to that of V_{gI} during the preceding trigger action. The new waveforms have therefore not been given in figs 18.7, 19.7, 20.7 and 21.7.

In the case of an asymmetrically loaded multivibrator, the situation is less simple, but the waveforms can nevertheless also be calculated; the results are shown by curves *c*.

Notwithstanding the presence of the load capacitance $C_{aI} = 110$ pF,

the switching time or the duration of the first trigger phase is now much shorter than in the first case *b*. This is due to the fact that the switching time is now defined by the waveform of V_{g1}, which is independent of C_{a1}. The switching time is about 0·6 μsec, whereas it was about 2 μsec in the first case.

It can, moreover, be seen that the trigger sensitivity will be better in the second case. In the first case the grid voltage of the initially conducting tube, V_{g1}, has almost reached its cut-off value at the instant

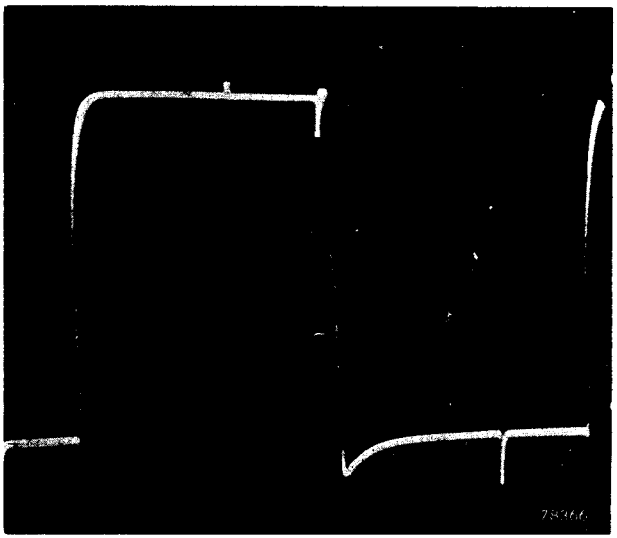

Fig. 26–7.
Oscillogram similar to that shown in fig. 24–7, displaying the anodevoltage variation V_{aII} of tube *II*.

at which tube *II* starts to draw anode current (at $t \approx 2$ μsec; see curve *b*, fig. 19.7). In the second case, however, the grid voltage of the initially conducting tube, V_{gII} (curve *c*, fig. 18.7), rises at a much slower rate, due to the influence of $C_{a1} = 110$ pF. At the instant at which tube *I* starts to draw current, the (negative) value of V_{gII} will still be almost three times that of V_{g1} in the first case. In other words: V_{g1} rises much faster than V_{gII} during the same periods of time.

The sensitivity of an asymmetrical multivibrator is thus not the same for the two stable conditions, and is smallest for the initial condition at which the capacitively loaded tube is conducting. In practice, this smallest sensitivity defines the usefulness of the circuit.

It can also be seen that sensitivity is improved by loading the multivibrator symmetrically (for example $C_{a1} = C_{aII} = 110$ pF). In that case

the grid voltage V_{g1} (curve *b*, fig. 19.7) will rise slower and reach the cut-off point later, so that it will be easier for the grid voltage of the other tube to reach the cut-off points.

This fact has been confirmed experimentally. As an example, the average values of V_{cr}, measured on a series of some 40 experimental types of double triodes, will be given. For symmetrical, unloaded multivibrator circuits, the critical trigger amplitude had an average value of 17 V. For an asymmetrical circuit (150 pF load in one of the anode

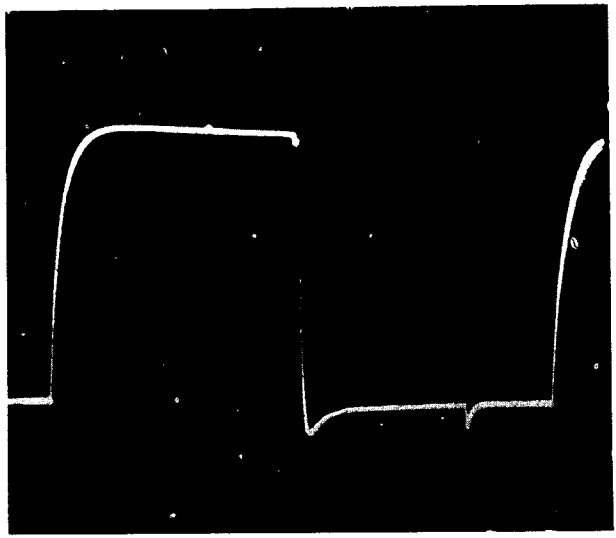

Fig. 27–7.
Oscillogram similar to that shown in fig. 24–7, displaying the anodevoltage variation V_{a1} of tube *I*.

circuits), this average value was 38 V. By connecting a load of 150 pF to both anode circuits, the sensitivity of the multivibrator was increased, the average value of V_{cr} then being 31·5 V.

7.2.5.4. Conclusion

The theoretical investigation of the operation of a bi-stable multivibrator has made it possible to gain an insight into the influence of the various tube characteristics on the behaviour of the circuit. For a given circuit, the dependence of the trigger sensitivity on the amplification factor, the internal resistance and the anode-to-grid capacitance can be calculated and graphically represented by curves similar to those shown in figs 14.7, 15.7, 16.7 and 17.7. For a complete survey, a family

of curves should be drawn giving the dependence of the sensitivity on one of the characteristics with the other two characteristics as parameters.

In the preceding sections, the influence of the tube characteristics on a given circuit has been investigated. It is of course also possible to take the tube as a given starting point and to investigate the circuit in order to determine the optimum results. The speed of the triggering, for example, is an important quantity, as this determines the maximum frequency of the input pulses at which the multivibrator will still operate in the correct way. It has for example been shown in the preceding pages that the switching time or duration of the first trigger phase depends on the capacitive load in one of the anode circuits.

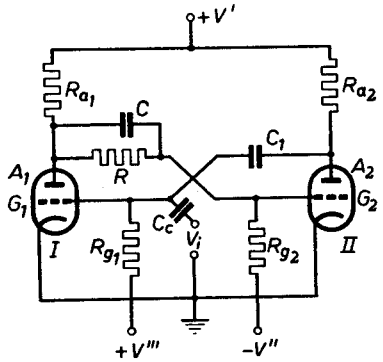

Fig. 28–7.

It can, moreover, be seen from eqs (65.7), (66.7), (67.7) and (68.7) that the amplitude V_0 of the input trigger pulses always occurs in combination with the time of rise t_0; in fact, the slope V_0/t_0 of the leading edge of the pulse is the principal quantity which determines the trigger action. The quantity t_0, moreover, occurs in a few exponential terms. In all preceding calculations, t_0 was assumed to be constant, namely 0·2 μsec. The dependence of the trigger action on the duration t_0 at a constant value of V_0 can obviously also be derived by proceeding in a similar way.

The most important result of representing the mechanism of the operation of a triggered bi-stable multivibrator in explicit formulae has been to enable the influence of several tube characteristics on the trigger action of the circuit in which the tube should operate satisfactorily, to be evaluated. This has led to the design of the double triode E 92 CC. Furthermore, it makes it possible to design a bi-stable multivibrator in such a way that optimum results are ensured.

7.3. THE MONOSTABLE MULTIVIBRATOR

7.3.1. INTRODUCTION

The monostable multivibrator can be analysed in the same way as the bi-stable multivibrator. Here the trigger pulses, assumed to be of the same shape as depicted in fig. 2.7, are applied to the control grid of the tube that is conducting.

The basic diagram of the circuit is given in fig. 28.7. As its name suggests, there is only one stable state of this type of multivibrator. Tube I will be conducting while tube II is cut off; this being caused by the supply voltage sources $+V'''$ and $-V''$. The anodes are fed from the supply voltage source $+V'$. All three sources are assumed to have negligibly small internal resistance, and the same is assumed for the trigger voltage source V_i.

Stray capacitances, except anode-to-grid capacitance, will be taken into account.

The negative-going front flank of the trigger pulse is assumed to be so steep that the time it takes to bring the control grid below the cut-off voltage is small compared with the time constants, which are typical for the circuit and which determine the transients. This means that the conducting tube is cut off about immediately at the instant $t = 0$ when the trigger pulse starts (see fig. 29.7).

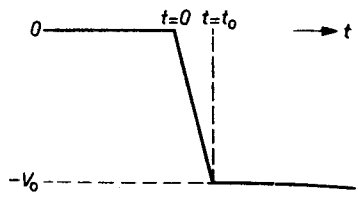

Fig. 29-7.

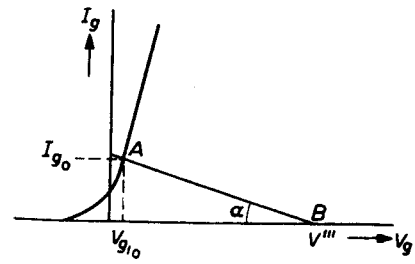

Fig. 30-7.

The complete trigger cycle can once again be distinguished by three phases. The *first phase* is the period immediately after the starting of the trigger pulse at the instant $t = 0$, when both tubes are cut off. If it is assumed that, at the instant $t = t_{II}$, the second tube, initially cut off, starts conducting, then this instant t_{II} is the commencement of the *second phase*.

Again, somewhat later, at the instant $t = t_3$, say, the grid voltage of tube I passes the cut-off value in the positive direction, and this tube starts conducting as well. At this instant, t_3, the *third phase* commences.

It is assumed that at times $t < 0$, the static condition, which is described in the following section, is present.

7.3.2. THE STATIC CONDITION

In this state of the monostable multivibrator, only direct currents

will flow in the circuit, and consideration of capacities in the diagram can be omitted.

It will be clear that the anode voltage of tube *II* will be

$$V_{aII_0} = V' \quad \ldots\ldots\ldots\ldots \quad (84.7)$$

The grid voltage of tube *I* will be dependent on the amount of grid current flowing. This, in turn, will be determined by the shape of the grid current-grid voltage characteristic and by the values of R_{g1} and V''' (see fig. (30.7)).

In fig. 30.7:

$$\cot \alpha = R_{g_1} \quad \ldots\ldots\ldots\ldots \quad (85.7)$$

The intersection of AB and the characteristic curve determines the value of I_{g_c}. The slope of the characteristic is assumed to be so high that

$$V_{g1_0} = 0 \quad \ldots\ldots \quad (86.7)$$

Then I_{g_0} is defined by

$$I_{g_0} = \frac{V'''}{R_{g_1}} \quad \ldots\ldots \quad (87.7)$$

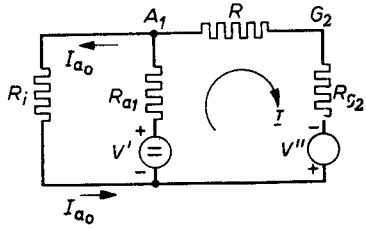

Fig. 31-7.

The voltages at A_1 and G_2 are to be determined from the diagram of fig. 31.7, which is only valid for the static condition (no capacitances as mentioned before).

In this diagram, r_a represents the internal anode resistance of tube *I*, through which an anode current I_{a_0} flows, thus:

$$V_{aI_0} = I_{a_0} r_a \quad \ldots\ldots\ldots\ldots \quad (88.7)$$

The current I_{a0} is distributed over the resistances R_{a_1} and $R + R_{g_2}$ in parallel, in such a way that the current through R_{a_1} is:

$$I_{Ra_1} = \frac{R + R_{g_2}}{R_{a_1} + R + R_{g_2}} I_{a_0} = (1 - \varepsilon_a) I_{a_0}.$$

The current through $R + R_{g_2}$ is:

$$I_{R+Rg_2} = \frac{R_{a_1}}{R_{a_1} + R + R_{g_2}} I_{a_0} = \varepsilon_a I_{a_0},$$

where:

$$\varepsilon_a = R_{a_1}/(R_{a_1} + R + R_{g2}) \quad \ldots\ldots\ldots \quad (89.7)$$

Moreover, apart from the fact that tube *I* is conducting or non conducting, a current I will flow in the circuit, defined by:

$$I = \frac{V' + V''}{R_{a_1} + R + R_{g_2}} \quad \ldots\ldots\ldots\ldots \quad (90.7)$$

The values of V_{aI_0} and V_{gII_0} are evidently:

$$V_{aI_0} = V' - \{(1 - \varepsilon_a)\, I_{a_0 0} + I\}\, R_{a_1},$$

or:

$$V_{aI_0} = (1 - \varepsilon_a)\,(V' - R_{a_1} I_{a_0}) - \varepsilon_a V'' \quad \ldots\ldots \quad (91.7)$$

$$V_{gII_0} = -V'' + (I - \varepsilon_a I_{a_0})\, R_{g_2}, \quad \ldots\ldots\ldots \quad (92.7)$$

or:

$$V_{gII_0} = -V'' + \varepsilon_g\,(V' + V'') - \varepsilon_a R_{g_2} I_{a_0},$$

where:

$$\varepsilon_g = R_{g_2}/(R_{a_1} + R + R_{g_2}) \quad \ldots\ldots\ldots\ldots \quad (93.7)$$

Thus:

$$V_{gII_0} = \varepsilon_g\,(V' - R_{a_1} I_{a_0}) - (1 - \varepsilon_g)\, V'' \quad \ldots\ldots\ldots \quad (94.7)$$

This is assumed to be sufficiently negative to keep tube II cut off. From (88.7) and (91.7) the value of I_{a0} can be determined:

$$I_{a_0} = \frac{(1 - \varepsilon_a)\, V' - \varepsilon_a V''}{r_a + (1 - \varepsilon_a)\, R_{a_1}} \quad \ldots\ldots\ldots\ldots \quad (95.7)$$

The value of r_a can be found from the $I_a - V_a$ characteristic of the tube, as it is the reciprocal of the slope of the characteristic at $V_{g_1} = 0$ (see fig. 54.6).

From the instant $t = 0$ onwards, transient phenomena are superimposed upon the static condition of the circuit, because of the occurrence of the trigger pulse. This dynamic condition will now be considered.

7.3.3. THE FIRST PHASE OF THE DYNAMIC CONDITION

The voltage changes at G_1, and A_2 will be derived with the aid of fig. (32.7), those at G_2 and A_1 with the aid of fig. 33.7.

The D.C. supply sources have been omitted in these figures, as they are accounted for in the static condition.

In fig. 32.7, the input-voltage source has been converted into an input current source I_i in the usual manner, where:

$$I_i = C_c \frac{dV_i}{dt} \quad \ldots\ldots\ldots\ldots \quad (96.7)$$

I_i is the superposition of two step functions, occurring at $t = 0$ and $t = t_0$ resp.:

$$I_i = C_c \frac{V_0}{t_0} \left\{ -U(t) + U(t - t_0) \right\} \quad \ldots\ldots\ldots (97.7)$$

At $t = 0$, the grid current I_{g_0} suddenly disappears. This is accounted for by the introduction of an input current step function $+I_{g_0}$, as indicated in fig. 32.7.

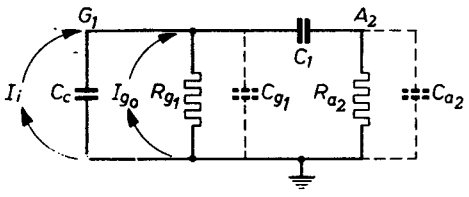

Fig. 32–7.

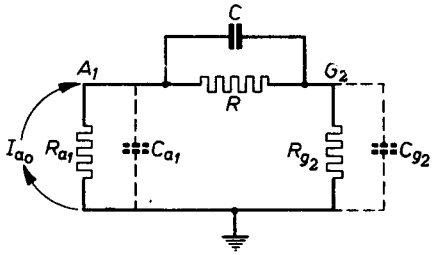

Fig. 33–7.

Stray capacitances at the input (and output) of the tubes are indicated by dotted lines (C_{g_1} and C_{a_2} resp.).

The sudden interruption of the anode current I_{a_0} in the first tube is accounted for by the input-current step function I_{a_0}, as indicated in fig. 33.7. Here stray capacitances are also indicated by dotted lines (C_{a_1} and C_{g_2}).

The voltage changes at the anodes A_1 and A_2 and at the grids G_1 and G_2 can now be calculated as the response of the circuits of figs 32.7 and 33.7 to the input current step functions I_i, I_{g_0} and I_{a_0}. First the voltage at G_1 will be derived.

This voltage, V_{g1}, is defined by the operational impedance Z_{g_1} between G_1 and earth. This impedance is:

$$Z_{g_1} = R_{g_1} \frac{1 + Ap}{1 + Bp + Ep^2}, \quad \ldots\ldots\ldots (98.7)$$

where: $p = \dfrac{d}{dt}$ = differentiation with respect to time

$$\left.\begin{aligned} A &= T_{a_2} + T_{21} \\ B &= T_{11} + T_{a_2} + T_{g_1} + T_{21} \\ E &= T_{11} T_{a_2} + T_{g_1} T_{a_2} + T_{21} T_{g_1} \\ T_{a_2} &= R_{a_2} C_{a_2} \\ T_{21} &= R_{a_2} C_1 \\ T_{11} &= R_{g_1} C_1 \\ T_{g_1} &= R_{g_1} (C_c + C_{g_1}) \end{aligned}\right\} \quad \ldots\ldots (99.7)$$

The voltage across this impedance as a result of the current step function $I_i + I_{g_0}$ occurring at the instant $t = 0$ will be:

$$V_{g1}(t) = (I_i + I_{g_0}) R_{g_1} \left\{1 + Ke^{p_1 t} - (1 + K) e^{p_2 t}\right\}, \quad . \quad (100.7)$$

where:

$$K = \frac{p_2 (1 + A_{p_1})}{p_1 - p_2} \quad . \quad . \quad . \quad . \quad . \quad . \quad . \quad . \quad . \quad . \quad . \quad . \quad . \quad (101.7)$$

$$p_1 = -\frac{B}{2E}\left\{1 - \sqrt{1 - \frac{4E}{B^2}}\right\} \quad . \quad . \quad . \quad . \quad . \quad . \quad . \quad . \quad . \quad . \quad . \quad (102.7)$$

$$p_2 = -\frac{B}{4E}\left\{1 + \sqrt{1 - \frac{4E}{B^2}}\right\} \quad . \quad . \quad . \quad . \quad . \quad . \quad . \quad . \quad . \quad . \quad . \quad (103.7)$$

(compare with section 5).

At the instant $t = t_0$, a current step function of amplitude I_i in the reverse direction is applied, giving rise to a transient voltage:

$$V_{g1}(t - t_0) = -I_i R_{g_1} \left\{1 + Ke^{p_1 (t - t_0)} - (1 + K) e^{p_2 (t - t_0)}\right\} . \quad . \quad (104.7)$$

In the static condition, $V_{g1} = 0$, so that the complete expressions for V_{g1} are:

$t \leqq 0 : V_{g1} = 0$

$$0 \leqq t \leqq t_0 : V_{g_1}(t) = (I_i + I_{g_0}) R_{g1} \left\{1 + Ke^{p_1 t} - (1 + K) e^{p_2 t}\right\} . \quad . \quad (105.7)$$

$$t \geqq t_0 : V_{g1}(t - t_0) = I_{g_0} R_{g_1} \left\{1 + Ke^{p_1 t} - (1 + K) e^{p_2 t}\right\} +$$

$$+ I_i R_{g_1} \left\{Ke^{p_1 t}(1 - e^{-p_1 t_0}) - (1 + K) e^{p_2 t}(1 - e^{-p_2 t_0})\right\} \quad . \quad . \quad . \quad . \quad (106.7)$$

At $t = \infty$, the voltage at G_1 would be: $V_{g1}(\infty) = I_{g_0} R_{g_1}$.

According to (87.7), this would be:

$$V_{g1}(\infty) = V''', \text{ which is evident.}$$

Secondly, the voltage at the anode A_2 will be derived from fig. 32.7. It depends on the transfer impedance

$$Z_{g_1 a_2} = R_{g_1} \frac{T_{21} p}{1 + Bp + Ep^2} . \quad . \quad . \quad . \quad . \quad . \quad . \quad . \quad (107.7)$$

The voltage at A_2 can be calculated to be:

$$t \leqq 0 : V_{a\text{II}} = V_{a\text{II}_0} = V'$$

$$0 \leqq t \leqq t_0 : V_{a\text{II}}(t) = V_{a\text{II}_0} + (I_i + I_{g_0}) R_{g1} \frac{T_{21}}{E(p_2 - p_1)} (e^{p_2 t} - e^{p_1 t}) \quad (108.7)$$

$$t \geqq t_0 : V_{a\text{II}}(t - t_0) = V_{a\text{II}_0} + I_{g_0} R_{g_1} \frac{T_{21}}{E(p_2 - p_1)}(e^{p_2 t} - e^{p_1 t}) +$$

$$+ I_i R_{g_1} \frac{T_{21}}{E(p_2 - p_1)} \left\{ e^{p_2 t}(1 - e^{-p_2 t_0}) - e^{p_1 t}(1 - e^{-p_1 t_0}) \right\} . \quad . \quad . \quad . \quad (109.7)$$

At $t = \infty$, this anode voltage would be:

$$V_{a\text{II}}(\infty) = V_{a\text{II}_0} = V' . \qquad \text{(see 84.7)}$$

The third voltage, to be derived with the aid of fig. 33.7, is the anode voltage of the first tube, $V_{a\text{I}}$.

The operational impedance between A_1 and earth is given by:

$$Z_{a_1} = R_{a_v} \frac{1 + Fp}{1 + Gp + Hp^2} , \quad . \quad . \quad . \quad . \quad . \quad . \quad . \quad . \quad . \quad . \quad . \quad (110.7)$$

where:

$$R_{a_v} = \frac{R_{a_1}(R + R_{g_2})}{R_{a_1} + R + R_{g_2}} = (1 - \varepsilon_a) R_{a_1} \quad . \quad . \quad . \quad . \quad . \quad (111.7)$$

$$F = \beta T_{g_2} + \beta_g T . \quad . \quad . \quad . \quad . \quad . \quad . \quad . \quad . \quad . \quad . \quad . \quad . \quad (112.7)$$

$$\beta = \frac{R}{R + R_{g_2}} ; \quad \beta_g = \frac{R_{g_2}}{R + R_{g_2}} \quad . \quad . \quad . \quad . \quad . \quad . \quad . \quad (113.7)$$

$$T_{g_2} = R_{g_2} C_{g_2} ; \quad T = RC. \quad . \quad . \quad . \quad . \quad . \quad . \quad . \quad . \quad . \quad (114.7)$$

$$G = (\varepsilon_g + \varepsilon) T_{a_1} + (\varepsilon_g + \varepsilon_a) T + (\varepsilon + \varepsilon_a) T_{g_2} \quad . \quad (115\,7)$$

$$T_{a_1} = R_{a1} C_{a1} \quad . \quad . \quad . \quad . \quad . \quad . \quad . \quad . \quad . \quad . \quad . \quad (116.7)$$

$$\left.\begin{aligned} \varepsilon_g &= \frac{R_{g_2}}{R_{a_1} + R + R_{g_2}} \\ \varepsilon &= \frac{R}{R_{a_1} + R + R_{g_2}} \\ \varepsilon_a &= \frac{R_{a_1}}{R_{a_1} + R + R_{g_2}} \end{aligned}\right\} \quad . \quad . \quad . \quad . \quad . \quad . \quad . \quad . \quad (117.7)$$

$$H = \varepsilon_a T T_{g_2} + \varepsilon T_{g_2} T_{a_1} + \varepsilon_g T_{a_1} T \quad . \quad . \quad . \quad . \quad . \quad . \quad (118.7)$$

A current step function with amplitude I_{a_0} at $t = 0$ causes a transient voltage across the impedance between A_1 and earth as given by the second right-hand term of expression (119.7). The total voltage is:

$$V_{a\text{I}} = V_{a\text{I}_0} + I_{a_0} R_{av} \left\{ 1 + L e^{p_3 t} - (1 + L) e^{p_4 t} \right\} \quad . \quad . \quad . \quad (119.7)$$

V_{aI_0} is given by (91.7)

and
$$L = \frac{p_4 (1 + F p_3)}{p_3 - p_4} \quad \ldots\ldots\ldots\ldots \quad (120.7)$$

$$p_3 = -\frac{G}{2H}\left\{1 - \sqrt{1 - \frac{4H}{G^2}}\right\} \quad \ldots\ldots \quad (121.7)$$

$$p_4 = -\frac{G}{2H}\left\{1 + \sqrt{1 - \frac{4H}{G^2}}\right\} \quad \ldots\ldots \quad (122.7)$$

At $t = \infty$, this anode voltage would be:

$$V_{aI}(\infty) = (1 - \varepsilon_a)\, V' - \varepsilon_a V'' \quad \ldots\ldots\ldots \quad (123.7)$$

Finally, the voltage at the grid of tube *II* will be given. This depends on the transfer impedance between A_1 and G_2:

$$Z_{a_1 g_2} = R_{ag}\,\frac{1 + Tp}{1 + Gp + Hp^2}, \quad \ldots\ldots\ldots \quad (124.7)$$

where:
$$R_{ag} = \frac{R_{a_1} R_{g_2}}{R_{a_1} + R + R_{g_2}} = \varepsilon_a R_{g_2} = \varepsilon_g R_{a_1} \quad \ldots\ldots \quad (125.7)$$

The total voltage at G_2 for $t > 0$ is:

$$V_{gII} = V_{gII_0} + I_{a_0} R_{ag}\left\{1 + M e^{p_3 t} - (1 + M)\, e^{p_4 t}\right\}, \quad \ldots \quad (126.7)$$

where:
$$M = \frac{p_4 (1 + T p_3)}{p_3 - p_4} \quad \ldots\ldots\ldots\ldots \quad (127.7)$$

V_{gII_0} is given by (94.7).

At $t = \infty$:

$$V_{gII}(\infty) = \varepsilon_g V' - (1 - \varepsilon_g)\, V'' \quad \ldots\ldots\ldots \quad (128.7)$$

Tube *II* was already in the cut-off condition; tube *I* is cut off suddenly by the trigger pulse at $t = 0$. Consequently, the first phase of the dynamic condition is characterized by the fact that both tubes are cut off. However, the grid voltages of both tubes tend to final positive values, namely:

$$V_{gI}(\infty) = V''' \text{ and } V_{gII}(\infty) = \varepsilon_g V' - (1 - \varepsilon_g)\, V'',$$

which is supposed to be positive.

At a given moment, one of the tubes reaches its cut-off point and will start conducting.

For correct operation of the monostable multivibrator it is necessary that tube *II* should reach its cut-off point sooner than tube *I*. The times t_I and t_{II} for which tubes *I* and *II* respectively reach their cut-off points can be calculated from the relations:

$$V_{gI}(t_I) = -\frac{1}{\mu} V_{aI}(t_I) \quad \ldots \quad (129.7)$$

$$V_{gII}(t_{II}) = -\frac{1}{\mu} V_{aII}(t_{II}), \quad \ldots \quad (130.7)$$

where μ = amplification factor of the tubes. (compare Sections 7.2.3.1 and 7.2.5.1)

Introducing a correction for the influence of the anode-grid capacitances, as in the sections mentioned, gives an extra component at grid 1:

$$\bar{V}_{gI}(t) = b_I I_{a_0} R_{a_v} \left\{1 + Le^{p_2 t} - (1 + L) e^{p_1 t}\right\}, \quad \ldots \quad (131.7)$$

and at grid 2:

$$\bar{V}_{gII}(t) = b_{II} \left[I_{g_0} R_{g_1} \frac{T_{21}}{E(p_2 - p_1)} (e^{p_2 t} - e^{p_1 t}) + \right.$$

$$\left. + I_i R_{g_1} \frac{T_{21}}{E(p_2 - p_1)} \left\{ e^{p_2 t} (1 - e^{-p_2 t_0}) - e^{p_1 t} (1 - e^{-p_1 t_0}) \right\} \right], \quad \ldots \quad (132.7)$$

where b_I and b_{II} are capacitive voltage divider factors

$$b_I = \frac{C_{aIgI}}{C_{aIgI} + C_c + C_{g_1} + \dfrac{C_1 C_{aII}}{C_1 + C_{a_2}}} \quad \ldots \quad (133.7)$$

$$b_{II} = \frac{C_{aIIgII}}{C_{aIIgII} + C_c + C_{g_2} + \dfrac{C C_{aI}}{C + C_{aI}}} \quad \ldots \quad (134.7)$$

The corrected equations (129.7) and (130.7) are then:

$$V_{gI}(t_I) + \bar{V}_{gI}(t_I) = -\frac{1}{\mu} V_{aI}(t_I) \quad \ldots \quad (135.7)$$

$$V_{gII}(t_{II}) + \bar{V}_{gII}(t_{II}) = -\frac{1}{\mu} V_{aII}(t_{II}) \quad \ldots \quad (136.7)$$

As stated already, the monostable multivibrator operates in the correct manner if $t_I > t_{II}$.

7.3.4. THE SECOND PHASE OF THE DYNAMIC CONDITION

With the aid of (130.7) or (136.7), t_{II} can be determined. Then, at the instant $t = t_{II}$, the second phase of the dynamic condition starts. The grid voltage $V_{gII}(t)$, which is an exponential function, traverses the grid base of tube *II*. This part of the exponential function in the grid base is assumed to be practically linear, as depicted in fig. (34.7) (compare section 7.2.3.2, fig. 8.7). The time function of V_{gII} between the instant t_{II} and t_4 will be:

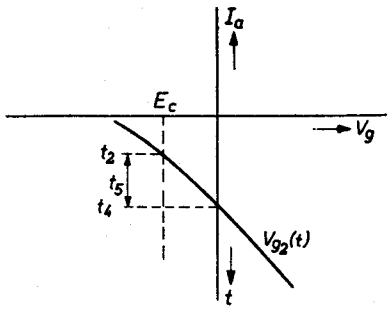

Fig. 34–7.

$$V_{gII}(t) = a\tau + E_c, \quad . \quad (137.7)$$

where:

$$\tau = t - t_2, \quad . \quad . \quad . \quad . \quad . \quad . \quad . \quad . \quad . \quad . \quad . \quad (138.7)$$

and a is a constant, given by:

$$0 = at_5 + E_c \quad \text{or} \quad a = -\frac{E_c}{t_5} = \frac{E_c}{t_4 - t_2}.$$

t_4 is to be calculated from $V_{gII}(t_4) = 0$

by substituting $t = t_4$ in expression (126.7).

It is further assumed that, at $t = t_{II}$, the anode voltage V_{aII} has practically reached the constant final value $V_{aI_0} = V'$.

The anode current for times $\tau = 0$ until $\tau = t_5$ is defined by:

$$I_a = \frac{V_{aII} + \mu V_{gII}}{r_a}, \quad . \quad . \quad . \quad . \quad . \quad . \quad . \quad . \quad . \quad . \quad (139.7)$$

whilst:

$$V_{aII} = V_{aII_0} - I_a Z_{a2}. \quad . \quad . \quad . \quad . \quad . \quad . \quad . \quad . \quad . \quad (140.7)$$

Z_{a2} is the impedance in the anode circuit, to be defined from fig. 32.7:

$$Z_{a2} = R_{a2} \frac{1 + Jp}{1 + Bp + Ep^2}, \quad . \quad . \quad . \quad . \quad . \quad . \quad . \quad . \quad (141.7)$$

where:

$$J = T_{g1} + T_{11} \text{ (see 99.7).}$$

Combination of (139.7) and (140.7) gives:

$$I_a = \frac{1}{r_a + Z_{a_2}} (V_{aII_0} + \mu V_{gII}) \quad . \quad . \quad . \quad . \quad . \quad (142.7)$$

Now:

$$V_{aII_0} + \mu V_{gII} = V' + \mu a\tau + \mu E_c = \mu a\tau \text{ (see 138.7).}$$

Thus:

$$I_a = \frac{1}{r_a + Z_{a_2}} (\mu a\tau) \quad \ldots\ldots\ldots \quad (143.7)$$

From (143.7) and (140.7):

$$V_{aII} = V_{aII_0} - \frac{Z_{a2}}{r_a + Z_{a_2}} (\mu a\tau) \quad \ldots\ldots \quad (144.7)$$

At $\tau = t_5$, or $t = t_4$, the grid voltage reaches zero and remains zero, as it is assumed that the internal grid resistance is negligibly small. This can be accounted for by assuming a new component of grid voltage to be present, given by:

$$V_{gII} (\tau - t_5) = -\mu a (\tau - t_5) \quad \ldots\ldots\ldots \quad (145.7)$$

Then, for times $\tau < t_5$ or $t < t_4$, the following expression holds:

$$V_{aII} (t - t_4) = V_{aII_0} - \frac{Z_{a_2}}{r_a + Z_{a_2}} \left[\mu a\tau - \mu a (\tau - t_5)\right] \quad \ldots\ldots \quad (146.7)$$

By operational methods, mentioned before, V_{aII} can be calculated. The final results are:

at $0 \leqq \tau \leqq t_5$ or $t_2 \leqq t \leqq t_4$

$$V_{aII} (t - t_2) = V_{aII_0} - \lambda_a V_{aII_0} \left[\frac{t - t_2}{t_4 - t_2} + \frac{N}{p_5 t_5} \left\{e^{p_5 (t - t_2)} - 1\right\} - \right.$$

$$\left. - \frac{1 + N}{p_6 t_5} \left\{e^{p_6 (t - t_4)} - 1\right\}\right] \quad \ldots\ldots\ldots\ldots\ldots\ldots \quad (147.7)$$

At $\tau \geqq t_5$ or $t \geqq t_4$:

$$V_{aII} (t - t_4) = V_{aII_0} - \lambda_a V_{aII_0} \left[1 + \frac{N}{p_5 t_5} e^{p_5 (t - t_2)} (1 - e^{-p_5 t_5}) - \right.$$

$$\left. - \frac{1 + N}{p_6 t_5} e^{p_6 (t - t_2)} (1 - e^{-p_6 t_5})\right] \quad \ldots\ldots\ldots\ldots\ldots\ldots \quad (148.7)$$

Where:

$$\lambda_a = \frac{R_{a_2}}{r_a + R_{a_2}} \quad \ldots\ldots\ldots \quad (149.7)$$

$$N = \frac{p_6(1 + Jp_5)}{p_5 - p_6} \quad \ldots\ldots\ldots \quad (150.7)$$

$$p_5 = -\frac{\lambda_i B + \lambda_a J}{2\lambda_i E}\left\{1 - \sqrt{1 - \frac{4\lambda_i E}{(\lambda_i B + \lambda_a J)^2}}\right\} \quad \ldots \quad (151.7)$$

$$p_6 = -\frac{\lambda_i B + \lambda_a J}{2\lambda_i E}\left\{1 + \sqrt{1 - \frac{4\lambda_i E}{(\lambda_i B + \lambda_a J)^2}}\right\} \quad \ldots \quad (152.7)$$

$$\lambda_i = 1 - \lambda_a = \frac{r_a}{r_a + R_{a_2}} \quad \ldots\ldots\ldots \quad (153.7)$$

The final value of $V_{a\text{II}}$ would be:

$$V_{a\text{II}}(\infty) = \lambda_i V_{a\text{II}_0} = \frac{r_a}{r_a + R_{a_2}} V_{a\text{II}_0} \quad \ldots\ldots \quad (154.7)$$

This is evident, for in this final state a constant anode current $I_{a_0\text{II}}$ would flow through the external and internal anode resistances, and have a value:

$$I_{a_0\text{II}} = \frac{V_{a\text{II}_0}}{r_a + R_{a_2}} \quad \ldots\ldots\ldots \quad (155.7)$$

This causes a voltage across r_a:

$$V_{a\text{II}}(\infty) = r_a I_{a_0\text{II}} = \frac{r_a}{r_a + R_{a_2}} V_{a\text{II}_0}.$$

The anode voltage $V_{a\text{II}}$ determines the grid voltage $V_{g\text{I}}$ by way of the voltage divider consisting of C_1 and Z_{g_1}.

$$V_{g\text{I}} = \frac{Z_{g_1}}{Z_{g_1} + \dfrac{1}{pC_1}} V_{a\text{II}}, \quad \ldots\ldots\ldots \quad (156.7)$$

or:

$$V_{g\text{I}} = T_{1\text{I}} \frac{p}{1 + (T_{1\text{I}} + T_{g_1})p} V_{a\text{II}} \quad \ldots\ldots \quad (157.7)$$

Keeping in mind that only variable components of $V_{a\text{II}}$ will be passed through the capacitance C_1, the steady state component $V_{a\text{II}_0}$ must not be substituted in expression (157.7) The final result of evaluating expression (157.7) is as follows:

$$\text{at } t_2 \leqq t \leqq t_4\text{: } V_{g\text{I}}(t-t_2) = -\lambda_a V_{a\text{II}_0}\frac{T_{11}}{t_5}\left[1-e^{-(t-t_2)/(T_{11}+T_{g1})}+\right.$$

$$+\frac{N}{1+p_5(T_{11}+T_{g_1})}\left\{e^{p_5(t-t_2)}-e^{-(t-t_2)/(T_{11}+T_{g1})}\right\}-$$

$$\left.-\frac{1+N}{1+p_6(T_{11}+T_{g_1})}\left\{e^{p_6(t-t_2)}-e^{-(t-t_2)/(T_{11}+T_{g1})}\right\}\right] \quad \ldots\ldots\ldots \quad (158.7)$$

$$\text{at } t \geqq t_4\text{: } V_{g_1}(t-t_4) = -\lambda_a V_{a\text{II}_0}\frac{T_{11}}{t_5}\left[e^{-(t-t_2)/(T_{11}+T_{g1})}\left(1-e^{t_5/(T_{11}+T_{g1})}\right)+\right.$$

$$+\frac{N}{1+p_5(T_{11}+T_{g_1})}\left\{e^{p_5(t-t_2)}\left(1-e^{-p_5t_5}\right)-e^{-(t-t_2)/(T_{11}+T_{g1})}\left(1-e^{t_5/(T_{11}+T_{g1})}\right)\right\}-$$

$$\left.-\frac{N}{1+p_6(T_{11}+T_{g_1})}\left\{e^{p_6(t-t_2)}\left(1-e^{-p_6t_5}\right)-e^{-(t-t_2)/(T_{11}+T_{g1})}\left(1-e^{t_5/(T_{11}+T_{g1})}\right)\right\}\right] \quad (159.7)$$

These two expressions must be added to the value of $V_{g\text{I}}$ originating from the first phase, i.e. to expression (106.7). The final value remains therefore: $V_{g\text{I}}(\infty) = V'''$. This is evident for tube I non-conducting.

Until the instant $t = t_4$, the anode voltage of tube I is represented by its first phase value, i.e. (119.7). At this instant, t_4, however, $V_{g\text{II}}$ shows a discontinuity, as it is suddenly kept at a constant value of zero. This causes transients at anode A_1 which can be calculated. However, since R_a will generally be small compared with R and R_{g_2}, the final contribution of these transients to the anode voltage of tube I will be small, and the complicated expression resulting from the calculations will be omitted.

Recapitulating the second phase voltage changes, it can be said that $V_{g\text{II}}$ is given by (126.7) for $0 \leqq t \leqq t_4$, and is zero for $t \geqq t_4$. $V_{a\text{II}}$ is given by (147.7) for $t_2 \leqq t \leqq t_4$, and by (148.7) for $t > t_4$, when it is assumed that the transients from the first phase have practically died out. $V_{g\text{I}}$ is given by expr. (106.7) from the first phase, to which must be added expression (158.7) for $t_2 \leqq t \leqq t_4$ and (159.7) for $t \geqq t_4$. $V_{a\text{I}}$ is given by expr. (119.7) from the first phase, if the effect of grid current in tube II is neglected.

7.3.5. THE THIRD PHASE OF THE DYNAMIC CONDITION

This phase commences as soon as the voltage at G_1 has increased to such a level that the cut-off value E_c is reached. Let this occur at the instant $t = t_6$. The tube I starts conducting, and the anode voltage

at A_1 decreases. This need only be a few volts for tube II to be cut off. Its anode voltage rises and adds in this way to the increase of V_{gI}; the whole process continuing more and more rapidly.

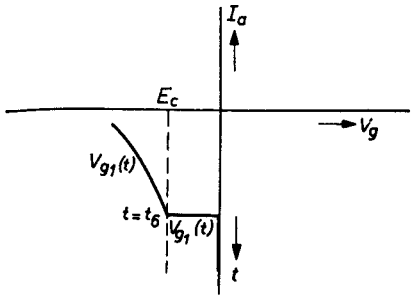

Fig. 35-7.

It will be assumed here that V_{gI} increases so rapidly that we can consider the change of V_{gI} to be a voltage step from the value E_c to zero, as represented in fig. 35.7:

$$V_{gI}(t-t_6) = E_c - E_c\,U(t-t_6), \tag{160.7}$$

where $U(t-t_6)$ is a unit-step function occurring at the instant $t = t_6$.

It is assumed that the final value of expr. (119.7) is practically reached for $t = t_6$.
This value is:

$$V_{aI}(\infty) = V_{aI_0} + I_{a_0} R_{av} \quad . \quad . \quad . \quad . \quad . \quad . \quad . \tag{161.7}$$

The anode current change is given by:

$$I_{aI} = \frac{V_{aI} + \mu V_{gI}(t-t_6)}{r_a}, \quad . \quad . \quad . \quad . \quad . \quad . \quad . \tag{162.7}$$

where:

$$V_{aI} = V_{aI}(\infty) - I_{aI} Z_{a_1} \quad . \quad . \quad . \quad . \quad . \quad . \quad . \quad . \tag{163.7}$$

Z_{a_1} is given by expr. (110.7).
From (162.7) and (163.7) it follows:

$$I_{aI} = \frac{V_{aI}(\infty) + \mu V_{gI}(t-t_6)}{r_a + Z_{a_1}} \quad . \quad . \quad . \quad . \quad . \tag{164.7}$$

Substituting (92.7) yields:

$$I_{aI} = \frac{1}{r_a + Z_{a_1}} \left[V_{aI}(\infty) + \mu \left\{ E_c - E_c U(t-t_6) \right\} \right] \quad . \quad . \tag{165.7}$$

However, $V_{aI}(\infty) + \mu E_c = 0$, as E_c is the cut-off voltage at an anode voltage $V_{aI}(\infty)$; then (165.7) becomes:

$$I_{aI} = \frac{1}{r_a + Z_{a_1}} V_{aI}(\infty)\, U(t-t_6) \quad . \quad . \quad . \tag{166.7}$$

According to (163.7) and (166.7):

$$V_{aI} = V_{aI}(\infty) - \frac{Z_{a_1}}{r_a + Z_{a_1}} V_{aI}(\infty)\, U(t - t_6) \quad . \quad . \quad . \quad (167.7)$$

The final result of the calculation will be:

$$V_{aI}(t - t_6) = V_{aI}(\infty) - \varrho_a V_{aI}(\infty)\left[1 + Pe^{p_7(t-t_6)} - (1+P)e^{p_8(t-t_6)}\right], \quad (168.7)$$

where:

$$\varrho_a = \frac{R_{av}}{r_a + R_{av}} \quad . \quad . \quad . \quad . \quad . \quad . \quad . \quad . \quad . \quad (169.7)$$

For R_{av}, see (111.7) $\qquad P = \dfrac{p_8(1 + Fp_7)}{p_7 - p_8}$

$$p_7 = -\frac{\varrho_i G + \varrho_a F}{2\varrho_i H}\left[1 - \sqrt{1 - \frac{4\varrho_i H}{(\varrho_i G + \varrho_a F)^2}}\right]$$

$$p_8 = -\frac{\varrho_i G + \varrho_a F}{2\varrho_i H}\left[1 + \sqrt{1 - \frac{4\varrho_i H}{(\varrho_i G + \varrho_a F)^2}}\right]; \quad \varrho_i = 1 - \varrho_a = \frac{r_a}{r_a + R_{av}}.$$

Another transient component will be caused by the sudden cessation of the flow of grid current in tube *II*. This will, for the same reason as we did not account for its sudden starting, be left out of consideration.

The final value of V_{aI} will be that of expression (168.7) at $t = \infty$:

$$V_{aI} \text{ final} = \varrho_i V_{aI}(\infty),$$

or, with expr. (161.7):

$$V_{aI} \text{ final} = \varrho_i \left(V_{aI_0} + I_{a_0} R_{av}\right).$$

According to (88.7):

$$I_{a_0} = \frac{V_{aI_0}}{r_a};$$

thus:

$$V_{aI} \text{ final} = \varrho_i V_{aI_0} \frac{r_a + R_{av}}{r_a} = (1 - \varrho_a)\, V_{aI_0} \frac{r_a + R_{av}}{r_a}.$$

Substituting (169.7) gives:

$$V_{aI} \text{ final} = V_{aI_0}.$$

In other words: the final value of V_{aI} is the same as the steady state value before triggering. A complete trigger cycle has elapsed.

We now consider the anode voltage of tube *II*. This can easily be determined by the following reasoning:

At the instant $t = t_6$, the grid G_1 is practically short-circuited to earth, and the anode impedance of tube *II* will be:

$$Z_{a_2} = \frac{R_{a_2}}{1 + R_{a_2}(C_1 + C_{a_2})\,p}, \quad \ldots\ldots \quad (170.7)$$

or:

$$Z_{a_2} = \frac{R_{a_2}}{1 + (T_{21} + T_{22})\,p} \quad \ldots\ldots \quad (171.7)$$

(compare expression (99.7)).

The anode current of tube *II* jumps at $t = t_6$ from zero to a value $I_{a_0 II}$, given by (155.7). This gives rise to a transient voltage at A_2, as represented by:

$$I_{a_0 II} \cdot R_{a_2}\,(1 - e^{-(t-t_6)/(T_{21}+T_{22})}) \quad \ldots\ldots \quad (172.7)$$

If it is assumed that the second phase transient (148.7) has reached its final state (154.7), viz.

$$V_{aII_6} = \frac{r_a}{r_a + R_{a_2}} V_{aII_0} \quad \ldots\ldots \quad (173.7)$$

at $t = t_6$, then the total voltage at A_2 is the sum of (172.7) and (173.7):

$$V_{aII}\,(t - t_6) = V_{aII_0} - \frac{R_{a_2}}{r_a + R_{a_2}} V_{aII_0}\, e^{-(t-t_6)/(T_{21}+T_{22})} \quad (174.7)$$

Again, the final state is equivalent to the static initial condition.

The grid voltage of tube *II*, V_{gII}, can be determined with the aid of the following considerations.

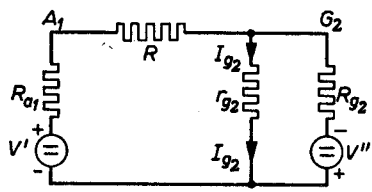

Fig. 36–7.

Immediately before the start of the third phase, a practically stationary situation was reached with tube *I* cut off and tube *II* conducting. Instead of fig. 31.7, the circuit of fig. 36.7 is representative for that part of the circuit at that instant. Without the grid current I_{g2}, the D.C. voltage sources V' and V'' would cause a potential between G and earth:

$$V_{gII} = -V'' + IR_{g_2}, \text{ where I is given by (90.7)}$$

Or:

$$V_{g\,II} = \varepsilon_g V' - (1 - \varepsilon_g)\, V'' ,$$

where ε_g is given by (93.7).

It is again assumed that I_{g_2} is such that it causes a voltage drop across the resistances R_{g_2} and $R + R_{a_1}$ in parallel, to compensate the value of V_{g_2} given above. This means a zero grid-to-cathode voltage. With this assumption we obtain the condition:

$$I_{g_2} \frac{R_{g_2}(R + R_{a_1})}{R_{g_2} + R + R_{a_1}} = \varepsilon_g V' - (1 - \varepsilon_g)\, V'' ,$$

from which I_{g_2} may be derived:

$$I_{g_2} = \frac{\varepsilon_g V' - (1 - \varepsilon_g)\, V''}{(1 - \varepsilon_g)\, R_{g_2}} \quad \ldots\ldots\ldots \quad (175.7)$$

At the instant $t = t_6$, tube I becomes conducting, tube II is cut off. Then the diagram of fig. 37.7 is valid for calculating the transients.

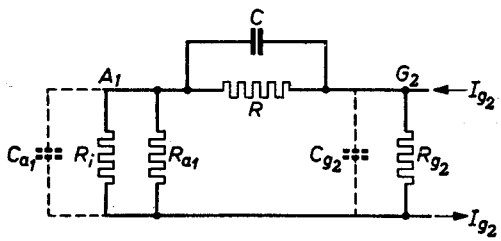

Fig. 37–7.

The anode voltage $V_{a\,I}(t—t_6)$ is known already and given by expr. (168.7). Part of this voltage is conducted to the grid G_2 by means of the voltage divider consisting of the $R-C$ parallel circuit and the $R_{g_2}-C_{g_2}$ parallel circuit.

In operational form, the voltage at G_2 as a result of $V_{a\,I}$ is:

$$V_{g\,II}(a_I) = \frac{R_{g_2}}{R_{g_2} + R} \frac{1 + Tp}{1 + (\beta_g T + \beta T_{g_2})\, p} V_{a\,It}(t - t_6) \cdot \quad (176.7)$$

For β and β_g, see (113.7); for T and T_{g_2}, see (114.7).

$V_{a\,It}$ represents the transient part of $V_{a\,I}$ from the instant $t = t_6$ onwards. This is the second term of the right-hand part of expr. (168.7)

$$V_{a\,It} = -\varrho_a V_{a\,I}(\infty) \left[1 + P e^{p_1 \tau} - (1 + P)\, e^{p_2 \tau}\right],$$

where: $$\tau = t - t_6.$$

This may be written in operational form as:

$$V_{a1t} = -\varrho_a V_{a1}(\infty)\left[1 + P\frac{p}{p-p_7} - (1+P)\frac{p}{p-p_8}\right] \quad (177.7)$$

(compare expr. (14.5)).

From (176.7) and (177.7) it follows that:

$$V_{g\text{II}}(a_1) = -\frac{R_{g_2}}{R_{g_2}+R}\,\frac{1+Tp}{1+(\beta_g T + \beta T_{g_2})p}\cdot$$
$$\cdot\,\varrho_a V_{a1}(\infty)\left[1 + P\frac{p}{p-p_7} - (1+P)\frac{p}{p-p_8}\right] \quad (178.7)$$

The influence of the sudden cessation of grid current I_{g_2} is again neglected, assuming that the positive voltage $\varepsilon_g V' - (1-\varepsilon_g)V''$ is small (see 175.7).

Expression (178.7) then represents the total grid voltage change. It must be superimposed on the D.C. voltage $-V'' + IR_{g_2}$ (for I, see expr. 90.7) and can be calculated in the same manner as already dealt with, namely by splitting into partial fractions. The rather cumbersome result will be given after examination of the final value for $t = \infty$. This can be found by putting $p = 0$ (equivalent to $t = \infty$)

$$V_{g\text{II}}(\infty) = -\frac{R_{g2}}{R+R_{g_2}}\varrho_a V_{a1}(\infty).$$

Substituting (161.7) and (169.7):

$$V_{g\text{II}}(\infty) = -\frac{R_{g2}}{R+R_{g_2}}\,\frac{R_{av}}{r_a+R_{av}}(V_{a1_0} + R_{av}I_{a_0})$$

According to (88.7):

$$V_{a1_0} = r_a I_{a_0}$$

Thus:

$$V_{g\text{II}}(\infty) = -\frac{R_{g_2}}{R+R_{g_2}}R_{av}I_{a_0}.$$

Introducing expr. (111.7) gives:

$$V_{g\text{II}}(\infty) = -\frac{R_{g_2}R_{a_1}}{R_{a_1}+R+R_{g_2}}I_{a_0} = -\varepsilon_a R_{g_2}I_{a_0}. \quad \text{(see 117.7)}$$

This is the final state of the transients, caused by the anode voltage change of tube I. This must be added to the ever present steady state components $V'' + IR_{g_2}$. Thus the final expression for $V_{g\text{II}}$ will be

$V_{gII}(\infty)$ total $= -V'' + (I - \varepsilon_a I_{a_0})\, R_{g2}$, and this is equal to the initial steady state value given by (92.7).

The total expression for the grid voltage of tube *II* in the third phase of the dynamic condition is the sum of the steady state components $-V'' + IR_{g_2}$ and the time function corresponding to the p-function (178.7):

$$V_{gII}(t - t_6) = \varepsilon_g V' - (1 - \varepsilon_g)\, V'' -$$
$$- \varepsilon_a R_{g_2} I_{a_0} \left[1 + \frac{T - S}{S} \left\{ 1 + \frac{P}{1 + Sp_7} - \frac{1 + P}{1 + Sp_8} \right\} e^{-(t-t_6)/S} + \right.$$
$$\left. + P \frac{1 + Tp_7}{1 + Sp_7} e^{p_7(t-t_6)} - (1 + P) \frac{1 + Tp_8}{1 + Sp_8} e^{p_8(t-t_6)} \right], \quad \ldots\ldots \quad (179.7)$$

where $S = \beta_g T + \beta T_{g_2}$.

Summarizing, the voltage changes derived for the third phase commencing at the instant $t = t_6$ are as follows:

$V_{gI} = 0$ for $t \geqq t_6$
V_{aI} is given by expr. (168.7)
V_{aII} ,, ,, ,, ,, (174.7)
V_{gII} ,, ,, ,, ,, (179.7)

7.3.6. EXPERIMENTAL VERIFICATION OF THE THEORY

A monostable multivibrator constructed to the circuit of fig. 28.7 with the following data was experimentally investigated.

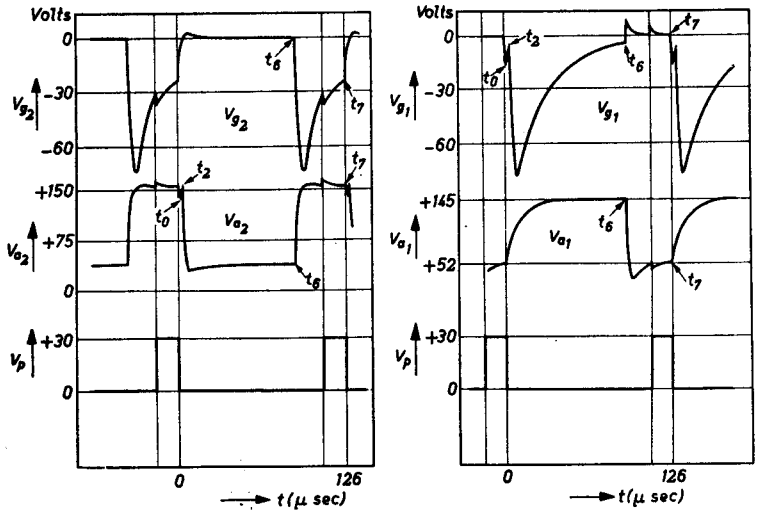

Fig. 38–7.

$V' = 150$ V $\qquad C_{a_1} = 500$ pF
$V'' = 100$ V $\qquad C_{a_2} = 1$ pF
$V''' = 0$ $\qquad C_{g_1} = C_{g_2} = 4$ pF
$C = C_1 = 100$ pF $\qquad C_c = 40$ pF
$R_{g_1} = R_{g_2} = R = 200$ kΩ
$R_{a_1} = R_{a_2} = 20$ kΩ

The tube was a development-type double triode with an amplification factor $\mu = 35$ and an internal anode resistance $r_a = 11.6$ kΩ.

The anode circuit of tube I was heavily loaded capacitively by $C_{a_1} = 500$ pF, with the intention of lengthening the duration of the very first period of the trigger cycle, in order to obtain a clear picture of these initial transients on an oscilloscope screen. If this is not done, then t_0 and t_{II} practically coincide, and the saw-tooth figure occurring at these instants in V_{gI} and V_{aII} would not be resolved by the oscilloscope (see fig. 38.7).

The following quantities can be calculated and are given below:

$I_{g_0} = 0$; $V_{aII_0} = 150$ V ; $\varepsilon_a = 0{\cdot}048$; $\varepsilon_g = \varepsilon = 0{\cdot}476$
$I_{a_0} = 4{\cdot}5$ mA (calculated with $r_a = 11{\cdot}6$ kΩ);
$V_{aI_0} = 52{\cdot}3$ V ; $V_{gII_0} = -23{\cdot}8$ V ; $V_{gI_0} = 0$;
$I_i = 6$ mA (calculated from $V_0 = 30$ V, $t_0 = 0{\cdot}2$ μsec)
$T = 20$ μsec ; $T_{a_2} = 0{\cdot}02$ μsec ; $T_{21} = 2$ μsec ;
$T_{11} = 20$ μsec ; $T_{g_1} = 8{\cdot}8$ μsec ; $T_{a1} = 10$ μsec ; $T_{22} = T_{g_2} = 0{\cdot}8$ μsec;
$A = 2{\cdot}02$ μsec ; $B = 30{\cdot}8$ μsec ; $E = 18{\cdot}18$ (μsec)^2 ;
$p_1 = -0{\cdot}034.10^6$ sec^{-1} ; $p_2 = -1{\cdot}66.10^6$ sec^{-1} ;
$K = -0{\cdot}952$; $R_{av} = 19$ kΩ
$R_{ag} = 9{\cdot}52$ kΩ
$\beta = \beta_g = 0{\cdot}5$;
$F = 10{\cdot}4$ μsec ; $G = 24{\cdot}2$ μsec ; $H = 100{\cdot}18$ (μsec)^2 ;
$p_3 = -0{\cdot}0537.10^6$ sec^{-1} ; $p_4 = -0{\cdot}19.10^6$ sec^{-1} ;
$L = -0{\cdot}613$; $M = +0{\cdot}103$;
$\lambda_a = 0{\cdot}633$; $\lambda_i = 0{\cdot}367$.
$J = 28{\cdot}8$ μsec ; $p_5 = -0{\cdot}0322.10^6$ sec^{-1} ;
$p_6 = -4{\cdot}38.10^6$ sec^{-1}.
$N = -0{\cdot}1$; $\varrho_a = 0{\cdot}62$; $\varrho_i = 0{\cdot}38$;
$p_7 = -0{\cdot}079.10^6$ sec^{-1} ; $p_8 = -0{\cdot}322.10^6$ sec^{-1} ;
$P = -0{\cdot}236$.

Photographs of the traces on the oscilloscope screen have been reproduced in figs 39.7 up till 43.7.

These pictures have been redrawn in fig. 38.7, in order to indicate several points of interest, and at the same time to give the phase re-

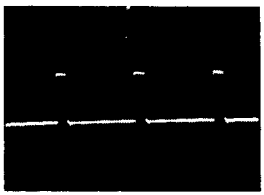

Fig. 39–7.

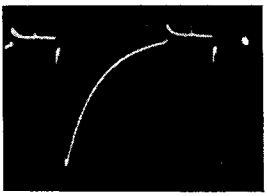

Fig. 40–7.

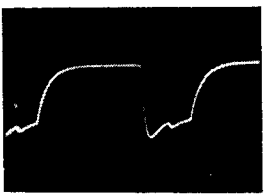

Fig. 41–7.

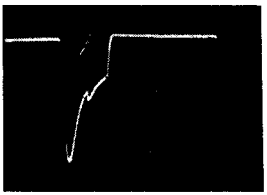

Fig. 42–7.

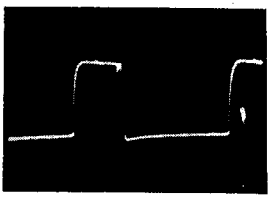

Fig. 43–7.

lationship between diverse signals at anodes and grids and the input trigger pulse.

The latter has a rectangular shape, a period of 126 μsec corresponding to about 8000 pulses per second.

The waveform of the voltages calculated with the aid of the values given above follows the experimental waveform so closely that the differences cannot be indicated in the drawing. Therefore it will be sufficient to compare some specific calculated and measured values.

Calculated values are as follows:

$t_0 = 0{\cdot}2$ μsec
$t_2 = 2{\cdot}5$,,
$t_4 = 3{\cdot}9$,,
$t_5 = t_4 - t_2 = 1{\cdot}4$ μsec
$t_6 = 90$ μsec (measured 89·6 μsec)

V_{gI}: at $t = t_0$: —23·3 V (measured —17 V)
,, $t = t_2$: —7·1 ,, (,, —6·5 ,,)
,, $t = t_4$: —69 ,, (,, —70 ,,)
,, $t = t_6$: —3·86 ,, (,, —4 ,,)
V_{aI}: at $t = t_2$: 71·32 V

At this value of the anode voltage the cut-off grid voltage of the tube is —3·1 V. However, at the instant $t = t_2$ V_{gI}, is below —6 V, so that there is no danger that the wrong tube, in this case tube *I*, will be conducting first.

At $t = t_6$ $V_{aI} = V_{aI}(\infty) = 138$ V
(measured 143 V)
V_{gII}: at $t = t_2$: —6 V (cut-off voltage at $V_{aII} = 150$ V)
at $t = t_7$ (end of the period) $V_{gII} = -26$ V
(measured —25 V)
V_{aII}: at $t = t_0$: 129·5 V (measured 135 V)
,, $t = t_2$: 150 V (,, 150 V)
,, $t = t_4$: 78·7 V

7.4. THE ASTABLE MULTIVIBRATOR

7.4.1. INTRODUCTION

The astable multivibrator (to be abbreviated in the following to AMV) differs fundamentally in its operation from both other types, mono- and bi-stable MV, in that the latter need external trigger signals to obtain any switching- or flip-flop action, whereas the AMV is provided with such a strong regeneration that it automatically and continuously goes on triggering itself internally. Thus it is essentially an astable device; hence its name. It never reaches a steady state. The monostable and bi-stable MV on the contrary, as their names suggest, possess one and two stable states respectively. This fact enabled us to describe their trigger or switching action by starting from their stable, steady state condition, and then calculating the transients caused by a single triggering signal. When these signals are of a periodic nature, the results of the analysis apply only when the periodic time of the triggering signals is large enough for the transients to have died out before further triggering takes place.

It is therefore evident that the problem with the AMV will have to be attacked in another way. However, one thing can be stated in advance:

If the AMV, which is in fact a (relaxation) oscillator, has reached a stationary state (to be distinguished from steady state), it must be true that any potential difference or current anywhere in the network must attain the same value periodically. This will be the starting point in solving the problem. In particular, the potential difference across the coupling capacitors between the anodes and grids of the tubes will be observed by giving it an as yet unknown value at the beginning of a period, then considering its evolution throughout the complete period, calculating its value at the end of the period, and finally putting this value equal to its initial value. This condition of equal values at the start and at the end of each cycle gives an equation which enables us to determine the frequency and the waveform of any potential difference or current in the circuit in general by a graphical method, and by an explicit expression under certain circumstances.

The method indicated will now be applied to several AMV circuits, namely to the symmetrical and the asymmetrical MV, both with and without a D.C. control voltage in the grid circuits of the tubes.

7.4.2. THE SYMMETRICAL AMV

7.4.2.1. Determination of the frequency of the AMV signal

The most general AMV circuit is represented in fig. 44.7.

A D.C. supply voltage source V feeds two tubes A and B, which need not be triodes as drawn in fig. 44.7, but may also be pentodes, through anode resistances R_{1A} and R_{1B} respectively.

Grid-leaks R_{2A} and R_{2B} are connected between the grids and the negative H.T. lead, to which both cathodes are also connected. This is the case of zero grid control voltage.

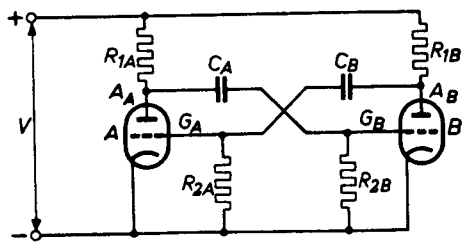

Fig. 44-7.

The anodes and grids are connected cross-wise by coupling capacitors C_A and C_B. With the following assumptions, a fairly quick method of obtaining the required results is possible:

The internal anode resistances of the tubes in the fully conducting state and the internal grid resistances at zero or positive grid-to-cathode potential are very small compared with the external resistances in the anode and grid circuits.

Furthermore it is assumed that the influence of the stray capacitances of the valve electrodes and the wiring, which shunt the resistances

and can have considerable effects on the wave shape of the relaxation signal at high frequencies, is negligible.

More precisely, this means that the time constants containing these stray capacitances are very small compared with the period and time of rise of the relaxation signal.

With these assumptions, the MV action may be described as a switching device that changes the two valves alternately from the conducting into the non-conducting state in a switching time that is negligibly small compared with the total period of the relaxation signal which results from this switching action.

The MV is symmetrical if tubes A and B are of the same type and

$$R_{1A} = R_{1B} = R_1,\ R_{2A} = R_{2B} = R_2,\ C_A = C_B = C.$$

Then, during one half of the total period of the MV signal, one of the tubes, say B, is conducting; the other tube, A, is cut off. During the second half of the period, the reverse process holds, namely tube B is cut off and tube A conducting. The equivalent circuit of the MV will be for the first half of the period as depicted in fig. 45.7, whilst for the second half period it is as represented in fig. 46.7.

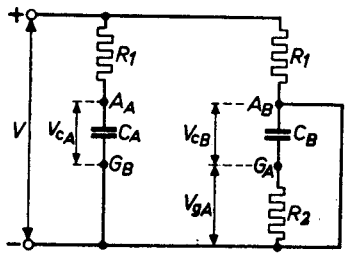

Fig. 45–7.

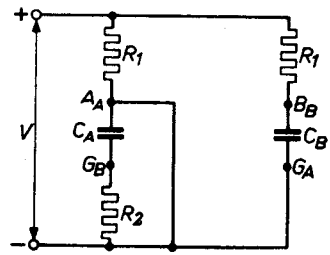

Fig. 46–7.

From fig. 45.7 it can be stated that the voltage across C_A, indicated by V_{CA}, will ultimately attain a value

$$V_{CA}\ (t = \infty) = V \quad \ldots\ldots\ldots \quad (180.7)$$

If its initial value, at the instant $t = 0$, when the MV was switched over to the state depicted in fig. 45.7, was also known, the time function according to which V_{CA} changes would be known, since it will be an exponential function with a time constant

$$T_C = R_1 C_A, \quad \ldots\ldots\ldots \quad (181.7)$$

extending from the initial value, as yet unknown, to the final value V. The unknown initial value, however, can be determined from consideration of fig. 46.7, since the final value of V_{CA} in this circuit will

be the same as the initial value of V_C from fig. 45.7. If the position in fig. 46.7 lasted indefinitely, it is clear that V_{CA} would attain a value of zero. This would, at the same time, be the case with the grid voltage V_{GB}, since $V_{GB} = -V_{CA}$. However, before this voltage V_{GB} can become zero, it passes the value $-E_C$, the cut-off grid voltage of the tubes. At this instant the MV switches over from one state into the other. So, the final value of V_{GB} in fig. 46.7 is $-E_C$, the final value of V_{CA} then being:

$$V_{CA} \text{ (final)} = +E_C \quad \ldots\ldots\ldots \quad (182.7)$$

This is, as already mentioned, the initial value in the circuit of fig. 45.7, It can therefore be written:

$$V_{CA}\,(t = 0) = E_C \quad \ldots\ldots\ldots \quad (183.7)$$

From (180.7), (181.7) and (183.7) it is now possible to write down the time function representing V_{CA} in the first half period, namely:

$$V_{CA} = V - (V - E_C)\, e^{-t/T_c} \quad \ldots\ldots \quad (184.7)$$

This voltage, V_{CA}, however, never reaches its ultimate value V, as, at a certain instant $t = t_1$, the voltage V_{CB} of circuit fig. 45.7 passes the value E_C, and at the same time the grid voltage V_{GA} is $-E_C$. This means that tube A starts conducting and the state of fig. 45.7 is switched over to the state of fig. 46.7.

If, at this instant, $t = t_1$, the voltage V_{CA} is V_0; then, from (184.7):

$$V_{CA}\,(t = t_1) = V_0 = V - (V - E_C)\, e^{-t_1/T_c} \quad \ldots \quad (185.7)$$

For a further t_1 seconds from the instant when $t = t_1$, the circuit of fig. 46.7 is valid.

We now know the initial value of V_{CA} (see (185.7)) and its ultimate value, namely:

$$V_{CA}\,(t = \infty) = 0 \quad \ldots\ldots\ldots \quad (186.7)$$

Between these values, V_{CA} changes exponentially with a time constant:

$$T_a = R_2 C_A \quad \ldots\ldots\ldots\ldots \quad (187.7)$$

and can be represented by the time function:

$$V_{CA} = V_0 e^{-t/T_a} \quad \ldots\ldots\ldots \quad (188.7)$$

Here the time-scale is different from that in the first half period. The instant $t = 0$ from expression (188.7) corresponds with $t = t_1$ from expression (184.7).

For $t = t_1$, expression (188.7) must be (in its own time-scale):

$$V_{CA}\,(t = t_1) = E_C = V_0\, e^{-t_1/T_a} \quad \ldots\ldots \quad (189.7)$$

Summarizing: expression (184.7) represents V_{CA} for the first half period of t_1 seconds, and expression (188.7) for the second half period of t_1 seconds. The initial value of (187.7) is equal to the final value of (188.7), namely E_C (see (184.7) and (189.7)). The final value of (184.7) is equal to the initial value of (188.7), namely V_0 (see (185.7) and (188.7)).

Now, from equations (185.7) and (189.7) it is possible to eliminate the unknown voltage V_0 to give one equation with one unknown, t_1.

It is convenient to introduce a new variable x, as follows:

$$x = e^{-t_1/T_d} \quad \ldots\ldots\ldots\ldots \quad (190.7)$$

Introducing x in (185.7) and (189.7) gives:

$$V_0 = V - (V - E_C)\, x^{T_d/T_c} \quad \ldots\ldots \quad (185a.7)$$

$$E_C = V_0 x. \quad \ldots\ldots\ldots\ldots \quad (189a.7)$$

Eliminating V_0 gives:

$$E_C = \left[V - (V - E_C)\, x^{T_d/T_c}\right] x \quad \ldots\ldots \quad (191.7)$$

In general, it will not be easy to solve this equation for x, and so a graphical method of obtaining x is proposed. In order to obtain a universal method, it is advantageous to introduce relative values of the voltages by dividing both (185a.7) and (189a.7) by the supply voltage V, giving:

$$\frac{V_0}{V} = 1 - (1 - D)\, x^{T_d/T_c} \quad \ldots\ldots \quad (185b.7)$$

$$\frac{V_0}{V} = \frac{D}{x}, \quad \ldots\ldots\ldots\ldots \quad (189b.7)$$

where:

$$D = \frac{E_c}{V}. \quad \ldots\ldots\ldots\ldots \quad (192.7)$$

D is practically constant for a given type of tube, when varying V.

According to (181.7) and (187.7):

$$\frac{T_d}{T_c} = \frac{R_2}{R_1} \quad \ldots\ldots\ldots\ldots \quad (193.7)$$

This is the ratio of the discharging to the charging time constant of the coupling capacitors C_A and C_B.

Now, the graphical method for solving x from (185b.7) and (189b.7) is as follows:

Draw $\frac{V_0}{V}$ according to these equations on the same graph. Then the point of intersection of the two curves gives the required value of x, and half the period of the MV signal is given by:

$$t_1 = T_d \ln \frac{1}{x}, \quad \ldots \ldots \ldots \quad (194.7)$$

as can be derived from (190.7).

The whole period will be:

$$T = 2t_1 = 2T_d \ln \frac{1}{x}, \quad \ldots \ldots \quad (195.7)$$

and the frequency is:

$$f = \frac{1}{T} = \frac{1}{2T_d \ln \frac{1}{x}} \quad \ldots \ldots \quad (196.7)$$

For examples of this graphical solution the reader is referred to the book mentioned in section 7.1.

It appears that, as D is decreased and T_d/T_c increased, V_0 more and more closely approaches V.

In practice, for $D < 0{,}1$ and $\frac{T_d}{T_c} > 1$, the approximation $V_0 \doteq V$ is valid. In that case, (189*b*.7) simplifies to:

$x = D$, and the following approximate formulae for the MV period and frequency hold:

$$T = 2T_d \ln \frac{1}{D} \quad \ldots \ldots \ldots \quad (197.7)$$

$$f = \frac{1}{2T_d \ln \frac{1}{D}} \quad \ldots \ldots \ldots \quad (198.7)$$

7.4.2.2. Waveform of the symmetrical AMV signal

The most important quantities, next to the frequency, which we like to know, are the changes in anode and grid voltages of both tubes.

These can be derived from the voltage changes across the coupling capacitors C_A and C_B. From fig. 45.7 it can be seen that for the first half-period the voltage of tube A is equal to V_{CA}; so, according to (184.7):

$$V_{A_1}(0 - t_1) = V_{CA} = V - (V - E_c)\, e^{-t/T_c} \quad . \quad (199.7)$$

During the second half-period this anode voltage is, according to fig. 46.7, given by:

$$V_{A_A}(t_1 - 2t_1) = 0 \quad \ldots\ldots\ldots \quad (200.7)$$

The grid voltage changes of tube B are:

for the first half period (see fig. 45.7):

$$V_{GB}(0 - t_1) = 0. \quad \ldots\ldots\ldots \quad (201.7)$$

for the second half period, according to fig. 46.7 and equation (188.7):

$$V_{GB}(t_1 - 2t_1) = -V_{CA} = -V_0 e^{-t/T_a} \quad \ldots \quad (202.7)$$

Because of the symmetrical properties of the circuit, the voltage changes across capacitor C_B will be equal to those across C_A, but shifted in time over half a period (t_1 sec).

So, during the first half period:

$$V_{C_B}(0 - t_1) = V_0 e^{-t/T_a}, \quad \ldots\ldots\ldots \quad (203.7)$$

and during the second half period:

$$V_{C_B}(t_1 - 2t_1) = V - (V - E_c) e^{-t/T_c} \quad \ldots \quad (204.7)$$

Then it is easy to see that:

$$V_{A_B}(0 - t_1) = 0. \quad \ldots\ldots\ldots\ldots \quad (205.7)$$

$$V_{A_B}(t_1 - 2t_1) = V - (V - E_c) e^{-t/T_c} \cdot \quad \ldots \quad (206.7)$$

$$V_{G_A}(0 - t_1) = -V_0 e^{-t/T_a} \quad \ldots\ldots\ldots \quad (207.7)$$

$$V_{G_A}(t_1 - 2t_1) = 0 \quad \ldots\ldots\ldots\ldots \quad (208.7)$$

In fig. 47.7 the various waveforms have been represented, namely:

V_{C_A}	according	to	equations	(184.7) and (188.7)
V_{C_B}	,,	,,	,,	(203.7) and (204.7)
V_{A_A}	,,	,,	,,	(199.7) and (200.7)
V_{G_A}	,,	,,	,,	(207.7) and (208.7)
V_{A_B}	,,	,,	,,	(205.7) and (206.7)
V_{G_B}	,,	,,	,,	(201.7) and (202.7)

If the value of x has been determined by graphical methods, as described in the previous section, then from (189a.7) it is found that:

$$V_0 = \frac{E_c}{x}.$$

The various waveforms are then known. In most practical cases, V_0 will be approximately equal to V, as already stated.

In the graphs of fig. 47.7, the difference between T_d and T_c has been chosen to be not very large. Therefore V_0 differs markedly from V. Should T_c be chosen much smaller, then all curves with the subscript T_c would rise much more steeply and attain the V_0 level in a much shorter time than t_1.

The stationary condition of the AMV will automatically correct this inequality of the two half-periods by taking a higher V_0 level such that the T_c-curves will reach this level at the correct instant $t = t_1$.

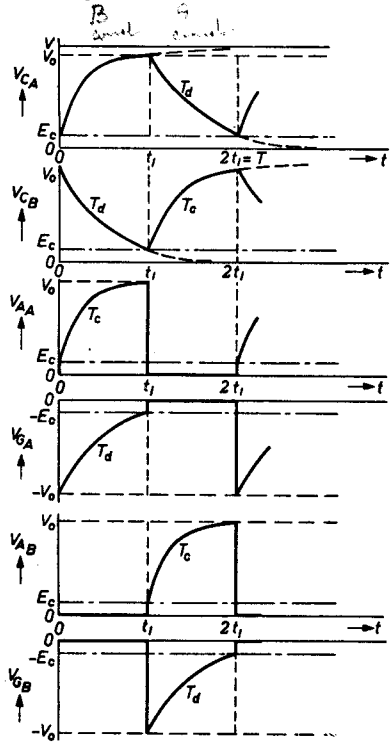

Fig. 47-7.

7.4.2.3. Influence of internal tube resistances

All previous derivations hold only for the case that the internal anode- and grid-resistances of the tubes are negligibly small compared with the circuit resistances. It can easily be shown that this is almost always satisfied as far as the internal grid resistance is concerned, but internal anode resistances may assume values up to tens of kilohms. With pentodes we have almost always to take into account the internal resistance below the "knee" of the $I_a V_a$-characteristic. This is because in the conducting state the tubes always have a grid-to-cathode potential very near to zero, and the anode load resistance will generally be large enough to have a voltage drop across this resistance sufficient to bring the anode-to-cathode voltage below the "knee" value. If this is not so, then the tube is not very suitable as a switching device. With triodes, on the other hand, rather high internal anode resistances may occur. It is therefore worth while to investigate the influence of this internal resistance. First the grid circuit will be considered. In fig. 48.7 the grid current - grid voltage characteristic is represented in a general form. Grid current starts at a negative grid voltage value of about 1 V and increases rapidly for positive values of V_g.

The straight lines l_1 and l_2 represent load lines for a certain value of grid leak resistance for D.C. grid-to-cathode bias voltages of 0 and $+V_c$ V respectively.

As can be seen from fig. 48.7, the grid-to-cathode voltage (V_{g_1} and V_{g_2}) will not be greatly influenced by large variations in grid bias voltage V_c, and we can assume values always very near to zero (in practice between —1 and +1 V). The assumption of a zero grid internalresistance implies that the I_gV_g-curve coincides with the vertical I_g-axis, thus always giving a zero grid-to-cathode voltage for every load line and bias voltage V_c. This approximation can be considered as sufficient to describe practical circumstances.

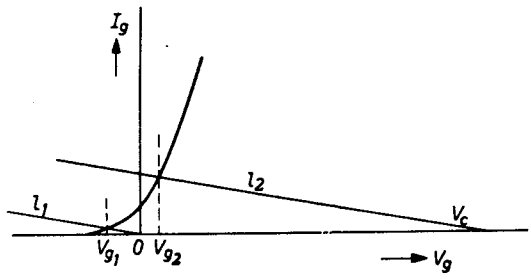

Fig. 48–7.

The influence of the anode internal resistance, however, needs closer examination. For both tubes, the introduction of an internal anode resistance r_a changes the equivalent circuits of the AMV (figs 45.7 and

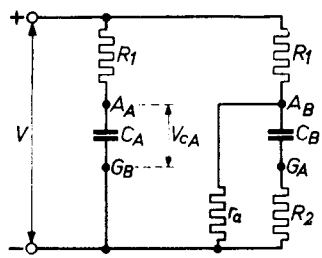

Fig. 49–7.

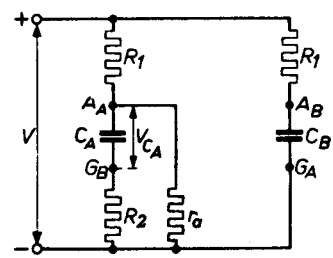

Fig. 50–7.

46.7) into those depicted in figs 49.7 and 50.7. The situation of fig. 49.7 starts at the instant $t = 0$ and ends at $t = t_1$. The voltage across capacitor G_A at the instant t_1 is again assumed to be

$$V_{C_A}(t = t_1) = V_0 \quad \ldots\ldots\ldots \quad (209.7)$$

This is, at the same time, the initial value in the situation of fig. 50.7, which lasts a further t_1 seconds. The value of V_{C_A} in this situation tends to $\frac{r_a}{R_1 + r_a} V$, as $t \to \infty$; so:

$$V_{C_A}(t=\infty) = \frac{r_a}{R_1 + r_a} V \quad \ldots\ldots \quad (210.7)$$

Thus, capacitor C_A discharges from the initial value V_0 (at $t = 0$ in a new time scale), to an ultimate value $\frac{r_a}{R_1 + r_a} V$, according to an exponential time function with a time constant

$$T_d' = C_A\left(R_2 + \frac{R_1 r_a}{R_1 + r_a}\right) = C_a R_2\left(1 + \frac{R_1 r_a}{R_2(R_1 + r_a)}\right) = T_d(1 + \lambda_g), \quad (211.7)$$

where:

$$\lambda_g = \frac{R_1 r_a}{R_2(R_1 + r_a)} \quad \ldots\ldots \quad (212.7)$$

(For the transients, R_1 and r_a may be considered to be in parallel between point A_A and the negative H.T. supply lead.)

Hence:

$$V_{C_A}(t_1 - 2t_1) = \frac{r_a}{R_1 + r_a} V + \left(V_0 - \frac{r_a}{R_1 + r_a} V\right) e^{-t/T_d'} . \quad (213.7)$$

Representing the parallel combination of R_1 and r_a by a value R_s,

$$R_s = \frac{R_1 r_a}{R_1 + r_a} \quad \ldots \quad (214.7)$$

the discharging circuit of C_A is given by fig. 51.7. From this circuit it can be easily seen that the change in grid voltage of tube B during the second half of the period is:

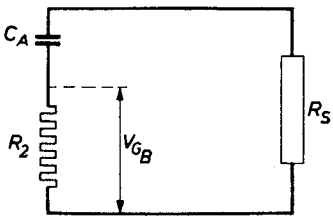

Fig. 51-7.

$$V_{G_B}(t_1 - 2t_1) = -\frac{R_2}{R_2 + R_s} \overline{V_{C_A}}.$$

Here $\overline{V_{C_A}}$ represents only the transient component of V_{C_A}, that is the second term in (213.7), since the D.C. component $\frac{r_a}{R_1 + r_a}$ does not affect the voltage across R_2. Thus:

$$V_{G_B}(t_1 - 2t_1) = -\frac{R_2}{R_2 + R_s}\left(V_0 - \frac{r_a}{R_1 + r_a} V\right) e^{-t/T_d'} \quad \ldots \quad (215.7)$$

This second half-period lasts t_1 seconds and ends when V_{G_B} attains the value $-E_c$, so that t_1 is defined by the relation:

$$E_c = \frac{R_2}{R_2 + R_s}\left(V_0 - \frac{r_a}{R_1 + r_a} V\right) e^{-t_1/T'_d} \quad . \quad . \quad . \quad . \quad (216.7)$$

From (213.7) and (216.7) it can be seen that the value of V_{C_A} at the end of the second half-period is:

$$V_{C_A}(2t_1) = \frac{r_a}{R_1 + r_a} V + \frac{R_2 + R_s}{R_2} E_c \quad . \quad . \quad . \quad (217.7)$$

But this is also its initial value for the first half-period:

$$V_{C_A}(0) = \frac{r_a}{R_1 + r_a} V + \frac{R_2 + R_s}{R_2} E_c , \quad . \quad . \quad . \quad (218.7)$$

whilst the ultimate value (for $t = \infty$) would be V. So, the time function representing V_{C_A} in the first half period is:

$$V_{C_A}(0 - t_1) = V - \left\{V - V_{C_A}(0)\right\} e^{-t/T_c} , \quad . \quad . \quad . \quad (219.7)$$

where $T_c = C_A R_1$, the same value as in previous sections. Substituting (218.7) and (219.7) gives:

$$V_{C_A}(0 - t_1) = V - \left(\frac{R_1}{R_1 + r_a} V - \frac{R_2 + R_s}{R_2} E_c\right) e^{-t/T_c} . \quad (220.7)$$

At the instant $t = t_1$, this capacitor voltage has attained the value V_0:

$$V_0 = V - \left(\frac{R_1}{R_1 + r_a} V - \frac{R_2 + R_s}{R_2} E_c\right) e^{-t_1/T_c} \quad . \quad . \quad (221.7)$$

Expression (216.7) can be rearranged as:

$$\frac{V_0}{V} = \lambda_a + (1 + \lambda_g)\frac{D}{x} \quad . \quad . \quad . \quad . \quad . \quad . \quad . \quad (216a.7)$$

and (221.7) as:

$$\frac{V_0}{V} = 1 - \left\{1 - \lambda_a - (1 + \lambda_g) D\right\} x^{T'_d/T_c} , \quad . \quad . \quad (221a.7)$$

where:

$$\lambda_a = \frac{r_a}{R_1 + r_a} \quad . \quad . \quad . \quad . \quad . \quad . \quad . \quad . \quad . \quad . \quad (222.7)$$

$$\lambda_g = \frac{R_s}{R_2} = \frac{R_1 r_a}{R_2 (R_1 + r_a)} \quad . \quad . \quad . \quad . \quad . \quad . \quad . \quad (223.7)$$

$$D = \frac{E_c}{V} \quad . \quad . \quad . \quad . \quad . \quad . \quad . \quad . \quad . \quad . \quad . \quad (192.7)$$

$$x = e^{-t_1/T'_d} \quad . \quad . \quad . \quad . \quad . \quad . \quad . \quad . \quad . \quad . \quad . \quad (224.7)$$

Expressions (216*a*.7) and (221*a*.7) must be compared with expressions (189*b*.7) and (185*b*.7) respectively from section 7.4. 2.1, to obtain an idea of the influence of the internal anode resistance r_a. Thus it will be seen that, where (189*b*.7) represents $\frac{V_0}{V}$ as a function of x by a hyperbola that is symmetrical with respect to the horizontal and vertical axis, (216*a*.7) represents a hyperbola shifted upwards by an amount λ_a with respect to the horizontal axis.

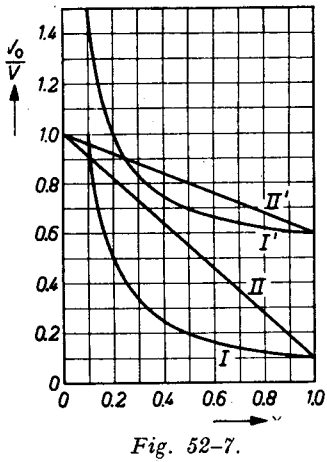

Fig. 52–7.

In addition, instead of D, a slightly larger value $(1 + \lambda_g)\, D$ must be substituted. In most practical cases, R_s will be much smaller than R_2, or $\lambda_g \ll 1$. Thus the apparent increase of D will be negligibly small. In fig. 52.7, equations (185*b*.7), (189*b*.7) (216*a*.7) and (221*a*.7) are represented graphically for a simple case, namely for

$$T_d/T_c = 1,\ T_d'/T_c = 1,\ \lambda_a = \tfrac{1}{2} \text{ and } D = \tfrac{1}{10}.$$

Then these equations are as follows:

$$\begin{cases} \dfrac{V_0}{V} = 1 - 0{,}9x \\ \dfrac{V_0}{V} = \dfrac{1}{10x} \end{cases} \quad \ldots\ldots\ldots\ldots\ldots \quad (185c.7),\ (189c.7)$$

$$\begin{cases} \dfrac{V_0}{V} = \lambda_a + (1 + \lambda_g)\dfrac{1}{10x} \\ \dfrac{V_0}{V} = 1 - \left\{1 - \lambda_a - (1 + \lambda_g)\tfrac{1}{10}\right\} x \end{cases} \quad \ldots\ldots \quad (216b.7),\ (221b.7)$$

The influence of λ_g has been neglected in the graphs of fig. 52.7. From equations (189*b*.7) and (185*b*.7), as well as from (216*a*.7) and (221*a*.7), it can be seen that a solution for $x = 1$ always occurs (intersection of both curves in fig. 52.7).

This solution, however, has no practical importance, as can easily be shown for the case of zero internal anode resistance; for according to (189.7) and (192.7), $V_0 = E_c$ if $x = 1$.

This means that the grid voltages would never exceed the cut-off

value, but only just reach this value, so that the tubes could not be switched from the conducting to the non-conducting state.

Also fig. 52.7 shows that there is always a second point of intersection of both curves. It can be seen that this occurs at practically the same value of $\frac{V_0}{V}$, viz. $\frac{V_0}{V} = 0{,}9$, but at different values of x. For the curves (185*c*.7) and (189*c*.7), the value of x is 0,11, which is quite near to the chosen value of D.

For the curves (216*b*.7) and (221*b*.7) the solution for x is $x = 0{,}25$.

Comparing the two cases, it follows from equation (196.7):

For $r_a = 0$, the frequency of the AMV signal will be:

$$f_0 = \frac{1}{2T_d \ln \frac{1}{0{,}11}}.$$

For $r_a = R_1$ ($\lambda_a = \frac{1}{2}$), the frequency will be:

$$f_1 = \frac{1}{2T_d' \ln \frac{1}{0{,}25}}.$$

Now, $T_d = T_d'$, as both $\frac{T_d}{T_c}$ and $\frac{T_d'}{T_c}$ have been chosen equal to unity; hence, the ratio:

$$\frac{f_1}{f_0} = \frac{\ln \frac{1}{0{,}11}}{\ln \frac{1}{0{,}25}} = 1{,}6.$$

It is apparent that the influence of the internal anode resistance is to increase the frequency of the AMV signal, although the charging and discharging time constants have been kept constant.

The value $\frac{T_d'}{T_c} = 1$ is rather exceptional in practice, as, in general, $\frac{T_d'}{T_c} \gg 1$, because $\frac{R_2}{R_1} \gg 1$. If this condition holds, it can easily be shown that in practice $\frac{V_0}{V}$ is unity for the point of intersection of the two curves that is of practical importance.

Taking $\frac{V_0}{V} = 1$ reduces equation (216*a*.7) to:

$$1 = \lambda_a + (1 + \lambda_g)\frac{D}{x},$$

or:

$$x = \frac{1 + \lambda_g}{1 - \lambda_a} D, \quad \ldots\ldots\ldots\ldots \quad (225.7)$$

and the AMV-frequency is:

$$f = \frac{1}{2T_d' \ln \dfrac{1 - \lambda_a}{(1 + \lambda_g) D}} \quad \ldots\ldots\ldots \quad (226.7)$$

As must be expected, this expression changes into (198.7) if r_a is taken as zero.

Substituting λ_a and λ_g (see (222.7) and (223.7)), respectively, in (226.7) gives:

$$f = \frac{1}{2T_d' \ln \dfrac{1}{D\left\{1 + r_a\left(\dfrac{1}{R_1} + \dfrac{1}{R_2}\right)\right\}}} \quad \ldots\ldots \quad (226a.7)$$

In fig. 53.7, curve I represents equation (216a.7) for $\lambda_a = 0{,}5$, $\lambda_g = 0$, $D = 0{,}1$ and $T_d'/T_c = 2$, whilst curve II represents equation (221a.7) for the same values of parameters. Curve II' also represents (221a.7), except that the value of T_d'/T_c is taken as unity. Thus, curves I and II' correspond with the upper two curves in fig. 52.7. It can be seen from fig. 53.7 that the point of intersection of curves I and II' $\left(\dfrac{V_0}{V} = 0{,}9;\ x = 0{,}25\right)$ shifts to the point $\dfrac{V_0}{V} = 0{,}99$, $x = 0{,}2$, where curves I and II intersect. The value of x would not have been changed much if it was taken from the intersection of curve I with the horizontal line $\dfrac{V_0}{V} = 1$. So, for values of $\dfrac{T_d'}{T_c} \geq 2$ and higher, it is a sufficiently good approximation to say that:

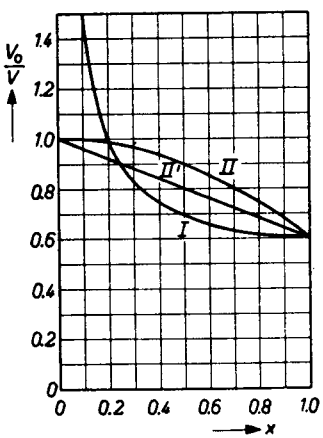

Fig. 53-7.

$$V_0/V = 1.$$

Consequently, equations (225.7), (226.7), (226*a*.7) are valid for these cases, which cover the majority of practical applications of the A.M.V.

The waveform of the different voltage changes can be derived from the expressions (220.7), (213.7), (215.7).

From fig. 49.7 it can be seen that:

$$V_{A_A}(0-t_1) = V_{C_A}(0-t_1) = V - \{(1-\lambda_a)\,V - (1+\lambda_g)\,E_c\}\,e^{-t/T_c} \quad (220a.7)$$

$$V_{G_B}(0-t_1) = 0 \quad (227.7)$$

From fig. 50.7:

$$V_{A_A}(t_1-2t_1) = V_{C_A}(t_1-2t_1) + V_{G_B}(t_1-2t_1) =$$

$$= \lambda_a V + (V_0 - \lambda_a V)\,e^{-t/T_d'} - \frac{1}{1+\lambda_g}(V_0 - \lambda_a V)\,e^{-t/T_d'},$$

or:

$$V_{A_A}(t_1-2t_1) = \lambda_a V + \frac{\lambda_g}{1+\lambda_g}(V_0 - \lambda_a V)\,e^{-t/T_d'} \quad (228.7)$$

$$V_{G_B}(t_1-2t_1) = -\frac{1}{1+\lambda_g}(V_0 - \lambda_a V)\,e^{-t/T_d'} \quad (215.7)$$

Because of the symmetrical properties of the AMV, it is clear that:

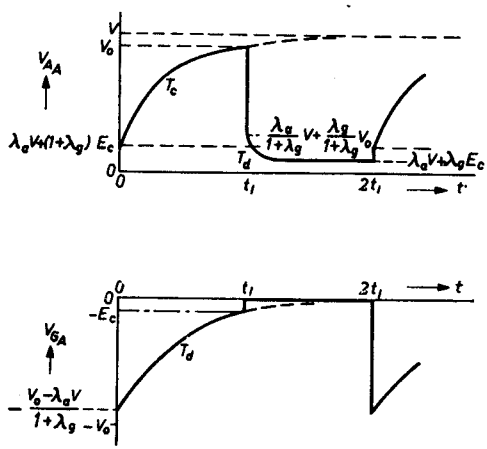

Fig. 54–7.

$$V_{A_B}(t_1-2t_1) = V_{A_A}(0-t_1)$$

$$V_{G_A}(t_1-2t_1) = 0$$

$$V_{A_B}(0-t_1) = V_{A_A}(t_1-2t_1)$$

$$V_{G_A}(0-t_1) = V_{G_B}(t_1-2t_1).$$

For $\lambda_a = \lambda_g = 0$, expression (220*a*.7) changes into (199.7), (228.7) into (200.7), and (225.7) into (202.7), as might be expected.

The initial value of V_{A_A} for the first half-period is:

$$V_{A_A}(0) = \lambda_a V + (1+\lambda_g)\,E_c \quad (229.7)$$

The final value of V_{A_A} for the first half-period is: $V_{A_A}(t_{1-}) = V_0$, as can be seen from (220*a*.7) and (221.7). The initial value of V_{A_A} for the second half-period is:

$$V_{A_A}(t_{1+}) = \frac{\lambda_a}{1+\lambda_g} V + \frac{\lambda_g}{1+\lambda_g} V_0 .$$

The final value of V_{A_A} for the second half-period is:

$$V_{A_A}(2t_1) = \lambda_a V + \lambda_g E_c ,$$

as can be seen from (228.7) and (216.7).

From (215.7) it follows:

$$V_{G_B}(t_{1+}) = -\frac{V_0 - \lambda_a V}{1+\lambda_g}$$

$$V_{G_B}(2t_1) = -\frac{V_0 - \lambda_a V}{1+\lambda_g} e^{-t_1/T_d'} = -E_c \quad \text{(according to (216.7))}$$

In fig. 54.7, V_{A_A} and V_{G_A} have been represented graphically.

V_{G_A} has the same waveform as V_{G_B} shifted in time over a period t_1 seconds.

A comparison of fig. 54.7 with fig. 47.7 shows the influence of the internal anode resistance r_a. The amplitudes of the different waveforms have been reduced, whilst the steep negative-going front of the anode voltage waveform is rounded off at its lower part.

7.4.2.4. Influence of a positive grid-bias voltage

Introducing a D.C. positive voltage source V' in both grid circuits changes the equivalent circuit diagrams of fig. 49.7 and 50.7 into those of fig. 55.7 and 56.7.

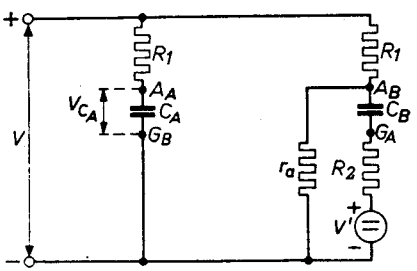

Fig. 55–7.

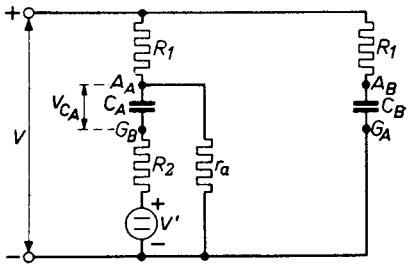

Fig. 56–7.

The complete derivation of the fundamental equations will not be repeated, but following the same reasoning as before, it is easy to arrive at the following expressions:

$$\frac{V_0}{V} = \lambda_a - \gamma + (1+\lambda_g)\frac{\gamma + D}{x} \quad \ldots\ldots\ldots\ldots \quad (230.7)$$

$$\frac{V_0}{V} = 1 - \{1 - \lambda_a - \lambda_g\gamma - (1 + \lambda_g)\, D\}\, x^{T_d'/T_c} \quad . \quad . \quad . \quad . \quad (231.7)$$

These equations may be compared with (216*a*.7) and (221*a*.7) respectivily, or with (189*b*.7) and (85*b*.7) respectively.

The quantity γ represents the ratio of the grid control voltage V' to the H.T. supply voltage V:

$$\gamma = \frac{V'}{V} \quad . \quad . \quad . \quad . \quad . \quad . \quad . \quad . \quad . \quad . \quad . \quad (232.7)$$

For $\gamma = 0$, equations (230.7) and (231.7) change into (216*a*.7) and (221*a*.7). If, moreover, λ_a and λ_g are taken to be zero, equations (230.7), (231.7) change into (189*b*.7) and (185*b*) respectivily.

The frequency of the AMV can be found from (230.7) and (231.7) by applying the same graphical procedure as before. Here again there will always be a solution of $x = 1$, as can be seen from (230.7) and (231.7), but this has no further practical importance. The other solution will, as a rule, be a value of x rather small with respect to unity, and therefore the term x^{T_d'/T_c} in (231.7) becomes negligible when the ratio T_d'/T_c assumes a value of, say, two or more. This will hold in most practical cases, so that (231.7) simplifies to $\frac{V_0}{V} = 1$, and consequently (230.7) becomes:

$$1 = \lambda_a - \gamma + (1 + \lambda_g)\frac{\gamma + D}{x},$$

or:

$$\frac{1}{x} = \frac{1 + \gamma - \lambda_a}{(1 + \lambda_g)(\gamma + D)} \quad . \quad . \quad . \quad . \quad . \quad . \quad . \quad . \quad (233.7)$$

x was defined by:

$$x = e^{-t_1/T_d'} \text{ (compare with (224.7))}.$$

This implies:

$$t_1 = T_d' \ln \frac{1}{x}.$$

The AMV signal frequency is:

$$f = \frac{1}{T} = \frac{1}{2t_1},$$

or:

$$f = \frac{1}{2T_d' \ln \frac{1}{x}}.$$

Substituting (233.7) yields:

$$f = \frac{1}{2T_d' \ln \dfrac{1 + \gamma - \lambda_a}{(1 + \lambda_g)(D + \gamma)}}, \quad \ldots \quad (234.7)$$

where:

$$T_d' = C\left(R_2 + \frac{R_1 r_a}{R_1 + r_a}\right)$$

$$\gamma = \frac{V'}{V}; \quad \lambda_a = \frac{r_a}{R_1 + r_a}; \quad \lambda_g = \frac{R_1 r_a}{R_2 (R_1 + r_a)}; \quad D = \frac{E_c}{V}.$$

The waveform of the capacitor and anode and grid voltages can be shown to be as follows:

In the first half-period lasting t_1 seconds:

$$V_{C_A} = V - \left\{(1 - \lambda_a)\, V - \lambda_g V' - (1 + \lambda_g)\, E_c\right\} e^{-t/T_c}. \quad \ldots \quad (235.7)$$

$$V_{G_B} = 0$$

$$V_{A_A} = V_{C_A} = V - \left\{(1 - \lambda_a)\, V - \lambda_g V' - (1 + \lambda_g)\, E_c\right\} e^{-t/T_c} \quad (236.7)$$

The initial values are:

$$V_{G_B}(0) = 0$$

$$V_{C_A}(0) = V_{A_A}(0) = \lambda_a V + \lambda_g V' + (1 + \lambda_g)\, E_c \quad \ldots \quad (237.7)$$

The final values are:

$$V_{G_B}(t_{1-}) = 0 \quad \ldots \quad (238.7)$$

$$V_{C_A}(t_{1-}) = V_{A_A}(t_{1-}) = V_0 \quad \ldots \quad (239.7)$$

In the second half-period lasting another t_1 seconds:

$$V_{C_A} = \lambda_a V - V' + (V_0 - \lambda_a V + V')\, e^{-t/T_d'} \quad \ldots \quad (240.7)$$

$$V_{G_B} = V' - \frac{1}{1 + \lambda_g}(V_0 - \lambda_a V + V')\, e^{-t/T_d'} \quad \ldots \quad (241.7)$$

$$V_{A_A} = \lambda_a V + \frac{\lambda_g}{1 + \lambda_g}(V_0 - \lambda_a V + V')\, e^{-t/T_d'} \quad \ldots \quad (242.7)$$

The initial values are:

$$V_{C_A}(t_1+) = V_0 \quad \ldots \quad (243.7)$$

$$V_{G_B}(t_1+) = \frac{\lambda_g V' + \lambda_a V - V_0}{1 + \lambda_g} \quad \ldots \quad (244.7)$$

$$V_{A_A}(t_1+) = \frac{\lambda_g (V_0 + V') + \lambda_a V}{1 + \lambda_g} \quad \ldots \quad (245.7)$$

The final values are:

$$V_{C_A}(2t_1) = \lambda_a V + \lambda_g V' + (1 + \lambda_g) E_c = V_{C_A}(0) \quad . \quad . \quad . \quad (246.7)$$

$$V_{G_B}(2t_1) = -E_c \quad . \quad . \quad . \quad . \quad . \quad . \quad . \quad . \quad . \quad . \quad . \quad . \quad . \quad . \quad . \quad . \quad . \quad . \quad (247.7)$$

$$V_{A_A}(2t_1) = \lambda_a V + \lambda_g (V' + E_c) \quad . \quad . \quad . \quad . \quad . \quad . \quad . \quad . \quad . \quad . \quad . \quad (248.7)$$

Comparing the amplitudes of the anode and grid voltages with those of fig. 54.7, it can be seen that the amplitude of the grid voltage is diminished by an amount $\frac{\lambda_g}{1 + \lambda_g} V'$, whilst that of the anode voltage is diminished by an amount $\lambda_g V'$. The general aspect of the waveforms will be the same as depicted in fig. 54.7. Furthermore, it should be noted that the ultimate value of the grid voltage in the first half of the period will not be zero (see dotted curve in V_{G_A} graph, fig. 54.7, following the instant t_1), but V'. So the angle of intersection between the exponential curve (T_d) and the cut-off level (dash-dot line) will be larger with a certain control voltage V' than without. The larger this angle, the better will be the frequency stability of the AMV signal, since the shift of the intersection point because of interference will be smaller for larger angles. Therefore, from the point of view of frequency stability, it is better to use a high positive grid-bias voltage with a larger time constant, T_d', than no bias at all with a smaller T_d', for generating the same frequency.

7.4.3. THE ASYMMETRICAL AMV

The fundamental circuit diagram is that of fig. 57.7. The period of the AMV signal now consists of two quasi-stable states with a different duration. The first state is assumed to last t_1 seconds, the second t_2 seconds, the total period T thus being $T = t_1 + t_2$.

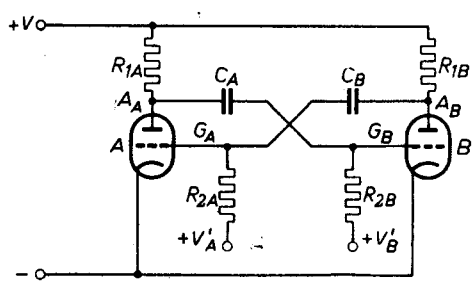

Fig. 57-7.

In fig. 58.7, the first state (from 0 to t_1 seconds) is represented in an equivalent diagram. The second state (from t_1 to $t_1 + t_2$ seconds) (or in a new time scale from 0 to t_2 seconds) is represented in fig. 59.7.

The final value at the instant t_1 of the voltage across C_A in fig. 58.7 is assumed to be:

$$V_{C_A}(t_1) = V_{O_A} \quad . \quad . \quad . \quad . \quad . \quad . \quad . \quad . \quad . \quad . \quad . \quad (249.7)$$

This is, at the same time, the initial value for the circuit of fig. 59.7. The ultimate value for infinite time would be:

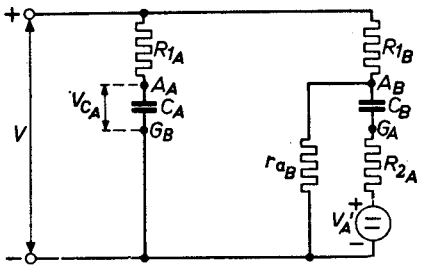

Fig. 58–7.

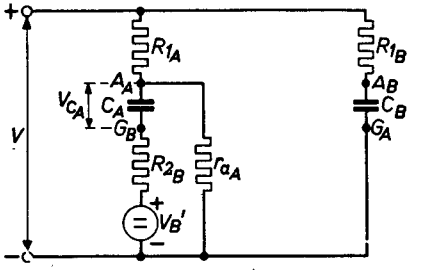

Fig. 59–7.

$$V_{C_A}(\infty) = \frac{r_{a_A}}{r_{a_A} + R_{1_A}} V - V'_B, \quad \ldots \quad (250.7)$$

or:

$$V_{C_A}(\infty) = \lambda_{a_A} V - V'_B, \quad \ldots \quad (251.7)$$

where:

$$\lambda_{a_A} = \frac{r_{a_A}}{r_{a_A} + R_{1_A}} \quad \ldots \quad (252.7)$$

During this second part of the period, the capacitor C_A will discharge with a time constant

$$T'_{d_A} = C_A \left(R_{2B} + \frac{r_{a_A} R_{1_A}}{r_{a_A} + R_{1_A}} \right), \quad \ldots \quad (253.7)$$

according to the exponential function:

$$V_{C_A} = \lambda_{a_A} V - V'_B + (V_{O_A} - \lambda_{a_A} V + V'_B)\, e^{-t/T'_{d_A}}. \quad (254.7)$$

The last right-hand component (the transient component) of (254.7) causes a current to flow through the grid leak R_{2_B}:

$$I_{2_B} = \frac{1}{R_{2_B} + \frac{r_{a_A} R_{1_A}}{r_{a_A} + R_{1_A}}} (V_{O_A} - \lambda_{a_A} V + V'_B)\, e^{-t/T'_{d_A}},$$

or a voltage drop appears across R_{2_B}:

$$V_{R_{2_B}} = - \frac{R_{2_B}}{R_{2_B} + \frac{r_{a_A} R_{1_A}}{r_{a_A} + R_{1_A}}} (V_{O_A} - \lambda_{a_A} V + V'_B)\, e^{-t/T'_{d_A}}.$$

Introducing

$$\lambda_{g_A} = \frac{r_{a_A} R_{1_A}}{R_{2_B}(r_{a_A} + R_{1_A})} \quad \ldots\ldots\ldots \quad (255.7)$$

gives:

$$V_{R_{2_B}} = -\frac{1}{1+\lambda_{g_A}} (V_{O_A} - \lambda_{a_A} V + V'_B)\, e^{-t/T'_{d_A}},$$

and the total voltage on the grid of tube B will be:

$$V_{G_B} = V'_B - \frac{1}{1+\lambda_{g_A}} (V_{O_A} - \lambda_{a_A} V + V'_B)\, e^{-t/T'_{d_A}} \quad \ldots \quad (256.7)$$

As soon as this voltage reaches the cut-off value $-E_{C_B}$ of tube B, the AMV switches from the state shown in fig. 59.7 to that in fig. 58.7. This occurs at the instant when $t = t_2$; so:

$$-E_{C_B} = V'_B - \frac{1}{1+\lambda_{g_A}} (V_{O_A} - \lambda_{a_A} V + V'_B)\, e^{-t_2/T'_{d_A}}, \quad \ldots \quad (257.7)$$

or:

$$(V_{O_A} - \lambda_{a_A} V + V'_B)\, e^{-t_2/T'_{d_A}} = (1+\lambda_{g_A})(E_{C_B} + V_B'). \quad (258.7)$$

From (258.7) and (254.7) it can be seen that the final value of V_{C_A} in the second part of the period will be:

$$V_{C_A}(t_2) = \lambda_{a_A} V - V_B' + (1+\lambda_{g_A})(E_{C_B} + V_B') \quad \ldots \quad (259.7)$$

This is also the initial value for the first part of the period (fig. 58.7).

$$V_{C_A}(0) = V_{C_A}(t_2).$$

The ultimate value for infinite time would be:

$$V_{C_A}(\infty) = V \quad \ldots\ldots\ldots\ldots \quad (260.7)$$

The capacitor C_A is thus charged with a time constant

$$T_{C_A} = C_A R_{1A}, \quad \ldots\ldots\ldots\ldots \quad (261.7)$$

according to an exponential function:

$$V_{C_A} = V - \left\{V - V_{C_A}(0)\right\} e^{-t/T_{C_A}},$$

or:

$$V_{C_A} = V - \left\{V(1-\lambda_{a_A}) + V_B' - (1+\lambda_{g_A})(E_{C_B} + V_B')\right\} e^{-t/T_{C_A}},$$

or:

$$V_{C_A} = V - \left\{(1-\lambda_{a_A})\, V - \lambda_{g_A} V_B' - (1+\lambda_{g_A})\, E_{C_B}\right\} e^{-t/T_{C_A}} \quad (262.7)$$

At the instant $t = t_1$, V_{C_A} reaches the value V_{O_A}; thus:

$$V_{O_A} = V - \{(1 - \lambda_{a_A})\, V - \lambda_{g_A} V_B' - (1 + \lambda_{g_A})\, E_{C_B}\}\, e^{-t_1/T_{C_A}}. \quad (263.7)$$

From equations (258.7) and (263.7) the unknown voltage V_{O_A} can be eliminated, giving one relation between t_1 and t_2.

Considering the voltage changes across capacitor C_B during the whole AMV signal period will give similar expressions as (258.7) and (263.7); only the indices A and B and t_1 and t_2 have been interchanged. From these expressions the unknown voltage V_{O_B} can be eliminated, giving another relation between t_1 and t_2. The complete derivation will be omitted here, giving only the final result:

$$y = \frac{(1 + \lambda_{g_A})\,(D_B + \gamma_B)}{1 - \lambda_{a_A} + \gamma_B - \{(1 - \lambda_{a_A} - \lambda_{g_A}\gamma_B - (1 + \lambda_{g_A})\, D_B\}\, x^{T'_{d_B}/T_{C_A}}} \quad (264.7)$$

$$x = \frac{(1 + \lambda_{g_B})\,(D_A + \gamma_A)}{1 - \lambda_{a_B} + \gamma_A - \{1 - \lambda_{a_B} - \lambda_{g_B}\gamma_A - (1 - \lambda_{g_B})\, D_A\}\, y^{T'_{d_A}/T_{C_B}}} \quad (265.7)$$

where:

$$x = e^{-t_1/T'_{d_B}}$$

$$y = e^{-t_1/T'_{d_A}}$$

$$T'_{dB} = C_B\left(R_{2_A} + \frac{r_{a_B} R_{1_B}}{r_{a_A} + R_{1_B}}\right);\ T'_{d_A} \text{ see (253.7)}$$

$$T_{C_B} = C_B R_{1_B};\ T_{C_A} \text{ see (261.7)}$$

$$\lambda_{g_A} \text{ see (255.7)};\ \lambda_{g_B} = \frac{r_{a_B} R_{1_B}}{R_{2_A}(r_{a_B} + R_{1_B})}$$

$$\lambda_{a_A} \text{ see (252.7)};\ \lambda_{a_B} = \frac{r_{a_B}}{r_{a_B} + R_{1_B}}$$

$$D_A = \frac{E_{C_A}}{V};\ D_B = \frac{E_{C_B}}{V}$$

$$\gamma_A = \frac{V_A'}{V};\ \gamma_B = \frac{V_B'}{V}$$

Now, t_1 and t_2, or x and y, can be solved graphically by plotting, in the same graph, y as a function of x according to (264.7), and x as a function of y according to (265.7). The point of intersection of both curves gives the solution for x and y. There will always be a solution $x = 1$, $y = 1$, which has no practical significance. The other solution will always be of such values that x and y are small compared with unity, so that it is

worthwhile to examine the power of x in (264.7) and that of y in (265.7). If these powers are sufficiently larger than unity, the last term in both denominators can be neglected. These powers are:

$$\frac{T'_{dB}}{T_{C_A}} \approx \frac{C_B}{C_A} \cdot \frac{R_{2_A}}{R_{1_A}} \text{ and}$$

$$\frac{T'_{dA}}{T_{C_B}} \approx \frac{C_A}{C_B} \cdot \frac{R_{2_B}}{R_{1_B}} \text{ respectively.}$$

Generally, the grid leak resistors R_{2_A} and R_{2_B} will be much larger than the anode resistors R_{1_A} and R_{1_B}. Consequently, the powers will be sufficiently large if C_B and C_A do not differ by a large amount. The asymmetry of the MV will mostly be determined by these capacitance values. A ratio $\frac{C_A}{C_B}$ of $\frac{1}{10}$ or 10 will not be exceeded very often. A ratio of $\frac{R_2}{R_1}$ larger than 10 will generally be used, so that, in the majority of practical applications, the powers of x and y may be neglected. Then expressions (164.8) and (265.7) are simplified to the following expressions:

$$y = \frac{(1 + \lambda_{g_A})\,(D_B + \gamma_B)}{1 - \lambda_{a_A} + \gamma_B} \quad \ldots\ldots\ldots \quad (264a.7)$$

$$x = \frac{(1 + \lambda_{g_B})\,(D_A + \gamma_A)}{1 - \lambda_{a_B} + \gamma_A}, \quad \ldots\ldots\ldots \quad (265a.7)$$

and the frequency is explicitly defined by:

$$f = \frac{1}{T} = \frac{1}{t_1 + t_2}$$

$$t_1 = T'_{d_B} \ln \frac{1}{x}, \quad t_2 = T'_{d_A} \ln \frac{1}{y}. \quad \ldots\ldots\ldots\ldots \quad (266.7)$$

$$f = \frac{1}{T'_{d_B} \ln \dfrac{1 - \lambda_{a_B} + \gamma_A}{(1 + \lambda_{g_B})\,(D_A + \gamma_A)} + T'_{d_A} \ln \dfrac{1 - \lambda_{a_A} + \gamma_B}{(1 + \lambda_{g_A})\,(D_A + \gamma_B)}} \quad (267.7)$$

In practice, the tubes will often be identical, for instance two halves of a double triode or pentode, whilst the grid bias voltages V'_A and V'_B are taken from the same source. Then, $D_A = D_B = D$ and $\gamma_A = \gamma_B = \gamma$.

Moreover, the resistances in both halves of the AMV will often be the same, i.e. $R_{1_A} = R_{1_B} = R_1$ and $R_{2_A} = R_{2_B} = R_2$. Then:

$$\lambda_{a_A} = \lambda_{a_B} = \lambda_a \text{ and } \lambda_{g_A} = \lambda_{g_B} = \lambda_g$$

and expression (267.7) is simplified to:

$$f = \frac{1}{(T'_{d_A} + T'_{d_B}) \ln \frac{1 - \lambda_a + \gamma}{(1 + \lambda_g)(D + \gamma)}} \quad \ldots \quad (268.7)$$

Once x and y have been defined, either graphically or explicitly, the voltages V_{O_A} and V_{O_B} can be determined, and the waveform of the different anode and grid voltages can be calculated.

If, in expression (268.7), the time constants T'_{d_A} and T'_{d_B} are equal, this expression is identical to (234.7), so that the AMV is symmetrical again.

7.4.4. CONCLUSION

In section 7.4 a graphical method of determining the frequency and waveform of an astable multivibrator signal is presented. In most practical cases simplifications are possible, to give explicit expressions for those quantities. The influence of internal anode resistance of the tubes is taken into account, whilst it is shown that the influence of internal grid resistance will, to a good approximation, always be negligible.

Summarizing the explicit expressions for the frequency gives the following:

a. Asymmetrical AMV with positive D.C. grid bias voltage:

$$f = \frac{1}{T'_{d_B} \ln \frac{1 - \lambda_{g_B} + \gamma_A}{(1 + \lambda_{g_B})(D_A + \gamma_A)} + T'_{d_A} \ln \frac{1 - \lambda_{a_A} + \gamma_B}{(1 + \lambda_{g_A})(D_B + \gamma_B)}} \quad \ldots \quad (267.7)$$

$$\lambda_{a_A} = \frac{r_{a_A}}{r_{a_A} + R_{1_A}}$$

$$\lambda_{a_B} = \frac{r_{a_B}}{r_{a_B} + R_{1_B}}$$

$$\lambda_{g_A} = \frac{R_{1_A}}{R_{2_B}} \lambda_{a_A}$$

$$\lambda_{g_B} = \frac{R_{1_B}}{R_{2_A}} \lambda_{a_B}$$

$$T'_{dA} = T_{dA}(1 + \lambda_{gA})$$
$$T'_{dB} = T_{dB}(1 + \lambda_{gB})$$
$$T_{dA} = C_A R_{2B}$$
$$T_{dB} = C_B R_{2A}$$
$$\gamma_A = \frac{V_A'}{V}$$
$$\gamma_B = \frac{V_B'}{V}$$
$$D_A = \frac{E_{cA}}{V}$$
$$D_B = \frac{E_{cB}}{V}$$

b. The quantity γ is a measure of the grid control voltage. If grid leaks are returned to the cathode (negative H.T. line), γ *is zero* and (267.7) is simplified to:

$$f = \frac{1}{T'_{dB} \ln \frac{1 - \lambda_{aB}}{(1 + \lambda_{gB}) D_A} + T'_{dA} \ln \frac{1 - \lambda_{aA}}{(1 + \lambda_{gA}) D_B}} \quad . \quad . \quad . \quad (269.7)$$

c. If corresponding quantities with indices A and B are equal, the AMV becomes *symmetrical*, and the frequency in the case of positive grid bias is:

$$f = \frac{1}{2T_d (1 + \lambda_g) \ln \frac{1 - \lambda_a + \gamma}{(1 + \lambda_g)(D + \gamma)}} \quad . \quad . \quad . \quad . \quad (270.7)$$

(see (234.7)).

Without positive grid bias:

$$f = \frac{1}{2T_d (1 + \lambda_g) \ln \frac{1 - \lambda_a}{(1 + \lambda_g) D}} \quad . \quad . \quad . \quad . \quad . \quad . \quad . \quad (271.7)$$

(see (226.7))

7.4.5. EXPERIMENTAL CHECK OF THE THEORY

A symmetrical astable multivibrator circuit according to the circuit of fig. 44.7 has been investigated. The only difference was in the con-

nection of the bottom of the grid leak resistances R_2. These were not connected to the negative terminal, but to the positive terminal of the H.T. supply. In this case we have to take into account a control voltage V' equal to the H.T. supply voltage V, so that $\gamma = \frac{V'}{V} = 1$. The ratio of the grid-leak resistance to the anode-load resistance was always sufficiently large to permit expression 234.7 to be used with reasonable accuracy to determine the frequency.

The tube used was a double triode type E 90 CC. The negative value of the grid voltage at which the anode current falls to 100 μA was rather arbitrarily chosen as the cut-off voltage, E_c. The mean value of E_c for 10 tubes was found to be 10.5 V, with a maximum value of 11.5 V and a minimum of 9.2 V. The mean value of the frequency of these ten tubes used in the circuit, was 1006 cycles per second, with a maximum value of 1060 c/s and a minimum value of 970 c/s. The circuit components were:

Anode load	$R_1 = 10{\cdot}1$ kΩ
Grid leak	$R_2 = 101$ kΩ
Coupling capacitor	$C = 10{,}000$ pF

Substituting these values and $E_c = 10{\cdot}5$ V, $V = 200$ V, $r_a = 4$ kΩ, $\gamma = 1$ in expression (234.7) gives a value of 1033 cycles per second for the frequency. This has a deviation of 2·7% from the measured value.

The influence of several circuit components has been calculated and measured. The results are given in the following table. The H.T. supply voltage throughout is $V = 200$ V, with r_a taken as 4 kΩ and E_c chosen to be 10·5 V.

R_1 (kΩ)	R_2 (kΩ)	C (kpF)	f (measured) (c/s)	f (calculated) (c/s)	Deviation (%)
10·1	101	10	1006	1033	2·7
10·1	101	15	690	689	0
10·1	101	5·6	1705	1840	7·8
10·1	560	10	191	182	—4·6
10·1	1000	10	109	102	—6·3
5·7	101	10	1134	1237	9·0
15·1	101	10	933	955	2·3

The waveforms of a few of these multivibrator circuits have been given in the oscillograms of figs 60.7 to 63.7. In figs 60.7 and 61.7

respectively, the changes of grid and anode voltage are shown. These waveforms should be compared with the calculated ones given in fig. 54.7. The circuit conditions were as follows: — Tube E 90 CC with $r_a = 4$ kΩ, $E_c = 10{\cdot}5$ V ($V = 200$ V). Coupling capacitors 10 kpF; anode load resistors $R_1 = 10{\cdot}1$ kΩ; grid leak resistors $R_2 = 1$ MΩ. The frequency measured which can be taken from the table above, amounts to 109 c/s. Thus, the duration of one complete cycle is practically 10 msec. The ratio $\frac{T'_d}{T_c}$, which is $\frac{R_2}{R_1}$ approximately, is large here (about 100), so that the anode voltage V_0 of the non-conducting tube will reach the value of the H.T. supply voltage V within a fairly short time. It can be seen from fig. 61.7 that the anode voltage in the non-conducting half-period does in fact reach "saturation", that is, the value V, in a time small compared with the total period of the signal.

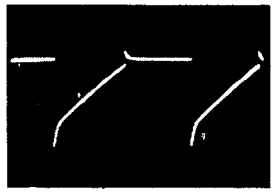

Fig. 60–7.

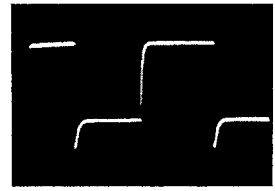

Fig. 61–7.

Fig. 62–7.

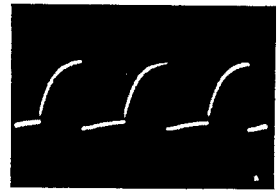

Fig. 63–7.

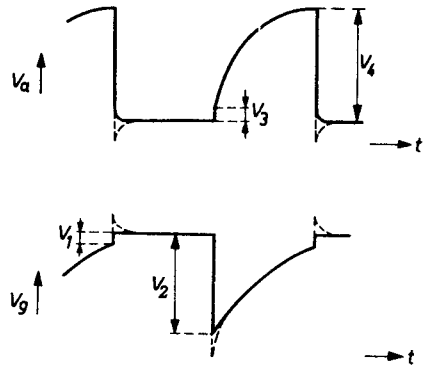

Fig. 64–7.

This time is defined by T_c, the period mainly by T_d. The case of figs 62.7 and 63.7 is more similar to the pictures of fig. 54.7, and the ratio $\frac{T_d}{T_c}$ is about 7. Details of circuit components and the valve are: E 90 CC with $r_a = 4\ k\Omega$, $E_c = 10{\cdot}5$ V ($V = 200$ V). Coupling capacitors $C = 10{,}000$ pF, anode load resistors $R_1 = 15{\cdot}1\ k\Omega$, grid-leak resistors $R_2 = 101\ k\Omega$. The frequency measured is 933 c/s, so that the duration of one complete cycle is 1·07 msec.

The general shape of the oscillograms is easily recognized to be that of the calculated waveforms of fig. 54.7. One deviation can be clearly distinguished. This is caused by the fact that the internal grid resistance of the tubes is not zero, as was assumed in the calculations, but has a finite, though small, value in practice. This causes a kind of overshoot in the grid-voltage change of the tube becoming conductive. This overshoot is also to be seen amplified in the anode voltage at the bottom of the steeply falling edge. This "negative overshoot" again appears, conducted through the coupling capacitor, at the grid of the other tube which is suddenly cut off. In fig. 64.7, these phenomena have been identified by dotted curves.

It is possible that the effect of finite anode internal resistance (rounding off the otherwise sharp edge at the bottom of the negative-going part of the anode voltage) nearly compensates for the overshoot effect of the finite grid internal resistance. This is shown in the oscillograms of figs 62.7 and 63.7. In the oscillograms of figs 60.7 and 61.7, on the other hand, the overshoot effect is clearly predominating.

The values of V_1 and V_2 from fig. 64.7 must be, according to fig. 54.7:

$$V_1 = E_c \text{ and}$$

$$V_2 = \frac{V_0 - \lambda_a V}{1 + \lambda_g} \text{ respectively.}$$

Evaluating these voltages for the multivibrator circuits of figs 60.7 and 62.7 gives a good agreement between the calculated and the measured values shown in the oscillograms. The ratio of V_3 to V_4 could be calculated and measured from the anode voltage waveform (see fig. 64.7). The agreement is less here, because it is more difficult to eliminate the disturbing effect of the overshoot of grid voltage.

8. BLOCKING-OSCILLATOR CIRCUITS

8.1. INTRODUCTION

Another well-known and frequently used circuit in pulse technique is the blocking oscillator. There are two main types to be distinguished, comparable with the monostable and astable multivibrators, viz. the triggered and the free-running blocking oscillators.

The point of comparison is that both circuit types can be described as consisting principally of a vacuum amplifier tube with strong positive feed-back; the point of difference is that with multivibrators an extra vacuum tube is used to feed back the signal in the proper polarity for regeneration, whereas with blocking oscillators a transformer serves this purpose.

The analysis of blocking-oscillator operation can be carried out according to the principles treated in foregoing sections, but in general the results are less accurate than with the multivibrator circuits. This is due to the fact that in general it is easier to avoid excessive stray inductance than stray capacitance in electronic circuits. The multivibrator circuits consist of resistances and capacitances only, and extra stray capacitances generally do not complicate the calculations of network response. Blocking-oscillator circuits, however, combine resistances and inductances; taking into account stray capacitances will generally increase the order of the differential equations to be solved in analysing the circuit behaviour. The above points should be remembered in the following analysis of the blocking-oscillator operation, where stray capacitances are not taken into account except when this is unavoidable.

Experience has shown, however, that the results of the relatively simple analysis can be useful in designing blocking oscillators for special purposes and in predicting their output-pulse shapes. Moreover, a good idea of the order of magnitude of anode- and grid dissipation can be gained.

Because of the flexibility of transformer coupling, several kinds of blocking-oscillator circuit can be designed. Positive feed-back can be attained by magnetically coupling either the anode circuit with the grid circuit, or the anode circuit with the cathode circuit, or the cathode circuit with the grid circuit.

The analysis is essentially the same for all three modes of feed-back, so that only one will be treated in detail; for the others the final results will be given.

The pulse duration of a monostable multivibrator is dependent on a time constant defined by the product of a resistance value and a capacitance value. With a blocking oscillator it is dependent on a time constant which is the quotient of a self-inductance value and a resistance value.

The frequency of an astable multivibrator is determined by *RC*-time constants. The treatment of the free-running blocking oscillator will be restricted to an analysis of the case where the current pulse through the vacuum tube has a very short duration with respect to the repetition period of the pulses; some reference will also be made to other possible cases.

8.2. ANALYSIS OF TRIGGERED BLOCKING OSCILLATOR

As mentioned in the preceding section, one type of triggered blocking oscillator will be analysed in detail. This type is the one using positive feed-back from the anode to the grid circuit. Its basic circuit is represented in fig. 1–8. It consists of tube I, whose anode is supplied from

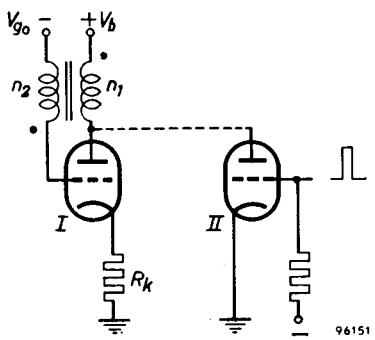

Fig. 1.8.

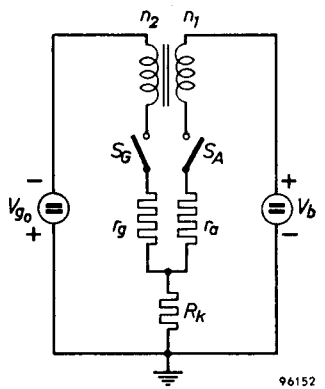

Fig. 2.8.

a source $+V_b$ volts via the primary winding (n_1 turns) of a transformer. The grid of tube I is connected via the secondary winding (n_2 turns) to a source of $-V_{g0}$ volts, which is sufficiently negative to keep the tube cut off if not triggered. A cathode resistor R_k is also incorporated. One way of triggering is by means of tube II, which is also normally cut off and only starts to conduct during a positive trigger pulse applied to the

grid. This induces in the transformer windings voltage pulses of such polarity as to make tube I conduct. Of course, other ways of triggering are also possible. For analysing the triggering process, the quiescent state equivalent circuit of fig. 2–8 is taken as a starting point.

Switches S_G and S_A are open and the voltages across them are $-V_{G0}$ and $+V_b$ respectively. The effect of a trigger pulse is to close these switches at, say, the instant $t = 0$. In foregoing sections we calculated the effect of suddenly closing a switch. One has to introduce a voltage equal to the voltage that would be present across the switch if it were not clossed but of opposite polarity.

This means, in the present case, voltage sources $+V_{g0}$ and $-V_b$ across S_G and S_A respectively. We then have to calculate the response of the circuit to these voltage sources and to superimpose it on the undisturbed state. The DC voltage sources $-V_{g0}$ and $+V_b$ can be replaced by short-circuits, as their internal resistance is neglected and their influence is already taken into account in the static condition. The equivalent circuit, therefore, is as represented in figure 3.8. To allow for the rectifying properties of the tube, two diodes D_G and D_A have been included, which ensures that the voltage source $V_{g0}U(t)$ cannot

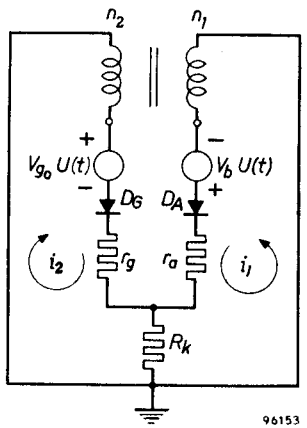

Fig. 3.8.

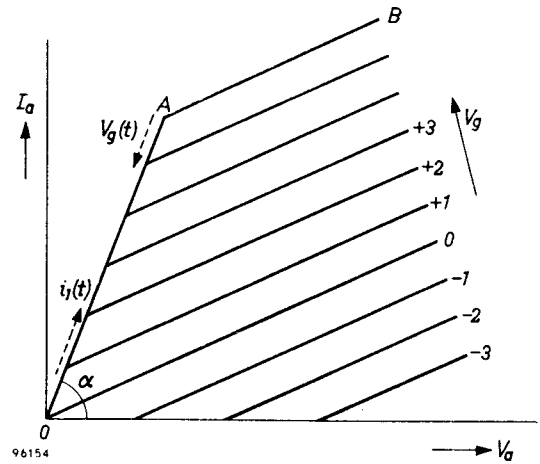

Fig. 4.8.

contribute to the current i_2. The latter can only be caused by induction from the right-hand mesh of the circuit. The function $U(t)$ is a unit step function as previously defined. The impedances r_g and r_a denote the internal resistances between grid and cathode and between anode and cathode respectively. As the positive feed-back is assumed to be so strong that the grid-to-cathode potential is positive, this means that

r_g is a kind of diode forward resistance, which can be of the order of a few hundred ohms. The impedance of the anode load is assumed to be so high that the anode current operating point moves along the "saturation" or "bottoming" line of slope α as indicated in fig. 4.8 for a triode and in fig. 50.6 for a pentode. The value of r_a is given by cot α, and can also be of the order of a few hundred ohms.

8.2.1. CALCULATION OF THE TRANSIENTS

By applying Kirchhoff's law, two equations can be derived, equation (1.8) being valid for the right-hand mesh and equation (2.8) for the left-hand mesh of the network of figure 3.8

$$V_b U(t) = i_1 (r_a + R_k) + i_2 R_k + L_1 \frac{di_1}{dt} - M \frac{di_2}{dt} \quad . \quad . \quad . \quad (1.8)$$

$$0 = i_2 (r_g + R_k) + i_1 R_k + L_2 \frac{di_2}{dt} - M \frac{di_1}{dt}, \quad . \quad . \quad . \quad (2.8)$$

L_1 is the self-inductance of the primary winding (n_1 turns), L_2 the self-inductance of the secondary winding (n_2 turns). M is the mutual inductance between primary and secondary windings.

In the following it will be assumed that the coupling is so close that

$$M^2 = L_1 L_2 \quad . \quad . \quad . \quad . \quad . \quad . \quad . \quad . \quad . \quad . \quad . \quad (3.8)$$

The following notation is also introduced:

$$r_a + R_k = R_1 \quad . \quad . \quad . \quad . \quad . \quad . \quad . \quad . \quad . \quad . \quad . \quad (4.8)$$

$$r_g + R_k = R_2 \quad . \quad . \quad . \quad . \quad . \quad . \quad . \quad . \quad . \quad . \quad . \quad (5.8)$$

$$\frac{d}{dt} = p \quad . \quad . \quad . \quad . \quad . \quad . \quad . \quad . \quad . \quad . \quad . \quad . \quad (6.8)$$

Equations (1.8) and (2.8) then become:

$$V_b U(t) = (R_1 + L_1 p) i_1 - (Mp - R_k) i_2 \quad . \quad . \quad . \quad . \quad . \quad . \quad (1a.8)$$

$$0 = (R_2 + L_2 p) i_2 - (Mp - R_k) i_1 \quad . \quad . \quad . \quad . \quad . \quad . \quad (2a.8)$$

From (2a.8):

$$i_2 = \frac{Mp - R_k}{L_2 p + R_2} i_1 \quad . \quad . \quad . \quad . \quad . \quad . \quad . \quad . \quad . \quad . \quad . \quad (7.8)$$

Substituting i_2 in (1a.8) gives:

$$V_b U(t) = \left[R_1 + L_1 p - \frac{(Mp - R_k)^2}{L_2 p + R_2} \right] i_1, \quad . \quad . \quad . \quad . \quad . \quad . \quad . \quad (8.8)$$

or:

$$i_1 = \frac{L_2 p + R_2}{(L_1 p + R_1)(L_2 p + R_2) - (Mp - R_k)^2} V_b U(t). \quad . \quad . \quad (9.8)$$

Introducing (3.8) gives:

$$i_1 = \frac{L_2 p + R_2}{(L_1 R_2 + L_2 R_1 + 2MR_k)\, p + R_1 R_2 - R_k^2} V_b U(t). \quad (10.8)$$

We can write:

$$L_1 = \frac{n_1^2}{n_2^2} L_2 \quad (11.8)$$

$$M = \frac{n_1}{n_2} L_2 \quad (12.8)$$

If, moreover, the following notation is introduced:

$$R_1 + \frac{n_1^2}{n_2^2} R_2 + 2\frac{n_1}{n_2} R_k = R \quad (13.8)$$

$$R_1 R_2 - R_k^2 = R_v^2, \quad (14.8)$$

then (10.8) can be written:

$$i_1 = \frac{L_2 p + R_2}{L_2 R p + R_v^2} V_b U(t) \quad (15.8)$$

and (7.8) becomes:

$$i_2 = \frac{Mp - R_k}{L_2 R p + R_v^2} V_b U(t) \quad (16.8)$$

From expressions (15.8) and (16.8) the time functions for i_1 and i_2 can be calculated. These are given here since we will want them in the following considerations:

$$i_1(t) = \frac{V_b}{R}\left[\frac{R_2 R}{R_v^2} + \frac{R_v^2 - R_2 R}{R_v^2} e^{-\frac{R v^2}{L_1 R} t}\right] \quad (17.8)$$

$$i_2(t) = \frac{n_1}{n_2}\frac{V_b}{R}\left[-\frac{n_2}{n_1}\frac{R_k R}{R_v^2} + \frac{R_v^2 + \frac{n_2}{n_1} R_k R}{R_v^2} e^{-\frac{R v^2}{L_1 R} t}\right] \quad (18.8)$$

8.2.2. DETERMINATION OF THE OUTPUT-PULSE WIDTH

Tube I cannot remain conducting for an infinitely long time. This can be seen from the expressions for the anode current $i_1(t)$ and the grid current $i_2(t)$ (see (17.8) and (18.8)).

The initial value (at $t = 0$) of $i_1(t)$ is:

$$i_1(0) = \frac{V_b}{R} \quad (19.8)$$

The final value (at $t = \infty$) would be:

$$i_1(\infty) = V_b \frac{R_2}{R_v^2} \quad \ldots\ldots\ldots \quad (20.8)$$

Now, it can be seen from (13.8) and (14.8) that $R > R_1$ and $\frac{R_v^2}{R_2} < R_1$; so: $R > \frac{R_v^2}{R_2}$, and consequently:

$$i_1(0) < i_1(\infty).$$

Thus, the anode current increases with time.

The initial value of $i_2(t)$ is:

$$i_2(0) = \frac{n_1}{n_2} \frac{V_b}{R} \quad \ldots\ldots\ldots\ldots \quad (21.8)$$

Its final value would be:

$$i_2(\infty) = -\frac{R_k}{R_v^2} V_b \quad \ldots\ldots\ldots \quad (22.8)$$

Hence, it is clear that the grid current decreases with time, and consequently also the grid-to-cathode voltage.

There must be a certain instant at which the decreasing grid voltage prevents the anode current from further increase. This will be explained with the aid of the (idealized) anode current/anode voltage characteristics of the tube, as represented in fig. 4.8. It is assumed that the anode current increases along the "bottoming" line OA, whereas the initial grid voltage is of such a value that it corresponds to the characteristic OAB.

If the grid voltage remained constant at this value, then the anode current could increase up to the point A, but as soon as it reaches this point, a discontinuity occurs in the slope of the increasing anode current. This causes a lower voltage to be induced in the secondary winding of the transformer; in other words, the grid voltage decreases.

This in turn reduces the anode current still more, again lowering the grid voltage, and so on. It will thus be clear that at the instant the anode current value reaches point A, the tube will be cut off with an avalanche effect. In practice, however, point A will not be reached, because during the increase of the anode current, the grid voltage decreases, and a point of discontinuity will be reached sooner at a lower point on the bottoming line.

The situation of the "knee"-points on the bottoming line is defined

by the following relation:

$$i_1 = S_b V_g, \quad \ldots \ldots \ldots \quad (23.8)$$

where S_b is the mutual conductance of the tube along the bottoming line, i.e. the increase of the anode current i_1 per volt increase of the grid voltage V_g.

Now, the increase of $i_1(t)$ and the decrease of $V_g(t)$, indicated by dotted arrows in figure 4, meet at a certain instant t_s, defined by expression (23.8):

$$i_1(t_s) = S_b V_g(t_s) \quad \ldots \ldots \quad (24.8)$$

This instant t_s marks the end of the conducting period of the tube, and is a measure of the width of the cathode-current pulse.

In order to determine the pulse width from expression (24.8), the grid voltage must be known. This voltage is equal to the potential drop across r_g (see fig. 3.8) caused by i_2; therefore:

$$V_g(t) = r_g i_2(t) \quad \ldots \ldots \quad (25.8)$$

Combining expressions (24.8), (25.8), (17.8) and (18.8) gives the following equation, from which t_s may be found:

$$\frac{V_b}{R}\left[\frac{R_2 R}{R_v^2} + \frac{R_v^2 - R_2 R}{R_v^2} e^{-\frac{t_s}{T}}\right] =$$

$$= S_b r_g \frac{n_1}{n_2}\frac{V_b}{R}\left[-\frac{n_2}{n_1}\frac{R_k R}{R_v^2} + \frac{R_v^2 + \frac{n_2}{n_1} R_k R}{R_v^2} e^{-\frac{t_s}{T}}\right], \quad \ldots \quad (26.8)$$

where T represents the time constant of the circuit:

$$T = \frac{L_2 R}{R_v^2} \quad \ldots \ldots \quad (27.8)$$

Expression (26.8) can be reduced to the following form:

$$e^{-\frac{t_s}{T}} = \frac{R_2 R + r_g S_b R_k R}{R_2 R - R_v^2 + r_g S_b \left(\frac{n_1}{n_2} R_v^2 + R_k R\right)}, \quad \ldots \quad (28.8)$$

or:

$$t_s = T \ln \frac{R_2 R - R_v^2 + r_g S_b \left(\frac{n_1}{n_2} R_v^2 + R_k R\right)}{R_2 R + r_g S_b R_k R} \quad \ldots \quad (29.8)$$

8.2.3. DISCUSSION OF THE TRANSIENT WAVEFORMS

The sum of the transient anode current and grid current, i.e. the cathode current, can easily be found by adding expressions (17.8) and (18.8). The voltage across R_k is proportional to this current and can be examined on an oscilloscope screen without being much influenced by the introduction of extra stray capacitances, R_k generally being a low impedance. Moreover, as no self-inductances of any importance are involved in the cathode circuit, the possibility of parasitic oscillations is much smaller here than in the anode or grid circuits.

The shape of the voltage $V(t)$ across R_k is given by the following expression, derived from R_k times the sum of $i_1(t)$ and $i_2(t)$:

$$V(t) = \frac{R_k}{R} V_b \left[\frac{r_g R}{R_v^2} + \frac{R_v^2 \left(1 + \frac{n_1}{n_2}\right) - r_g R}{R_v^2} e^{-\frac{t}{T}} \right] \quad . \quad . \quad (30.8)$$

From expression (30.8) some interesting properties of the shape of the voltage pulse $V(t)$ can be derived.

Firstly, it is easy to see that the front-flank is a step-function, since for $t = 0$:

$$V(0) = \left(1 + \frac{n_1}{n_2}\right) \frac{R_k}{R} V_b \quad . \quad . \quad . \quad . \quad . \quad . \quad . \quad (31.8)$$

When substituting (4.8), (5.8) and (13.8), this becomes:

$$V(0) = \frac{\left(1 + \frac{n_1}{n_2}\right) R_k}{r_a + \frac{n_1^2}{n_2^2} r_g + \left(\frac{n_1^2}{n_2^2} + 2\frac{n_1}{n_2} + 1\right) R_k} V_b,$$

or:

$$V(0) = \frac{R_k}{\left(1 + \frac{n_1}{n_2}\right) R_k + \frac{r_a + \frac{n_1^2}{n_2^2} r_g}{1 + \frac{n_1}{n_2}}} V_b \quad . \quad . \quad . \quad . \quad . \quad (32.8)$$

Secondly, if it is assumed that the tube is suddenly cut off at the instant defined by expression (29.8), then the rear flank of the output pulse is a negativegoing step-function.

It must be noted that in practice there will always exist a certain stray capacitance from cathode to earth, so that no sudden voltage steps across R_k are possible. Nevertheless, if the time constant in the cathode circuit can be kept small, very steep pulse-flanks can be obtained.

A third interesting aspect is that expression (30.8) shows that there must be a condition for which the flatness of the pulse-top is maximal, in which case the pulse amplitude remains constant at the initial value $V(0)$ during its whole duration. This situation exists when the exponential time function of (30.8) has no influence. This leads to the condition:

$$R_v^2 \left(1 + \frac{n_1}{n_2}\right) = r_g R \quad \ldots\ldots\ldots \quad (33.8)$$

If the tube characteristics and the circuit resistances are known, then condition (33.8) affords the possibility of calculating the turns ratio $(n_1/n_2)_m$ at which maximal flatness occurs.

Substitution of (13.8) and (14.8) in (33.8) gives:

$$(R_1R_2 - R_k^2)\left(1 + \frac{n_1}{n_2}\right) = r_g R_1 + r_g R_2 \left(\frac{n_1}{n_2}\right)^2 + 2r_g R_k \frac{n_1}{n_2}.$$

The solution of this second-order equation is:

$$\frac{n_1}{n_2} = \frac{R_k(r_a - r_g) + r_a r_g \pm \sqrt{\{R_k(r_a - r_g) + r_a r_g\}^2 + 4r_a r_g R_k (r_g + R_k)}}{2r_g (r_g + R_k)} \quad (34.8)$$

For a positive, real value of n_1/n_2 we need only the plus sign.

8.2.4. COMPARISON OF THEORY AND PRACTICE

The circuit of figure 1.8 has been investigated, using an experimental double-triode type of tube and the following values of circuit components and supply voltages:

$V_b = 150$ volts, $V_{g0} = 6$ volts, $R_k = 47$ ohms, transformer windings $n_1 = 70$ turns, $n_2 = 50$ turns, ferroxcube core of permeability μ appr. 2000.

The waveform of the output voltage across R_k was observed on an oscilloscope screen and appeared to have the shape shown by the dotted curve of figure 5.8.

This voltage pulse has a sharp front-flank and a more gradually falling rear flank. The latter may be caused by the cathode circuit time-constant (stray capacitances) and the fact that the tube characteristics do not possess the sharp bends as assumed in figure 4.8.

Moreover, the primary of the transformer is shunted by a resistor of 1000 ohms, which proved to be necessary to avoid excessive ringing effects and consequent free-running of the blocking oscillator.

Figure 5.8 shows that the total duration of the pulse is 7 μsec,

whereas at about 6 μsec the switch-back operation starts. Finally, some droop is present in the flat part of the pulse.

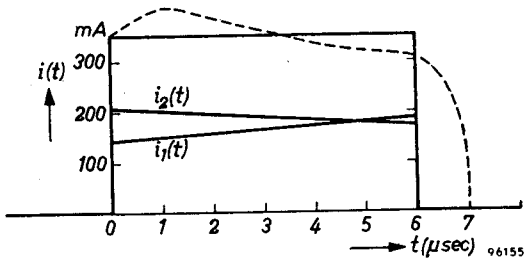

Fig. 5.8.

The self-inductance of the secondary winding of the transformer, with primary winding open-circuited, is measured to be $L_2 = 2.8$ mH.

The tube anode current/anode voltage characteristics with control-grid voltage values ranging from —2 to +10 volts show that the internal anode resistance along the bottoming line is about 400 ohms and the slope in this region is about 7 mA/V. For complete calculation of the circuit, only the value of the internal grid-to-cathode resistance is wanted. As it is rather difficult to determine this value experimentally at very high grid-to-cathode voltages without damaging the tube, the following procedure has been adopted to determine r_g. From the waveform, observed on the oscilloscope, it appears that at $t = 0$ the output voltage $V(0) = 17$ volts. Substituting this value in equation (30.8) makes it possible to find the value of r_g, which proved to be $r_g = 164$ ohms.

Other quantities can be calculated, and it is found that the time constant $T = 28$ μsec, the pulse duration $t_s = 6$ μsec. The anode current and grid current as functions of time are given in the following table.

Time t (μsec)	Anode current $i_1(t)$ (mA)	Grid current $i_2(t)$ (mA)	Total cathode current $i(t)$ (mA)
0	150	211	361
1	156	201.5	357.5
2	162	192	354
3	167	183	350
4	172	174	346
5	177	165	342
6	182	157	339

These currents as functions of time have also been represented in figure 5.8. Comparison of the calculated waveform of $i\,(t)$ with the experimental one shows that the latter has some overshoot and more droop. This can possibly be attributed to some oscillating effect due to stray capacitances, damped by the heavily conducting tube. In conclusion, however, it can be said that the calculation method gives a good approximation to the behaviour of the circuit in practice, and it certainly offers the possibility to have in advance, before designing such a circuit, an idea of the waveform to be expected and the demands made of the tube.

8.2.5. SOME DESIGN CONSIDERATIONS

The presence of a cathode resistor R_k greatly complicates the formulae derived in the preceding sections. In many applications one may be more interested in the current pulse than in the voltage pulse, as for instance in the case of driving magnetic cores in a memory matrix or switching circuits.

Therefore it is worth-while to rearrange the formulae by putting $R_k = 0$.

A striking example of simplification gives the expression for the ratio of the transformer-winding turns that is required for optimum flatness of the current pulse (see expression (34.8)). This reduces with $R_k = 0$ to

$$\left(\frac{n_1}{n_2}\right)_{opt} = \frac{r_a}{r_g} \quad \ldots\ldots\ldots\ldots \quad (35.8)$$

With practical values as used in the preceding section, this gives $(n_1/n_2)_{opt} = 2.44$, whereas expr. (34.8) would give a value 2.4. A negligible error is made when using the simplified formula. A survey of the expressions valid for $R_k = 0$ will be given.

$$R_1 = r_a \quad \ldots\ldots\ldots\ldots \text{ see expr. } (4.8)$$

$$R_2 = r_g \quad \ldots\ldots\ldots\ldots \text{ see expr. } (5.8)$$

$$R = r_a + \left(\frac{n_1}{n_2}\right)^2 r_g \quad \ldots\ldots\ldots \text{ see expr. } (13.8)$$

$$R_v{}^2 = r_a r_g \quad \ldots\ldots\ldots\ldots \text{ see expr. } (14.8)$$

$$i_1\,(t) = \frac{V_b}{r_a + \left(\frac{n_1}{n_2}\right)^2 r_g}\left[1 + \left(\frac{n_1}{n_2}\right)^2 \frac{r_g}{r_a}\left(1 - e^{-\frac{t}{T}}\right)\right] \quad (36.8)$$

$$i_2(t) = \frac{V_b}{r_a + \left(\frac{n_1}{n_2}\right)^2 r_g} \frac{n_1}{n_2} e^{-\frac{t}{T}} \quad \ldots\ldots\ldots \quad (37.8)$$

$$i_1(t) + i_2(t) = i(t) =$$

$$= \frac{V_b}{r_a + \left(\frac{n_1}{n_2}\right)^2 r_g} \left[1 + \left(\frac{n_1}{n_2}\right)^2 \frac{r_g}{r_a} + \frac{n_1}{n_2}\left\{1 - \frac{n_1}{n_2}\frac{r_g}{r_a}\right\} e^{-\frac{t}{T}}\right] \quad \ldots \quad (38.8)$$

The time constant

$$T = L_2\left\{\frac{1}{r_g} + \left(\frac{n_1}{n_2}\right)^2 \frac{1}{r_a}\right\}. \quad \ldots\ldots\ldots \quad (39.8)$$

The pulse width

$$t_s = T \ln \frac{1 + \frac{n_2}{n_1} r_a S_b}{1 + \left(\frac{n_2}{n_1}\right)^2 \frac{r_a}{r_g}} \quad \ldots\ldots\ldots \quad (40.8)$$

In most applications the need will be for a current pulse of a given amplitude and duration with a flat top; so condition (35.8) will nearly be satisfied. Introducing this in the expressions for currents and pulse duration gives the following equations:

$$i_1(t) = \frac{V_b}{r_a\left(1 + \frac{r_a}{r_g}\right)}\left\{1 + \frac{r_a}{r_g}\left(1 - e^{-\frac{t}{T}}\right)\right\} \quad \ldots \quad (41.8)$$

$$i_2(t) = \frac{V_b}{r_g\left(1 + \frac{r_a}{r_g}\right)} e^{-\frac{t}{T}} \quad \ldots\ldots\ldots \quad (42.8)$$

$$i(t) = \frac{V_b}{r_a}. \quad \ldots\ldots\ldots\ldots\ldots \quad (43.8)$$

$$T = \frac{L_2}{r_g}\left(1 + \frac{r_a}{r_g}\right) \quad \ldots\ldots\ldots\ldots \quad (44.8)$$

$$t_s = T \ln \frac{1 + r_g S_b}{1 + \frac{r_g}{r_a}} \quad \ldots\ldots\ldots\ldots \quad (45.8)$$

For the design of this kind of blocking-oscillator circuit it will be useful to have available values of r_a, r_g and S_b of the tube types suitable for this purpose.

The design procedure is then very simple. Suppose a pulse is wanted of amplitude I_0 and duration τ. Substituting I_0 in expression (43.8) gives the value wanted for V_b. Substituting τ in expression (45.8) gives the value of the time constant T, and consequently from expression (44.8) the value of L_2 is known. Depending on the permeability and dimensions of the transformer-core material, the number of secondary turns n_2 is defined by this value of L_2, and as $\frac{n_1}{n_2} = \frac{r_a}{r_g}$, the number of primary turns n_1 is also known.

8.2.6. THE BLOCKING CONDITION

The width t_s of the transient current pulses in grid and anode is given by expression (29.8), which can be written

$$t_s = T \ln \left[1 + \frac{(r_g S_b n - 1) R_v^2}{R_2 R + r_g S_b R_k R} \right], \quad \ldots\ldots\ldots \quad (46.8)$$

where $n = n_1/n_2$.

This formula shows that for

$$n < \frac{1}{r_g S_b} \quad \ldots\ldots\ldots\ldots \quad (47.8)$$

no positive real value of t_s can be found.

What this means, physically, can easily be seen. From (17.8) and (18.8) the initial values of anode and grid currents (at the instant $t = 0$) prove to be:

$$i_1(0) = \frac{V_b}{R} \quad \ldots\ldots\ldots\ldots \quad (48.8)$$

and

$$i_2(0) = n \frac{V_b}{R} \quad \ldots\ldots\ldots\ldots \quad (49.8)$$

Referring to fig. 4.8 it can be seen that blocking-oscillator action can only occur if the initial value of i_1 is smaller than S_b (slope) times the grid-to-cathode voltage V_g, or: $i_1(0) < S_b V_g(0)$.

Now $V_g = r_g i_2$, so $i_1(0) < S_b r_g i_2(0)$.

Substituting (48.8) and (49.8) gives

$$\frac{V_b}{R} < S_b r_g n \frac{V_b}{R}$$

or

$$n > \frac{1}{S_b r_g} \quad \ldots\ldots\ldots\ldots \quad (50.8)$$

This is the condition for correct blocking operation. Comparison with (47.8) shows that the latter indeed represents the condition for wrong operation.

Condition (50.8) thus represents, for given tube characteristics (r_g and S_b), the minimum amount of positive feedback required from anode to grid.

8.2.7. ANODE CURRENT AND VOLTAGE

It could happen that use is to be made of the anode-current pulse instead of the cathode-current pulse. It can then be of interest to investigate whether the anode-current pulse can also have a flat top. For the general case of expression (17.8) it leads to the following condition:

$$R_2 R = R_v^2 .$$

Introducing (14.8), (13.8) and (5.8) leads to the condition:

$$n = -\frac{R_k}{r_g + R_k},$$

which can never be satisfied, as n cannot be negative.

At $R_k = 0$, the flat-top condition is $n = 0$, which is meaningless.

Conclusion: a flat-topped pulse can only be found in the cathode lead.

If the anode-voltage pulse is of interest, it is easy to derive the following the time function:

$$V_a(t) = -V_b n^2 \frac{r_g}{r_a + n^2 r_g} e^{-\frac{t}{T}} \text{ (assuming } R_k = 0) \ldots \quad (51.8)$$

8.2.8. ENERGY DISSIPATION IN GRID AND ANODE CIRCUITS

Generally, the transient anode and grid currents can be expressed in the following form:

$$i_1(t) = A + B e^{-\frac{t}{T}} \ldots \quad (52.8)$$

$$i_2(t) = D + E e^{-\frac{t}{T}} \ldots \quad (53.8)$$

(Compare (17.8) and (18.8))

It is clear that, if these currents flow through resistances r_a and r_b, resp. during a time interval t_s, then the dissipated energies in anode and grid circuits are:

$$W_a = \int_0^{t_s} i_1^2(t)\, r_a\, dt \ldots \quad (54.8)$$

and

$$W_g = \int_0^{t_s} i_2^2(t)\, r_g\, dt \quad \ldots\ldots\ldots\ldots \quad (55.8)$$

respectively.

The solution of the integrals is:

$$W_a = A^2 t_s r_a - 2ABT\,(e^{-\frac{t_s}{T}} - 1)\, r_a - \tfrac{1}{2}TB^2\,(e^{-\frac{2t_s}{T}} - 1)\, r_a \quad \ldots \quad (56.8)$$

and

$$W_g = D^2 t_s r_g - 2DET\,(e^{-\frac{t_s}{T}} - 1)\, r_g - \tfrac{1}{2}TE^2\,(e^{-\frac{2t_s}{T}} - 1)\, r_g \quad \ldots \quad (57.8)$$

The mean power during the pulse is:

$$\hat{P}_a = \frac{W_a}{t_s} = A^2 r_a - 2AB\frac{T}{t_s}\,(e^{-\frac{t_s}{T}} - 1)\, r_a - \tfrac{1}{2}\frac{T}{t_s}B^2\,(e^{-\frac{2t_s}{T}} - 1)\, r_a \quad (58.8)$$

and

$$\hat{P}_g = \frac{W_g}{t_s} = D^2 r_g - 2DE\frac{T}{t_s}\,(e^{-\frac{t_s}{T}} - 1)\, r_g - \tfrac{1}{2}\frac{T}{t_s}E^2\,(e^{-\frac{2t_s}{T}} - 1)\, r_g \quad (59.8)$$

If trigger pulses are regularly applied, having a repetition period t_r, then the long term average power is:

$$\bar{P}_a = \frac{W_a}{t_r} = \frac{W_a}{t_s}\frac{t_s}{t_r} = \frac{W_a}{t_s}\delta = \hat{P}_a\delta \quad \ldots\ldots \quad (60.8)$$

$$\bar{P}_g = \hat{P}_g\delta, \quad \ldots\ldots\ldots\ldots \quad (61.8)$$

$$\delta = \frac{t_s}{t_r} \text{ duty cycle of the pulses} \quad \ldots \quad (62.8)$$

a. *General case*

From (17.8) and (18.8) the constants A, B, D and E can be taken:

$$A = V_b\frac{R_2}{R_v^2},\quad B = \frac{V_b}{R} - A,\quad D = -n^2 V_b\frac{R_k}{R_v^2},\quad E = n\frac{V_b}{R} - D. \quad (63.8)$$

$e^{-\frac{t_s}{T}}$ is given by expression (28.8).

Thus, all terms for determining the power dissipations, as given by (58.8), (59.8), (60.8) and (61.8) are, known.

b. *Special case*

The experimental case treated in section 8.2.4 and represented in

fig. 5.8 has been calculated as regards the grid and anode dissipation, and the following data resulted:

$$\hat{P}_a = 11 \text{ watts} \quad . \quad . \quad . \quad . \quad . \quad . \quad . \quad . \quad . \quad . \quad . \quad (64.8)$$

$$\hat{P}_g = 5.6 \text{ watts} \quad . \quad . \quad . \quad . \quad . \quad . \quad . \quad . \quad . \quad . \quad . \quad (65.8)$$

If the maximum permitted anode dissipation were 1,5 watt, then, disregarding grid ratings, this would limit the duty cycle to:

$$\delta = \frac{\bar{P}_a}{\hat{P}_a} = \frac{1{,}5}{11} = 0.136,$$

or

$$t_r = \frac{t_s}{0.136}.$$

Now $t_s = 6$ μsec; so $t_r = 44$ μsec.

Or the maximum repetition frequency of the pulses, as limited by anode dissipation, would be

$$f_{max} = \frac{1}{t_r} = 23 \text{ kc/s}.$$

A maximum permitted grid dissipation of 30 mW would, by similar reasoning, lead to a max. repetition frequency $f_{max} = 0.9$ kc/s. Life tests at 1 kc/s and 5 kc/s show that probably more grid dissipation could be permitted.

5 kc/s operation gives a main grid dissipation

$$\bar{P}_g = \delta \hat{P}_g = \tfrac{6}{200} 5.6 \text{ watts} = 0.17 \text{ watts}.$$

c. *Requirements for magnetic core drivers*

Suppose a vacuum tube of the type mentioned in section 8.2.4 ($r_a = 400$ ohms, $r_g = 164$ ohms, $S_b = 7$ mA/V) is to supply current pulses of 2 μsec width, 370 mA amplitude, optimum flatness, to switch small ferroxcube matrix cores (switching time 1.5 μsec, outer diameter 2 mm.).

Following the design procedure of section 8.2.5 (final paragraph), this gives the requirements:

$$V_b = 148 \text{ volts}$$
$$T = 4.75 \text{ } \mu\text{sec},$$
$$L_2 = 0.23 \text{ mH}.$$

With the aid of the small Fxc closed pot-core D-14/8, it is possible to make the required transformer. With an air-gap of 0.2 mm, 106 turns are required for 1 mH self-inductance. For 0.23 mH, therefore, the required number is $n_1 = 106 \sqrt{0.23} = 50$ turns.

Since we want a flat-topped pulse, the condition is

$$\frac{n_1}{n_2} = \frac{r_a}{r_g} \text{ or } n_1 = \tfrac{400}{164} \cdot 50 = 122 \text{ turns.}$$

The design of the blocking oscillator is now completely defined. The power dissipation can be calculated. For the flat-topped case, the quantities A, B, D and E become (see (52.8), (53.8), (41.8) and (42.8)):

$$A = \frac{V_b}{r_a},\ B = -\frac{V_b}{r_a + r_g},\ D = 0,\ E = \frac{V_b}{r_a + r_g}. \qquad (66.8)$$

Calculation of expressions (58.8) and (59.8) gives:

$$\hat{P}_a = 10.3 \text{ watts},\ \hat{P}_g = 7.56 \text{ watts}.$$

Max. anode dissipation of 1.5 watt would limit the maximum repetition frequency to $f_{max} = 73$ kc/s.

Max. grid dissipation of 30 mW would permit $f_{max} = 2$ kc/s.

Max. grid dissipation, as in the former case, of 0.17 watt (life-tests) would permit $f_{max} = 11.3$ kc/s.

If $f_{max} = 100$ kc/s is required, the average anode and grid dissipations must be at least:

$$\bar{P}_a = 2 \text{ watts},\ \bar{P}_g = 1.5 \text{ watts}.$$

d. *Experimental check*

The blocking oscillator just described has been built, and the output pulse checked. The measured value of L_2 was 0.243 mH. The pulse width, instead of 2 μsec, should then be $\frac{0.243}{0.23} \cdot 2\ \mu\text{sec} = 2.15\ \mu\text{sec}$.

The cathode-current pulse ($= i_1(t) + i_2(t)$) is observed on an oscilloscope screen as the voltage developed across a resistor of 3.1 ohm in the cathode lead. The oscillograms are shown in fig. 6.8 for four different tubes of the same type. The scales of the axes are: vertically 1 division = 0.5 volt, horizontally 1 division = 0.25 μsec. The pulse-width and the amplitudes at the central vertical axis are listed below.

Case	Pulse-width (μsec)	Amplitude (volts across 3.1 ohm)	Current (mA)
a	2.8	1.2	387
b	3.1	1.3	420
c	3.4	1.8	580
d	3.1	1.4	450

We estimated a pulse-width of 2.15 μsec, a current of 370 mA. Practice shows a considerable spread in different tubes and a mean result that is only a rough approximation of the calculated values. However, this is sufficient for practical purposes, since the current value, for instance, can easily be corrected by means of the anode supply voltage, while the pulse-width can be corrected by means of the self-inductance.

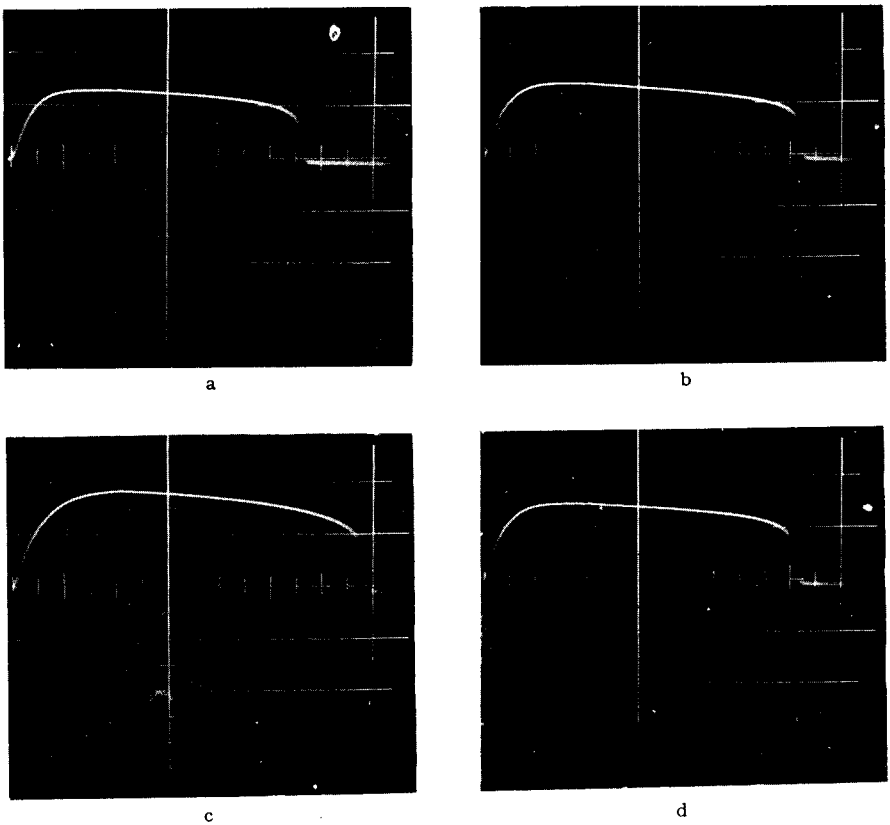

Fig. 6.8.

e. *Variation of pulse-width*

With the closed pot-core D 14/8, the effective air-gap can be varied; for this purpose a F_{xc} control slug can be screwed into the centre-core. At an air-gap of 0.2 mm this allows for a total variation of the self-inductance of 15%. The pulse-width of the current pulses of all four cases, *a*, *b*, *c* and *d* mentioned before, could also be varied by about the same amount.

8.3. OTHER MODES OF FEED-BACK

The method of analysis treated in section 8.2 for the anode-to-grid coupled blocking oscillator can also be adopted with the other types of blocking oscillator, characterized by feed-back from anode to cathode or from cathode to grid.

There appears to be great conformity between the three feedback cases of a blocking oscillator. Whether feed-back is applied from anode to grid, from anode to cathode, or from cathode to grid, the following *general expressions* are valid:

The anode transient current

$$i_1(t) = \frac{V_b}{r_v}\left[\frac{r_v}{r_a} + \left(1 - \frac{r_v}{r_a}\right) e^{-\frac{t}{T}}\right] \quad . \quad . \quad . \quad . \quad . \quad . \quad . \quad . \quad (67.8)$$

The grid transient current

$$i_2(t) = N\frac{V_b}{r_v} e^{-\frac{t}{T}} \quad . \quad . \quad . \quad . \quad . \quad . \quad . \quad . \quad . \quad . \quad (68.8)$$

The pulse-width:

$$t_s = T \ln\left[1 + \frac{r_a}{r_v}(N r_g S_b - 1)\right] \quad . \quad . \quad . \quad . \quad . \quad . \quad . \quad . \quad (69.8)$$

Where:

$$r_v = r_a + N^2 r_g \quad . \quad . \quad . \quad . \quad . \quad . \quad . \quad . \quad . \quad . \quad . \quad (70.8)$$

$$T = \frac{r_v}{r_a}\tau \quad . \quad . \quad . \quad . \quad . \quad . \quad . \quad . \quad . \quad . \quad . \quad (71.8)$$

N is a coupling factor, depending on the mode of feed-back used. τ is a time constant, also depending on the system of feed-back. A survey of expressions to be substituted for N and τ with the three types of feed-back is given below.

a. *Feed-back from anode* (n_1 turns, self-inductance L_1) *to grid* (n_2, L_2)

$$N = \frac{n_1}{n_2} \quad . \quad . \quad . \quad . \quad . \quad . \quad . \quad . \quad . \quad . \quad . \quad (72.8)$$

$$\tau = \frac{L_2}{r_g} \quad . \quad . \quad . \quad . \quad . \quad . \quad . \quad . \quad . \quad . \quad . \quad (73.8)$$

b. *Feed-back from anode* (n_1, L_1) *to cathode* (n_2, L_2)

$$N = \frac{n_1}{n_2} - 1 \quad . \quad . \quad . \quad . \quad . \quad . \quad . \quad . \quad . \quad . \quad (74.8)$$

$$\tau = \frac{L_2}{r_g} \quad . \quad . \quad . \quad . \quad . \quad . \quad . \quad . \quad . \quad . \quad . \quad (75.8)$$

c. *Feed-back from cathode* (n_1, L_1) *to grid* (n_2, L_2)

$$N = \frac{1}{\frac{n_2}{n_1} - 1} \quad \ldots\ldots\ldots\ldots \quad (76.8)$$

$$\tau = \frac{1}{N^2} \frac{L_1}{r_g} \quad \ldots\ldots\ldots\ldots \quad (77.8)$$

General condition for a flat-topped $(i_1 + i_2)$ *pulse*

$$N = \frac{r_a}{r_g} \quad \ldots\ldots\ldots\ldots \quad (78.8)$$

Then:

$$r_v = r_a + \frac{r_a^2}{r_g} \quad \ldots\ldots\ldots\ldots \quad (79.8)$$

$$T = \left(1 + \frac{r_a}{r_g}\right) \tau \quad \ldots\ldots\ldots\ldots \quad (80.8)$$

$$i_1(t) = \frac{V_b}{r_a} \left(1 - \frac{e^{-\frac{t}{T}}}{1 + \frac{r_g}{r_a}}\right) \quad \ldots\ldots\ldots\ldots \quad (81.8)$$

$$i_2(t) = \frac{V_b}{r_a} \frac{e^{-\frac{t}{T}}}{1 + \frac{r_g}{r_a}} \quad \ldots\ldots\ldots\ldots \quad (82.8)$$

$$t_s = T \ln \left(1 + \frac{r_a S_b - 1}{1 + \frac{r_a}{r_g}}\right) \quad \ldots\ldots\ldots\ldots \quad (83.8)$$

8.3.1. SOME EXPERIMENTAL CHECKS

A relative quantity was calculated and checked by measurements, viz. the ratio t_s/L.

a) Anode-to-grid feed-back

According to expressions (39.8) and (40.8):

$$\frac{t_s}{L_2} = \left(\frac{1}{r_g} + n^2 \frac{1}{r_a}\right) \ln \left(1 + \frac{n r_g S_b - 1}{1 + n^2 \frac{r_g}{r_a}}\right), \quad \ldots\ldots \quad (84.8)$$

if no cathode resistor R_k is present.

Experiments have been carried out with an E88CC double triode, using a transformer with constant turns ratio $n = 3$. The value of n_1, however, (and consequently n_2) was varied through values of $n_1 = 90$, 120 and 165 turns, and the air-gap in the core (pot-core type D-18/12 Fxc 3 B) was varied through 0.3, 0.5 and 1.0 mm resp.

Characteristics of the E88CC for positive grid voltages up to 10 volts were available. From the characteristics $I_a = f(V_a)$ with V_g as parameter, the values of r_a and S_b can be found and prove to be

$$r_a = \tfrac{1}{3} \text{ kilo-ohm } S_b = 14 \text{ mA/V}.$$

From the characteristics $I_g = f(V_a)$ with V_g as parameter, the value of r_g can be found; $r_g = \frac{1}{5}$ kilo-ohm.

With these values, expression (84.8) proves to be:

$$\frac{t_s}{L_2} = 0{,}0246 \frac{\text{sec}}{H} \quad \ldots\ldots\ldots\ldots \quad (85.8)$$

A mean value of 0.0224 sec/H can be obtained from the measurements, which is in fairly good agreement with (85.8).

b) Anode-to-cathode feed-back.

From expressions (69.8), (70.8), (71.8) and (74.8) it follows that

$$\frac{t_s}{L_2} = \left\{ \frac{1}{r_g} + (n-1)^2 \frac{1}{r_a} \right\} \ln \left\{ 1 + \frac{(n-1)\, r_g S_b - 1}{1 + (n-1)^2 \frac{r_g}{r_a}} \right\} \quad (86.8)$$

Substituting the same values as in the former case gives

$$\frac{t_s}{L_2} = 0.0145 \frac{\text{sec}}{H} \quad \ldots\ldots\ldots\ldots \quad (87.8)$$

The mean measured value is 0.0158 sec/H, which again shows a good agreement.

c) Cathode-to-grid feed-back.

From expressions (69.8), (70.8), (71.8) and (76.8) it can be calculated

that $$\frac{t_s}{L_1} = 0.0069 \frac{\text{sec}}{\text{H}} \quad \ldots\ldots\ldots\ldots \quad (88.8)$$

The mean experimental value is found to be 0.0097 sec/H. The agreement is less satisfactory in this case.

In conclusion, it can be stated that an approximate calculation of the transient behaviour of a triggered vacuum tube blocking oscillator is possible. Three modes of operation can be used, and they are described

by quite similar expressions. In all cases anode dissipations and grid dissipations can be determined, and for given maximum permissible values of these dissipations, the maximum permissible trigger pulse repetition frequency can be derived. The formulae can be used to design a blocking oscillator. For this purpose it will be helpful if tube characteristics of the following functions are available:

a) $I_a = f(V_a)$ with $+V_g$ as parameter.

b) $I_g = f(V_a)$ with $+V_g$ as parameter.

8.4. FREE-RUNNING BLOCKING OSCILLATOR

There are several possible ways of converting a triggered blocking oscillator into a free-running one. An *RC*-timing circuit may be incorporated either in the grid circuit or in the cathode circuit. In both cases the pulse width is determined by the magnetic circuit (the transformer) and associated resistances, whilst the period of the pulses is determined by the *RC*-time constant. Another possibility is to have both pulse-width and pulse-period determined by the magnetic circuit.

8.4.1. *RC*-TIMING CIRCUIT IN THE GRID LEAD

The magnetic feed-back circuit may be any of the three types treated in sections 8.2 and 8.3. In fig. 7.8 it is only schematically indicated by dotted windings. Also drawn in dotted lines is a circuit across the capacitor, with which it is possible, by closing switch S, to keep the capacitor charged to a voltage V_0, such that the grid-to-cathode voltage $V_g = V_{g0} - V_0$ is below the cut-off value $-V_{c0}$, so that no currents flow in the anode and grid circuits. Supposing, now, that switch S is opened at the instant $t = 0$, the capacitor starts to discharge to a final voltage of zero according to the time function

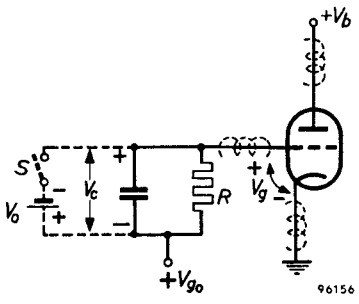

Fig. 7.8.

$$V_c = -V_0 e^{-\frac{t}{RC}} \quad \ldots\ldots\ldots \quad (89.8)$$

The voltage between grid and cathode varies according to the time function

$$V_g = V_{g0} + V_c = V_{g0} - V_0 e^{-\frac{t}{RC}} \quad \ldots \quad (90.8)$$

Now, it is supposed that $V_{g0} > V_{c0}$, so that, after a certain time t_r, the

value of V_g must be equal to $-V_{c0}$, equation (90.8) then reading

$$-V_{c0} = V_{g0} - V_0 e^{-\frac{tr}{RC}}, \quad \ldots\ldots\ldots \quad (91.8)$$

from which t_r can be found:

$$e^{-\frac{tr}{RC}} = \frac{V_{g0} + V_{c0}}{V_0} \quad \ldots\ldots\ldots\ldots \quad (92.8)$$

V_0, however, has to be defined further. This can be done by assuming that the free-running oscillator has reached a stationary state. Each time the grid voltage reaches the cut-off value V_{c0}, a de-blocking action occurs, a current pulse flows in the anode and grid circuit, the duration t_s of which is assumed to be very small with respect to the pulse repetition time t_r. The grid-current pulse $i_2\,(t)$ charges the capacitor C in such a short time t_s that the capacitor does not loose an appreciable amount of charge during the charging time t_s (this implies $t_s \ll RC$). The value of the charge surge from the grid current, stored in the capacitor C, will be

$$Q = \int_0^{t_s} i_2\,(t)\,dt, \quad \ldots\ldots\ldots\ldots \quad (93.8)$$

and the corresponding voltage increase across the capacitor

$$\Delta V = \frac{1}{C} Q \quad \ldots\ldots\ldots\ldots \quad (94.8)$$

If a stationary state is reached, this increase first brings back the capacitor voltage to its initial value V_0. The decrease of the capacitor voltage during the cut-off period t_r is to be derived from equation (89.8):

$$-\Delta V_c = V_c\,(0) - V_c\,(t_r) = -V_0 + V_0 e^{-\frac{tr}{RC}},$$

or:

$$\Delta V_c = V_0\left(1 - e^{-\frac{tr}{RC}}\right). \quad \ldots\ldots\ldots\ldots \quad (95.8)$$

Thus, in the stationary state we have $\Delta V_c = \Delta V$.

Substituting expressions (94.8) and (95.8) gives:

$$\frac{Q}{C} = V_0\left(1 - e^{-\frac{tr}{RC}}\right). \quad \ldots\ldots\ldots\ldots \quad (96.8)$$

Eliminating V_0 from expressions (92.8) and (96.8) results in:

$$e^{\frac{tr}{RC}} = 1 + \frac{Q}{C\,(V_{g0} + V_{c0})} \quad \ldots\ldots\ldots \quad (97.8)$$

Introducing expression (93.8) gives:

$$t_r = RC \ln \left[1 + \frac{\int_0^{t_s} i_2 (t)\, dt}{C (V_{g0} + V_{c0})} \right] \quad \ldots\ldots \quad (98.8)$$

With expressions (68.8), (69.8) and (71.8) it is easy to calculate the integral of (98.8), the final result being:

$$Q = \int_0^{t_s} i_2 (t)\, dt = \frac{V_b}{r_a} \tau \frac{N r_g S_b - 1}{N \frac{r_g}{r_a} + r_g S_b} \quad \ldots\ldots \quad (99.8)$$

Expressions (98.8) and (99.8) combined, give:

$$t_r = RC \ln \left[1 + \frac{\tau (N r_g S_b - 1)}{r_a C (\gamma + D) \left(N \frac{r_g}{r_a} + r_g S_b \right)} \right], \quad \ldots\ldots \quad (100.8)$$

where

$$\gamma = \frac{V_{g0}}{V_b}, \quad \ldots\ldots\ldots\ldots \quad (101.8)$$

a relative expression for the grid-bias voltage, and

$$D = \frac{V_{c0}}{V_b}, \quad \ldots\ldots\ldots\ldots \quad (102.8)$$

which is nearly the reciprocal value of the amplification factor of the tube.

The time constant τ is given by expressions (73.8), (75.8) and (77.8), depending on the mode of feed-back used.

Expressions (101.8) and (102.8) are introduced to obtain a better comparison between expression (100.8) and the expressions for the repetition frequency of the astable multivibrator given in section (7.4.4.).

8.4.2. *RC*-TIMING CIRCUIT IN THE CATHODE LEAD

Similar reasoning to that in the previous section leads to the same expression as (97.8), with the understanding that Q now represents the charge given to the capacitor by the sum of the current pulses in anode and grid circuits; in other words:

$$Q = \int_0^{t_s} \{ i_1 (t) + i_2 (t) \}\, dt. \quad \ldots\ldots \quad (103.8)$$

$$Q = \frac{V_b}{r_v} \left[\frac{r_v}{r_a} t_s + T \left(1 - \frac{r_v}{r_a} + N \right) \left(1 - e^{-\frac{t_s}{T}} \right) \right]. \quad . \quad (104.8)$$

The repetition period of the pulses is thus given by expressions (97.8) and (104.8) (for further reference, see the beginning of section 8.3).

It is true that the expressions become rather cumbersome, but they

do give an idea of the influence of various tube and transformer properties, circuit component values and bias voltages on the repetition period of this type of free-running blocking oscillator.

8.4.3. FREQUENCY NOT DEFINED BY AN *RC*-NETWORK

Up till now we have not taken into account the effects of stray capacitances. At the instant the tube starts to conduct, its internal resistances (r_a and r_g) have such a strong damping effect that no serious complications due to ringing of parasitic resonance circuits have to be considered. However, at the end of the pulse current, when the tube is suddenly cut off again, the transformer windings are no longer damped, and heavy oscillatory effects would occur in the anode and grid circuits as a result of ringing. To get rid of them, one of the transformer windings is often shunted by a suitable damping resistance. Preferably, this should be a non-linear resistance, causing little or no damping during the "forward stroke" (current pulse) and heavy damping during the back stroke (non-conducting period); for this purpose a diode is often employed (see fig. 8.8).

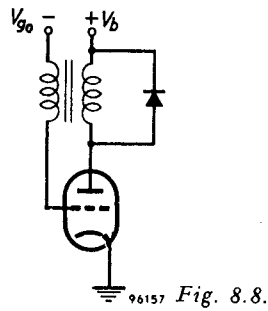

Fig. 8.8.

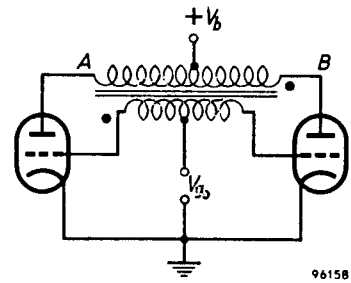

Fig. 9.8.

This principle can be used to give another kind of free-running blocking oscillator, viz. the push-pull type, sometimes used in chopper circuits. The basic circuit is given in fig. 9.8. Each tube, with the associated transformer windings, represents a blocking-oscillator circuit, but at the same time it is the damping "diode" for the other tube. The output signal across points AB will be symmetrical and more or less square-wave shaped. Its repetition period is twice the width of the current pulses flowing in each tube. The grid-bias voltage V_{g0} must be above the cut-off value for free-running operation. The amplitude of the output pulses is within certain bounds proportional to the anode-supply voltage V_b. This property can be used for converting a DC-voltage into a proportional AC-voltage, which is generally easier to amplify than DC-signals.

BIBLIOGRAPHY

I. BISTABLE MULTIVIBRATOR

1. W. H. Eccles, F. W. Jordan: *"A Trigger Relay utilising Three-Electrode Thermionic Vacuum Tubes"*, The Radio Review **1**, (Dec. 1919), **143**.
2. M.I.T. Radiation Lab. Series, Vol. 19, *"Waveforms"*.
3. B. E. Phelps: *"Dual-Triode Trigger Circuits"*, Electronics **18**, (July 1945), 110.
4. W. L. Buys: *"Analysis of Scale Units"*, Nucleonics **3**, (Nov. 1948), 49.
5. J. R. Tillman: *"Transition of an Eccles-Jordan Circuit"*, Wireless Engineer **28**, (April 1951), 101.
6. M. Rubinoff: *"Notes on the Design of Eccles-Jordan Flip-Flops"*, Communication and Electronics 1, (July 1952), 215.
7. R. F. Johnson, A. G. Ratz: *"A Graphical Method for Flip-Flop Design"*, Communication and Electronics **5**, (March 1953), 52.
8. R. Pressman: *"How to Design Bistable Multivibrators"*, Electronics **26**, (April 1953), **164**.
9. D. K. Ritchie: *"The Optimum D.C.Design of Flip-Flops"*, Proc. I.R.E. **41**, (November 1953), 1614.
10. R. Piloty: *"Die Dimensionierung der Eccles-Jordan Schaltung"*, Archiv d. Elektr. Übertragung **7**, (Nov. 1953), 537.
11. S. Higashi, I. Higashino, S. Kaneko, T. Oshio: *"Flip-Flop Circuits"* Part I, *"Analysis"*, Jl. Inst. Polytechnics, Osaka City University, **4**, Series B, (1953), 7. Part II, *"Methods of Design"*, Idem, **5**, Series B, (1954), 37.
12. H. Harmuth: *"Multivibratoren"* E. und M. **71**, Heft 6, (March 1954), 136.
13. R. Favre: *"Circuits Électroniques Multistables et Décades"*, Helvetica Physica Acta, **27**, Nr. 3, (June 1954), 235.
14. K. Gosslau, H. J. Harloff: *"Untersuchungen über das Gleichstrom- und Wechselstrom-Verhalten von Bistabilen Kippschaltungen"* Nachr. Techn. Zeitschrift, **8**, Heft 10, (Oct. 1955), 521.
15. P. A. Neeteson: *"Analysis of Bistable Multivibrator Operation"*, Book of the Philips' Technical Library (1956).
16. M. Bataille: *"Étude des États d'Équilibre d'un Basculeur Bistable en Vue d'un Fonctionnement sûr et durable"*, L'Onde Électrique **36**, no. **347** (Feb. 1956), **94**.
17. G. G. E. Low: *"Two Trigger Circuits useful as Sources of Rectangular Pulses"* Electronic Engineering **28**, (April 1956), 158.
18. G. Thiele: *"Berechnungsanleitung für Flip-Flop-Schaltungen"*, Elektr. Rundschau (1957) Nr. 7, 212, Nr. 8, 250, Nr. 9, 274.

II. MONOSTABLE MULTIVIBRATOR

1. M.I.T. Radiation Lab. Series, Vol. 19, *"Waveforms"*.
2. H. Harmuth: *"Multivibratoren"*, E. und M. **71**, Heft 6 (March 1954), 136.
3. A. C. Luther, Jr: *"Stabilization of Pulse Duration in Monostable Multivibrators"*, RCA Review, (Sept. 1955), 403.
4. G. Haas: *"Untersuchungen über die Zeitverzögerung der Impulsauslösung beim Monostabilen Multivibrator"*, A.E.U. 9, (1955), 272.
5. B. R. Johnson: *"A Method of Multivibrator Timing Stabilisation"* A.W.A. Technical Review, **10**, Nr. 1, (1956), 33.
6. W. Gruhle: *"Multivibratorschaltung für Millimikrosekunden-Impulse"*, Elektronik, Nr. 9, (1957), 261.

III. ASTABLE MULTIVIBRATOR

1. H. Abraham, E. Bloch: *"Mesure en Valeur Absolue des Périodes des Oscillations Électriques de Haute Fréquence"*, Annales de Physique **12**, (1919), 237.

2. F. C. WILLIAMS, A. FAIRWEATHER: *"A 'Chopped- Signal' Vacuum Tube Generator with good Voltage Regulation"*, Post Office Electrical Engineers' Journal, 32, (1939), 104.
3. F. VECCHIACCHI: *"Meccanismo di Funzionamento e Frequenza del Multivibratore"* Altafrequenza 9, (1940), 745.
4. E. H. B. BARTELINK: *"A Wide-Band Square-Wave Generator"*, A.I.E.E. Transactions 60, (June 1941), 371.
5. M. V. KIEBERT Jr, A. F. INGLIS: *"Multivibrator Circuits"*, Proc. I.R.E. 33, (1945), 534.
6. N. W. MATHER: *"Multivibrator Circuits"*, Electronics 19 (Oct. 1946), 136.
7. S. BERTRAM: *"The Degenerative Positive Bias Multivibrator"* Proc. I.R.E., 36, (Feb. 1948), 277.
8. A. E. ABBOT: *"Multivibrator Design by Graphical Methods"*, Electronics 21, (June 1948), 118.
9. R. FEINBERG: *"On the Performance of the Push-Pull Relaxation Oscillator (Multivibrator)"*, Phil. Mag., 39, (April 1948), 268.
10. R. FEINBERG: *"Symmetrical Multivibrators"*, Wireless Engineer, 26, (May 1949), 153.
11. R. FEINBERG: *"Asymmetrical Multivibrators"*, Wireless Engineer, 26, (Oct. 1949), 325.
12. M.I.T. Radiation Lab. Series, Vol. 19, *"Waveforms"*.
13. B. BANERJEE: *"A Study of the Switching Action in a Multivibrator Circuit"*, Indian Jl. of Physics 24, nr. 8, (Aug. 1950), 361.
14. D. C. SARKAR, R. AHMED: *"Analysis of the Relaxation Period of a Multivibrator"*, Indian Jl. of Physics 28, nr. 11, (Nov. 1954), 533.

IV. BLOCKING-OSCILLATOR CIRCUITS

1. R. BENJAMIN: *"Blocking Oscillators"*, Jl. Inst. El. Engs., 93, Part IIIa, nr. 7, (1946), 1159.
2. M.I.T. Radiation Lab. Series, Vol. 19, *"Waveforms"*.
3. L. FLEMING: *"The Blocking Oscillator as a Variable-Frequency Source"* (Correspondence) Proc. I.R.E., 37, (Nov. 1949), 1293.
4. J. RACKER, P. SELVAGGI: *"Television Synchronizing Circuits"*, Part 1, Radio and Television News, 45, (Jan. 1951), 70.
5. A. F. GIORDANO: *"Blocking-Tube Oscillator Design for Television Receivers"*, Electrical Engineering, 70, nr. 12 (Dec. 1951), 1050.
6. K. G. BEAUCHAMP: *"Blocking Oscillators"*, Electronic Engineering, 25, (June 1953), 239.
7. P. R. GILETTE, K. W. HENDERSON, K. OSHIMA: *"Blocking Oscillator Transformer Design"*, I.R.E. Convention Record, vol. 3, Part 3, (1955), 75.
8. J. MAC DONALD SMITH: *"Millimicrosecond Blocking Oscillators"*, Electronic Engineering, 29, (April 1957), 184.
9. C. H. R. CAMPLING: *"Magnetic Inverter uses Tubes or Transistors"*, Electronics, 31, nr. 11 (March 14, 1958), 158.

LIST OF SYMBOLS AND INDEX

G constant (expr. 39*b*.7; p. 102).

H constant (p. 102; 123).

I, i current.

I_a anode current of a tube.

I_g grid current of a tube.

I_i input current of a network (p. 36).

I_o auxiliary current source used to account for the effect of opening a switch in a network (p. 6).

y constant (p. 126).

j imaginary unit ($\sqrt{-1}$) (p. 21).

K constant (expr. 21*a*.5; p. 102).

L constant (expr. 21.7).

M constant (p. 124).

Multivibrator (p. 18, 75)
- astable, (p. 18, 75; section 7.4)
- bi-stable, (p. 18, 75; section 7.2)
- monostable, (p. 18, 75; section 7.3)

N constant (p. 128).

Operational calculus section 5 (p. 19).

P constant (expr. 21.7).

p operator of dimension frequency or reciprocal time (p. 19).

Q constant (expr. 40*a*.7).

R resistance.

r internal resistance.

r_a internal anode resistance of a tube.

r_g internal grid resistance of a tube.

S mutul conductance of a tube (p. 61); constant (p. 135).

Superposition theorem (p. 25).

T time constant; period of astable multivibrator (expr. 195.7, p. 143).

t time.

$U(t)$ unit-step function: $U(t) = 0$ at $t < 0$
$U(t) = 1$ at $t > 0$.

$U(t-t_o)$ unit-step function occurring at the instant $t = t_o$
$U(t-t_o) = 0$ at $t < t_o$
$U(t-t_o) = 1$ at $t > t_o$.

V voltage.

V_a anode voltage of a tube.

V_b, V_b battery- or H.T. supply voltage.

V_c auxiliary voltage source used to account for the effect of closing a switch in a network (p. 4); voltage across a capacitor (p. 20).

V_{cr} minimum trigger voltage of a bistable multivibrator (p. 103).

V_g grid voltage of a tube.

V_i input voltage (p. 19).

x unknown in an equation (p. 102).

y unknown in an equation (p. 103).

Z impedance.

α angle (p. 30); ratio of times (expr. 94.6); slope of a voltage pulse (p. 81).

β angle (p. 59);
ratio of voltages (expr. 93.6).

γ ratio of voltages (expr. 50*a*.7).

Δ small variation (p. 26).

ε ratio of resistances (p. 23).

λ time (fig. 4.5); ratio of resistances (expr. 121.6).

μ amplification factor of a tube (p. 60, 61).

ω angular frequency (p. 21).

τ time (p. 31).

ϱ ratio of resistances (expr. 169.7).

∞ infinite (time) (p. 11).